Université Catholique de Louvain

Secteur des Sciences de la Santé

Louvain Drug Research Institute

SELF-EMULSIFYING SYSTEMS FOR THE ORAL DELIVERY OF ANTI-SICKLING AGENTS

Aristote Buya Banzenga

Thèse présentée en vue de l'obtention du grade de docteur en Sciences biomédicales et pharmaceutiques

Pr Véronique Préat
Pr Ana Beloqui, Patrick Memvanga

2021

In memory of my dear mother

(Longombanga Sukani Bibi)

This project would not have been possible without the support of many people.

First, I would like to thank my advisor Professor Préat Véronique for her guidance, patience, and support. I have benefited greatly from your immense knowledge and meticulous scientific approach. I am extremely grateful that you took me as a student and continued to trust me over the years. I could not have imagined having a better advisor for my doctoral studies.

I would also like to thank Professors Beloqui Ana and Memvanga Patrick for guiding me and for all valuable contributions and motivations to move ahead. Professor Memvanga Patrick has always been by my side. From my first trip to Europe until the end of my thesis, he was always available to discuss. I am grateful for the excellent example he is providing as a successful scientist and Professor.

Besides my supervisors, I would like to thank my PhD committee members: Professors Gallez Bernard, Leclercq Joëlle, Elens Laure and Van Bambeke Francoise for their insightful comments and feedback at each step of my PhD studies.

Thanks to the Professors of the Faculty of Pharmaceutical Sciences (UNIKIN) for providing me the required training and scientific foundation for the realization of this thesis.

The work reported in this thesis would not have been possible without the financial support of UCLouvain (Bourse de la coopération au développement), for which I am grateful.

I would like to extend my thanks to Professors Evrard Brigitte (Ulg) and Vandamme Thierry (Université de Strasbourg) for accepting to take part of thesis jury.

My special thanks to Catherine Rasse (SMCS-UCLouvain), Tanguy Missoul (Mettler Toledo), Marjorie Vermeersch (CMMI-ULB), Danisa Zapparrata (UCLouvain) and Koen Robeyns (IMCN-UCLouvain) for training and support during my studies.

I would like to take this opportunity to thank Bernard Ucakar, Kevin Vanvarenberg and Murielle Callier for their help and support. Thanks to my office colleagues (Thibaut, Yasmine, Mingchao and Alessio) and all the labmates from ADDB for their kindness and help.

Thanks to the Congolese community (Ange, Hervé, Espoir, Papa Marcel and Maman Gaby) for memorable moments and funny talks.

I would like to thank my family to whom I owe a great deal. To my late mother Longombanga Sukani, I could not imagine you would leave so early. My love for you is eternal. Without you, I would not be the person I am today. I hope you can see and be proud of your son.

Finally, I would like to thank my best friend and wife, Loris Gloria Mukuzo, who supported me in all my sorrows and absences. She gave me love, help and prevented several wrong turns. I will never forget our evening calls on Messenger.

TABLE OF CONTENTS

LIST OF ABBREVIATIONS

BBPI	Bowman-Birk protease inhibitor
BCRP	Breast cancer resistance protein
BCS	Biopharmaceutical classification system
DL-PA	Dalargin-palmitic acid
DLS	Dynamic light scattering
DoE	Design of experiment
DSC	Differential scanning calorimetry
EMA	European medicines agency
FCS	Fluorescence correlation spectroscopy
FDA	Food and Drug Administration
FeSSGF	Fed state simulated gastric fluid
FeSSIF	Fed state simulated intestinal fluid
FTIR	Founier-transform infrared spectroscopy
GMP	Good manufacturing practice
GRAS	Generally regarded as safe
HbF	Fetal hemoglobin
HbS	Hemoglobin S
HBSS	Hank's salt balanced solution
HLA	Human leukocyte antigen
IFN	Interferon
iNKT	Invariant natural killer T
IRP	Intestinal recirculating perfusion
IVIVC	In vitro-in vivo correlation
LCT	Long chain triglycerides
LDH	Lactate dehydrogenase
LFCS	Lipid formulation classification system
MCT	Medium chain triglycerides
MTD	Maximum tolerated dose
NaTDC	Sodium taurodeoxycholate
NO	Nitric oxide
P-gp	P-glycoprotein
PAMPA	Parallel artificial membrane permeability assay
PBS	Phosphate-buffered saline
QbD	Quality-by-design
RBC	Red blood cell
s-SNEDDS	Supersaturated SNEDDS
SA	Surfactant
SCD	Sickle cell disease
SEDDS	Self-emulsifying drug delivery system
SEM	Scanning electron microscopy
SEN	Senicapoc
SNEDDS	Self-nanoemulsifying drug delivery system

SPIP	Single-pass intestinal perfusion
sSAXS	Synchrotron small-angle x-ray scattering
TDA	Taylor dispersion analysis
TEM	Transmission electron microscopy
TGA	Thermal gravimetric analysis
VOC	Vaso-occlusive crisis
VOX	Voxelotor
WHO	World Health Organization
XRPD	X-ray powder diffraction

CHAPTER I

INTRODUCTION

TABLE OF CONTENTS

PART I.
SICKLE CELL DISEASE

ABSTRACT

Sickle cell disease is one of the most common genetic blood disorders arising from a mutation in the β-globin gene that leads to the substitution of glutamic acid by valine at the sixth position of the β-chain of hemoglobin. This substitution causes mutant hemoglobin polymerization in low oxygen tension. The polymerized hemoglobin leads to erythrocyte rigidity, vaso-occlusion and anemia. As a result, occlusion of the microcirculation occurs which may lead to infraction, ischemia and ultimately, long term organ failure. Simple, rapid and affordable tests are being developed to facilitate universal screening of the disease, especially in low-income countries. Current therapies in sickle cell disease are focused on reducing hemoglobin polymerization and anemia. Hydroxyurea, which increases fetal hemoglobin production and blood transfusion are now largely used. Several new therapeutic agents are being investigated, including erythrocyte ion-channels blockers, anti-oxidative, antiadhesion and anti-inflammatory agents. The advancements in the field of translational research in sickle cell disease have led to the application of stem cell transplantation and gene therapy as promise curative option of the disease. This part offers an updated overview of sickle cell disease, including epidemiology, physiopathology, screening and therapeutic strategies.

I. INTRODUCTION

Sickle cell disease (SCD), one of the most common inherited hemoglobinopathy worldwide is now understood to be an increasing global health problem. A single mutation in the hemoglobin gene causes glutamic acid to be replaced by valine at the sixth codon of the growing protein chain [1,2]. Under deoxygenated conditions, mutant hemoglobin namely sickle hemoglobin (HbS) polymerizes, which results in the sickling of the erythrocyte. In addition, polymerized hemoglobin leads to stiffness of erythrocyte membrane, hemolysis and anemia. Later, occlusion of the microcirculation occurs which may lead to infraction, ischemia and ultimately, long term organ failure. Every year, approxymativly 300.000 infants are born with sickle cell anemia, the most common form of SCD, and referring to homozygosity for the β-globin gene [3]. The highest prevalence of SCD occurs in sub-Saharan Africa, more than 75% of affected individuals are born in this area [4]. The co-occurrence SCD-malaria among populations sparked an interest to study the link between the two diseases. Taylor et al. [5] demonstrated that a SCD mutation deters progression to severe malaria by enhancing the clearance of infected red blood cell thereby stopping malarial parasite growth. Several other studies revealed the protective effect of SCD against malaria [6-8]. SCD care and management remain costly, patients spend over $1 billion per year in the United States [9], where the median of life expectancy is only ~45-58 years [10]. Despite the high incidence of SCD in sub-Saharan Africa, not much information is available on the estimated life expectancy of those affected by SCD [11, 12].

II. DISTRIBUTION AND BURDEN OF DISEASE

SCD was originally distributed throughout sub-Saharan Africa, the Middle East, Mediterranean and India. This large distribution is indicative of relative protection that provides sickle cell trait (heterozygous HbAS) against *Plasmodium falciparum* infection [13]. Because of population movement from tropical areas, the HbS allele has spread far beyond its origin [1,14]. In addition, with the increase in number of migrants from those tropical regions, the prevalence of SCD in new populations is increasing (Figure 1) [15].

Nowadays, there is no reliable global estimate, but a recent estimate in newborn suggests that approximatively 300.000 babies per year are born with SCD [1, 16] and this number could rise to 400.000 by 2050 [17]. Most of these births occur in Democratic Republic of the Congo, Nigeria and India, where half of the world's affected SCD individuals lives [15,18]. The vast majority (up to 90%) of children with SCD do not reach their fifth birthday. Despite this high mortality associated with SCD in these regions, little is known about the cause of death in affected children. Generally, routine neonatal screening and diagnostic facilities are lacking in these countries. Consequently, most infants die undiagnosed due to acute complications, notably supported by malaria, bacterial sepsis and anemia [19, 20]. In contrast, live expectancy of infants with SCD in high-income countries has remarkably improved. This has been achieved by the application of care programs, which comprise systematic neonatal screening, diagnostic, hydroxyurea treatment and penicillin prophylaxis [15, 21].

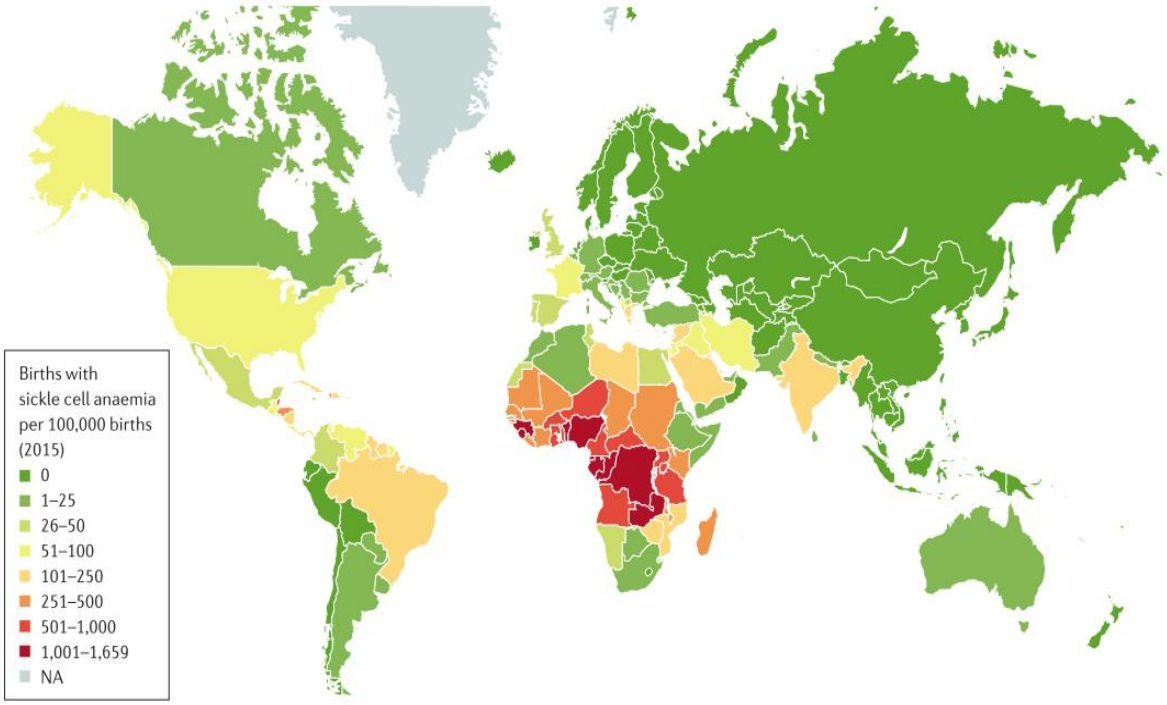

Figure 1. Map of the estimated numbers of births with sickle cell anemia per 100.000 births per country in 2015. From [1].

III. PATHOPHYSIOLOGY

SCD is an autosomal recessive inherited disorder caused by a single mutation in the β-globin gene. This mutation is located in exon I on both 11-chromosome homologues that changes the 17th nucleotide thymine to adenine, causing the substitution of valine to glutamate in the 6th amino acid of the β-globin chain [22]. The loss of glutamate, a negatively charged amino acid alters electrostatic mobility and under low oxygen tension, valine promotes hydrophobic interactions between β1 and β2 of two HbS molecules. As consequence, HbS molecules polymerize and deform the structure of the erythrocyte, referred as "sickle red blood cell" (Figure 2). The rate and extent of HbS polymerization is proportional to the intra-erythrocytic concentration of HbS and duration of hemoglobin deoxygenation [15]. Sickle red blood cell resumes its normal form once there is reoxygenation; however, recurrent sickling upon deoxygenation causes damage of erythrocyte membrane. Sickle red blood cell is rigid, dehydrated, lysis-prone and interacts with vascular endothelium and leucocytes. This results in hemolysis and occlusion of small vessels, which are the main pathophysiological process of SCD.

Hemolysis has long been recognized to be the cause of anemia but its contribution to the development of several intravascular events is now described [23]. Erythrocyte hemolysis leads to plasma release of HbS, arginase-1 and reactive oxygen species. Those in turn promote oxidative and inflammatory stress, especially to blood cells and vessels [24]. The released free HbS and arginase-1 scavenge nitric oxide (NO) and its precursor L-arginine, causing a decrease in NO bioavailability [25]. NO is an important paracrine factor that initiates and maintains the smooth muscle dilatation and contributes to endothelial function [26]. In addition, NO ensures the

hemostatic balance and inhibits adhesion molecules and platelet activation [27, 28]. In view of this, persistent erythrocyte hemolysis promote vasocontraction and progressive vasculopathy [29].

Erythrocyte sickling, the leading cause of ischemia, is the predominant pathophysiological process responsible for vaso-occlusion associated with severe pain and inflammation [30]. Several events may induce vaso-occlusion, but the three important factors include HbS polymerization, erythrocyte hemolysis and increased blood viscosity. Due to the HbS polymerization, erythrocyte may become rigid and poorly deformable, that results in their mechanical sequestration in the small vessels promoting vaso-occlusion. Another cause of vaso-occlusion is the scavenging of NO, as consequence of persistent erythrocyte hemolysis. Low levels of NO alter its endothelial functions, such as repression of cell adhesion molecules and inhibition of platelet activation, and shift vasoconstriction/vasodilatation balance towards vasoconstriction, which favors the occurrence of vaso-occlusion [31]. The increase in adhesion molecules expression promotes intense erythrocyte interaction with endothelial cells. Sickle erythrocyte presents an increase expression of adhesion molecules, especially integrin $\alpha_4\beta_1$ and CD36 that interact with vascular cell adhesion molecule-1 and thrombospondin, respectively [3]. High blood viscosity, which occurs as result of persistent hemolysis and reduced sickle red blood cell flexibility due to HbS polymerization contributes to the microvascular occlusion and ischemia.

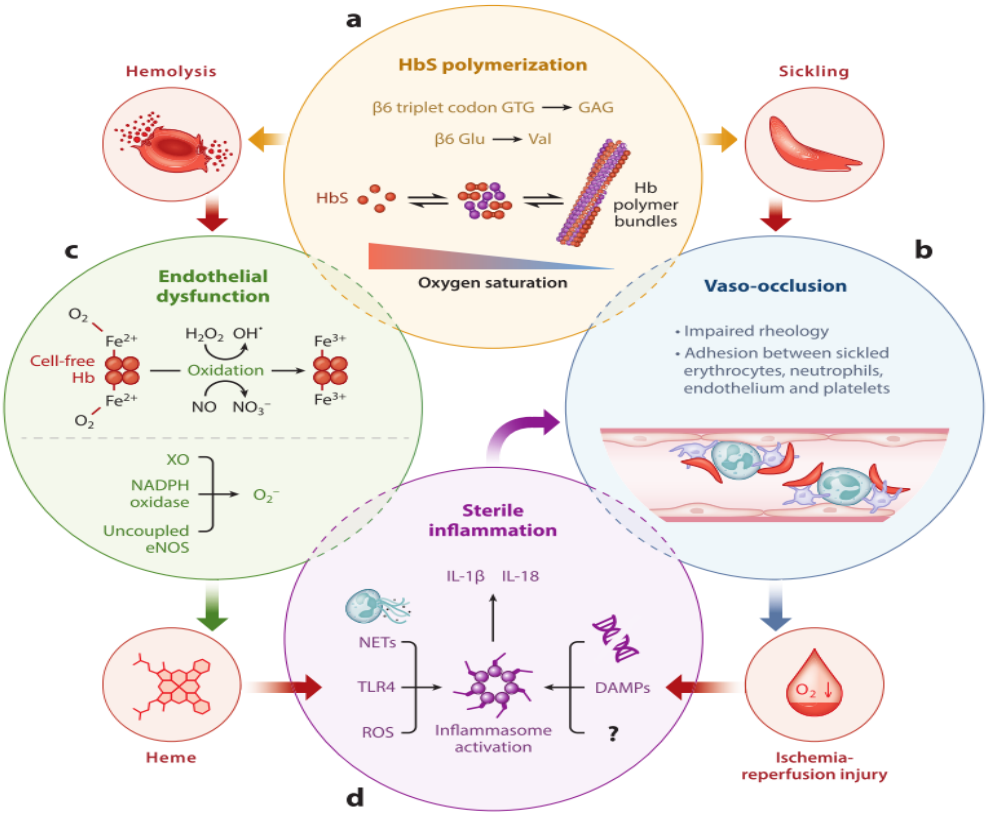

Figure 2. Molecular pathophysiology of sickle cell disease. From [22].

IV. CLINICAL COMPLICATIONS OF SICKLE CELL DISEASE

Overall, complications of SCD can be divided into two main categories: those related to erythrocyte hemolysis and functional NO deficiency, responsible of progressive vasculopathy (pulmonary hypertension, cerebrovascular disease, nephropathy, leg ulcers and priapism) and those related to microvascular occlusion and ischemia (vaso-occlusion, pain, infection diseases, retinopathy, osteonecrosis and hyposplenism) [23]. The main clinical complications of SCD are discussed below.

IV.1. VASO-OCCLUSIVE CRISIS

Vaso-occlusive crisis (VOC) are the clinical hallmark of SCD, and the main reason for emergency care of SCD patients. These crisis are known as recurrent painful crisis, in which episodic microvascular occlusion in many sites leads to hypoxia, ischemia and ultimately to the release of inflammatory mediators [32]. This in turn activate nociceptive afferent nerve fibers, causing the pain response.

The occurrence of VOC is not predictable and may be triggerred by hypoxia, dehydration, cold, acidosis and stress [32]. Affected areas are long bone chest, head, pelvis and spine.

IV.2. CEREBROVASCULAR ACCIDENTS

The central nervous system is severely affected in SCD, both children and adults suffer from cerebrovascular complications. Cerebrovascular accidents are the most devastating striking and complication of SCD, with the high stroke incidence in early childhood (aged 2-9 years) [33]. In absence of systematic newborn screening, stroke occurs in 5-10% of children affected by SCD [22]. Stroke can be either hemorrhagic or ischemic; however, the most occurring type in SCD patients is ischemic related to vascular occlusion [34]. Risk factors include raised systolic blood pressure, HbS phenotype, high steady-state HbS concentration, previous transient ischemic attack, acute chest syndrome and high leucocyte counts [34].

IV.3. INFECTIOUS DISEASE

Infections are probably the most significant contributors to morbidity and mortality in SCD patients, especially in children [35]. Splenic dysfunction, which is already present at childhood has a key role in increasing the susceptibility to bacterial infections [36]. SCD children lack IgM memory B cells that can mount a specific response to microorganisms. Most common infections seen in children with SCD are from encapsulated organisms, including *Salmonella species*, *Escherichia coli*, *Streptococcus pneumoniae*, *Neisseria meningitidis* and *Haemophilis influenza* [37,38]. Less commonly, *Klebsiella* and *Pseudomonas* are found.

In contrast to relative protection that provides sickle cell trait (heterozygous HbAS) against *Plasmodium falciparum*, homozygous SS patients are highly vulnerable to malaria. Co-existence of the two contributes to excess mortality, and malaria is a significant precipitating cause of VOC in endemic areas [39].

IV.4. ACUTE CHEST SYNDROME

Acute chest syndrome is a frequent cause of hospital admission and an important precipitating cause of death in young adults [5]. It is defined as an acute lung injury accompanied by respiratory symptoms and fever [40]. The injured lung fails to be reoxygenated, and ultimately causes chronic pulmonary disease, including inflammation and hypertension.

The underlying risk factors of acute chest syndrome are not fully understood; however, some suspect factors include vaso-occlusion, red blood cell adhesion, lower fetal hemoglobin (HbF) concentration, hypoxia, fat embolism and infections [41, 42].

IV.5. OTHER COMPLICATIONS

Patients with SCD suffer from a wide range of complications, including priapism, leg ulcers, retinopathy, nephropathy, osteonecrosis and cardiomyopathy [43-45]. These complications are thought to derive from both repeated hemolysis as well as small vessels occlusion. Recently, a clear distinction has been made between the two phenotypes of SCD. On the first hand, the vaso-occlusive phenotype characterized by a relatively higher hematocrit and less intravascular hemolysis that results in more VOC, acute chest syndrome and osteonecrosis. On the other hand, the hemolytic phenotype characterized by low hemoglobin levels and high LDH concentrations, resulting in complications such priapism, leg ulcers, nephropathy and cardiomyopathy. However, mostly in practice, the clinical picture of SCD reflects a mixture of these two phenotypes.

V. DIAGNOSIS AND SCREENING

An early screening of SCD is not a common practice, especially in low-income countries, and the diagnosis is usually made when complications occur. Diagnosis of SCD is based on the complete blood count and analysis of hemoglobin. Widely used hemoglobin analysis techniques include hemoglobin solubility testing, hemoglobin profile analysis by electrophoresis or chromatography [46, 48]. Recently, thermogravimetric analysis has been proposed as novel test for SCD screening [49, 50].

DNA analysis is being increasingly used in pregnant women to determine the risk of SCD in fetus [51-53]. Despite the advantages of these techniques in improving SCD detection, their costs and the lack in 100% accuracy limit their application.

VI. EXISTING THERAPIES FOR THE MANAGEMENT OF SCD

VI.1. HYDROXYUREA

Hydroxyurea was the first Food and Drug Administration (FDA) approved drug for the treatment of SCD. It is a ribonucleotide reductase inhibitor that is easily absorbed after oral administration and turns into a free radical nitroxide before diffusing through cell membranes [54]. Several mechanisms of action have been attributed to hydroxyurea, one such being the increase in HbF concentrations, which can inhibit HbS polymerization, red blood cell sickling and vaso-occlusion [55]. Hydroxyurea is also known to act as a NO generator and causes a significant reduction in number of platelet and white blood cells. Other mechanisms of action have emerged, including a reduced expression of adhesion molecules that promote vaso-occlusion [56, 57].

A randomized controlled trial was performed to assess the benefits versus risks of hydroxyurea treatment in adult patients [58]. According to this study, hydroxyurea decreased the frequency of blood transfusion, painful crisis, acute chest and hospitalization. Several subsequent trials have shown similar benefit of hydroxyurea treatment among adults [59-61].

Because hydroxyurea is a cytotoxic and was initially tested in patients with severe SCD symptoms, its use was only reserved for adult patients. The FDA restricts the indication of hydroxyurea only to SCD adults with recurrent moderate to severe vaso-occlusive crisis (at least 3 in the previous 12 months). The effects of hydroxyurea are dose-dependent and clinical studies have shown that the optimal benefit of hydroxyurea is obtained at the maximum tolerated dose (MTD). The major drawbacks of the use of hydroxyurea at the MTD is its reported toxicity in many cases. Further, being a cytotoxic, the effect of hydroxyurea in long-term therapy remains unknown and requires specific investigations. Another concern related to hydroxyurea is inter-patient variability in both the MTD and the percentage of HbF.

Although hydroxyurea nonresponders are rare in childhood, approximately one-third of adults will not respond, making alternative and combination therapies a worthwhile endeavor [54, 62]. The literature reports that the ability to respond to hydroxyurea administration might depend on the

bone marrow capacity to withstand moderate dose of hydroxyurea, so allowing the generation of erythroid precursors that produce HbF [54].

Early evidence studies supporting the use of hydroxyurea in children were inadequate. Clinical studies and resulting data analysis have not provided satisfactory results to support its use in pediatric population [7]. Nowadays, many clinical studies (Toddler HUG, BABY HUG, HUG-KIDS, and NHLBI) were carried out to assess the risk of hydroxyurea treatment in children. These clinical trials and observations demonstrated the clinical befits of hydroxyurea in children and have proven that 85-90 % of children were capable to tolerate hydroxyurea 20 mg/kg per day [7]. It was reported that early initiation of hydroxyurea therapy might prevent cerebrovascular, kidney and spleen complications without a delay in growth or other toxicity [63-65].

VI.2. L-GLUTAMINE

L-glutamine (Endari®) is the second FDA-approved therapy of SCD. L-glutamine undergoes intestinal metabolization to citrulline and subsequently to arginine, the amino acid substrate for NO production that becomes deficient in SCD patients. Moreover, L-glutamine is a substrate of nicotinamide adenine dinucleotide (NAD) that modulates oxidation-reduction potential in sickle red blood cells and reduces oxidative damage.

Niihara et colleagues conducted a pilot study with seven patients (aged 19-60 years) who were administered 3 g of L-glutamine orally per day for 4 weeks. They demonstrated a modest decrease in painful crisis and hospitalization among treated group versus placebo [66]. L-glutamine gained approval based on results of a placebo-controlled, double-blind and phase multicenter randomized clinical trial [67, 68]. It was hypothesized that L-glutamine administration (0.6 g/kg/day) reduces the frequency of vaso-occlusive crisis, hospitalization, acute chest syndrome.

However, the main concern limiting long-term compliance of L-glutamine is that its oral administration is onerous, the patients have to take the drug, mix it up in water and drink it two or three times a day [69].

VI.3. EMERGING TREATMENT APPROACH FOR SCD

VI.3.1. Hemoglobin F inducing agents

One of the mechanisms that interfere with the polymerization of deoxygenated HbS is the induction of HbF. It is a known fact that increasing the levels of HbF is a therapeutic opportunity to reduce the mortality in SCD [70]. There are many agents that are being studied for their ability to increase HbF production. Some of them are discussed below.

- Decitibine and 5-Azacytidine

Human gamma globin genes are hypomethylated in fetal cells and methylated in adult cells. The genes are silenced during childhood and expressed through adulthood via epigenetic gene regulation carried out by DNA methyltransferase 1 (DNMT1). The methylation of DNA achieved by DNMT1 is responsible for the shift in production from the gamma globin chain (HbF) in

childhood to beta globin beta chain (HbS) in adulthood. Several studies have shown that the inhibition of DNMT1 could prevent the switch of HbF production [71-73]. Decitibine and its prodrug 5-azacytidine have been found to cause resistance to DNA methylation, inactivate DNMT1 and induce gamma globin gene expression in primates and SCD patients [54, 74]. In preliminary studies, decitibine increased HbF production (up to 14%) and hemoglobin levels in patients who failed to respond to hydroxyurea administration [75-76]. This promising drug has completed phase II clinical trials. However, decitibine has many shortcomings, including brief half-life, low oral bioavailability and negligible tissue distribution [77-78]. Out of decitibine and 5-Azacytidine, other HbF inducing agents are presented in table 1.

VI.3.2. Anti-Adhesion Agents

Deoxygenated HbS causes damage to red blood cell membrane through the formation of polymers. In addition, HbS can undergo auto-oxidation and precipitation on the surface of red blood cell that result in oxidants generation, which increases membrane damage [80]. Blood cells adhesion is among the many changes that result from damage of erythrocyte membrane.

Blood cells interactions with the endothelium have been well established in SCD and require the involvement of several cellular and endothelial proteins [80, 81]. These interactions may lead to the release of oxygen radical species from endothelial cells and the activation of NF-kB transcription factor that upregulates the expression of various adhesion molecules, including P-selectin, E-selectin, ICAM-1 and ICAM-1 on the surface of the endothelium.

Of particular interest has been the family of adhesion molecules known as selectin, especially P-selectin which is upregulated during SCD steady-state and is the initiating factor of erythrocyte adhesion and vaso-occlusion seen in inflammation or pain crisis [82-84]. It was thus stated that blocking P-selectin could decrease inflammation and pain crisis in SCD patients.

In this section, we briefly discuss some promissing agents that target intercellular adhesion (table 1).

- Crizanlizumab

Crizanlizumab (ADAKVEO) is the lastest FDA approved treatment for SCD. It is a monoclonal antibody that specifically binds and blocks P-selectin. In double-blind randomized phase II trials, SCD patients were administered either crizanlizumab low dose (2.5 mg/kg/day), high dose (5 mg/kg/day) or placebo [85, 86]. There was a lower (43%) median pain crisis rate per year in patients who received high dose of crizanlizumab versus placebo group. The drug was given by intravenous infusion and has shown to have a relatively long half-life (30-days). The investigators concluded that crizanlizumab is effective in preventing vaso-occlusive pain crisis in SCD patients. The phase III study to instigate the efficacy of crizanlizumab in adolescents and adults with SCD is ongoing (NCT03814746).

However, the fact that crizanlizumab is given intravenously could possibly be a drawback to its long-term use. Also, studies assessing appropriate dosing and safety of crizanlizumab in pediatric population are not yet available.

- Rivipansel

Rivipansel (GMI-1070) is a small P-selectin antagonist found to inhibit selectin binding *in vitro* and selectin-related effects *in vivo* [87]. A phase I studies reported that infusion of rivipansel at 10 mg/kg/day achieved plasma level expected to have activity in SCD patients, with an estimated half-life of 7.7h [88]. A phase II trial in hospitalized SCD patients with recurrent vaso-occlusive pain showed a "clinically meaningful" ability of rivipansel to shorten the time to resolution of vaso-occlusive pain and a significant reduction in the mean cumulative intravenous opioid antalgic usage [89]. A phase III trial assessing the time to readiness-for-discharge, cumulative IV opioid and re-hospitalization for vaso-occlusive crisis is ongoing (NCT02187003).

VI.3.3. Antioxidant agents

Increased oxygen radical species production plays a key role in the pathophysiology of SCD by leading to membrane damage, expression of adhesion molecules and hemolysis. HbS nonenzymatic auto-oxidation and iron-mediated Fenton chemistry reactions are sources of oxygen radical species production in sickle red blood cells [90]. In addition, SCD patients show lower levels of reduced glutathione, which is an important endogenous antioxidant and a pivotal component of the enzymatic antioxidant system [91].

The promising antioxidants agents, both in preclinical and clinical trials used to mitigate oxidative stress are shown in table 1 and some of them are described below.

- Omega-3 fatty acids

A lower content of omega-3 fatty acids is observed in SCD patients [92]. Tomer et colleagues reported a lower frequency of pain episodes in SCD patients who were treated with omega-3 fatty acids (0.1 g/kg/day) compared to placebo group treated with olive oil [93]. A randomized, placebo-controlled, double-blind trial was carried out at a single hospital in Sudan. Patients with SCD (N=140) were enrolled and monitored for 1 year. The investigators demonstrated that omega-3 treatment reduced vaso-occlusive events and frequency of blood transfusions [94].

- N-acetyl cysteine

N-acetyl cysteine inhibits dense cell formation, *in vitro* sickling of red blood cells and restores reduced glutathione amount toward normal [95]. In an open label randomized pilot study of oral N-acetylcysteine, 11 consecutive patients were randomly assigned to receive 1.2 mg or 2.4 mg N-acetylcysteine daily for 6 weeks. The results indicate an increase in whole blood glutathione levels and a decrease in cell-free hemoglobin, red blood cell outer membrane phosphatidylserine exposure and plasma levels of advanced glycation products following 6 weeks of N-acetylcysteine treatment in both dose groups [96].

- Natural antioxidants

Some phytochemicals or herbals act directly to induce the resolution of anemia through their antioxidant activity. The advantage of using them is that they are available, especially in low-income countries. Many plants extracts, including *Brassica oleracea var italica*, *Hypoestes triflora, Phyllanthus niruri* and *Beta vulgaris* have shown pharmacological effects in hemolytic anemia treatment [97].

VI.3.4. Anticoagulant Agents

There is evidence that even during steady state, SCD patients exhibit increased platelet and fibrinolytic system activation which results in a "hypercoagulable state" [28]. In addition, patients with SCD exhibit increased thrombin generation, abnormal activation of coagulation cascade and decreased levels of anticoagulant proteins in the no-crisis state. Furthermore, procoagulant activity and tissue factor antigen are reported to be high in the blood of SCD patients compared to normal controls [98, 99].

A growing body of evidence suggests that complications from coagulation pathways likely contribute to the pathophysiology of SCD and, therefore, has been a new target for researchers hoping to alleviate complications of SCD. In this section, we review anticoagulant agents studied for their efficacy in SCD management and some of them are presented in table1.

VI.3.4.1. Agents that interfere with coagulation

- Rivaroxaban

Sparkenbaugh et al. [100] demonstrated the contribution of Xa factor in the coagulation process in murine model of SCD. Factor Xa activates serine proteases responsible of coagulation cascade and inflammation in many vascular disorders. Thus, preventing the activation of Xa factor could lower serine proteases levels and consequently improve the phenotype of SCD. Rivaroxaban, a direct factor Xa inhibitor is under phase II studies for its effects on coagulation, interleukin-6 levels and vascular cell adhesion molecule-1 in SCD patients.

- Low-molecular-weight heparin

A randomized, double-blind, placebo-controlled study showed the clinical benefit of low-molecular-weight heparin tinzaparin and dalteparin in the treatment of acute vaso-occlusive pain in patients with SCD [101, 102]. However, it is not clear whether the reported effects were a result of the anticoagulation activity or the P-selectin inhibition effect of the drugs. Sevuparin, a negatively charged polysaccharide derived from heparin is now undergoing phase II trial. The drug has low anticoagulant effect but shows a strong activity to block cell adhesion molecules and plasma factors involved in SCD vaso-occlusion [103].

VI.3.4.2. Antiplatelet agents

- Prasugrel

Prasugrel is a novel thienopyridine P2Y12 ADP receptor antagonist that blocks ADP-mediated platelet activation and aggravation. A large pediatric trial of prasugrel showed a reduction in vaso-occlusive pain episodes compared with placebo [104]. However, this reduction did not reach statistical significance. A study in adults with SCD showed that plasma soluble P-selectin and platelet surface P-selectin, both biomarkers of platelet activation, were significantly reduced in patients with SCD compared with the placebo [105].

- Ticagrelor

Ticagrelor is another thienopyridine P2Y12 ADP receptor antagonist; however, it differs from prasugrel in the fact that it does not require metabolic activation, and has additional vasodilator and anti-inflammatory effects [104, 106]. A phase II study to instigate the efficacy of ticargrlor has recently been completed and results are pending (NCT02482298).

VI.3.5. Agents that reduce Inflammation

Growing evidence demonstrates that chronic hemolysis and vaso-occlusion may contribute to vascular inflammation associated with SCD [100]. The endothelial cells activation by plasma free heme can trigger a cascade of proinflammatory cytokines. In addition, sickle erythrocyte, platelets and leucocytes can activate endothelial cells and contribute to the inflammation seen in SCD [107]. We review some agents under investigation to downregulate inflammatory consequence of patients with SCD (table 1).

- Regadenoson

Regadenoson is an A_2 receptor agonist reported to reduce iNKT cells activation in phase I study [108]. iNKT cells activation in patients with SCD was associated with increased IFN-gamma and phospho-NK-kB levels, both responsibles of inflammatory response [108]. Based on positive results, ragadenoson was tested under phase II randomized placebo-controlled trial. However, data demonstrated that a 48-hour continuous infusion of 1.44 mg/kg per hour regadenoson intended to reduce the activity of iNKT cells was not sufficient to produce a statistically significant reduction in such activation or in measure of clinical efficacy compared to placebo [109].

- Simvastatin and atorvastatin

A pilot study was conducted to evaluate markers of vascular dysfunction in SCD patients treated with simvastatin [110]. The study showed that simvastatin could increase the levels of NO and decrease interleukin-6 and C-reactive protein in a dose-dependent manner. A phase II study to investigate the efficacy of simvastatin was recently completed (NCT01702246) and results are pending. The effets of atorvastatin on endothelial dysfunction are under investigation (NCT01732718).

Table 1. New therapeutic agents for the treatment of SCD

Class	Drug name	Mechanism	Route	Phase	ClinicalTrials.gov Identifier
Antihemolytic and anti-sickling agents	Senicapoc	Inhibit gardos channel	PO	Completed Phase II	NCT00040677
	Voxelotor	Increase oxygen affinity	PO	Completed Phse III	NCT03036813
	Panobinostat	Increase hemoglobin F	PO	Phase I	NCT01245179
	Decitabine	Increase hemoglobin F	PO	Phase II	NCT01375608
	Metformin	Increase hemoglobin F	PO	Phase I	NCT02981329
	Sanguinate	Oxygen transfer agent	IV	Phase II	NCT02672540
	Pomalidomide	Increase hemoglobin F	PO	Completed Phase I	NCT01522547
Anti-Adhesion Agents	Rivipansel	Anti-adhesion (panselectin inhibitor)	IV	Phase III	NCT02187003
	Crizanlizumab	Anti-adhesion (anti-P- selectin agent)	IV	Phase III	NCT03814746
	Sevuparin	Anti-adhesion (anti-P- selectin agent)		Phase II	NCT02515838
	Poloxamer 188	Anti-adhesion	IV	Completed phase III	NCT01737814
	Propranolol	Anti-adhesion	PO	Completed phase II	NCT01077921
	Gammaglobulin	Anti-adhesion	IV	Phase II	NCT01757418
	Montelukast	Anti-adhesion	PO	Phase II	NCT01960413
	N-acetyl cysteine	Antioxidant	PO	Phase I/II	NCT01800526
	Omega-3 fatty acids	Antioxidant	PO	Phase I/II	NCT02947100

Antioxydant Agents	Arginine	Antioxidant/vasodilator	IV	Phase II	NCT02536170
	L-citrulline	Antioxidant/vasodilator	PO	Phase I	NCT02659644
Anticoagulant Agents	Ticagrelor	Antiplatelet agent	PO	Completed phase II	NCT02482298
	Prasugrel	Antiplatelet agent	PO	Phase III	NCT01794000
	Rivaroxaban	Anticoagulant	PO	Phase II	NCT02072668
	Apixaban	Anticoagulant	PO	Phase III	NCT02179177
	Unfractionated heparin	Anticoagulant, anti-adhesion	IV	Phase II	NCT02580773
	Low-molecular-weight heparin	Anticoagulant	SQ	Phase III	NCT02580773
Anti-inflammatory agents	Simvastatin	Anti-inflammatory	PO	Phase II	NCT00508027, NCT01702246
	Atorvastatin	Anti-inflammatory	PO	Phase II	NCT01732718
	Vitamin D	Anti-inflammatory	PO	Phase II	NCT01443728
	Mometasone	Anti-inflammatory	IN	Phase II	NCT02061202
	Budesonide	Anti-inflammatory	IN	Completed phase I	NCT02187445
	Regadenoson	Anti-inflammatory	IV	Phase II	NCT01788631
	Zileuton	Anti-inflammatory	PO	Completed phase I	NCT01136941
	NKTT120	Anti-inflammatory	IV	Completed phase I	NCT01783691

PO : oral, IN : intranasal, IV: intravenous, SQ: subcutaneous

VI.4. BLOOD TRANSFUSION

Erythrocyte transfusions have an established role in the prevention and treatment of both acute and chronic complications of SCD. Studies have proven that transfusions may increase hemoglobin levels, correct anemia, decrease the percentage of HbS and reduce erythrocyte hemolysis, all of which lower the risk of ischemia and vaso-occlusion [111-113]. Erythrocyte transfusions are more likely to be necessary if there is an urgent need to decrease HbS concentration without causing an increase in blood viscosity, typically in patients with acute neurological complications. A pediatric study was conducted to compare the occurrence of strokes between children on regular blood transfusions and those who received standard therapy. The participants enrolled were between 1 and 15 years and were followed for 3 years. The study demonstrated that regular blood transfusions significantly lower the incidence of strokes in the transfused group compared to other standard care [114].

Blood transfusion can be administered as a simple top-up transfusion or as an automated exchange transfusion where there is simultaneous collection and replacement of blood. The top-up transfusion is mainly indicated in severe anemia, in particular due to erythrocyte aplasia caused by splenic sequestration or infections. The aim is to correct anemia and improve oxygen carrying capacity of the blood. On the other hand, indications of exchange transfusion are clinical complications which require a rapid and significant decrease in HbS concentration, including acute stroke, acute chest, acute multiorgan failure and severe sepsis [115, 116].

Although blood transfusions have proven to be essential in the management of acute crisis, they are also associated with risks and patients must be carefully monitored. Common complications include iron overload, hemolytic transfusion reaction caused by erythrocyte alloimmunization and risk of transmission of infection disease (HIV, hepatitis C, malaria, etc.) [117-119]. Most iron deposition occurs in the liver, with little cardiac loading and is known to be a major cause of tissue damage [120]. Nowadays, ion-chelating agents (deferoxamine, deferiprone and deferasirox) are increasingly studied for chronically transfused individuals with SCD to avoid liver damage [121-123]. However, the use of ion-chelators has been associated with toxicity in certain cases. Whitley et al. [124] reported auditory and visual neurotoxicity with the use of deferoxamine. In the same way, other studies showed that deferoxamine could interfere with natural growth due to skeletal dysplasia [125,126]. Erythrocyte alloimmunization occurs approximately in 30% of chronically transfused SCD patients compared to 2-5% of all transfusion recipients [127]. Alloantibodies are known to be persistent for several years and can cause a significant delayed hemolytic transfusion reaction.

Although red blood transfusions have proven to be important for SCD patients, more studies are needed, and benefits and risks of blood transfusions should be fully discussed with patients and their familes before initiating a long-term transfusion program.

VI.5. STEM CELL TRANSPLANTATION

Currently, hematopoietic stem cell transplantation is the curative treatment for SCD patients. The first successful case of stem cell transplantation was reported in 1984 in a SCD child who had

developed acute myeloid leukemia [128]. Globally, up to 1.000 SCD patients have received hematopoietic stem cell transplantation, and survival analysis from 1986 to 2013 has revealed excellent results, with both children and adults showing an overall survival of 92.9 % (95% confidence interval 91.1-94.6%) [129]. Change to the intensity of conditioning has expended stem cell transplantation as a curative approach for adult patients with severe organ dysfunction, who were otherwise ineligible for hematopoietic stem cell transplantation using standard myeloablative conditioning regime [130]. Although promising results have been shown through several studies [131-133], stem cell transplantation has certain limitations. Controversies have arisen not only about the optimal age to transplant but also about whom to transplant. High mortality rate reported in patients older than 16 years age and the difficulty in obtaining HLA-compatible donors are major conserns [135]. Less than 14% of patients with SCD have HLA-compatible donors [134] and the estimated risk of death from HLA-compatible-stem-cell transplantation in SCD is about 5 % [135]. Alternative source of HLA-haploidentical such family donors have been therefore actively explored to make stem cell transplantation accessible to more patients [136]. Late effect of transplantation such as hypogonadism, growth failure, sterility have also been reported [137-140].

VI.6. GENE THERAPY

Gene therapy to edit SCD has been ongoing for several years. This therapy involves *ex vivo* gene modification of autologous hematopoietic stem cells and their transplantation into the bone marrow tissue. As gene therapy does not require the selection of HLA-haploidentical donor and avoid risk of graft rejection, it appears to be an attractive alternative to hematopoietic stem cell transplantation [141]. Several gene therapy approaches have been developed. Lentiviral vector approach is one of the most used strategies to transfer a modified gene into hematopoietic stem cell [142]. Lentiviruses have been established as efficient and relevant globin vectors for correcting the hemoglobin gene in SCD. Pawliuk et al. [143] applied gene therapy to cure sickle cell transgenic mice. A lentiviral vector containing a β-globin gene variant to produce HbF was constructed and transferred to hematopoietic stem cells. Transduced hematopoietic stem cells were transplanted into SCD mice by marrow ablation. Results showed that long-term expression was achieved, and erythroid-specific accumulation of targeted protein was about 52% of total hemoglobin in all circulating erythrocytes. Moreover, the mice showed inhibition of erythrocyte dehydration and sickling.

Recently, a young boy (13 years old) with SCD was treated with a lentivieral vector. Once the transduced stem cells had transplanted, hemolysis was corrected, and normal blood count were achieved in all lineages. The level of therapeutic antisickling β-globin remained high (approximately 50% of β-like–globin chains) in long-term without recurrence of vaso-occlusive crisis and with correction of the biologic markers of SCD [144]. So far, six clinical trials are ongoing to evaluate long-term efficacy and safety of gene therapy in SCD patients [15, 145, 146].

VII. SENICAPOD AND VOXELOTOR IN THE TREATMENT OF SCD

VII.1. SENICAPOC

VII.1.1. Senicapoc: chemistry and properties

Senicapoc [bis(4-fluorophenyl) phenyl acetamide] (Figure 3), previously known as ICA-17043 is a small organic compound with a molecular mass of 323 g/mol [147]. The chemical synthesis of senicapoc and evaluation of its pharmacokinetic properties compared to others structurally similar analogs have been reported by McNaughton-Smith et al. [148].

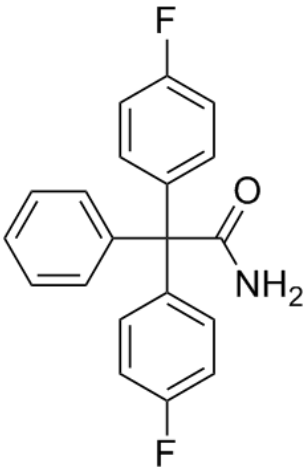

Figure 3. Chemical structure of Senicapoc

Senicapoc is a potent and selective blocker of the calcium-activated potassium (Gardos) channel located on the human erythrocytes, thereby inhibiting the efflux of potassium through this channel (Figure 4) [149]. When washed erythrocytes were loaded with rubidium ($^{86}Rb^{+}$), increasing concentrations of senicapoc produces a consistent and increasing block of rubidium ($^{86}Rb^{+}$) efflux through the Gardos channel with an IC_{50} (drug concentration that inhibits 50% of K^{+} efflux from erythrocytes) of 11 ± 2 nM compared to an IC_{50} of 100 ± 12 nM for clotrimazole [147]. In addition, *in vitro* incubation of washed erythrocytes with increasing concentrations of senicapoc show dose-dependent inhibition of erythrocytes dehydration following exposure of the cells to Ca^{2+} ionophore A23187 [147].

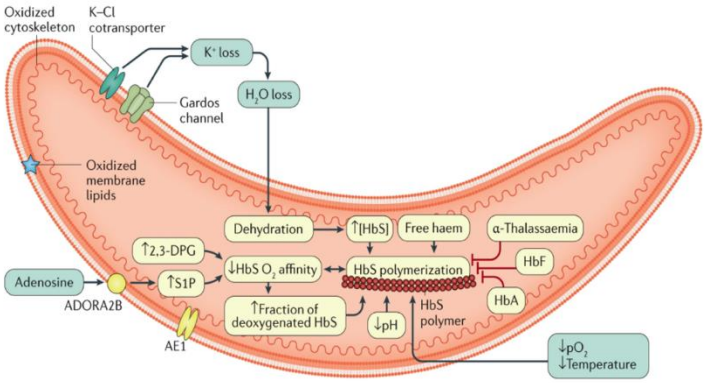

Figure 4. Mechanism of action of Senicapoc. From [149].

VII.1.2. Preclinical studies of senicapoc

Oral administration of senicapoc to transgenic sickle mice (10 mg/kg twice daily) for 21 days resulted in a significant decrease in Gardos channel activity. In addition, an increase erythrocyte K^+ content, an increase in hematocrit, a decrease in erythrocyte density and a decrease in mean corpuscular hemoglobin concentration (MCHC) were observed, all together indicated a reduction in erythrocyte dehydration following senicapoc administration [147]. The reduced cell dehydration was evidenced by a decrease in the average erythrocyte density and high cell K^+ content in treated mice compared to placebo group.

Pharmacokinetics (table 2) and safety evaluations of senicapoc in rats have been reported. Senicapoc is a hydrophobic drug (logP 3.59) with poor aqueous solubility (975 ng/mL) [147] and moderate oral bioavailability (51%). It has been reported that senicapoc has a half-life of 1 h in rats, with a maximum concentration attained after 4 h when administered orally [149]. At high dose (1000 mg/kg), senicapoc produced minimal effects on animal behaviors, and had no impact on either intestinal motility or locomotor activity [149]. *In vitro* and *in vivo* genetic toxicity studies showed that senicapoc was not mutagenic and exhibited no reproductive toxicity in rats or rabbits at doses ranged from 100 to 1500 mg/kg. No effects were observed on the QT/QTc interval in conscious dogs. The only consistent finding in rats and monkeys after chronic administration of senicapoc (up to 100 mg/kg/day) was an increase in liver weight, which was explained as result of adaptation to the dosing regimen change [149].

VII.1.3. Clinical development of senicapoc

A Phase I dose-escalation studies in both healthy subjects and SCD patients has been conducted to evaluate the pharmacokinetics and safety of senicapoc. In a double-blind, randomized, placebo-controlled study of healthy subjects who received oral doses of senicapoc ranging from 25 to 200 mg in capsule, the C_{max} and AUC increased proportionally from 25 to 150 mg and a plateau was reached at 200 mg [150]. Gardos channel inhibition was obtained at mean senicapoc plasma concentrations ranging from 136 to 170.5 ng/mL following the administration of two high doses (150 and 200 mg) [150]. When healthy subjects and SCD patients received senicapoc, elimination half-life ranged between 12 -17 days and 9-15 days for healthy subjects and SCD patients, respectively [150]. Dose-escalation studies were carried out in SCD patients to determine senicapoc tolerated doses and safety. Single senicapoc oral doses of 50, 100 and 150 mg were well tolerated, and no dose-limiting adverse effects were reported. The concurrency of nausea was more frequent in treated group in a dose-dependent manner [151]. No significant change in blood parameters, ECG parameters (including QT/QTc) or vitals parameters were observed between the active and placebo groups.

A 12-weeks phase II randomized double-blind study assessing the efficacy of senicapoc in SCD patients was conducted. The patients were randomized into three groups: placebo, low-dose (6 mg/day) and high dose (10 mg/day). The study showed that oral administration of senicapoc reduced erythrocytes hemolysis as indicated by an increase in hemoglobin levels and concomitant decrease in indirect bilirubin, lactate dehydrogenase (LDH) and number of circulating dense erythrocytes and reticulocytes [152]. In addition, a dose-dependent inhibition of Gardos channel

was observed in both the low- and high-dose senicapoc groups. All of these results are in line with an increase in life span of erythrocyte and an improvement of anemic state [152]. Senicapoc was well tolerated in SCD patients during the 12 weeks of administration. Nausea and diarrhea occurred more frequently in treated group compared to placebo, and their incidence seemed to be dose-dependen [152].

Following the results from phase II study, a subsequent phase III study was conducted in 298 SCD patients who were randomized to receive senicapoc or placebo for 48 weeks. The study aims to compare the rate of acute vaso-occlusive pain crisis occurring in SCD patients receiving 10 mg of senicapoc versus placebo. In accordance with previous findings, patients on senicapoc exhibited increased hemoglobin levels and decreased markers of hemolysis compared to placebo group. However, the study was terminated early owing to no significant improvement in the rate of acute vaso-occlusive pain crisis in the senicapoc group compared to placebo (0.38 vs 0.31, p= 0.054) [149, 153]. This study showed that improvements in hematological parameters following senicapoc administration may not result in an improvement in vaso-occlusive complications.

VII.2. VOXELOTOR

VII.2.1. Voxelotor: chemistry and properties

Voxelotor (2-hydroxy-6-({2-[1-(propan-2-yl)-1H-pyrazol-5-yl]pyridin-3-yl}methoxy)benzaldehyde) (Figure 5), previously known as GBT 440 is a small organic compound with a molecular mass of 337 g/mol. Voxelotor is a hydrophobic drug (logP 3.54) with poor aqueous solubility (43 μg/mL) [154]. Voxelotor is a first-in-class oral molecule developed for the treatment of SCD based on its properties as hemoglobin-oxygen affinity allosteric modifier [154]. Voxelotor mechanism of action consists of the reversibly bind with the N-terminal valine of the α-chain of hemoglobin, leading to an allosteric modification of hemoglobin and stabilization of the oxygenated HbS conformation (Figure 6). As oxygenated HbS does not polymerize, voxelotor can reduce polymerization and sickling of erythrocytes in SCD patients [154, 155].

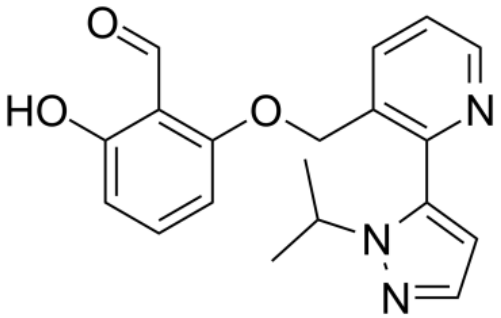

Figure 5. Chemical structure of Voxelotor

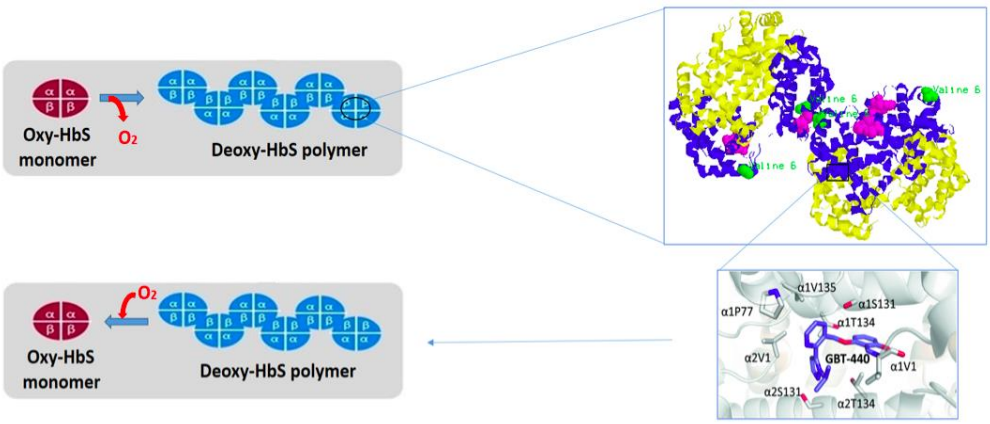

Figure 6. Mechanism of action of Voxelotor.

VII.2.2. Preclinical studies of voxelotor

The administration of voxelotor (100-150 mg/kg) to SCD mice prolongs the half-life of erythrocytes, decrease *ex-vivo* erythrocytes sickling, and reticulocytes counts [154]. In addition, voxelotor was found to improve erythrocyte deformability, reduce blood viscosity and reverse erythrocyte sickling under hypoxic conditions [156, 157].

Pharmacokinetics studies (table 2) conducted in rats, dogs, and monkeys showed that voxelotor is well tolerated and is readily portioned into erythrocytes. Voxelotor is absorbed into plasma and is then distributed predominantly into RBCs due to its preferential binding to Hb. Voxelotor is primarily eliminated by hepatic metabolism with subsequent excretion of metabolites into urine and feces. In vitro and in vivo studies indicate that voxelotor is extensively metabolized through Phase I (oxidation and reduction), Phase II (glucuronidation) and combinations of Phase I and II metabolism. Oxidation of voxelotor is mediated primarily by CYP3A4, with minor contribution from CYP2C19, CYP2B6, and CYP2C9. The pharmacokinetics is linear and voxelotor exposures increase proportionally with either single or multiple doses in whole blood, plasma, and RBCs. Steady-state after repeated administration is reached within 8 days and exposures of voxelotor are consistent with accumulation predicted based on single dose data in patients with SCD [155]. Following multiple doses, voxelotor was well tolerated up to 900 mg daily for 15 days and no serious side effects were reported [155]. Voxelotor showed variable oral bioavailability of 60, 36.6, and 36.1 % in rats, dogs, and monkeys, respectively, with similar half-lives approximatively 20 h [155]. The high partitioning into erythrocyte implies that voxelotor is rapidly sequestered into erythrocyte. No significant time-dependent inhibition of the major human CYP isozymes was observed following voxelotor administration [155].

Table 2. Summary of Pharmacokinetics data for Senicapoc and Voxelotor [148, 155]

	Animal model	Dose (mg/kg)	Solubility (μg/mL)	F %	$T_{1/2}$ (h)	T_{max} (h)	C_{max} (μg /mL)
Senicapoc	Rat	10	620	51	1.0	4	0.4
Voxelotor	Monkey	4.25	31	36.1	28.8	18	25.2
	Mouse	30	31	70.5	24	4	81.9
	Rat	7.2	31	59.8	19.1	5	71.2

VII.2.3. Clinical development of voxelotor

The first-in-human study was conducted in healthy volunteers and SCD patients to evaluate safety, tolerability, pharmacokinetics and pharmacodynamics of voxelotor [158]. A total of 40 healthy subjects were randomized to receive a single dose of voxelotor (100, 400, 1000, 2000 or 2800 mg) and 2 SCD patients receiving 1000 mg voxelotor. The study demonstrated that voxelotor was well tolerated across a wide dose range and showed dose proportionality and predictable pharmacokinetics and pharmacodynamics. Voxelotor showed a dose-dependent increase in hemoglobin-oxygen affinity in both healthy and SCD patients, and a significant reduction in erythrocytes sickling was observed in patients with SCD [159]. All the adverse events reported (nausea, diarrhea, and headache) following voxelotor administration in healthy volunteers and SCD patients were grade 1 (mild) [155]. Voxelotor demonstrated a terminal half-life ranged from 26 to 72 h and was mainly eliminated by metabolism in healthy subjects with less than 1% of the given dose excreted unchanged into urine [160]. Inter-subject variability for Cmax and AUC values was observed following voxelotor administration and was likely caused by variability in dissolution of voxelotor in gut of subjects due to its poor aqueous solubility [158].

A multicenter, phase III, double-blind randomized trial was conducted to compare the efficacy and safety of two dose of voxelotor (900 mg and 1500 mg) with placebo in SCD patients [161,162]. A total of 274 SCD subjects were randomly assigned to receive a once-daily oral dose of voxelotor 900 mg, 1500 mg, or placebo for 24 weeks. The study demonstrated that voxelotor increased hemoglobin levels and reduced markers of hemolysis compared to placebo. These finding were consistent with inhibition of HbS polymerization and indicated voxelotor disease-modifying potential. Based on its favorable properties, OXBRYTA® (tablets), a specialty of voxelotor has been given accelerated approval by the U.S. Food and Drug Administration (FDA) for patients aged 12 and older [162].

PART II.
SELF-NANO-EMULSIFYING DRUG-DELIVERY SYSTEMS: FROM THE DEVELOPMENT TO THE CURRENT APPLICATIONS AND CHALLENGES IN ORAL DRUG DELIVERY

Aristote B. Buya, Ana Beloqui, Patrick B. Memvanga, Véronique Préat

Adapted from Pharmaceutics 2020, 12, 1194

ABSTRACT

Approximately one third of newly discovered drug molecules show insufficient water solubility and therefore low oral bioavailability. Self-nanoemulsifying drug-delivery systems (SNEDDSs) are one of the emerging strategies developed to tackle the issues associated with their oral delivery. SNEDDSs are composed of an oil phase, surfactant, and cosurfactant or cosolvent. SNEDDSs characteristics, their ability to dissolve a drug, and *in vivo* considerations are determinant factors in the choice of SNEDDSs excipients. A SNEDDS formulation can be optimized through phase diagram approach or statistical design of experiments. The characterization of SNEDDSs includes multiple orthogonal methods required to fully control SNEDDS manufacture, stability, and biological fate. Encapsulating a drug in SNEDDSs can lead to increased solubilization, stability in the gastro-intestinal tract, and absorption, resulting in enhanced bioavailability. The transformation of liquid SNEDDSs into solid dosage forms has been shown to increase the stability and patient compliance. Supersaturated, mucus-permeating, and targeted SNEDDSs can be developed to increase efficacy and patient compliance. Self-emulsification approach has been successful in oral drug delivery. The present review gives an insight of SNEDDSs for the oral administration of both lipophilic and hydrophilic compounds from the experimental bench to marketed products.

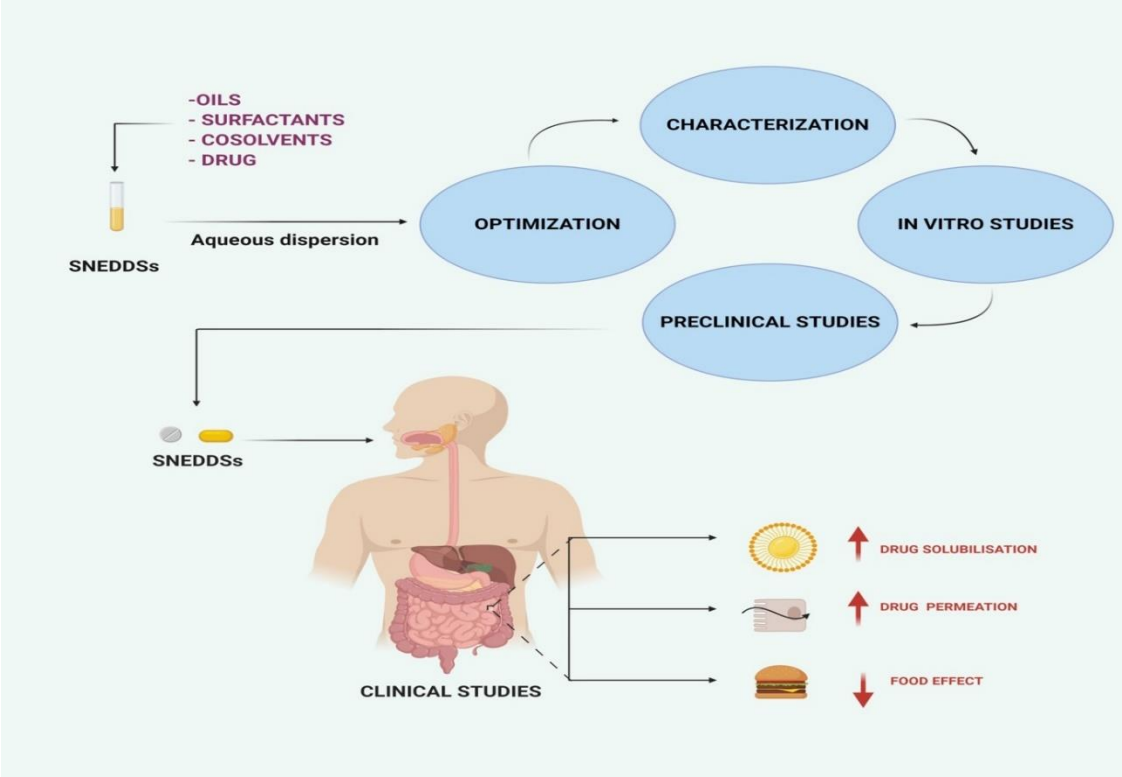

I. INTRODUCTION

The oral administration route remains the best choice for drug delivery owing to its safety, patient compliance, and capacity for self-administration. In addition to being the most convenient route of administration, oral delivery has been limited owing to the numerous barriers present at the gastro-intestinal (GI) tract [163]. The solubilization of the drug within the GI tract is a mandatory for the drug absorption, as insufficient drug dissolution may lead to incomplete absorption, low bioavailability, and high variability following oral administration [163]. The oral delivery of drugs may also be associated with precipitation, food and drug interactions, susceptibility to degradation, and first-pass metabolism, leading to low oral bioavailability. According to the BCS (Biopharmaceutical Classification System), most of the drugs discovered thus far are classified into class II (low solubility, high permeability) and class IV (low solubility, low permeability). Class II drugs exhibit good permeability but low aqueous solubility; therefore, the limiting step in their absorption is the dissolution. A slight increase in drug solubility produces a significant increase in its oral bioavailability. Therefore, there is an urgent need to develop new drug carriers for their oral delivery. Several techniques have been reported relating to improving the solubility of poorly soluble drugs, including, solid dispersions, nanosuspensions, structural modification, and cyclodextrin complexes.

Solid dispersions consist of two (or more) component systems in which the drug is dispersed monomolecularly or as small particles in a hydrophilic matrix [164]. Formulation of solid dispersion helps in converting the crystalline form of the drug into its amorphous form to enhance the bioavailability of such drugs by improving the aqueous solubility. Crystalline compounds consist of highly ordered crystal lattice which needs more energy to disorder as compared to highly disordered amorphous form. Increased aqueous solubility can be attributed to a strongly enhanced surface area of the drug, to an improved wetting and to the amorphous state of the drug. Generally, either polyvinylpyrrolidone or polyethylene glycol are used as matrix materials. Due to their solubility enhancement potential, solid dispersions have drawn increasing interest over the last decade, in both academia and industry. Some US Food and Drug Administration (FDA)-approved pharmaceutical products based on solid dispersion include Nabilone (Cesamet®), Verapamil (Isoptin® SR), Itraconazole (Sporanox®) and Tacrolimus (Prograf®). However, the solubilization capacity of solid dispersion systems can decrease over the time, resulting in recrystallization or precipitation of the drug. Another obstacle is the amount of polymer needed i.e. more than 50% to 80% is required to achieve desired solubilization. Also, the polymers use for the formulation can absorb moisture which may result in phase separation, crystal growth or conversion to the crystalline form.

Nanosuspensions are submicron colloidal dispersions of nanosized drug particles stabilized by surfactants. They consist of the poorly water-soluble drug without any matrix material suspended in an aqueous vehicle [165]. Drug particle size reduction leads to an increase in surface area and consequently in the drug solubility. Nanosuspensions are suitable for the compounds with high log P value, high melting point and high dose. They can be used to enhance the solubility of drugs that are poorly soluble in water and oils.

Subtle structural modifications which reduce log *P* or melting point can lead to improved drug solubility. These modifications include removing hydrophobic groups, modifying geometry by altering the position of functional groups, changing stereochemistry, reducing or increasing the degree of unsaturation, or adding substituents such as methyl or fluorine [166]. By the addition of polar groups like carboxylic acids, ketones and amines, solubility is improved by increasing hydrogen bonding and the interaction with water. However, these modifications can alter the pharmacological activities of the compound.

Cyclodextrins have been widely investigated as pharmaceutical excipients for past few decades and is still explored for new applications. They are macrocyclic oligosaccharides consisting of a hydrophilic outer surface and a hydrophobic inner cavity where guest molecules having a lipophilic nature can be accommodated. Thus, the drugs get encapsulated in the cavity and results in improved aqueous solubility [167]. However, the formation of cyclodextrin complexes requires specific molecular properties, which may not work for certain compounds, and the toxicity of cyclodextrin complexes at high concentrations, which limits the dose level, are the major limitations of this technique.

All of these techniques suffer from limitations such as poor industrial scalability, poor stability, complex chemical synthesis and requirement of sophisticated equipment that reduce manufacturing ease and ultimately lack commercialization prospects. To overcome this, the literature has encouraged considering alternative technologies, including lipid-based formulations, to solve the problem of aqueous solubility and oral bioavailability of BCS class II drugs.

The fact that the oral absorption of poor water-soluble drugs could be improved once given with food rich in lipids has brought the use of lipids-based formulations as means to improve the drug solubility and absorption following the oral administration [163]. Lipid-based formulations are considered to be a promising approach to enhance the water solubility and oral absorption of lipophilic drugs. The main goal of these formulations is to maintain the drugs in solution within the GI tract [163]. Among the wide number of lipid-based drug-delivery systems, self-nanoemulsifying drug delivery systems (SNEDDSs) are one of the most investigated in oral drug delivery.

SNEDDSs have been described as a blend of oils, surfactants, and cosurfactants or cosolvents [168]. Following aqueous dispersion and mild agitation (such in GI tract), SNEDDSs spontaneously form fine oil-in-water nano-emulsions with droplet size of 200 nm or below [169], as shown in Figure 1. The spontaneous emulsification takes place when the entropy change favoring dispersion exceeds the energy required to increase the surface area of the dispersion [170,171]. SNEDDSs have shown immense potential in overcoming limitations related to the oral administration of several compounds. Such limitations include low solubility in the GI tract, inconsistent dissolution, enzymatic degradation, and erratic intestinal absorption. Surfactants and lipid components used in SNEDDSs can cooperate to enhance the GI absorption drugs. Furthermore, these components can be modified easily according to the need to make SNEDDSs feasible for both hydrophilic and hydrophobic drugs. Recent studies have shown that SNEDDSs could be effective oral drug carriers of peptides and proteins by preventing their GI degradation and improving their intestinal membrane permeability [172–174].

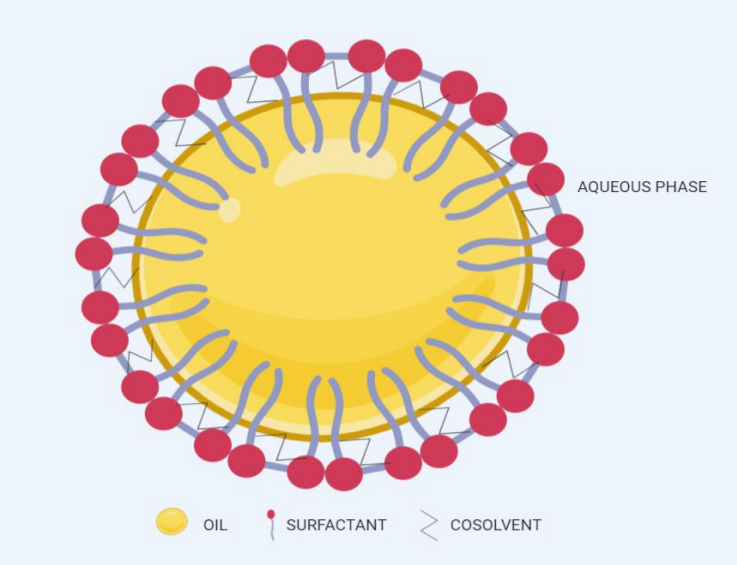

Figure 1. Typical structure of SNEDDSs after aqueous dispersion.

In comparison to other lipid nanocarriers such as nanostructured lipid carriers (NLCs), solid lipid nanoparticles (SLNs), liposomes or solid dispersions, SNEDDSs can be easily scaled up by mixing components with conventional equipment and then including the mixture in solid dosage form, i.e., capsule or tablet. Furthermore, drug-delivery-system-related issues such as a tendency to aggregate during the storage or to release the drug are not relevant to SNEDDSs, as fine dispersion are directly produced in the GI tract [175]. Therefore, SNEDDSs display better pharmaceutical properties for enhancing solubility and oral bioavailability [169,175]. More recently, however, the development of marketed SEDDSs formulations, such as Norvir® (ritonavir), Sandimmune® (cyclosporine), Fortavase® (saquinavir) and Neoral® (cyclosporine), has stimulated a growing interest in the use of SNEDDSs to improve the drug solubility and oral bioavailability.

To date, there are several studies that focus on SNEDDSs use for the oral delivery of lipophilic compounds, yet relatively few that introduce the potential of SNEDDSs for improving the oral delivery of hydrophilic macromolecules.

This paper offers a comprehensive overview of SNEDDSs development, characterization and *in vitro*/*in vivo* evaluation (Figure 2). We focus on SNEDDSs use for the oral delivery of both lipophilic and hydrophilic drugs, with special emphasis on the primary mechanisms by which components used to prepare SNEDDSs can improve the drug solubility, stability, and bioavailability after oral administration. Additionally, we discuss some advancements and promising techniques, such as solidification techniques for transforming liquid SNEDDSs into solid SNEDDSs formulations, as well as supersaturated SNEDDSs to enhance the drug-loading capacity. Lastly, we highlighted the most important challenges ahead related to SNEDDSs formulations.

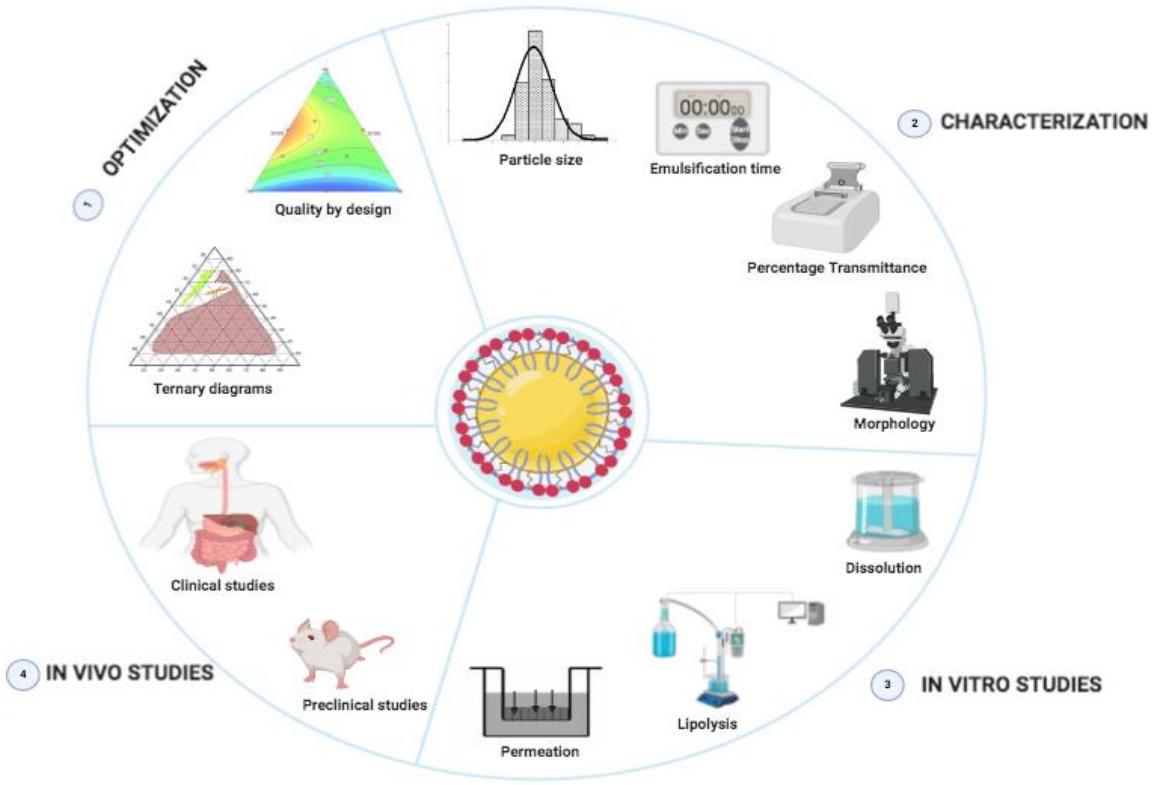

Figure 2. Overview of the design of SNEDDSs formulations.

II. GENERAL COMPONENTS OF SNEDDS AND THEIR ROLE IN FORMULATION PERFORMANCE

To enable differentiation among various lipid-based carriers, Pouton et al. [169] introduced the lipid formulation classification system (LFCS). According to LFCS, SNEDDSs belong to class III compositions, which are composed of oils and water-soluble surface-active agents (surfactants and cosurfactants) and may also include cosolvents. Successful formulation of a SNEDDS requires attention when selecting formulation ingredients. Preformulation studies (e.g., solubility, emulsification efficiency) should be carried out to guide the right selection of SNEDDSs ingredients.

The general components used for SNEDDSs formulation are summarized below.

II.1. OIL PHASE

Generally, medium- and long-chain triglycerides (TG) containing oils presenting varying degrees of saturation are used to formulate SNEDDSs. The oil with maximum ability to solubilize a specific drug is usually selected due to its key influence in both formulation-loading capacity and drug absorption [176]. However, one exception to this general rule was reported by Larsen et al. [177], who demonstrated that SNEDDS containing an oil with the lowest solubilization capacity exhibited the highest drug absorption, indicating that the high solubilization in an oil is not always the best indicator of better *in vivo* performance.

Natural edible oils (i.e., castor oil, soybean oil, coconut oil, etc.) remain the logical and desired oil ingredients, but they exhibit relatively low drug-loading capacity and poor emulsification efficiency [178]. Modified medium-chain triglycerides (MCTs) and long-chain triglycerides (LCTs) are mostly employed to enhance the drug solubility in the formulation and are presented in Table 1.

MCTs are predominantly composed of triglycerides with lipid chain lengths ranged from C_8 to C_{10} (i.e., Capryol® 90, Captex® 300, Labrafac® CC), whereas LCTs consist of TG with lipid chain lengths greater than C_{10} (e.g., Maisine®-35, Lauroglycol® 90, Peceol®) [180]. After oral administration of these lipids, gastric, and pancreatic lipases break down TG into diglyceride, monoglyceride, and fatty acids. Once within the small intestine, those products stimulate the release of endogenous biliary lipids from the gall bladder, including bile salt, lipoprotein, phospholipid, and cholesterol, which enhance the solubilization and absorption ability of the intestinal tract via the formation of micelles (Figure 3) [181–183].

MCTs are preferred because of their better solubilizing ability and self-emulsification capacity [184]. C_{10} remains the only enhancer that has been used clinically in the intestine for oral drug delivery [185]. MCTs can increase the drug transport through the portal vein, but they have a limited capacity to enhance the lymphatic transport of the drugs [186,187]. Conversely, LCTs are directly encapsulated into chylomicrons, before their passage into the lymphatic system, bypassing the hepatic first-pass metabolism [166,187,188]. LCTs increase the transport of drugs through lymph vessel; however, sometimes, they are difficult to emulsify [189]. Thus, a mixture of MCTs and LCTs can be considered to meet optimum properties and improve pharmacokinetics.

Table 1. Commonly used oils, surfactants, and cosolvents.

General Class	Example	Molecular Structure	Commercial Name	Accept ability
OILS				
Medium-chain	Triglycerides of capric/caprylic acids	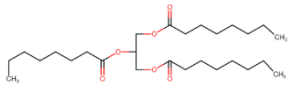	Captex® 300, 350, Labrafac® CC, Crodamol GTCC	P/O/T/ Oc/M
	Di-glycerides of capric/caprylic acids	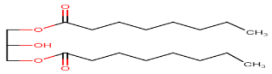	Capmul® MCM, Akoline® MCM	O/T
	Monoglycerides of capric/caprylic acids	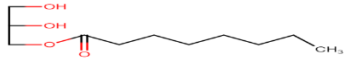	Capryol® 90, Capryol® PGMC, Imwitor® 742	O/T
Long-chain	Glyceryl monooleate	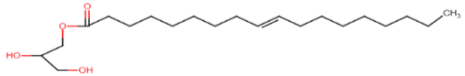	Peceol®, Capmul®-GMO	O/T
	Glyceryl monolinoleate	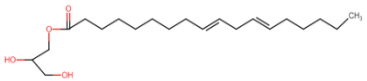	Maisine®-35	O/T
Propylene glycol fatty acid esters	Propylene glycol monocaprylate	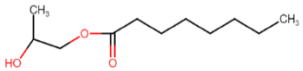	Capmul® PG-8, Sefsol 218	O/T
	Propylene glycol dicaprylate/caprate	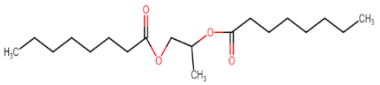	Miglyol® 840, Captex® 200	O/T

	Propylene glycol Monolaurate	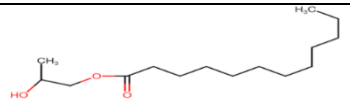	Lauroglycol® 90, Capmul® PG-12, Lauroglycol® FCC	O/T
SURFACTANTS				
Polysorbates	Polysorbate esters	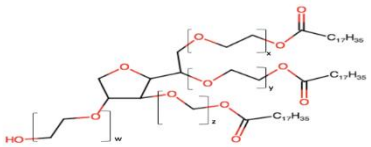	Tween® 20, Tween® 80	P/O/T/ Oc M
Sorban esters	Sorban esters	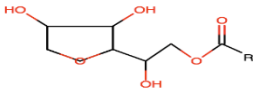	Span® 20,80, Crill® 4	P/O/T/ Oc M
Castor oil esters	Ethoxylated castor oil	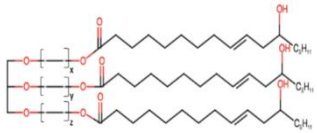	Cremophor®-EL, Etocas® 35 HV	O/T
	Hydrogenated castor oil	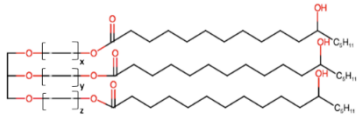	Cremophor® RH40, 60, Croduret® 40	O/T

Polyglycolyzed glycerides	Linoleoyl/Oleoyl Macrogol glycerides	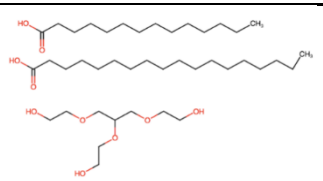	Labrafil® 1944, 2121 CS	O/T
	Caprylocaproyl macrogol glycerides	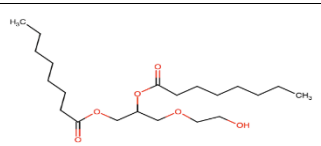	Labrasol®	O/T
COSOLVENTS				
Alcohols	Short chain Alcohols	R-OH	Ethanol, benzyl alcohol	P/T/Oc /M
	Alkane diols		Propylene glycol	P/T/Oc /M
Polyethylene glycols	Polyethylene glycols	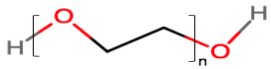	PEG 400, 600	P/T/Oc /M
Esters	Glycerol esters	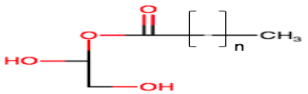	Transcutol®	O/T

M: Mucosal; P: Parenteral; O: Oral; Oc: Ocular; T: Topical. *Adapted from [179].*

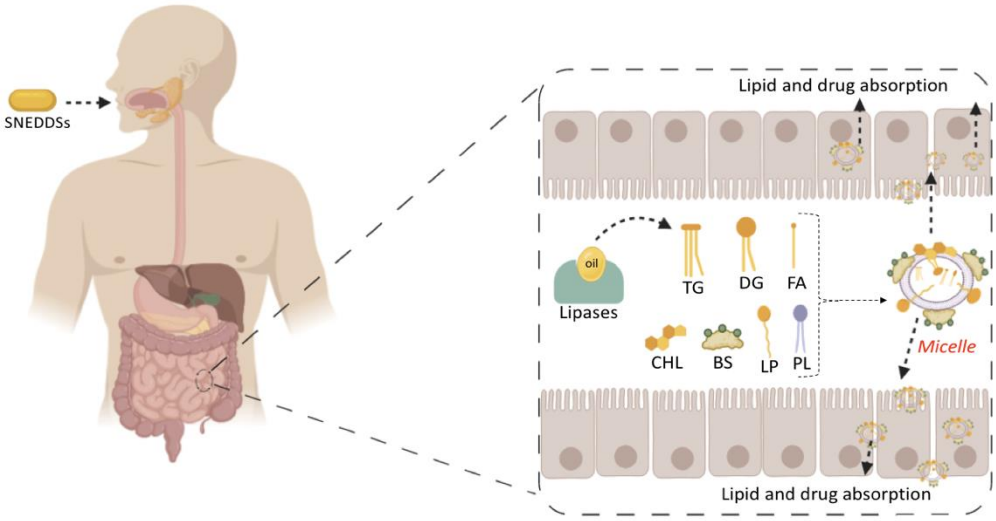

Figure 3. Lipid digestion and drug solubilization process in the small intestine. Abbreviation: triglycerides (TG), diglycerides (DG), monoglycerides (MG), fatty acids (FA), cholesterol (CHL), bile salts (BS), lipoproteins (LP), phospholipids (PL).

II.2. SURFACTANTS

The second obligatory components in SNEDDSs are surfactants. Due to their amphiphilic properties, surfactants are found at the oil–water interface and help in the stabilization of the nanoemulsion by reducing the surface tension. Generally, surfactants are classified based on their charge and hydrophilic-lipophilic balance (HLB) value. Regarding their charge, surfactants are categorized as ionic (anionic, cationic, and zwitterionic) and non-ionic surfactants. As compared with ionic surfactants, non-ionic surfactants are generally used because of their lower toxicity and ability to stabilize emulsion over a wider range of nanoemulsion pH and ionic strength [190]. Regarding their HLB value, surfactants can be classified as lipophilic (HLB < 10) or hydrophilic (HLB > 10) surfactants. The non-ionic surfactants with HLB > 12 are the most recommended, as they enable a spontaneous nanoemulsification with particle sizes less than 200 nm after aqueous dispersion.

The emulsification ability of a surfactant, its HLB value and the maximum solubility of the drug are three important factors to keep in mind when selecting surfactant in SNEDDSs. Furthermore, the concentration of surfactant has been demonstrated to affect the emulsion particle size. Increasing the amount of surfactant can reduce the emulsion particle size due to the surface tension lowering property of the surfactant at the oil and water interface that reduces the free energy for emulsification [176]. However, in some cases, an increase in surfactant amount results in higher particle size, due to the excess penetration of water into the lipid droplet which cause massive disruption of the oil–water interfacial and relaxation of high polydisperse nanoemulsion droplets [191,192]. Other than fine globule formation, many non-ionic surfactants, such Tween® 80 and Cremophor® EL, possess the ability to increase membrane fluidity [193] and to inhibit efflux transporters (e.g., P-gp, BCRP) [194,195], which are contributing factors in enhancing the drug bioavailability.

The surfactant acceptability for the oral delivery and its regulatory status (e.g., GRAS—generally regarded as safe) should also be taken into consideration during the selection. Table 1 presents common non-ionic surfactants along with their acceptability. It should be noted that surfactant molecules are not always innocuous, they can exhibit structure or concentration-dependent toxicity [179]. Some of them might cause irritation to the GI epithelium following oral administration. Thus, the amount of surfactant in SNEDDSs must be maintained at a low level as much as possible.

II.3. COSURFACTANTS/COSOLVENTS

A single surfactant is rarely able to provide low interfacial tension; therefore, the addition of another surfactant (cosurfactant) or cosolvent usually is necessary. They can synergically cooperate with surfactants to enhance the drug solubility and surfactant dispersibility in the oil, thus promoting nanoemulsion stability and homogeneity [196]. The use cosurfactants or cosolvents can reduce the local irritancy of the surfactant and dose variability of the formulation by improving interfacial fluidity [197]. The weight ratio of surfactant/cosurfactant or cosolvent has also been reported to have an important impact on size distribution and the extent of nanoemulsion area [198,199]. Commonly used cosolvents include propylene glycol, ethanol, poly (ethylene glycol) (PEG) and other newer cosolvents, such as Transcutol® HP [200,201], which are presented in Table 1.

However, while cosolvents can improve drug solubilization in the formulation, their amount should be kept at minimal level because of their polarity. Cosolvent readily migrate toward the water phase following aqueous dispersion, leading to drug precipitation [202]. Furthermore, alcohols and other volatile cosolvents can evaporate into shells of capsules, resulting in drug precipitation [203].

In the SNEDDS formulation, apart from previously presented components, other ingredients such antioxidants, viscosity enhancers and ingredients for modified drug release can be used [204–207].

III. OPTIMIZATION OF SNEDDS FORMULATIONS

After selecting potential components of SNEDDSs, optimization studies are performed to obtain the optimum amounts of oily phase, surfactants, and cosolvents that might yield spontaneous nanoemulsion [208]. Ternary phase diagrams are largely employed to identify the emulsification area for selected components. In ternary diagrams, the ratio of one component varies while the concentrations of the other two are fixed. The emulsification area is identified visually or by measuring the particle size of the emulsion/nanoemulsion resulting after aqueous dispersion. All the SNEDDSs composition from the emulsification area yield spontaneous nanoemulsions, with globule sizes less than 200 nm after aqueous dispersion [209]. In some cases, the drugs can influence the emulsification region. Date et al. [210] demonstrated that cefpodoxime proxetil could significantly reduce the emulsification region in the ternary phase diagram.

Khattab et al. [211] developed SNEDDSs to enhance aliskiren hemi-fumarate oral absorption. Capryol® 90 (oily phase), Cremophor® RH and Tween® 20 (surfactants) and Transcutol® HP (cosurfactant) were selected from the solubility study. The formulations were further optimized using a pseudo-ternary phase diagram in which an area of emulsification was identified (Figure 4a). The region of nanoemulsification was defined as the region where homogenous and clear systems were obtained after aqueous dispersion. A large nanoemulsion area indicates better emulsification efficiency of the surfactant toward oil. For Tween® 20/Transcutol® HP systems, they showed that increasing the Tween® 20 to Transcutol® HP ratio increased the nanoemulsion area, which was explained by the increase in surfactant adsorption at the emulsion interface leading to decreases in surface tension and formulation droplet sizes. For Cremophor® RH 40/Transcutol® HP systems, the opposite was noted. They observed that increasing the Cremophor® RH 40 to Transcutol® HP ratio resulted in a notable decrease in the nanoemulsion region. The fact was explained by the high viscosity of Cremophor® RH 40, preventing a rapid breakage of the oil–water interface, and thus decreasing the area of nanoemulsion. The authors concluded that Tween® 20 could better emulsify Capryol® 90 compared to Cremophor® RH 40. The final SNEDDS consisted of Capryol® 90 (oil), Tween® 20 (surfactant), Transcutol® HP (cosolvent) and improved the oral bioavailability of aliskiren hemi-fumarate in rats compared to drug solution.

In addition to a ternary phase diagram, SNEDDSs optimization can also be done with numerous types of statistical experimental design, such as Box–Benkhen design [212–214], central composite design [215], simplex lattice design [216], full-factorial design [217], and D-optimal design [218].

Box–Benkhen design is a response surface design based on three levels (−1, 0, +1) which provides an appropriate model for the quadratic behavior of factors [219]. The number of runs (N) needed to develop Box–Benkhen design is given as $N = 2k(k - 1) + C_0$, (where k and C_0 are the numbers of independent variables and central points, respectively). Garg et al. [220] formulated SNEDDSs of polypeptide-k that were optimized by Box–Benkhen design (Figure 4b). Seventeen runs were performed to study the impact of SNEDDS factors on the selected responses (dependent variables). From the study, a decrease of size (Y1) was observed at a higher level of surfactant (Tween® 80, X2), while size increased at higher levels of oil (oleoyl polyoxyl-6 glycerides, X1) and cosolvent (diethylene glycol monoethyl ether, X3). The drug loading (Y3) increased with the increases in X1, X2, and X3 ratios, as shown in Figure 4b. Furthermore, more negative values of

zeta potential (Y4) were observed when the concentration of oil (oleoyl polyoxyl-6 glycerides, X1) increased. The optimized SNEDDS showed values of droplet size (Y1), 32nm, drug loading (Y3), 73%, and zeta potential (Y4), −15.6 mV, and enhanced the oral bioavailability of polypeptide-k in rats.

Central composite designs are the most largely employed response surface designs. They are fractional factorial or factorial designs containing center points, along with a group of axial points which enable the estimations of curvature [221]. The experimental design must have at least three levels of each factor another to establish the coefficients of a polynomial with quadratic terms. A central composite design requires $2^k + 2k + n_c$ experiments, where k and n_c are the numbers of factors and central points, respectively.

Panigrahi et al. [215] optimized by central composite design bosentan loaded SNEDDSs composed of Capmul® and Labrasol® (surfactants, X1), MCM (oil, X2), and PEG 600 (cosolvent, X3). Preliminary Taguchi design studies revealed surfactant and oil as important factors in SNEDDSs that were further screened and optimized by central composite design. For particle size (Y1), it was observed that at a medium to high concentration of surfactant, Y1 increased only when the amount of oil was reduced. Furthermore, particle size (Y1) was increasing with the gradient declination of surfactant amount. For emulsification time (Y2), it was observed that the gradient increase in surfactant amount reduced Y2. It also signified that an increase in oil amount will increase the Y2. In the case of percentage drug release in 15 min (Y3), it was observed that at a low level of oil, Y3 was high only when the amount of surfactant was higher. Y3 was decreasing on the gradient declination of surfactant amount (Figure 4c). The optimized SNEDDS revealed values of particle size (Y1), emulsification time (Y2) and percentage drug release in 15 min(Y3) as 62.5 nm, 12 s, and 98.5%, respectively, and improved bosentan oral bioavailability as compared to pure drug in rabbits.

Simplex lattice design is defined as a space-filling design which creates a triangular grid of experiments (runs). In this design, the fractions of excipients that make up any composition must add to unity; hence, a regular simplex represents factor space. Mixture points are evaluated in accordance with a lattice arrangement, and a simplified polynomial function is used to represent dependent variables [222]. This function represents how the components affect the response. This design offers an effective tool for investigating the properties of blends over wide ranges of composition, especially for mixtures of four or more components.

With the aim of improving the dissolution rate of pentagamavunon, Astuti et al. designed SNEDDSs formulations that were optimized using simplex lattice design. The factors were the concentrations of oil (oleic acid, X1), surfactants (Tween® 20 and Labrasol®, X2), and cosolvent (PEG 400, X3). Particle size (Y1) increased when the amounts of oil (X1), surfactants (X2), and cosolvent (X3) increased (Figure 4d). Moreover, oil concentration had the highest effect on particle size, while the effects of surfactants and cosolvent were more limited. For the drug solubility in the formulations (Y3), the main effect shows a positive coefficient, following the order: cosolvent >surfactants> oil. In addition, the authors showed that the most significant antagonistic interactive effect was X1X2X3; thus, the effect of the three factors together was less than the sum of the three factors taken independently of each other, while the most significant synergistic interaction effect

was X1X2. The optimum SNEDDSs consists of 18.6% oleic acid, 51.4% Tween® 20: Labrasol® (1:1) and 30% PEG 400 and showed a size of 75 nm (Y1) and drug solubility of 31.80 mg/mL (Y3) [223].

Full-factorial design is composed of two or more independent variables interacting each other at different levels. This design is used to study the main effects and interactions of independent variables on dependent variables. The number of runs needed to study n independent variables at 2-levels is 2^n. The full-factorial design is particularly useful in the early stage of the experimental work, especially when the number of independent variables is ≤4 [224].

Karamanidou et al. [225] formulated SNEDDSs for the successful oral delivery of insulin. The authors applied a 3^3 full-factorial design for selecting the quantities of the components (oil, surfactant and cosurfactant/cosolvent) to be used for each composition. The optimum SNEDDSs were composed of Lauroglycol® FCC as the oily phase, Cremophor® EL as the surfactant, and Transcutol® P or Labrafil® M 1944 CS as the cosurfactant. The systems were characterized by average droplet sizes of 30-45 nm and percentages of insulin loading between 0.27 and 1.12%. They demonstrated that insulin-phospholipid (dimyristoyl phosphatidylglycerol) encapsulation into SNEDDSs improved enzymatic stability of the formulations and a sustained release of insulin from the formulations was observed. The SNEDDSs were innocuous up to concentrations of 2 mg/mL and improved insulin permeability.

D-optimal design is among designs generated by a computer algorithm. This design should be applied when classical experimental designs cannot be used. Unlike classical experimental designs, D-optimal design usually contains no orthogonal matrices, and effect estimates are correlated [226]. D-optimal design is always applicable regardless of the type of mathematical model used or the specified objective of the experiment. It is a straight response surface design based on a selected optimality criterion and the best fitting model (i.e., first order plus interaction, cubic, full quadratic, etc.) [227,228].

Ujilestari et al. formulated and characterized SNEDDSs of cardamom (Amomum compactum) essential oil. The SNEDDSs formulations were optimized by D-optimal design by varying amounts of coconut oil (X1), Tween® 80 (X2) and PEG 400 (X3). Emulsification time (Y1) and transmittance percentage (Y2) were chosen as response variable for the optimization. They observed a significant ($p < 0.05$) relationship between the factors (X1, X2, X3) and the emulsification time (Y1), while no significant ($p > 0.05$) relationship was observed between the factors and the transmittance percentage (Y2) (Figure 4e). The optimized SNEDDS was composed of 10% cardamom essential oil, 10% coconut oil (X1), 65.7% Tween® 80 (X2), and 14.3% PEG 400 (X3). The SNEDDS exhibited an emulsification time of 46.38 s, 99.37% of transmittance percentage, a viscosity of 187.5 mPa, a particle size of 13.97 nm, and zeta potentials ranging from 28.8 to 45.9 mV. The studies demonstrated that the SNEDDSs had enhanced water solubility and stability of cardamom essential oil [218].

Compared with ternary phase diagrams, the key advantage of these statistical experimental designs is that they can minimize expenditure in terms of time, resources, and developmental efforts.

Moreover, the simultaneous influence of factors (oil, surfactant and cosolvent) on the SNEDDS' characteristics (i.e., droplet size, PDI, time of emulsification, etc.) can be studied.

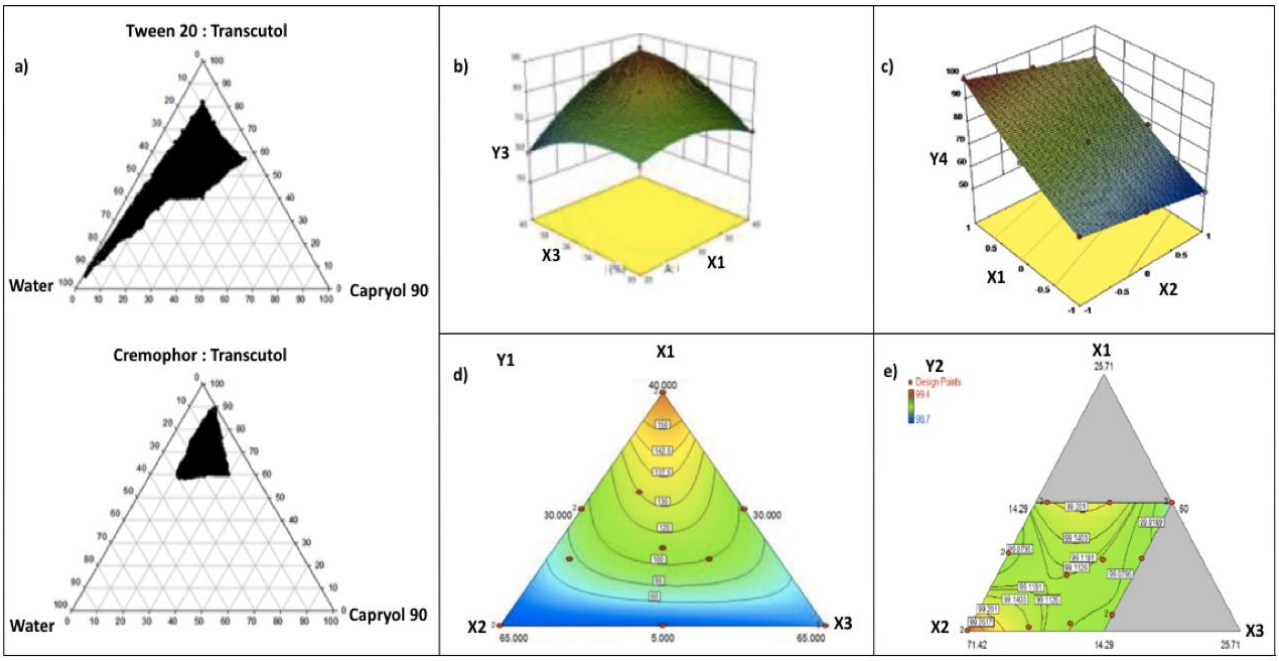

Figure 4. Optimization of SNEDDSs (**a**) ternary diagrams from [211], (**b**) Box–Benkhen design from [220]. Drug: polypeptide-k, Factors Oleoyl polyoxyl-6 glycerides (oil, X1), Tween® 80 (surfactant, X2), diethylene glycol monoethyl ether (cosolvent, X3); responses: percentage drug loading (Y3), (**c**) central composite design from [215]. Drug: Bosentan, Factors: Capmul® and Labrasol® (surfactants, X1), MCM (oil, X2), and PEG 600 (cosolvent, X3); responses: percentage drug release in 15 min (Y4), (**d**) simplex lattice design from [223]. Drug: pentagamavunon-0, Factors: oil (oleic acid, X1), surfactants (Tween® 20 and Labrasol®, X2), cosolvent (PEG 400, X3); response: particle size (Y1) **(e)** D-optimal design from [218]. Drug: cardamom essential oil, Factors: coconut oil (X1), Tween® 80 (X2) and PEG 400 (X3); response: transmittance percentage (Y2).

IV. PHYSICO-CHEMICAL CHARACTERIZATION OF SNEDDSS FORMULATION

It is always important to evaluate the final SNEDDSs for several parameters. The general techniques and methods that have been employed for SNEDDSs characterization are summarized below (Table 2).

Table 2. The general methods and models used to evaluate SNEDDSs.

	Method/Model	Information Provided
Physico-chemical characterization	DLS	Droplet size, PDI, thermodynamic stability
	Electrophoretic velocimetry	Zeta potential
	Spectrophotometry	Transmittance percentage, cloud point, thermodynamic stability
	TEM, SEM	Morphology, droplet size
	Viscosimeter	Viscosity, thermodynamic stability
	Dissolution apparatus	Drug dissolution, emulsification time
Preclinical in vitro and ex vivo evaluation	pH-stat unit	Formulation digestion, drug distribution across aqueous/oil phase
	PAMPA	Permeation across intestinal barrier
	SPIP	Permeation across intestinal barrier
	IRP	Permeation across intestinal barrier
	CaCO-2	Permeation across intestinal barrier, cytotoxicity
Preclinical In vivo evaluation	Animals	Pharmacokinetic, toxicity, pharmacodynamic
Clinical trials	Humans	Pharmacokinetic, bioequivalence toxicity, pharmacodynamic

PAMPA: parallel artificial membrane permeability assay, SPIP: single-pass intestinal perfusion, IRP: intestinal recirculating perfusion.

IV.1. PARTICLE SIZE

The droplet size of a SNEDDS is often measured after aqueous dispersion via dynamic light scattering (DLS) [229]. The availability of DLS made it a popular technique for droplet size determination; however, the measure can be biased in the presence of large aggregates which scatter more than the nanoparticles, especially at low scattering angles [230,231]. To overcome this limitation, fluorescence correlation spectroscopy (FCS) and Taylor dispersion analysis (TDA) can be used as complementary techniques. In FCS, the fluorescence fluctuations from a fluorescent probe which diffuses in and out of a tiny observation volume is measured [232]. Its high sensitivity allows it to work in dilute solutions; however, FCS applications for larger-sized particles (i.e., emulsion) are still limited, probably owing to the difficulty involved in measuring particle sizes larger than 1/10th of the observation volume's size [233,234]. Conversely, as a microcapillary-based flow method, TDA allows the characterization of particle size and the stability of small compounds in solution, even for complex composition [235]. TDA quantifies the broadening of the peaks of a specific molecule plug in a Poiseuille laminar flow to determine the molecular diffusion coefficient and subsequently, the hydrodynamic radius [236]. TDA is advantageous as it is less affected by the presence of large-particle aggregates or the sample viscosity; hence, the solutions can be run without any filtration or dilution [237]. However, it usually requires a lipophilic marker which travels in the droplet or micelle [238,239]. The Taylorgrams are plotted as optical

density versus time, and the hydrodynamic radius are generated from the molecular diffusion coefficient [235,236]. Chamieh et al. [237] used TDA coupled with a fluorescence detector for the particle size characterization of Labrasol®. The particle size characterization was performed at two different temperatures (25 °C and 37 °C) and increasing concentration (from 1 to 70 $g \cdot L^{-1}$). The authors showed that when combined, DLS and TDA allowed determining the proportion and coacervates size in the dispersion as well as the PDI of the sample.

Size characterization is one of the most essential examinations for SNEDDSs development since the size of the particles can directedly affect not only the *in vitro* tested characteristics (i.e., dissolution, stability) but also the *in vivo* performance of a SNEDDS. (i.e., drug absorption) [240,241]. The literature reported that smaller particle size has a positive effect on the oral bioavailability of a drug encapsulated into SNEDDSs [242,243]. The plausible explanation for the improved oral bioavailability could be that the smaller the particle size, the larger interfacial area, which improves the drug solubilization and permeability. However, it is not a general rule that a smaller globule size of dispersion will always lead to higher oral absorption. Yap et al. [244] compared the oral bioavailability of tocotrienols from two SEDDSs, the first one yields a large emulsion that readily lipolyzed (E1), while the second produced a smaller emulsion with negligible digestion (E2).

Both E1 and E2 showed the same oral bioavailability even though E2 yield dispersion with a smaller particle size. Thus, it appears that droplet size taken together with other SNEDDSs parameters (i.e., susceptibility to lipolysis) have direct impact on the oral absorption of a compound encapsulated into SNEDDSs. However, despite a lack of consistent correlation between emulsion droplet size and oral absorption, generating a smaller dispersion following aqueous dilution or lipolysis is generally necessary since, it is a known fact that these formulations can minimized dose variability after oral ingestion [245–247].

IV.2. ZETA POTENTIAL

The zeta potential provides information about the colloidal stability. It is estimated by measuring the electrophoretic mobility of the droplets. The presence of a high zeta potential value (±40 mV) exhibits repulsive electrostatic forces, which reduces the possibility of particle aggregation [248]. The nanoparticle charge can affect the oral absorption of the drug encapsulated into SNEDDSs. Charge-dependent interaction with mucus and cell membrane barriers with respect to absorption enhancement has been reported [249]. The mucus thin layer protects the GI epithelium from xenobiotics and pathogens, but it also acts as a strong barrier for nanoparticles [250]. The mucus gel exhibits negatively charged substructure made of sulfonic and sialic acid, which hinders positively charged nanoparticles from diffusing into deeper mucus regions owing to electrostatic interactions. Accordingly, negatively charged nanoparticles can more easily permeate the mucus gel compared to positively charged nanoparticles. However, the apical side of the intestinal epithelial cells exhibits negative charges related to the mucosal solution in the lumen. Accordingly, nanoparticles with positive charges can interact with the negative charges of the intestinal mucosal and enhance the cellular uptake of the encapsulated molecule [251,252]. In view of this, Salimi et al. [253] developed SEDDSs that can change their zeta potential via a flip-flop mechanism. They synthesized and incorporated into SEDDSs a conjugate compound that carries both an amino

group and a phosphate group. Particles exhibited both a negative value of zeta potential during the mucus transport and a positive zeta potential value after enzymatic degradation of the phosphate ester group, resulting in high cell association and uptake.

IV.3. EMULSIFICATION TIME MEASUREMENT

The emulsification time can be measured on a USP II dissolution apparatus [184]. The formulation is added to a basket containing water and is maintained at 37 °C under agitation (100 rpm). The emulsification time is recorded as the time required to obtain a clear dispersion [254]. The emulsification time is dependent on the oil/surfactant concentration. A spontaneous emulsification is observed with surfactant concentrations less than 60% (*w/w*) because of the quick release of oil droplets by water penetration into the oil–water interface. However, above the surfactant concentration of 60% (*w/w*), there is an increase in the time of emulsification due to the high viscosity of the surfactants [183]. A rapid emulsification can contribute to a quick drug release and a subsequently rapid onset of action [255,256].

IV.4. TRANSMITTANCE PERCENTAGE MEASUREMENT

The transmittance percentage is the measurement of optical clarity of the diluted SNEDDSs with water. The transmittance usually described in percentage is the measurement of how much light passes through a sample. It can be assessed by spectroscopy using water as a blank [257,258]. The increase in transmittance can be used to monitor the self-emulsification rate, and the final transmittance percentage is usually correlated with the nanoparticle droplet size [259,260].

IV.5. MORPHOLOGY

The morphology of the nanoemulsion droplets can be determined by scanning electron microscopy (SEM) and transmission electron microscopy (TEM). SEM is based on back-scattered electrons, which informs the droplet morphology. In TEM, electrons are transported through the dispersion to generate the morphology of the droplets and differentiate several chemical molecules with the respect to their density. Recently, cryo-SEM and cryo-TEM have been developed to study the real morphological information of nanoparticles [236].

IV.6. VISCOSITY MEASUREMENT

Generally liquid SNEDDSs formulations are filled into capsules. Low-viscosity formulations face leakage concerns, whereas overly viscous SNEDDSs are hardly filled into capsules due to flowability problems [261]. Generally, a viscosity ranging between 0.1–1.0 Pa at 25 °C implies that the formulated SNEDDSs can easily be filled into capsules by liquid filling equipment [262]. The viscosity of SNEDDSs is determined with viscometers.

IV.7. CLOUD POINT MEASUREMENT

The cloud point is known as the temperature at which the nano/emulsion is broken. The cloud point is determined to investigate the stability of SNEDDSs in the Gl tract. Formulations are diluted with distilled water and placed in a water bath with gradually increasing temperature.

Furthermore, spectrophotometric analyses are carried out to determine the transmittance percentage of the sample. At the cloud point, the decrease in dispersion transmittance percentage from the zero point is noted [263,264]. The cloud point of SNEDDSs should be more than 37 °C; otherwise, absorption of the drug can be interrupted, as cloudy emulsion affects the absorption by the dehydration of components used in SNEDDSs formulations [265].

IV.8. THERMODYNAMIC STABILITY STUDIES

The thermodynamic stability is an indicator of the kinetic stability of a dispersion and is generally used to study the chemical reactions occurring between the components of a dispersion. Poor stability of dispersion can lead to precipitation or phase separation, which could affect drug absorption as well as therapeutic efficacy [266,267]. Generally, centrifugation, heating-cooling, and freeze-thaw cycles are carried out for these studies. Various aspects such as phase separation, turbidity, and particle size are observed during these experiments. Subsequently, stable formulations are selected for further evaluation.

V. IN VITRO ASSESSMENT OF SNEDDSS FORMULATIONS

The literature reports the potential of SNEDDSs in improving the oral bioavailability of several compounds. It is a known fact that the performance of any SNEDDS depends on a complex interplay between physiological processes in the GI tract. Following oral ingestion, the digestion of SNEDDSs is initiated in the stomach, where digestible excipients (oils and surfactants) are lysed by the action of gastric lipase at the interface. Gastric digestion releases approximatively 15% of fatty acids from lipids. Within the small intestine, pancreatic lipase together with its co-lipase complete the breakdown of dietary glycerides to di-glycerides, monoglycerides, and fatty acids. The presence of exogenous lipids in the small intestine also stimulates secretion of endogenous biliary lipids, including bile salt, phospholipid, and cholesterol from the gall bladder. In the presence of an elevated bile salts concentration, lipid digestion products are subsequently incorporated into a series of colloidal structures, including multilamellar/unilamellar vesicles and bile salt phospholipid mixed micelles [181–183]. Together, these vesicles significantly increased the solubilization ability of the small intestine for both lipid digestion products and drugs before their absorption.

Although this knowledge is useful, the prediction of the *in vivo* performance of a SNEDDS remains challenging. For this purpose, a series of *in vitro* models or tests have been developed to simulate main processes related to the absorption of drugs. These processes are usually evaluated in various *in vitro* models testing dissolution, digestion, and permeation. The in *vitro* models employed vary depending on their physiological relevance and complexity, ranging from single unit to multi-compartmental models. More elaborate *in vitro* models evaluate dissolution, digestion, and permeation simultaneously [268,269]. Different *in vitro* models that have been used to evaluate SNEDDSs are described below.

V.1. IN VITRO DISSOLUTION

The *in vitro* dissolution test is routinely employed as an indicator of the likely GI drug dissolution and, consequently, as a tool to predict the rate and extent of absorption for poorly water-soluble drugs. The rate of drug dissolution relies on many factors, including the degree of wetting, the drug solubility in the intestinal contents, medium viscosity, emulsion droplet size and the volume of the intestinal contents [270]. The pH has also a key impact on drug dissolution characteristic. Generally, simulated gastric fluid without enzymes (pH 1.2) and phosphate buffer (pH 6.8–7.4) have been used to test drug dissolution. In general, the *in vitro* dissolution from a SNEDDS formulation is faster compared with native drug due to the reduction in particle size and the increase in surface area [255,256,271].

Eleftheriadis et al. [272] studied the dissolution behavior of SNEDDSs loaded with fenofibrate or itraconazole in comparison with the pure drugs. Dissolution studies were performed using a USP dissolution apparatus II in 900 mL of simulated intestinal fluid at 75 rpm paddle rotation and 37 °C. The results showed that the incorporation of these molecules in SNEDDSs significantly enhanced their dissolution rate. Regarding the pure drugs, only 6.6% of fenofibrate and 1.6% of itraconazole were dissolved in 45 min. Almost 100% of the active contents were dissolved from the SNEDDSs formulations in the same period ($p > 0.05$). At the end of the experiment, the total amounts of pure fenofibrate and itraconazole released were 11% and 4%, respectively. In another

example, Abouhussein et al. [273] investigated the *in vitro* dissolution of rivaroxaban loaded SNEDDSs in comparison with the drug powder. The standard USP II paddle method was used at 37 ± 0.5 °C, and 900 mL of sodium lauryl sulfate (0.6%) in acetate buffer pH 4.5 was employed as the dissolution medium. From the studies, it was found that the two developed SNEDDSs provided significantly higher rates of release (100% and 78% in 5 min, respectively) compared to pure raw drug powder (15%).

However, the use of simple aqueous media to test the dissolution behaviors of poorly water-soluble drugs is often limited by two factors: 1) the poor solubility of the drug (and, therefore, the difficulty to maintain sink conditions), which, when coupled with analytical sensitivity issues such as drug binding to filters can make reproducible *in vitro* dissolution evaluation difficult, and 2) the lack of similarities between the simple aqueous media and the likely GI tract environment, which reduces the *in vivo* prediction. In attempt of improving the accuracy of *in vivo* prediction through *in vitro* dissolution test, many studies have developed and used biorelevant media that more accurately reflect the solubilization capacity of the GI tract [274–277]. The compositions of these biorelevant media have been inspired mainly by the likely concentration of endogenous phospholipids and bile salts in the stomach and the proximal part of the small intestine [278,279].

Dressman and al. [280] have studied the dissolution behavior of many lipophilic drugs using various dissolution media [281]. Consistent correlations were found for nonionizable drugs between the type of media and the dissolution profiles of the drugs. For example, the percentage release of danazol in fed state intestinal conditions (FeSSIF media) was three-fold higher compared to fasted state intestinal media (FaSSIF). For molecules with appreciable ionization over the physiological pH range, the situation is complicated by the impact of both ionization and media on the drug solubility.

It was observed for a weak base such as ketoconazole (pKa 6.5, 2.9) that the ionized species at pH 1.2 was much soluble than the unionized at pH 6.5. Furthermore, the percentage of drug dissolved in simulated fasted gastric fluid (FaSSGF) was significantly higher compared to the simulated fasted intestinal fluid (FaSSIF). However, the improved solubilizing capacity of the fed intestine is, at least in part, sufficient to overcome the poor intrinsic solubility of the unionized ketoconazole and the amount of ketoconazole dissolved under fasted gastric state is not notably different from that dissolved under simulated fed state intestinal [282,283]. Memvanga and Préat [203] developed SEDDSs composed of groundnut or sesame oil, Maisine® 35-1, Tween® 80 or Cremophor® EL, and absolute ethanol for the oral delivery of β-Arteether. The *in vitro* dissolution test using gastric (HCl 0.1 N) and intestinal (phosphate buffer pH 6.8) media showed an increase in drug solubilization over time (Figure 5a). Mendes et al. [284] evaluated the dissolution of hydrochlorothiazide from two SNEDDSs and pure drug. Studies were performed using USP apparatus III containing 200 mL of FaSSGF pH 1.6 or FaSSIF pH 6.5, both at 37 ± 0.5 °C as dissolution media. In the first step of the assay, the dissolution was performed in FaSSGF (20 dips/min); subsequently, the dissolution medium was replaced with FaSSIF for more 180 min (15 dips/min). They demonstrated that both SNEDDSs allowed a faster release rate of hydrochlorothiazide when compared to the free drug. An *in vitro* release of 27.4% was achieved after 30 min for the hydrochlorothiazide powder, while release rates of 81.9 and 75.6% were achieved by SNEDDS-1 and SNEDDS-2, respectively.

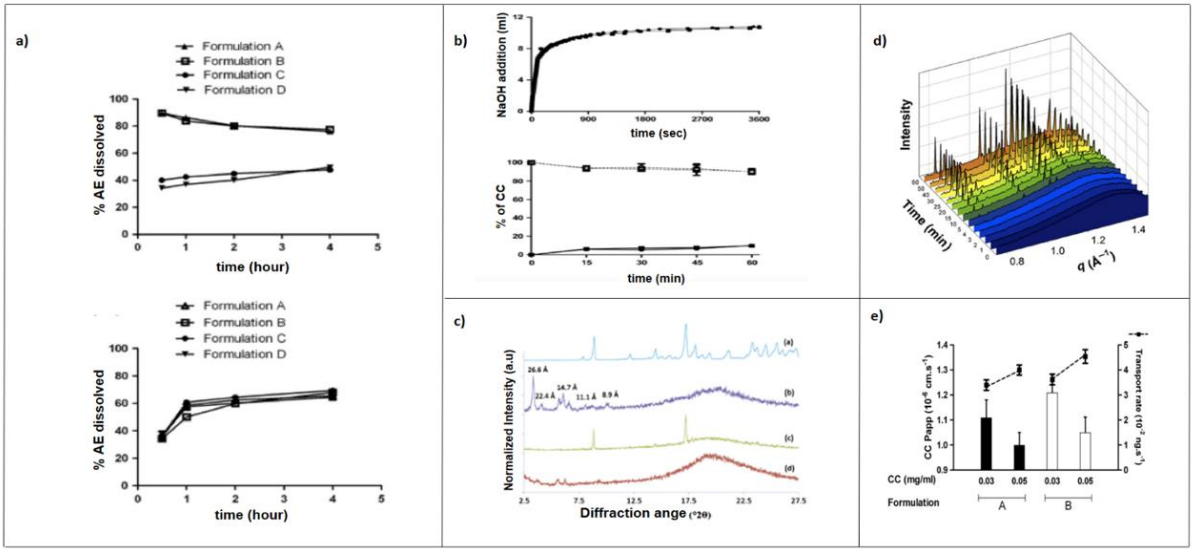

Figure 5. (**a**) Solubilization and stability of beta-Arteether in 0.1 N HCl (pH = 1) (top) and in phosphate buffer (pH = 6.8) (bottom) as a function of time. Each point represents the mean ± SD (n = 3). From [203]. (**b**) Quantity of 0.2 M NaOH added to titrate the fatty acids that were released during lipid digestion (top) and the distribution profile of curcumin in the aqueous phase (open shapes and dotted lines) and in the pellet phase (filled shapes and lines) as a function of lipolysis time (bottom). From [202]. (**c**) The X-ray powder diffraction patterns of (a) crystalline, (b) CC pellet, (c) blank pellet spiked with CC and (d) blank pellet from the lipolysis of a SNEDDS formulation. The numbers over the peaks indicate d-spacings. From [202]. (**d**) In situ SAXS profiles during the lipolysis of the MC-SNEDDS formulation containing fenofibrate. Drug precipitation was evident at 4 min after the addition of pancreatic lipase, with the characteristic diffraction peaks for fenofibrate. From *[285]*. (**e**) Apparent permeability and transport rate of curcumin-loaded SEDDS across Caco-2 monolayers with two different drug concentrations (0.03 and 0.05 mg/mL). From [202].

V.2. *IN VITRO* LIPOLYSIS

In vitro lipolysis has increasingly been used to assess the likely impact of digestion by gastric/pancreatic enzymes and the dispersion in intestinal fluids on lipid-based formulations, including SEDDSs [235,286,287]. The most frequently employed *in vitro* lipolysis model to evaluate SNEDDSs is the pH-stat lipolysis model [288–290]. The experimental setup generally consists of different equipment used to mimic the intestinal environment, as depicted in Figure 6. The *in vitro* lipolysis is generally carried out in a thermo-controlled reaction vessel containing a lipolysis medium representative of either fed or fasted GI fluid, formulated with an accurate pH buffer capacity along with bile salt, phospholipids, and NaCl.

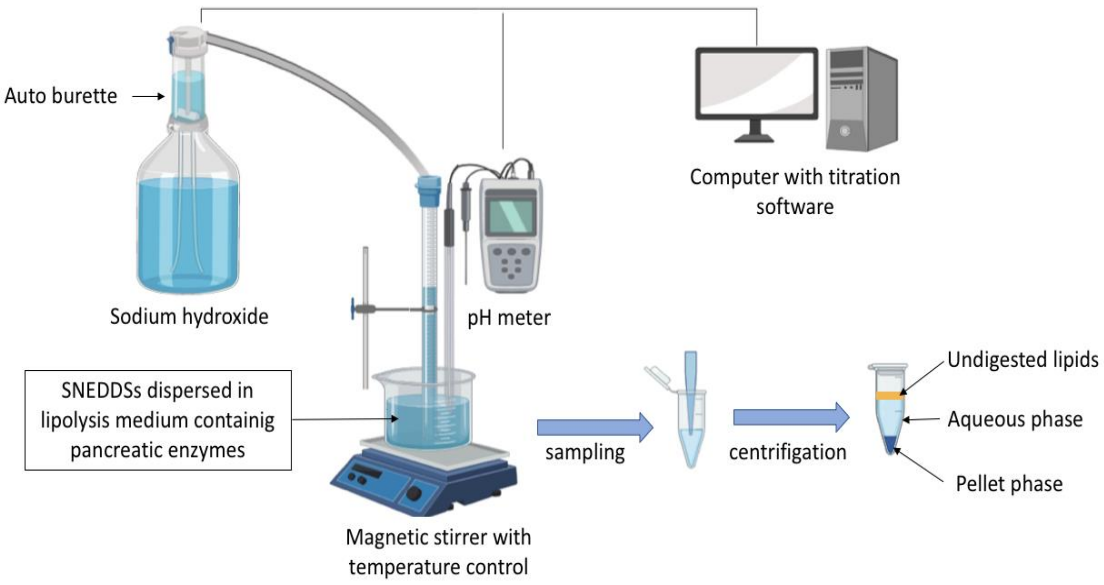

Figure 6. pH-stat lipolysis model for the *in vitro* assessment of lipid-based drug-delivery systems.

The digestion is triggered by addition of pancreatin extract containing lipases and other pancreatic enzymes (amylase, protease, and ribonuclease). These enzymes hydrolyze TG and other digestible SNEDDSs components (i.e., surfactants), which subsequently release free fatty acids. The fatty acids released are automatically titrated with sodium hydroxide to neutralize the drop in pH caused by the enzymatic lipolysis. The addition of calcium is important to form insoluble soaps with free fatty acids and thereby removes them from the system. Free fatty acids could migrate at the oil–water interface and inhibit enzyme activity [291]. Assuming that a high *in vitro* drug solubilization equals a high oral absorption, the percentage of drug dissolved in the aqueous phase during the *in vitro* lipolysis has been related to high oral drug absorption [268]. With this relationship, many studies have described rank-order correlation between the patterns of drug solubilization obtained on *in vitro* lipolysis and the plasma profiles after oral administration [292–295]. Thus, SNEDDSs that show evidence of drug precipitation during the digestion appear more likely to result in poorer *in vivo* drug exposure [296]. The additional solid-state characterization of the precipitates (nature/form) formed during SNEDDSs lipolysis may therefore contribute to the improvement of quality of data interpretation. A drug precipitation in amorphous form (or molecular dispersed state) might be expected to lead to rapid *in vivo* drug re-dissolution in comparation to the precipitation in the crystalline form [297–299]. Several techniques can be used to study the solid-state of the precipitates, including UV imaging, X-ray diffraction and in-line Raman spectroscopy [300–303].

Moreover, advances in synchrotron small-angle x-ray scattering (sSAXS) are providing greater details of the real-time structural configuration and colloidal phase transitions of lipolyzed formulations [304,305]. sSAXS has been used to control the structural evolution of colloidal structures on a shorter time scale and drug behaviors (solubilization and/or precipitation) on a longer time scale during lipolysis in real time [306]. This technique avoids the need for sample

inhibition, time point collections, extended storage and sample retrieval for test, further improving the accuracy and efficiency of the process [236].

Memvanga et al. [202] developed SEDDSs to increase the oral bioavailability of curcumin. Results from the *in vitro* lipolysis showed that 90–95% of curcumin remained solubilized (Figure 5b), and X-ray powder diffraction analysis of the pellets revealed that 5–10% of the drug precipitated in amorphous form (Figure 5c). Christophersen et al. [295] evaluated the ability of a GI *in vitro* digestion model to predict the *in vivo* performance of two SNEDDSs formulations and a commercial tablet of cinnarizine, both in the fasted and fed states in dogs. A SNEDDS (sesame oil, oleic acid, Brij 97, Cremophor® RH 40, ethanol) was either filled into a gelatin capsule (SNEDDS-A) or loaded onto a porous tablet core (SNEDDS-B) and compared to a commercial tablet in an *in vitro* digestion model. The results in the fasted state showed that the percentage of dissolved drug decreased in the following order: SNEDDS-A > SNEDDS-B > tablet, which correlated well with the *in vivo* bioavailability. In the fed state *in vitro* digestion model, the amount of cinnarizine dissolved was similar for all formulations. The authors noted the increase in conventional tablet performance explained by food effect. The X-ray powder diffraction (XRPD) analysis of the pellets obtained at the end of the *in vitro* digestion showed that the drug from the commercial tablets precipitated in crystalline forms. Khan et al. [285] coupled *in vitro* lipolysis with sSAXS to simultaneously monitor the solid-state characteristic of precipitated fenofibrate from the lipolysis of a SNEDDS. Results showed that fenofibrate precipitates in its thermodynamically stable crystalline form upon lipolysis of the SNEDDSs, and an increase in scattering intensity over time corresponded well to an increase in concentration of precipitated fenofibrate in the pellet phase (Figure 5d).

However, while the pH-stat lipolysis model provides one means of predicting the oral absorption, it is a closed system, and many studies have since revealed a lack of *in vitro–in vivo* correlation (IVIVC) using the same lipolysis model [307–309]. Moreover, the lack of the absorption sink that is present *in vivo* will most likely lead to an overestimation of drug precipitation, which may produce an incorrect estimation of the *in vivo* performance [310,311].

In an attempt to simulate the *in vivo* conditions as closely as possible, recent research has developed several digestion models, including a high-throughput lipolysis model [312,313], a Permeapad® lipolysis/permeation model [298], two compartmental simultaneous setups [314,315] and the μFLUX system [269].

V.3. *IN VITRO* PERMEATION STUDIES

The parallel artificial membrane permeability model (PAMPA) and the Caco-2 cell model are the two most often used to evaluate the drug permeation *in vitro* [316].

PAMPA is a high-throughput technique, based on an artificial lipidic membrane that is useful in predicting the passive oral drug absorption [317,318]. Initially, drug is placed at the donor compartment, and the apical compartment is drug-free. After the incubation time, the quantity of drug is determined in each compartment. The compartments may also contain some additional compounds to bind the drug as it permeates [319,320]. PAMPA is especially advantageous in early

drug discovery and, since it is easy to automate, cost-effective and compatible for high-amount solubilizers [321,322]. Nekkanti et al. [323] developed SNEDDSs and proliposomes for valsartan and compared their *in vitro*/*vivo* performance. SNEDDSs were developed using varying amount of Labrafil® M 2125, Capmul® MCM, and Tween® 80, while proliposomes containing soy phosphatidylcholine, hydrogenated soy phosphatidylcholine, a distearyl phosphatidylcholine were developed by a thin-film hydration technique. Results from *in vitro* drug permeation studies using PAMPA showed an increase in drug permeability from SNEDDSs and proliposomes over the pure drug. The effective permeability values for the pure drug, proliposomes, and SNEDDSs formulations were found to be 1.0×10^{-5}, 1.7×10^{-5}, and 1.8×10^{-5}, respectively. However, the limitations of PAMPA are that the lipidic membrane is slightly different from the biological membrane and the presence of organic solvent in the membrane, which could result in a non-bilayer membrane structure. Furthermore, PAMPA is limited to passive permeation evaluation [321,324].

The Caco-2 cell line is routinely cultivated as monolayers on permeable filters to study intestinal drug absorption. The drug transport across the GI epithelium cells may occur by several pathways, including the passive paracellular and transcellular routes, the carrier-mediated pathways and transcytosis. Mature Caco-2 cells have been used to study transport of drugs by all these pathways [325–328]. Although Caco-2 originated from human colon carcinoma, they develop numerous features of absorptive GI cells during culture, such as microvillous structure, hydrolysis enzymes, tight junctions, and carrier-mediated transport system of fatty acids, amino acids, sugars, and many drugs [329–331]. Similar to *in vivo* conditions in intestinal cells, once in contact with lipids, they can synthetize and secrete chylomicrons [332]. Caco-2 cells can be pretreated with different inhibitors to elucidate the uptake mechanisms of drugs and lipid nanocarriers [212,333]. Several studies have shown enhanced drug permeation from SNEDDSs using Caco-2 monolayers [334–338]. Memvanga et al. [202] demonstrated that the transport of the curcumin-SEDDSs across Caco-2 monolayers was improved compared with that of free drug (Figure 5e).

Apart from the permeability assessment, Caco-2 cells could be used to evaluate the safety of many lipid-based formulations. In these assays, Caco-2 cells are treated with increasing amounts of the formulation dispersed in a suitable buffer and left to incubate. Many cellular processes such as DNA synthesis metabolic activity and proliferation can be used to evaluate cell viability after the incubation [339–341]. Widely used *in vitro* cytotoxicity assays include 3-(4,5-dimethylthiazol-2-yl)-2,5-diphenyltetrazolium bromide (MTT), 3'-[1-[(phenylamino)-carbonyl]-3,4-tetrazolium]-bis(4-methoxy-6-nitro)benzene-sulfonic acid hydrate (XTT) and 3-(4,5-dimethylthiazol-2-yl)-5-(3-carboxymethoxyphenyl)-2-(4-sulfophenyl)-2*H*-tetrazolium (MTS), which give direct indications of metabolism activity [342–345]. These assays are based on mitochondrial reduction of tetrazolium salts to dyed formazan-based products, providing information on cell activity and metabolism [346]. The main differences between them rely on the chemical compositions of tetrazolium salts. MTT is a positively charged compounds that easily diffuses viable cells and converts to insoluble formazan products, whereas MTS and XTT are negatively charged compounds that are readily transformed into soluble formazan products [316].

Lactate dehydrogenase (LDH) assay is commonly used to access cell membrane damage [339]. The activity of LDH released in the cell culture medium after nanoparticle treatment is

spectrophotometrically measured. Released LDH converts pyruvate into lactate resulting in the chemical reduction of NADH into NAD^+. A drop in NADH absorption peak correlates to an increase in extracellular concentration of LDH [316].

Desai et al. [347] compared the cytotoxicity of MCT- and LCT-containing SEDDSs on Caco-2 cells of varying maturity (1-, 5-, and 21-day cultures). The cell viability was determined using MTT assy. They demonstrated that the oil-surfactant mixtures had greater tolerance than surfactants alone, and LCT-SEDDSs were well-tolerated at almost 10-fold higher concentrations than the corresponding MCT-SEDDSs. Moreover, the LCT-SEDDSs showed better tolerance compared to MCT-SEDDSs after lipolysis. The authors concluded that MCT and LCT lipids are well-tolerated at normal human dose, and LCT lipids were less toxic than MCT lipids in a Caco-2 cell model.

VI. Ex vivo permeation studies

Intestinal absorption has been recognized as a crucial factor affecting the plasma concentration of compounds loaded in SNEDDSs. Several isolated systems have been used to determine the GI absorptive ability of a drug and the mechanism behind this process. These systems contribute to the reduction of live animal in experimentation. Frequently used systems are single-pass intestinal perfusion (SPIP) and intestinal recirculating perfusion that provide conditions closer to what is faced after oral ingestion [347–349]. The SPIP is based on the principle that the amount drug in perfusion nanoemulsion decreases over time due to the drug permeation [350]. It allows the determination of the rate and extent of permeation through the intestinal segment (i.e., duodenum, jejunum) after cannulating at both ends. The SPIP is advantageous for compounds that are rapidly absorbed [208,351]. In the intestinal recirculating perfusion (IRP), the process is repeated many times with the same perfusate. Due to the longer retention time within the intestine, the probability of drug absorption is considerably increased. Then, it is dedicated to drugs that are absorbed slowly to amplify the concentration change [352,353].

Kazi et al. [354] investigated the *in vitro* and *in vivo* performance of SNEDDSs loaded with talinolol. The *in vitro* dissolution revealed a significantly higher drug dissolution rate from SNEDDSs (>92% in 2 h) compared to pure drug. The data from *in vitro* lipolysis showed that SNEDDSs presented comparably higher amounts of drug in aqueous phase under both fed and fasted (60% and 67%, respectively) conditions. The *ex vivo* permeability by SPIP showed a 4-fold increase in permeability from SNEDDSs compared to pure drug. In another study, Beg et al. [355] used the quality-by-design (QbD) approach to design and optimize SNEDDSs of paclitaxel with improved biopharmaceutical attributes. Following appropriate mathematical models, the optimized SNEDDSs were earmarked by QbD optimization. Next, cationic SNEDDSs were formulated for both LCT- and MCT-containing SNEDDSs and were subjected to *in vitro* testing. The *in vitro* dissolution study indicated a 2.7-fold enhancement in dissolution rate from optimum cationic SNEDDSs over free drug. *Ex vivo* SPIP study exhibited nearly 6- to 8-fold enhancement in absorption and absorption parameters of the drug from the optimized cationic SNEDDSs as compared to the pure drug.

VII. IN VIVO PHARMACOKINETICS STUDIES

In addition to primary *in vitro* studies, animal pharmacokinetics studies play a major role in predicting the oral bioavailability in humans during drug development [356]. Generally, an oral dose of the drug loaded in SNEDDSs are given to animals (preconcentrate or dispersed in water). To analyze the absorbed drug in the plasma, various analytical techniques such as liquid chromatography-UV and liquid chromatography-mass spectrometry are commonly used [299,357]. The pharmacokinetic parameters (i.e., $t^{1/2}$, $C_{max,}$ $T_{max,}$ AUC_{0-t}) from animals are extrapolated to humans to select a suitable dose to use during the first trials in humans. When compared to dogs, rabbits, or pigs, rats are an economical, convenient, and relatively high-throughput animal model. Another advantage of rats is the potential of inhibition of efflux pumps, transporters, and enzymes, allowing the evaluation of their impact on drug absorption [247]. However, it should be noted that one of the major issues of extrapolating bioavailability from animals to humans is the fact that the anatomy and physiology of animals vary largely; therefore, the oral absorption of a drug dose varies across species.

There are hundreds of published articles on pharmacokinetics studies with SNEDDSs in animals such as rats, dogs, or rabbits. Diverse SNEDDSs have been formulated and have shown superior *in vitro/in vivo* performance compared with native drugs. Some preclinical studies reporting enhanced bioavailability from SNEDDSs formulations are presented in Table 3, with a brief description that gives an overview of this field.

Aside from improved oral absorption, SNEDDSs have been reported to minimize the impact of food effect and bile secretion on the oral drug absorption [246,275]. Perlman et al. developed SEDDSs that provided considerably higher fasted exposures of torcetrapib than the formulation containing Miglyol® 812, previously employed in the clinic. SEDDSs composed of 30% Capmul® MCM, 20% MCT, 30% Triacetin, and 20% Polysorbate 80 enhanced fasted exposure and thus decreased the effect of food from 5- to 3-fold in dogs at a dose of 90 mg [383]. Moreover, reduced intra- and inter-subject variabilities by SNEDDSs were reported [246,384].

In contrast, a literature review revealed fewer clinical studies in which the absorptions of drugs were enhanced by administration in the form of SNEDDSs. Some examples are given here, and Table 4 summarizes them.

Table 3. Examples of preclinical studies reporting enhanced dissolution and bioavailability of drugs upon their incorporation into SNEDDSs.

Class	Drug	Components	In Vitro/Vivo Observation	References
ANTI-CANCER	Docetaxel	Capryol® 90, Labrasol®, Transcutol® HP	AUC_{0-t} and C_{max} increased 6.4 and 6.5-fold, respectively compared to docetaxel aqueous solution.	[358]
	Erlotinib	Labrafil® M2125 CS, Labrasol®, Transcutol® HP, Aerosil® 200, Dextran 40	AUC_{0-t} and C_{max} increased 2.1 and 2.4-fold, respectively in case of dextran-based solid SEDDS compared to erlotinib powder.	[359]
	Paclitaxel	Sesame oil, Labrasol®, Sodium deoxycholate	AUC_{0-t} and C_{max} increased to 2.7 and 3.99-fold, respectively compared to drug suspension.	[356]
ANTI-CANCER	Lycopene	LCT, Tween® 85, Cremophor® RH, Gelucire®	AUC_{0-t} and C_{max} increased 2.3 and 2.85-fold, respectively compared to Lycovit®.	[360]
	Methotrexate	Ethyl oleate, Tween® 80, Propylene glycol	AUC_{0-24} and C_{max} increased 1.57 and 1.68-fold, respectively compared to native drug.	[361]

	Irinotecan	Capmul® CM-C8, Cremophor® EL, Pluronic L-121	AUC_{0-t} and C_{max} increased 4.2 and 1.7-fold, respectively compared to drug suspension.	[362]
CARDIOVASCULAR AND ANTI-HYPERTENSIVE	Carvedilol	Labrafil® M1944CS, Tween® 80, Transcutol®	Relative bioavailability enhanced by 4.1 times compared with tablet.	[363]
	Felodipine	Miglyol® 812, Cremophor® RH 40, Tween® 80, Transcutol® HP, Silicon dioxide	AUC_{0-t} increased 2-fold compared to conventional tablets.	[364]
	Clinidipine	Capryol® 90, Tween® 80, Transcutol®	The absorption of the drug was enhanced from liquid-SEDDS as 99 % of the drug was transported from mucosal to serosal side of the rat intestine within 90 min from SEDDS in comparison to only 42.2% from that of the pure drug suspension.	[365]
	Valsartan	Triacetin or Castor oil, Tween® 80, PEG 600	For triacetin-SNEDDS 5 and 2.4-fold increase in Cmax and AUC, respectively; for castor oil SNEDDS 8 and 3.6-fold increase in Cmax and AUC, respectively.	[366]
	Rosuvastatin	Peceol®, Tween® 80, Transcutol® HP	In vivo pharmacokinetic studies revealed 1.8 and 5.7-fold enhancement in AUC_{0-t} and C_{max}, respectively, and 0.33-fold reduction in T_{max} of drug from the SNEDDS vis-à-vis the pure drug suspension.	[335]

	Atenolol	Tartaric acid, Captex®, Span® 80, Oleic acid	*Ex vivo* intestinal permeability studies revealed that atenolol SDEDDS exhibited better drug permeation compared to atenolol or atenolol-tartaric acid suspension.	[367]
	Ramipril	Sefsol, Tween® 80, Carbitol	2.29-fold improvement in oral bioavailability compared with free drug suspension.	[266]
ANTI-DIABETIC	Insulin	Miglyol®, Cremophor® RH40, MCM C-10, Ethanol	AUC_{0-t} increased 2.7-fold compared to insulin solution.	[368]
	Glibenclamide	Cotton oil, Tween® 80, Propylene glycol	AUC_{0-t} increased 1.4-fold compared to free drug.	[369]
	Trans-cinnamic acid	Isopropyl myristate, Cremophor® EL, PEG 400	The efficacy of trans-cinnamic acid in both hyperglycemia and glucolipid metabolic disorder was enhanced in SNEDDS compared to the drug suspension.	[370]
	Gliclazide	Capryol® 90, Cremophor® EL, Akoline® MCM	Enhancement in oral bioavailability as compared to the free drug.	[371]
	Exenatide	Cremophor® EL, Labrafil® 1944, Capmul®-PG 8, propylene glycol	14.6-fold higher relative bioavailability versus subcutaneous exenatide solution.	[372]
ANTIOXIDANT	Quercetin	Capmul®, Tween® 20, Ethanol	23.7-fold increase in the cell uptake of quercetin when incorporated in SEDDS compared to free drug.	[373]

	Resveratrol	Miglyol® 812, Montanox, Labrasol®, Gelucire®, Ethanol	The absorptive fluxes through the intestinal epithelium from the nano-emulsions were significantly increased compared to an ethanolic control solution.	[374]
	Genistein	Labrafac® lipophile 1349, Maisine®-35, Cremophor® EL, Labrasol®, Transcutol®	95% of drug release in 5 min.	[375]
	Retinol acetate	Soybean oil, Capmul®, Cremophor® EL	Improved in dissolution rate.	[376]
	Coenzyme Q10	Lauroglycol® FCC, Witepsol® H335, Solutol® HS 15	5-fold improvement in oral bioavailability compared to free drug.	[201]
ANTI-VIRAL, ANTI-BACTERIAL, ANTI-FUNGAL, AND ANTIPROTOZOAL	Darunavir	Lauroglycol® 90, Tween® 80, Transcutol® HP	Enhancement in AUC_{0-t}, oral bioavailability and C_{max}, 1.45,5.8 and 7.5-fold, respectively compared to free drug.	[377]
	Nelfinavir mesylate	Maisine® 35-1, Tween® 80, Transcutol® HP	4.5-fold improvement in permeability and 3.6-fold improvement in bioavailability.	[275]

Lopinavir	Maisine®, Tween®-80, Transcutol® HP	Enhanced oral bioavailability (3.9-fold) compared to the pure drug.	[378]
Acyclovir	Sunflower oil, Tween® 60, Glycerol	3.5-fold increase in oral bioavailability compared to the pure drug suspension.	[379]
Rifampicin	Capmul® MCM C, Cremophor®-EL, Labrasol®	3.72 and 5.22-fold improvement in AUC_{0-t} and C_{max}, respectively compared to drug suspension.	[380]
Amphotericin B	Peceol®, PEG-200, Distearoylphos-phatidylethanolamine	Amphotericin B-SEDD treatment significantly decreases total fungal colony forming unit concentrations compared to non-treated controls without significant changes in plasma creatinine levels in the A. fumigatus infected rats.	[381]
Satranidazole	Oleic acid, Tween® 20, PEG 400	SNEDDSs formulations showed a drug release of greater than 70% in 45 minutes whereas marketed preparation showed more than 70% of drug release in 90 minutes.	[382]

Table 4. Pharmacokinetics data reporting enhanced bioavailability from Self-Emulsifying Drug Delivery Systems (SEDDS) in human subjects

Drug	Components	In Vivo Observation	References
Vitamin E	Palm oil, Tween® 80, Span® 80	3-fold higher oral bioavailability from SEDDSs.	[385]
Cyclosporin	Corn oil glycerides, Cremophor® RH40, PG, DL-α-tocopherol and ethanol	AUC_{0-t} and C_{max} increased 1.18 and 1.17-fold, respectively from SEDDSs.	[386]
Tocotrienols	Tocomin, Soybean oil Tween® 80 Labrasol®	2 to 3-fold higher oral bioavailability from SEDDSs.	[244]
Saquinavir (Fortovase®)	Medium-chain mono- and di-glycerides	Increased oral bioavailability up to 331% from Fortovase® compared to Invirase®.	[360]
Simvastatin	Labrafil®, Tween® 80, Transcutol® HP	1.55 and 1.5 increased in Cmax and AUC_{0-t}, respectively from SNEDDSs.	[387]
Vitamin K	Vitamin K, Labrasol®, Transcutol® HP	Enhancement in vitamin K relative bioavailability from SNEDDSs.	[384]

Julianto and colleagues [385] conducted a single-dose study to evaluate the oral bioavailability of a ∝-tocopherol SEDDS in comparison with that of a commercial product, Natopherol®, available as soft gelatin capsules. The SEDDS contained 40% palm oil, 20% Span® 80, 40% Tween® 80, and alpha-tocopherol (333.3 IU/mL), whereas the commercial formulation contained alpha-tocopherol (400 IU) dissolved in soybean oil. They demonstrated that SEDDS formulation enhanced the oral bioavailability of alpha -tocopherol between 210 and 410% compared with the commercial formulation in healthy male volunteers (Figure 7a).

Postolache et al. [386] compared the oral bioavailability of cyclosporine SEDDSs with a marketed semi-solid oily solution cyclosporine on 24 human healthy volunteers. The results showed that both the $AUC_{0-\infty}$ and C_{max} values of the SEDDSs were higher than those of the oily solution. The authors concluded that the oily solution was not bioequivalent with the SEDDSs formulations owing to the lower absorption rate.

A comparative pharmacokinetic study was conducted to evaluate the oral bioavailability of tocotrienols from SEDDSs and an oily solution. Liquid formulations loaded with 200 mg mixed tocotrienols administrated in healthy adults as SEDDSs or simple solution of soybean oil stated that SEDDSs showed a rapid onset of absorption, with a marked increase in the extent of the drug bioavailability by almost three-fold compared to the soybean oily solution under fasted condition [244].

Roche Laboratories enrolled human subjects to compare the bioavailability of Fortovase® and Invirase®, both available in the market as soft and hard gelatin capsules, respectively. Fortovase® was a SEDDS containing saquinavir (200 mg) dissolved in medium-chain mono and di-glycerides, povidone and ∝-tocopherol, whereas Invirase® contained saquinavir (500 mg), microcrystalline lactose, sodium starch glycolate, povidone, magnesium stearate, and talc. The study demonstrated a significant improvement of the oral bioavailability up to 331% from Fortovase® compared with Invirase® [388]. Due to pill burden and GI tolerability issues, Fortovase® was later discontinued from the market [388].

The pharmacokinetic parameters of vitamin K self-nano-emulsifying lyophilized tablets (SNELTs) were evaluated and compared with marketed tablets and ampoules on human volunteers [384].

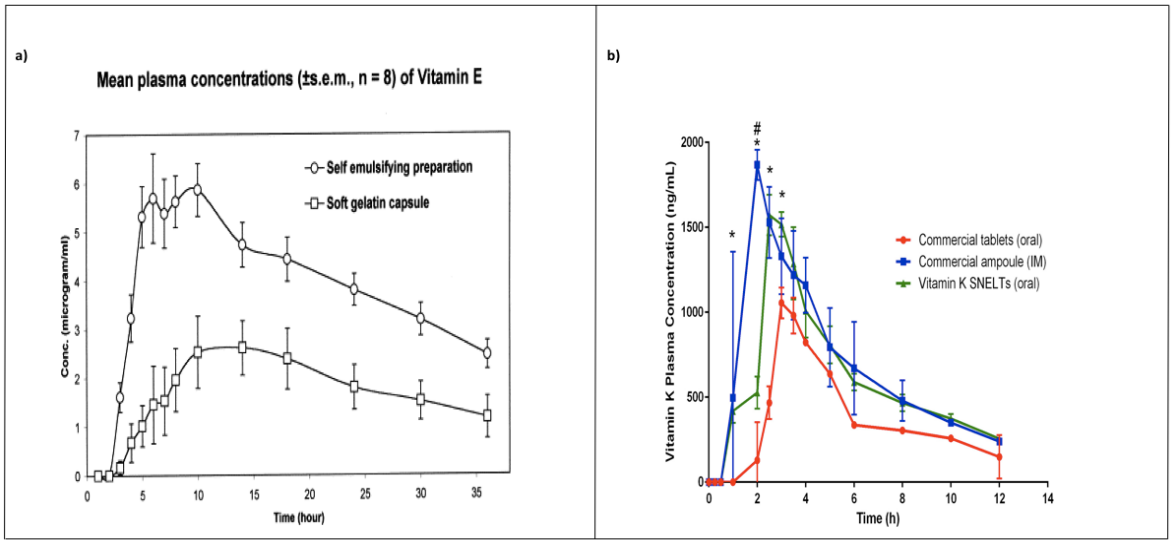

SNELTs enhanced vitamin K's relative bioavailability (170%) in comparison with the marketed tablets. Moreover, promisingly, SNELTs showed no statistically significant difference in the AUC compared with the marketed IM injectable ampoules (Figure 7b).

Figure 7. (**a**) Mean plasma concentration (± SEM, n=8) of a-tocopherol as a function of time following oral administration of vitamin E (400 IU) in the form of a self-emulsifying preparation and soft gelatin capsule after subtraction of endogenous vitamin E from each subject. From [385]. (**b**) Plasma concentration-time profiles of vitamin K after intramuscular and oral administration of commercial vitamin K products and oral administration of vitamin K SNELTs to human volunteers. Each value represents the mean ± SD (n = 6). *$p < 0.05$ compared to the commercial vitamin K tablet (oral); #$p < 0.05$ compared to the commercial vitamin K ampoule (IM). From [384].

VIII. ADVANCEMENTS IN SNEDDSS

VIII.1. SUPERSATURATED SNEDDSS

Drug solubility in lipidic components is the key factor that determines the dose of a drug to be administered in a SNEDDS formulation [389,390]. As the oil content is reduced during the dispersion or digestion, the solubilizing capacity of SNEDDSs declines *in vivo,* leading to drug precipitation [391]. Therefore, most SNEDDSs contain drugs below their equilibrium solubility, typically between 50% and 90%, limiting the access of many drugs to this promising technology, especially drugs that should be given at a high dose [392–394].

To overcome this drawback, supersaturated SNEDDSs (s-SNEDDSs) containing precipitation inhibitors have been suggested [390]. s-SNEDDSs are thermodynamically stable SNEDDSs containing a polymer (such as poly vinyl pyrrolidone (PVP) or hydroxypropylmethylcellulose) that should inhibit the nucleation process and subsequent drug precipitation, thus temporarily maintaining a supersaturated solution of the drug in the GI tract [395–397]. Supersaturation enhances the thermodynamic stability of the drug above its solubility limit, thus improving both the extent and rate of drug absorption [165]. Moreover, the higher drug loading in the formulation increases the flux over the GI epithelium [398]. Bannow et al. studied the impact of the polymeric precipitation inhibitor (polyvinylpyrrolidone-co-vinyl acetate) PVP/VA-64 on the *in vitro* performance and physical stability of s-SNEDDS containing simvastatin. They demonstrated that s-SNEDDSs containing 20% (*w*/*w*) of PVP/VA-64 and a simvastatin load of 200% enhanced formulation performance during *in vitro* digestion, achieving a 2.5-fold higher degree of drug supersaturation after 15 min of lipolysis in comparison with PVP/VA-64-free s-SNEDDSs of the same simvastatin load [399].

As per the literature, many researchers have indicated that the bioavailability of a drug in s-SNEDDSs is enhanced and is greater than that in the traditional SNEDDSs [394,400]. s-SNEDDSs have also been employed to reduce the oil/surfactant content in the conventional SNEDDSs formulations. The high concentrations of these surfactants typically present in SNEDDSs can lead to GI side effects. It has been noted that the significantly reduced amount of oil/surfactant in s-SNEDDSs offers an improved safety/toxicity profile than the classical SNEDDSs [393].

VIII.2. MUCUS-PERMEATING SNEDDSS

Due to faster clearance rates and rapid secretion, the mucus barrier sets a challenge for conventional drug-delivery systems to reach the GI epithelial cell surface and remain there for a sufficient amount of time [401,402]. It has been reported that SNEDDSs composition and resulting nanoemulsion droplet size are the most important factors influencing the mucus-permeating ability of a SNEDDS formulation [403,404]. Most SEDDSs formulations contain surfactants made of PEGylated groups to ensure self-emulsification process, so their relatively high mucus-permeating abilities can be explained by those PEGylated groups located at the surface of the oil droplets, making SNEDDSs highly muco-inert [405].

Friedl et al. observed the permeation of different droplet-sized SNEDDSs across mucus membranes and demonstrated that SNEDDS with a particle size of 12 nm had greater diffusion potential (70%) compared to the diffusion (8%) of the large SNEDDS (450 nm) [406].

Currently, several strategies are used to improve mucus permeation of SNEDDSs, including surface charge modification [407–410], mucoadhesive polymer incorporation [411,412] and the inclusion of mucolytic agents [413,414].

SNEDDSs that can change their zeta potential from negative to positive were formulated. Those SNEDDSs containing highly phosphorylated molecules have a negative zeta potential and change their zeta potential to positive once coming into contact with intestinal alkaline phosphatase, an enzyme presents in the GI mucus gel layer [253,408]. The advantages of this approach are that negatively charged SNEDDSs formulation can diffuse more quickly across the mucus gel layer, and zeta potential are shifted to positive once in contact with GI epithelium, allowing improved cellular uptake.

Mucoadhesive SNEDDSs are developed to prolong nanoparticle residence time at GI epithelium surfaces, thus avoiding pre-systemic drug metabolism. The choice of an appropriate mucoadhesive polymer in terms of lipophilic properties and compatibility is primarily important. The classical polymers (e.g., carboxymethyl cellulose, chitosan) adhere by forming hydrogen bonds or weak electrostatic interactions, resulting in a relatively low muco-adhesion, generally insufficient to ensure a prolonged localization at a specific target site [175]. To address this issue, thiolated polymers were introduced as a new generation of mucoadhesive polymers [411,412]. In contrast to classical mucoadhesive polymers, these novel polymers have the capability of enhanced attachment via covalent bonding [415]. Leonaviciute et al. provided a proof-of-concept that mucoadhesive Self-Emulsifying drug delivery systems (SEDDS) can be obtained using hydrophobic mucoadhesive polymers. A thiolated Eudragit® S100 was synthesized and incorporated into SEDDSs (T-SEDDSs). They demonstrated that T-SEDDSs led to markedly improved muco-adhesiveness compared with blank SEDDSs. Blank SEDDSs were totally removed from the GI mucosa after 15 min, whereas more than 60% of T-SEDDSs were still attached to it [416].

Mucolytic agents can improve the SNEDDSs permeation across the GI barrier by breaking down certain three-dimensional substructures within the mucus network [250,417]. Instead of cleaving the entire mucus network and consequently its important protective role, these agents break down the mucus gel layer only where they are in contact with it. Leichner et al. developed SEDDS with mucolytic properties following the incorporation of papain. The enzyme was encapsulated into SEDDS via hydrophobic ion pairing technique using sodium deoxycholate. The formulated SNEDDS exhibited an almost 3-fold increase in mucus diffusion and an extended residence time at the mucosal (up to 3- and 5-fold) compared to the control [418].

VIII.3. SOLID SNEDDSS

Despite the benefits provided by liquid SNEDDSs, drawbacks such as drug/components precipitation when stored, interactions between the filling and the capsule shell, and formulation stability during storage are common issues faced by them [189,190,419]. The main strategy applied

to overcome these challenges is to transform liquid SNEDDSs into solid dosage SNEDDSs formulations. It is believed that the conversion of liquid SNEDDSs to solid SNEDDSs provides relatively lower production cost, better formulation stability, ease of handing, precise dosing, and, consequently, better patient compliance [420–423].

Generally, the techniques employed to develop solid SNEDDSs include adsorption onto inert carriers [424,425], spray drying [426,427], melt granulation [428,429] and extrusion-spheronization [430] and are described below.

VIII.3.1. Methods of production

Adsorption onto solid carriers with high specific area and/or high porosity is the most studied technique to produce solid SNEDDSs [431]. The process of adsorption is easy and just implies addition of the liquid SNEDDSs onto solid carriers with gentle mixing in a blinder. The solid carriers commonly used include silicates such silicon dioxide (i.e., Aerosil®), magnesium aluminometasilicate (Neusilin®), micronized porous silica (i.e., Syloid®) and dibasic calcium phosphate anhydrous (Fujicalin®). The obtained solid SNEDDS can directly be filled into gelatin capsules or, alternatively, mixed with appropriate ingredients prior compression into tablets. Benefits of this technique include the avoidance of organic solvents and the small number of excipients required for the formulation [432]. Furthermore, liquid SNEDDSs can be adsorbed at high levels (>60% *w/w*) onto a suitable solid carrier [433].

Spray drying is a simple one-step technique for producing solid micro/nanoparticles including solid SNEDDSs [434]. The solid carrier is mixed with the liquid component using a solvent followed by solubilization. The solubilized liquid formulation is then sprayed into a hot-air compartment to remove the volatile solvents, which can be organic solvents or water in the case of nano-emulsion. Dried particles under controlled temperature and flow rate are prepared. Such micro/nanoparticles can be further filled into capsules or converted into tablets.

Solid SNEDDSs production by spray-drying technique is feasible with several solid carriers, whether hydrophobic or hydrophilic. The choice of a solid carrier can impact the release profile and the oral absorption of the drug by affecting the formulation droplet size and entrapment after reconstitution [435–437]. The sprayer, the airflow, the chamber temperature, and the design of drying chamber are chosen with the respect to the powder specifications and product drying characteristics.

Melt granulation is a technique in which agglomeration of powder is obtained through the addition of a softening or binder at low temperature (50–80 °C). The melted binder establishes liquid bridges between particles and forms small granules that are transformed into spheronized pellets under specific conditions. Generally, 15–25% of the binder can be used depending on the powder fineness [438]. Melt granulation offers several advantages in comparison to conventional wet granulation, as it is a simple operation, in which the addition of the liquid component and the subsequent drying phases are excluded. The process parameters to be considered include mixing time, binder particle size, viscosity of the binder on melting and impeller speed [439,440].

Extrusion/spheronization is one of the pelletization methods employed in the pharmaceutical industry to manufacture a series of solid dosage forms, including pellets, granules and tablets [434,435,441]. Extrusion is technique used to convert a raw material with plastic characteristics into a product of uniform shape and density by forcing it through a die under controlled conditions of temperature, pressure, and product flow. Extrusion is then followed by a spheronization process, in which the product (extrudate) is broken and transformed into round pellets [442]. The following steps are applied during extrusion/spheronization process: mixing of the liquid SNEDDSs and components including adsorbent to form a homogenous powder; wet massing binder; extrusion into a spaghetti-like product; spheronization from the extrudate to spheroids of uniform particle size; drying; and sifting to achieve the desired particle size distribution. The characteristics of the SNEDDSs pellets formed greatly depend on the pellet composition. A balance between the smallest quantity of absorbent required and the largest quantity of liquid SNEDDSs is necessary to formulate pellets with desired biopharmaceutical attributes and the highest possible drug loading [443,444]. The drawbacks of this technique often include the high-energy input manly attributed to temperature and shear forces.

VIII.3.2. Solid-state characterization of Solid SNEDDSs

In addition to characterization techniques used for liquid SNEDDSs, solid SNEDDSs require further specified solid-state characterization. The inner physical structure of the powder particles is mainly verified by thermal analysis and X-ray diffraction, while different component interactions are studied by Fourier-transform infrared spectroscopy (FTIR).

Differential scanning calorimetry (DSC) and thermal gravimetric analysis (TGA) are mostly used to evaluate the thermal behavior of solid SNEDDSs. In these techniques, samples are subjected to heating at a specified temperature rate under different atmospheres such as argon, oxygen, and nitrogen [216]. The main information generated from these techniques is the melting point, crystallinity, polymorphism, and endothermic and exothermic behaviors of the sample, which are related to a reference standard [445].

X-ray diffraction is used to determine the crystallization and polymorphism of drugs in solid SNEDDSs [446]. Most drugs, lipids and surfactants have several polymorphic forms that can change after the encapsulation [447]. Since the biological activity of molecules also relies on polymorphic form, it is very important to ensure the stability of an appropriate form after the solidification. The X-ray pattern of the encapsulated drug is compared with the reference, and any difference indicates the impact of the solidification process on the drug stability.

FTIR is used to analyze intermolecular interactions and drug-carrier compatibilities. It provides information about functional groups and different chemical bonding between molecules. FTIR allows a study of the functional and structural modifications during the formulation and possible interactions between oils, surfactants, cosurfactants/cosolvents and molecules [216,390].

VIII.4. SNEDDSs FOR THE ORAL DELIVERY OF HYDROPHILIC MACROMOLECULES

The use of hydrophilic macromolecules (polysaccharides, peptides, protein and genes) has attracted growing interest presently owing to their high specificity, selectivity, and reduced side effects. Currently, more than 120 biopharmaceuticals, especially proteins, are approved for the use in clinic by the US Food and Drug Administration [448–450]. However, there are many challenges towards the oral administration of these hydrophilic macromolecules due to GI barriers that limits their oral absorption [451]. The low oral bioavailability of these drugs is a result of many factors, including poor diffusion related to hydrophilicity and large size, mucus barrier, gastric acidity, and enzymatic degradation [403,452].

Advanced SNEDDSs provide novel nanoemulsions with improved functional characteristics such as prolonged GI residence time, increased stability in GI fluids, improved mucus diffusion, improved permeation, and enhanced cell uptake, leading consequently to increased oral bioavailability of the encapsulated drugs [172,173,453,454]. Bravo-Alfaro et al. [455] developed SNEDDSs containing an insulin complex along with modified or unmodified phosphatidylcholine to increase insulin oral bioavailability. Under *in vitro* GI conditions, SNEDDSs showed 35.7% of drug availability upon reaching the final stage of the simulated small intestine. *In vivo* studies using diabetic rats showed a 36.1% decrease in plasma glucose levels after 4 h of SNEDDS administration and only 1.8% bioavailability after subcutaneous insulin administration.

SNEDDSs are also considered to be an innovative alternative for oral delivery of gene among the non-viral vectors. Incorporation of nucleic acids (e.g., pDNA, siRNA, microRNA) into nanoemulsions formed upon SNEDDSs dispersion could protect them from enzymatic metabolism and enhance their cellular uptake [456,457]. Mahmood et al. [453] loaded a pDNA into SNEDDS formulation as a pDNA/cetrimide complex at a molecular ratio of 1/2. Furthermore, the transfection efficiency was improved by encapsulating HIV-1 Tat protein (a cell-penetrating protein). The transfection efficiency tested on HEK-293-cells was found to be 1.7 and 1.8-fold higher for SNEDDSs loaded with Tat protein in comparison to Lipofectin and control, respectively.

However, the incorporation of any hydrophilic drug in the oily phase of a SNEDDS is difficult due to its low lipid solubility, which is responsible for low drug loading [408,458]. Several strategies have been developed to increase the lipid solubility of hydrophilic macromolecular drugs to facilitate their encapsulation into SNEDDSs formulations. These strategies are presented here:

VIII.4.1. Ion pairing

The hydrophobic ion paring process for hydrophilic drugs is based on partial or full binding of the drug with an amphiphilic ligand with opposite charge, or lipophilic pro-drug to increase the hydrophobicity and lipid solubility [459]. This association is a reversible and cost-effective method that enhances the lipid solubility along with the ability to cross membranes without changing the native structure of the molecule [459]. The potential of this method in the oral delivery of hydrophilic drugs has been examined *in vitro* and *in vivo*. Menzel et al. demonstrated the high impact of ion paring on the oral bioavailability of exenatide. Exenatide was lipidized via hydrophobic ion

pairing with sodium docusate (DOC) and encapsulated into a SEDDS consisting of 25% Labrafil® 1944, 30% Capmul®-PG 8, 35% Cremophor® EL, and 10% propylene glycol. The results from *in vivo* evaluation in rats showed a 14.6-fold higher relative bioavailability versus subcutaneous exenatide solution [372]. In another study, Hauptstein et al. [452] successfully encapsulated pDNA as a hydrophobic ion-paired complex with different cationic lipids into a SNEDDS formulation composed of 30% Capmul® MCM, 30% Captex® 355, 30% Cremophor® EL, and 10% propylene glycol. *In vitro* degradation studies via DNase I revealed that pDNA encapsulation into SNEDDS formulation led to significantly prolonged resistance time against enzymatic degradation (up to 8-fold) in comparison to pDNA–lipid complexes and naked pDNA. Furthermore, transfection studies showed a significantly improved transfection efficiency compared to naked pDNA. Many other amphiphilic molecules have been studied for hydrophobic ion paring and encapsulation into SNEDDSs [225,460–463]. Indeed, soybean phosphatidylcholine remains the most largely investigated amphiphilic molecule to facilitate the encapsulation of hydrophilic drugs into SNEDDSs.

VIII.4.2. Double emulsification technique

Double emulsification technique is an alternative method used to encapsulate hydrophilic drugs into SNEDDSs via the formation of self-double nanoemulsifying drug-delivery systems (SDNEDDSs), as depicted in Figure 8.

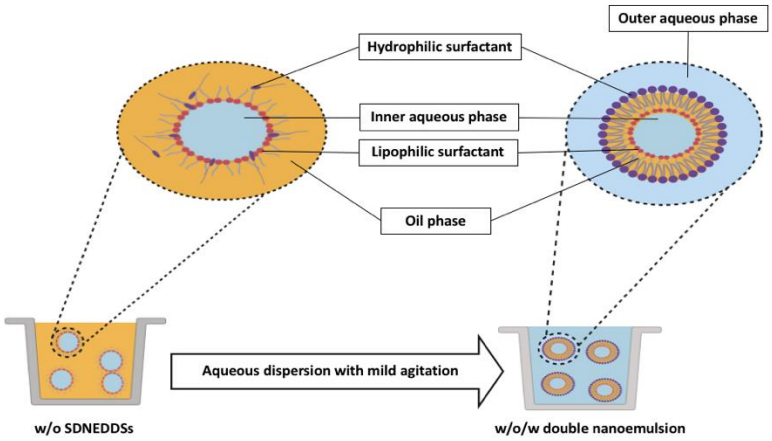

Figure 8. Schematic illustration of the double emulsification technique. Adapted from [367].

In this process, hydrophilic drugs are first dissolved in the inner water phase, whereas lipophilic excipients are dissolved in lipids. The water phase is then dispersed in the oily phase to form preconcentrate w/o SDNEDDSs. SDNEDDSs undergo self-emulsification to w/o/w double nanoemulsion upon aqueous dispersion in the GI tract [464]. SDNEDDSs can save protein and other macromolecular drugs from enzymatic degradation in the GI tract, improve efficacy and reduce the drug dose [465–467]. However, the drug stability in the inner water phase always represent a challenge.

VIII.4.3. The use of hydrophilic cosolvent

The use of a suitable cosolvent can facilitate the incorporation of hydrophilic macromolecular drugs into SNEDDSs formulations. The popular cosolvents used include propylene glycol, polyethylene glycol (PEG)-400, glycerol, and ethanol as mentioned earlier. They enhance the solvent capacity of the formulation and increase the dispersibility of surfactant in the oily phase, thus promoting SNEDDSs homogeneity and stability. Winarti et al. [468] used glycerin as a cosolvent to incorporate bovine serum albumin into a SNEDDS formulation. Bovine serum albumin was first dissolved in glycerin and then encapsulated into the oil phase using surfactants that have HLB values ranging between 11–15. However, there are several limitations related to these cosolvents, including the incompatibility of low-molecular-weight cosolvents with capsule shells and immiscibility of some of them with oils [469].

VIII.4.4. Chemical modification

One attractive strategy for improving the solubility and diffusion properties of hydrophilic macromolecular drugs is to combine them with membrane-binding carrier molecules. Hydrophobic carrier molecules such as fatty acids are among the most potentially useful categories of carriers, and studies showed that fatty acid-conjugated peptides and proteins may cross cell membranes, including the blood-brain barrier [470,471].

To develop a Bowman–Birk protease inhibitor (BBPL) into an effective cancer chemo-preventive agent, Wang et al. developed a technique to prepare a reversibly conjugated BBPL with palmitic acid (PA-BBPL) [472]. The results of the study showed that pharmacokinetic parameters of PA-BBPL were largely different from those of free BBPL. An extended plasma half-life and increase (11-fold) in the $AUC_{0-\infty}$ were observed for the lipidized form of BBPL. In addition, owing to the reversibility of the combination, PA-BBPL was showed to be equally potent as the free BBPL in the prevention of carcinogen-induced transformation of C3H10T1/2 cells in culture [473]. In another example, the lipophilicity of dalargin was enhanced by 0-esterification of tyrosine with palmitic acid. Dalargin-palmitic acid complex (DL-PA) was encapsulated into selected SEDDSs composed of 40% Cremophor® EL ,50% Capmul® 90, and 10% propylene glycol and SEDDS composed of 30% Capmul® MCM, 30% Captex® 8000, 30% Cremophor® EL, and 10% propylene glycol. Both SEDDSs showed significant mucus-permeating potential as well as protective effects against dalargin degradation by trypsin, elastase and α-chymotrypsin [474].

VIII.5. TARGETED SNEDDSS

Drugs in clinical trials may fail to reach favorable outcomes because they cannot target a desired site of action. A successful strategy to overcome this issue is to develop targeted drug-delivery carriers that release the drugs at a specific site of action [475]. SNEDDSs can be considered for this approach. Surface-modified nanoemulsions have been developed to reach animals and human liver in a similar way to chylomicrons [476,477]. SNEDDSs can drastically increase the concentration of the drug in liver and/or spleen and can be a smart way to reach these organs [478–480].

Another key aspect of SNEDDSs is their ability to be taken up into the lymphatic system. Many diseases, including HIV, lymphoma, autoimmune diseases, leukemia, tissue rejection, and tumor metastasis, require the lymphatic system for their progress [166,481–483]. Furthermore, passive and active targeting is achievable by attaching suitable ligands (antibodies, nucleic acid or peptides) to target a specific site of action [484,485]. Batool et al. developed a papain-grafted S-protected hyaluronic acid-lithocholic acid co-block (P-G-S-P-H-L-AC) amphiphilic polymer as a muco-permeating stabilizer to target MCF-7 breast cancer epithelial cells. The P-G-S-P-H-L-AC amphiphilic polymer was incorporated into a SNEDDS loaded with tamoxifen. An *ex vivo* permeation study revealed 7.11-fold higher diffusion of tamoxifen by tamoxifen P-G-S-P-H-L-AC SNEDDS compared to free tamoxifen. Furthermore, the formulated SNEDDS was safe and compatible against macrophages. It could efficiently kill MCF-7 breast cancer cells compared to free drug [207].

VIII.6. SNEDDSS FOR THE ORAL DELIVERY OF NATURAL DRUGS

Presently, the use of natural medicines has been increased owing to their therapeutic effects and fewer side effects compared with synthetic drugs [208,486–488]. It has been estimated by the World Health Organization (WHO) that more than 70% of the world's population, mostly in low-income countries, rely on plant medicines for primary health care [489–492]. Worldwide, plant medicines represent approximately 25% of the pharmaceutical arsenal [493]. However, most of natural extracts and natural drugs exhibit poor *in vivo* activity related to their low solubility, poor gastric stability, high metabolism and, hence, poor bioavailability [184,494,495]. Thus, SNEDDSs represent a very attractive drug-delivery carrier for natural medicines.

Qian et al. developed SNEDDSs of myricetin to improve its solubility and oral absorption. These myricetin-SNEDDSs had high solubility, fast drug release characteristics (>80% in 1 min), improved permeability and low cytotoxicity compared with the free myricetin. The oral bioavailability of myricetin was improved 2.5- to 6.3-fold compared to myricetin alone in rats [184]. To improve the aqueous solubility and oral absorption of bruceine D, Dou et al. [496] developed a SNEDDS composed of Solutol® HS-15, MCT, and propylene glycol. Bruceine-D-SNEDDS exhibited improved pharmacokinetic parameters as compared with the suspension. Furthermore, bruceine D-SNEDDS formulation significantly restored the body weight and colon length, reduced the disease activity index and colon pathology in a rat model. Tung et al. [497] developed and optimized s-SNEDDSs for the oral delivery of silymarin. s-SNEDDSs containing silymarin, Labrafil® M 1944, Kolliphor RH40 and Transcutol® HP were prepared, and Poloxamer 407 was chosen as the optimal precipitation inhibitor. The relative bioavailability of s-SNEDDSs versus Legalon® (silybum marianum) determined in mice was approximately 760%. Furthermore, s-SNEDDSs revealed a significantly higher hepatoprotective activity in CCl_4-induced model in contrast to the commercial product and decreased the plasma levels of lipid peroxidation and transaminases along with glutathione and superoxide dismutase activities under tested doses calculated as silybin. Shanmugam et al. used a spray-drying technique to prepare solid SNEDDSs for the oral delivery of the bioactive carotenoid lutein. The solid SNEDDSs contained 25% phosphatidylcholine, 60% Labrasol®, 14% Transcutol® HP, and Aerosil® 200 as the inert solid carrier. The pharmacokinetic evaluations performed in rabbits resulted in increased values of C_{max} and $AUC_{0\text{-}t}$ of carotenoid lutein loaded in solid SNEDDSs. The enhancements of C_{max} for solid

SNEDDSs were approximately 21- and 8-fold compared with free lutein (FL) and marketed product (MP), respectively. The relative bioavailability of solid SNEDDSs compared with MP and FL were 2.7- and 11.8-fold, respectively [498]. Recently, Kazi et al. designed solid SNEDDSs consisting of curcumin and piperine by incorporating bioactive natural oils (avocado, apricot, black seed and *Zanthoxylum rhetsa*) in the formulations. The optimal liquid SNEDDSs were solidified using Aeroperl® or Neusilin®. SNEDDS consisting of 20% black seed oil, 20% Imwitor® 988, 10% Transcutol® HP, 50% Cremophor® RH40 and Neusilin® enhanced curcumin and piperine release (up to 60% and 77%, respectively). In addition, these formulations could efficiently deliver the black seed oil to the patient [499]. Many other studies showed the potential of SEDDSs in the oral delivery of natural drugs, including [500–506].

IX. CHALLENGES

Even though SNEDDSs show considerable benefits over available drug-delivery systems today, still there are aspects that need to be further studied to make SNEDDSs future drug carriers.
Certain biopharmaceutical issues involving SNEDDSs include the drug-loading capacity and risk of precipitation upon dispersion or digestion. As mentioned above, the formulation-loading capacity could be improved via s-SNEDDSs. The risk of drug precipitation upon aqueous dilution could be minimized by keeping a good balance between oil and the surfactant/cosolvent ratio during the formulation. Many studies demonstrated that small changes in SNEDDSs composition are not expected to bring huge changes in drug solubility, but there could be a crucial decrease in formulation solvent capacity following aqueous dispersion [507,508]. For many years, SNEDDSs that showed evidence of drug precipitation upon aqueous dispersion or digestion appeared more likely to result in lower *in vivo* drug absorption. This thought process led to widespread use of *in vitro* dissolution and lipolysis test to evaluate performance of SNEDDSs using GI simulated fluids and the overarching assumption that a high water solubilization *in vitro* equals a high oral absorption. Although this assumption remains true for several drugs, for certain drugs (i.e., fenofibrate), oral absorption may still be consistent, even in light of notable drug precipitation. Accordingly, supersaturation rather than solubilization is emerging as an important drug driver flux across absorptive membranes [247,290,397,509].

The use of lipids and surfactants as excipients of SNEDDSs requires special attention regarding their safety after oral administration. First, the amount of these excipients in a SNEDDS is usually very high, and second, due to the complexity of their characteristics, these components can create multiple interactions and reactions with the physiological environment that could be difficult to control *in vivo*. More mechanistic studies will need to be performed to track these ingredients and the potential interactions involved after their ingestion. Moreover, such components, especially surfactants, should be identified as safe, less toxic, and compatible, even at high amounts [510,511]. It is also worth to highlight some drawbacks to which much major attention should be paid, such as the interaction drug-excipients and phenomenon associated with lipid oxidation [512–514]. Currently, drug-delivery research groups are working to surmount the aforementioned issues.

In the field of solid SNEDDSs, adsorbency, an indicator of the ability to carry greater amounts of liquid SNEDDSs should be searched. The advantages attributed to converting liquid SNEDDSs into solid dosage forms should be weighed against any potential decline in biopharmaceutical performance brought by the solidification process. The development of such SNEDDSs requires better understanding of SNEDDS factors (oil, surfactant, cosolvent, absorbent, etc.) that might impact the biopharmaceutical performance of the products. Accordingly, the implementation of a QbD approach is useful in the development of SNEDDSs as it takes several parameters.
Although the harmonization and standardization of several efficient *in vitro* tests such as lipolysis have already been established, the knowledge about the *in vivo* pharmacokinetic parameters and processes involved after SNEDDSs administration remains a gray area, especially in human volunteers [286]. Understanding the *in vivo* pharmacokinetic parameter is helpful in designing both optimized SNEDDSs and *in vitro* robust models that can be employed to predict *in vivo* characteristic accurately, thereby establishing the IVIVC [186,515]. To date, modeling of IVIVC is being increasingly applied as a prediction tool of drug plasma concentration versus time from the

in vitro data [293,516,517]. Both processes of formulation dispersion and digestion from SNEDDSs have been grouped into a mathematical model using a series of differential equations [518,519].

Out of all the *in vitro* tests commonly available for SNEDDSs evaluation, *in vitro* lipolysis test is found to be more relevant for predicting the *in vivo* behavior, even though it still has limits, including lack of a sink condition and the inability to predict the fraction of drugs that is absorbed via the lymphatic system and transported by efflux [181]. Attempts have been made to combine artificial membranes or a cell-based permeation step with the current *in vitro* digestion model [269,298,314], but they may not be able to remove enough drug to mimic effective *in vivo* drug absorption. Another approach is the use of models that incorporate a means to accurately monitor *in vitro* lipolysis and to simultaneously assess lipids and drug absorption in rats, as described by Crum et al. [290]. In doing so, they allow for real-time observation of the SNEDDSs lipolysis and drug absorption. However, as in most of *in vitro* lipolysis models, the experimentations are carried out under conditions not reflecting rat GI fluids but humans or large animals (i.e., dogs). To overcome these conditions, efforts were underway to develop a suitable *in vitro* rat model of digestion that accurately simulates the composition of rat GI fluids [520].

Although the majority of *in vitro* digestion tests have been carried out under fasted conditions, it has been recognized that these tests should also include fed conditions, with an additional step mimicking gastric lipolysis. One study was conducted to develop a model that initially mimics gastric digestion, then immediately followed by intestinal conditions simulation. The study was conducted under both fasted state and fed state conditions, wherein, after gastric digestion, the experiment was continued after addition of simulated intestinal fluid [295].
Considerable efforts are currently underway to generate interesting information that can be used to further refine available *in vitro* tests in order to design robust models for SNEDDSs evaluation.

X. SNEDDS FROM AN INDUSTRIAL PERSPECTIVE

SNEDDSs are initially developed in the lab, and there is a considerable gap between lab and large-scale production. SNEDDSs developments at the lab-scale are well documented. However, literature research revealed that little attention has been paid to challenges related to the large-scale production. This outcome could be explained by several reasons, including the limited experiments, the insufficient information on the large-scale process, the lack of experience and capabilities to cover all the manufacturing processes, or bias towards academic publication [521,522]. The success of any formulation, including SNEDDSs, relies on the bench to large-scale translation. Such translation, however, still possesses serious hurdles related to product stability and batch-to-batch variations that can significantly modify the formulation characteristics, which ultimately impact the therapeutic outcome [522]. However, large-scale production should be conducted in a manufacturing environment that meets Good Manufacturing Practice (GMP) requirements, which rely on strict and robust protocols, validated technical facilities, and well-trained personnel. GMP implementation requires a significant financial support to build a qualified facility.

From the safety point of view, the regulatory status with regard to the toxicity of components is important for the development of a marketed product [189,523]. It should be noted that all excipients are not inert, certain may be toxic, especially at high amounts. SNEDDS components must be chosen from the listed oils, surfactants, and cosolvents provided by the FDA and EMA (GRAS excipients). Moreover, the FDA updates the list of excipients in the database quarterly regarding those that are newly approved and incorporated in marketed products, referred to as the Inactive Ingredient Guide (IIG), which are approved and can be added in marketed products. Both IIG and GRAS data can be used by industry as an aid in the development of SNEDDSs formulations [523].

The regulatory landscape for SNEDDSs marks a considerable change in formulation approach, moving from the empirical-based formulation method to a more logical formulation approach, such as the QbD approach. The QbD boost in the pharmaceutical industry has been widely recognized and subsequently imbibed due to the guidelines provided by the FDA, EMA, and ICH. QbD, a regulatory-driven approach, aims to build quality from the first design stages with predefined goals by controlling and understanding processes, on basis of a solid science and quality risk management [228]. By doing so, it improves manufacturing processes and ensures the final product quality. Furthermore, this approach saves cost and simplifies production process through the implementation of product quality specifications related to clinical performance, preventing of dose variability as well as improving process design, manufacturing efficiency and post-approval change facility [219].

From the formulation point of view, Williams et al. [524] suggested a flowchart that provides a decision tree to formulate a lipid-based drug-delivery system (Figure 9).

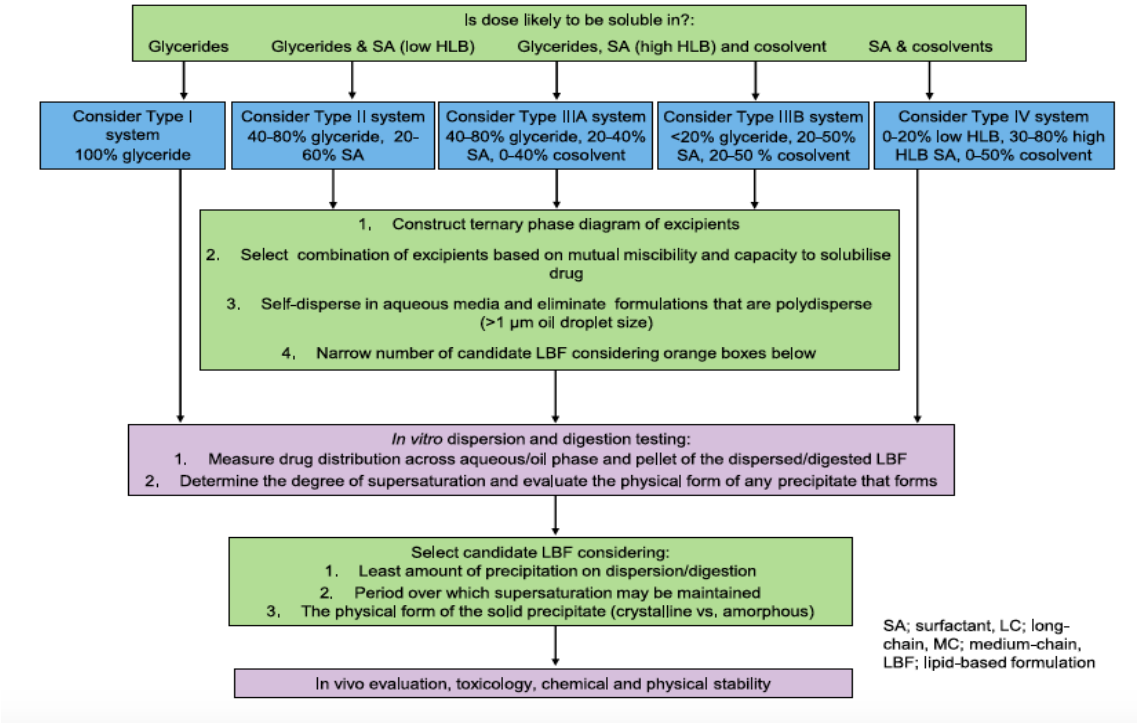

Figure 9. A flowchart providing a general guide to lipid-based formulation design. From [524].

This flowchart was developed as part of consortium efforts to rationalize the formulation of lipid-based drug-delivery systems and to elucidate the fate of a drug after its administration via a lipid-based formulation. However, this flowchart provides an academic view of the formulation; thus, a flow diagram representing industrial view is still needed in the public domain.

According to the US FDA, two formulations are therapeutic equivalents if they are pharmaceutical equivalents and can be expected to have the same therapeutic effect and toxicity profile after administration under specified conditions [525]. Two approved drug products are considered therapeutic equivalents if their bioequivalence has been demonstrated, and they can be expected to have the same clinical effect and safety profile when administered to patients under the conditions specified in the labeling [525]. Many drug applications for lipid-based formulations have been based on the drug approval in the conventional dosage form given by the same route of administration [526]. Since both tested formulations should contain the same active molecule, comparison of products should be based on single-dose pharmacokinetics and mass balance profile studies [526]. Data obtained from these evaluations will help in determining the dosing regimen for the new formulation. Therefore, regulatory agencies recommend dose-proportionality and multiple-dose studies for the investigated formulation. Additional investigations such as drug interaction studies and studies in special population category may be required to refine the dosing regimen of the product [527]. Currently, there are no specific requirements in place within the FDA or EMA for the preclinical and clinical evaluation of lipid-based formulations in general and SNEDDSs in particular [528,529]. Only reflection articles providing guidelines on the pharmaceutical drug development of a specific type of formulation are found in the literature [530–532], and the approval process is essentially the same as that for any other regulated drug device or biologic [529].

A review of the literature revealed many SNEDDSs formulations that were approved (EMA and FDA) for the oral delivery of different drugs (Table 5).

Some of the approved SNEDDSs have been further discontinued. According to the Federal Register, none have been discontinued for efficacy or safety issues. Fortovase® (Saquinavir) was discontinued because a new tablet dosage form with a comparatively low pill burden has been introduced. Kaletra® (Lopinavir/ritonavir lopinavir) was discontinued and replaced by a stable solid dispersion formulation that had higher drug loading, low pill burden, and did not require refrigeration. Agenerase® (Amprenavir) was replaced by a pro-drug (fosamprenavir). The successful marketed products illustrate how SNEDDSs can pass clinical evaluation and result in products providing better care for patients.

Table 5. Non-exhaustive list of marketed SNEDDSs for oral administration

Drug Name	Trade Name (Company)	Composition	Dosage Form
Ritonavir	Norvir® (Abbott Laboratories)	Ole Oleic acid, Cremophor®-EL, ethanol, butylated hydroxytoluene	Soft capsules
Tipranavir	Aptivus® (Boehringer Ingelheim)	Mono/di-glycerides of caprylic acids, Cremophor® EL ethanol, propylene glycol	Soft capsules
Cyclosporine	Sandimmune® (Novartis)	Corn oil/olive oil, Labrafil® M 1944 CS, ethanol, α-tocopherol	Soft capsule
	Neoral® (Novartis)	Mono-, di- and triglycerides of corn oil, Cremophor® RH40, propylene glycol, ethanol, D-α-tocopherol	Oral solution and soft capsules
Isotretinoin	Accutane® (Roche)	Beeswax, hydrogenated soybean oil flakes, hydrogenated vegetable oil, soybean oil Olive, polyoxyethylated oleic glycerides, ethanol	Soft capsules
Sirolymus	Rapamune® (Wyeth-Ayerst)	Phosphatidylcholine, mono- and di-glycerides, soy fatty acids, Tween® 80, ethanol, propylene glycol, ascorbyl palmitate	Oral solution

XI. CONCLUSIONS

Drug discovery programs provided many new chemical species that are poorly water-soluble. The use of lipid-based formulations in general and SNEDDSs in particular shows great potential in enhancing aqueous solubility, stability, oral absorption and in minimizing inter/intra-patient dose variability. SNEDDSs improve the absorption of drugs by several pathways, including increasing membrane fluidity, bypassing the first-pass effect, and inhibition of P-gp efflux. As described in Figure 2, after SNEDDSs dispersion in the GI tract, nanoemulsions are formed, which facilitate oil hydrolysis by lipases on the oil–water interface. Following this process, micelles along with other colloidal structures made of phospholipids, bile salt, and triglycerides are formed, which increase the transport of the drug through the intestinal barrier. The submicron size of the system with enhanced surface activity allows more robust drug transport through the GI boundary layer, ultimately resulting in better drug absorption and a rapid onset of action.

Previously, SNEDDSs formulations were used to overcome issues related to low aqueous solubility and oral bioavailability drugs. However, the scope of SNEDDSs is far beyond the solubility and dissolution issues. Presently, they have evolved into mucus-permeating, supersaturated, solid and targeted SNEDDSs to tackle issues related to classical SNEDDSs and to make new changes for several applications. Many anti-cancer, anti-diabetic, and anti-viral drug solubility, stability, and bioavailability characteristics were improved via SNEDDSs formulations.

Despite the above-mentioned advancements and modifications in SNEDDSs, there are still areas that need to be addressed to make SNEDDSs commercially attractive. The priority of future research should be based on the mechanisms of action of different SNEDDSs formulations and pharmacokinetic studies, especially on human subjects.

REFERENCES

1. Kato, G. J.; Piel, F. B.; Reid, C. D.; Gaston, M. H.; Ohene-Frempong, K.; Krishnamurti, L.; Smith, W. R.; Panepinto, J. A.; Weatherall, D. J.; Costa, F. F.; Vichinsky, E. P. Sickle Cell Disease. *Nat. Rev. Dis. Prim.* **2018**, *4*, 1–22,https://doi.org/10.1038/nrdp.2018.10.
2. Carden, M. A.; Fasano, R. M.; Meier, E. R. Not All Red Cells Sickle the Same: Contributions of the Reticulocyte to Disease Pathology in Sickle Cell Anemia. *Blood Rev.* **2020**, *40*, 100637, https://doi.org/10.1016/j.blre.2019.100637.
3. Palomo, M.; Diaz-Ricart, M.; Carreras, E. Is Sickle Cell Disease-Related Neurotoxicity a Systemic Endotheliopathy? *Hematol. Oncol. Stem Cell Ther.* **2020**, *13*, 111–115, https://doi.org/10.1016/j.hemonc.2019.12.005.
4. Macharia, A. W.; Mochamah, G.; Uyoga, S.; Ndila, C. M.; Nyutu, G.; Makale, J.; Tendwa, M.; Nyatichi, E.; Ojal, J.; Shebe, M.; Awuondo, K. O.; Mturi, N.; Peshu, N.; Tsofa, B.; Scott, J. A. G.; Maitland, K.; Williams, T. N. The Clinical Epidemiology of Sickle Cell Anemia In Africa. *Am. J. Hematol.* **2018**, *93*, 363–370,https://doi.org/10.1002/ajh.24986.
5. Taylor, S. M.; Parobek, C. M.; Fairhurst, R. M. Haemoglobinopathies and the Clinical Epidemiology of Malaria: A Systematic Review and Meta-Analysis. *Lancet Infect. Dis.* **2012**, *12*, 457–468,https://doi.org/10.1016/S1473-3099(12)70055-5.
6. Marsh, V. M.; Kamuya, D. M.; Molyneux, S. S. "All Her Children Are Born That Way": Gendered Experiences of Stigma in Families Affected by Sickle Cell Disorder in Rural Kenya. *Ethn. Heal.* **2011**, *16*, 343–359,https://doi.org/10.1080/13557858.2010.541903.
7. Fernandes, Q. Therapeutic Strategies in Sickle Cell Anemia: The Past Present and Future. *Life Sci.* **2017**, *178*, 100–108. https://doi.org/10.1016/j.lfs.2017.03.025.
8. Rogers, K.; Balachandren, N.; Awogbade, M.; Johns, J. Sickle Cell Disease in Pregnancy. *Obstet. Gynaecol. Reprod. Med.* **2019**, *29*, 61–69,https://doi.org/10.1016/j.ogrm.2019.01.006.
9. Kauf, T. L.; Coates, T. D.; Huazhi, L.; Mody-Patel, N.; Hartzema, A. G. The Cost of Health Care for Children and Adults with Sickle Cell Disease. *Am. J. Hematol.* **2009**, *84*, 323–327,https://doi.org/10.1002/ajh.21408.
10. Telen, M. J.; Malik, P.; Vercellotti, G. M. Therapeutic Strategies for Sickle Cell Disease: Towards a Multi-Agent Approach. *Nat. Rev. Drug Discov.* **2019**, *18*, 139–158, https://doi.org/10.1038/s41573-018-0003-2.
11. Serjeant, G. R. Mortality from Sickle Cell Disease in Africa. *Br. Med. J.* **2005**, *330*, 432–433,https://doi.org/10.1136/bmj.330.7489.432.
12. Aggarwal, A.; Mehta, S.; Gupta, D.; Sheikh, S.; Pallagatti, S.; Singh, R.; Singla, I. Clinical & Immunological Erythematosus Patients Characteristics in Systemic Lupus Maryam. *J. Dent. Educ.* **2012**, *76*, 1532–1539,https://doi.org/10.4103/ijmr.IJMR.
13. Rogers, K.; Balachandren, N.; Awogbade, M.; Johns, J. Sickle Cell Disease in Pregnancy. *Obstet. Gynaecol. Reprod. Med.* **2019**, *29*, 61–69,https://doi.org/10.1016/j.ogrm.2019.01.006.
14. Piel, F. B.; Tatem, A. J.; Huang, Z.; Gupta, S.; Williams, T. N.; Weatherall, D. J. Global Migration and the Changing Distribution of Sickle Haemoglobin: A Quantitative Study of Temporal Trends between 1960 and 2000. *Lancet Glob. Heal.* **2014**, *2*,https://doi.org/10.1016/S2214-109X(13)70150-5.
15. Houwing, M. E.; de Pagter, P. J.; van Beers, E. J.; Biemond, B. J.; Rettenbacher, E.; Rijneveld, A. W.; Schols, E. M.; Philipsen, J. N. J.; Tamminga, R. Y. J.; van Draat, K. F.; Nur, E.; Cnossen, M. H. Sickle Cell Disease: Clinical Presentation and Management of a Global Health Challenge. *Blood Rev.* **2019**, *37*, 100580,https://doi.org/10.1016/j.blre.2019.05.004.

16. Palomo, M.; Diaz-Ricart, M.; Carreras, E. Is Sickle Cell Disease-Related Neurotoxicity a Systemic Endotheliopathy? *Hematol. Oncol. Stem Cell Ther.* **2020**, *13*, 111–115,https://doi.org/10.1016/j.hemonc.2019.12.005.
17. Piel, F. B.; Hay, S. I.; Gupta, S.; Weatherall, D. J.; Williams, T. N. Global Burden of Sickle Cell Anaemia in Children under Five, 2010-2050: Modelling Based on Demographics, Excess Mortality, and Interventions. *PLoS Med.* **2013**, *10*, https://doi.org/10.1371/journal.pmed.1001484.
18. Piel, F. B.; Steinberg, M. H.; Rees, D. C. Sickle Cell Disease. *N. Engl. J. Med.* **2017**, *376*, 1561–1573,https://doi.org/10.1056/NEJMra1510865.
19. Rees, D. C.; Williams, T. N.; Gladwin, M. T. Sickle-Cell Disease. *Lancet* **2010**, *376*, 2018–2031, https://doi.org/10.1016/S0140-6736 (10)61029-X.
20. McGann, P. T.; Hernandez, A. G.; Ware, R. E. Sickle Cell Anemia in Sub-Saharan Africa: Advancing the Clinical Paradigm through Partnerships and Research. *Blood* **2017**, *129*, 155–161, https://doi.org/10.1182/blood-2016-09-702324.
21. Quinn, C. T.; Rogers, Z. R.; McCavit, T. L.; Buchanan, G. R. Improved Survival of Children and Adolescents with Sickle Cell Disease. *Blood* **2010**, *115* (17), 3447–3452,https://doi.org/10.1182/blood-2009-07-233700.
22. Sundd, P.; Gladwin, M. T.; Novelli, E. M. Pathophysiology of Sickle Cell Disease. *Annu. Rev. Pathol. Mech. Dis.* **2019**, *14*, 263–292,https://doi.org/10.1146/annurev-pathmechdis-012418-012838.
23. Kato, G. J.; Steinberg, M. H.; Gladwin, M. T. Intravascular Hemolysis and the Pathophysiology of Sickle Cell Disease. *J. Clin. Invest.* **2017**, *127*, 750–760,https://doi.org/10.1172/JCI89741.
24. Alayash, A. I. Oxidative Pathways in the Sickle Cell and beyond. *Blood Cells, Mol. Dis.* **2018**, *70*, 78–86,https://doi.org/10.1016/j.bcmd.2017.05.009.
25. Morris, C. R.; Kato, G. J.; Poljakovic, M.; Wang, X.; Blackwelder, W. C.; Sanchdev, V.; Hazen, S. L.; Vichinsky, P.; Jr, S. M. M.; Gladwin, M. T. NIH Public Access. **2007**, *294*, 81–90.
26. Cabrales, P.; Friedman, J. M. HBOC Vasoactivity: Interplay Between Nitric Oxide Scavenging and Capacity to Generate Bioactive Nitric Oxide Species. *Antioxid. Redox Signal.* **2013**, *18*, 2284–2297,https://doi.org/10.1089/ars.2012.5099.
27. Kyle Mack, A.; Kato, G. J. Sickle Cell Disease and Nitric Oxide: A Paradigm Shift? *Int. J. Biochem. Cell Biol.* **2006**, *38*, 1237–1243,https://doi.org/10.1016/j.biocel.2006.01.010.
28. Ataga, K. I.; Brittain, J. E.; Desai, P.; May, R.; Jones, S.; Delaney, J.; Strayhorn, D.; Hinderliter, A.; Key, N. S. Association of Coagulation Activation with Clinical Complications in Sickle Cell Disease. *PLoS One* **2012**, *7* , https://doi.org/10.1371/journal.pone.0029786.
29. Potoka, K. P.; Gladwin, M. T. Vasculopathy and Pulmonary Hypertension in Sickle Cell Disease. *Am. J. Physiol. - Lung Cell. Mol. Physiol.* **2015**, *308* (4), L314–L324, https://doi.org/10.1152/ajplung.00252.2014.
30. McGann, P. T.; Nero, A. C.; Ware, R. E. Current Management of Sickle Cell Anemia. *Cold Spring Harb. Perspect. Med.* **2013**, *3*, 1–17. https://doi.org/10.1101/cshperspect.a011817.
31. Halphen, I.; Elie, C.; Brousse, V.; Le Bourgeois, M.; Allali, S.; Bonnet, D.; De Montalembert, M. Severe Nocturnal and Postexercise Hypoxia in Children and Adolescents with Sickle Cell Disease. *PLoS One* **2014**, *9*, 1–8,https://doi.org/10.1371/journal.pone.0097462.
32. Ballas, S. K.; Gupta, K.; Adams-Graves, P. Sickle Cell Pain: A Critical Reappraisal. *Blood* **2012**, *120* (18), 3647–3656,https://doi.org/10.1182/blood-2012-04-383430.
33. Stuart, MJ; Nagel RL. Sickle-cell disease. The Lancet **2004**, 364:1343-60, https://doi.org/10.1016/S0140-6736(04)17192-4
34. Yuditskaya, S.; Suffredini, A. F.; & Kato, G. J. The proteome of sickle cell disease: insights from exploratory proteomic profiling. *Expert review of proteomics* **2010**, *7*, 833–848.
35. Manci, E. A.; Culberson, D. E.; Yang, Y. M.; Gardner, T. M.; Powell, R.; Haynes, J.; Shah, A. K.; Mankad, V. N. Causes of Death in Sickle Cell Disease: An Autopsy Study. *Br. J. Haematol.* **2003**, *123*, 359–365,https://doi.org/10.1046/j.1365-2141.2003.04594.x.

36. Saraf, S. L.; Shah, B. N.; Zhang, X.; Han, J.; Tayo, B. O.; Abbasi, T.; Ostrower, A.; Guzman, E.; Molokie, R. E.; Gowhari, M.; Hassan, J.; Jain, S.; Cooper, R. S.; Machado, R. F.; Lash, J. P.; Gordeuk, V. R. APOL1,α-Thalassemia, and BCL11A Variants as a Genetic Risk Profile for Progression of Chronic Kidney Disease in Sickle Cell Anemia. *Haematologica* **2017**, *102*, e1–e6, https://doi.org/10.3324/haematol.2016.154153.
37. De Montalembert, M. Advances in Sickle Cell Disease. *Bull. Acad. Natl. Med.* **2008**, *192*, 1375–1381,https://doi.org/10.1016/S0001-4079(19)32687-1.
38. M.I., S.; V.E., P. Preventing and Treating Infections in Children with Asplenia or Hyposplenia. *Paediatr. Child Heal.* **2014**, *19*, 271–274.
39. Makani, J.; Williams, T. N.; Marsh, K. Sickle Cell Disease in Africa: Burden and Research Priorities. *Ann. Trop. Med. Parasitol.* **2007**, *101*, 3–14,https://doi.org/10.1179/136485907X154638.
40. Stuart, M. J.; Setty, B. N. Y. Acute Chest Syndrome of Sickle Cell Disease: New Light on an Old Problem. *Curr. Opin. Hematol.* **2001**, *8*, 111–122, https://doi.org/10.1097/00062752-200103000-00009.
41. DeBaun, M. R.; Rodeghier, M.; Cohen, R.; Kirkham, F. J.; Rosen, C. L.; Roberts, I.; Cooper, B.; Stocks, J.; Wilkey, O.; Inusa, B.; Warner, J. O.; Strunk, R. C. Factors Predicting Future ACS Episodes in Children with Sickle Cell Anemia. *Am. J. Hematol.* **2014**, *89*, E212–E217, https://doi.org/10.1002/ajh.23819.
42. Alkindi, S.; Al-Busaidi, I.; Al-Salami, B.; Raniga, S.; Pathare, A.; Ballas, S. K. Predictors of Impending Acute Chest Syndrome in Patients with Sickle Cell Anaemia. *Sci. Rep.* **2020**, *10*, 1–6, https://doi.org/10.1038/s41598-020-59258-y.
43. Montague, D. K.; Jarow, J.; Broderick, G. A.; Dmochowski, R. R.; Heaton, J. P. W.; Lue, T. F.; Nehra, A.; Sharlip, I. D. American Urological Association Guideline on the Management of Priapism. *J. Urol.* **2003**, *170*, 1318–1324,https://doi.org/10.1097/01.ju.0000087608.07371.ca.
44. Minniti, C. P.; Eckman, J.; Sebastiani, P.; Steinberg, M. H.; Ballas, S. K. Leg Ulcers in Sickle Cell Disease. *Am. J. Hematol.* **2010**, *85*, 831–833,https://doi.org/10.1002/ajh.21838.
45. Ware, R. E.; Rees, R. C.; Sarnaik, S. A.; Iyer, R. V.; Alvarez, O. A.; Casella, J. F.; Shulkin, B. L.; Shalaby-Rana, E.; Strife, C. F.; Miller, J. H.; Lane, P. A.; Wang, W. C.; Miller, S. T. Renal Function in Infants with Sickle Cell Anemia: Baseline Data from the BABY HUG Trial. *J. Pediatr.* **2010**, *156*, 66–70.e1, https://doi.org/10.1016/j.jpeds.2009.06.060.
46. Clarke, G. M.; Higgins, T. N. Laboratory Investigation of Hemoglobinopathies and Thalassemias: Review and Update. *Clin. Chem.* **2000**, *46*, 1284–1290, https://doi.org/10.1093/clinchem/46.8.1284.
47. Urrechaga, E.; Borque, L.; Escanero, J. F. The Role of Automated Measurement of RBC Subpopulations in Differential Diagnosis of Microcytic Anemia and β-Thalassemia Screening. *Am. J. Clin. Pathol.* **2011**, *135*, 374–379,https://doi.org/10.1309/AJCPJRH1I0XTNFGA.
48. Greene, D. N.; Vaugn, C. P.; Crews, B. O.; Agarwal, A. M. Advances in Detection of Hemoglobinopathies. *Clin. Chim. Acta* **2014**, *439*, 50–57,https://doi.org/10.1016/j.cca.2014.10.006.
49. De Angelis Curtis, S.; Kubiak, M.; Kurdziel, K.; Materazzi, S.; Vecchio, S. Crystal Structure and Thermoanalytical Study of a cadmium(II) Complex with 1-Allylimidazole. *J. Anal. Appl. Pyrolysis* **2010**, *87*, 175–179,https://doi.org/10.1016/j.jaap.2009.11.007.
50. Risoluti, R.; Caprari, P.; Gullifa, G.; Massimi, S.; Sorrentino, F.; Maffei, L.; Materazzi, S. Innovative Screening Test for the Early Detection of Sickle Cell Anemia. *Talanta* **2020**, *219*, 121243, https://doi.org/10.1016/j.talanta.2020.121243.
51. Ryan, K.; Bain, B. J.; Worthington, D.; James, J.; Plews, D.; Mason, A.; Roper, D.; Rees, D. C.; De La Salle, B.; Streetly, A. Significant Haemoglobinopathies: Guidelines for Screening and Diagnosis. *Br. J. Haematol.* **2010**, *149*, 35–49,https://doi.org/10.1111/j.1365-2141.2009.08054.x.
52. Daniel, Y., Van Campen, J., Silcock, L., Yau, M., Ahn, J. W., Ogilvie, C., … Oteng-Ntim, E. (2019). Non- Invasive Prenatal Diagnosis (NIPD) of Sickle-Cell Disease By Massively Parallel Sequencing

of Cell-Free Fetal DNA in Maternal Serum. *Blood*, *134*(Supplement_1), 2085. https://doi.org/10.1182/blood-2019-127945

53. Alapan, Y.; Fraiwan, A.; Kucukal, E.; Hasan, M. N.; Ung, R.; Kim, M.; Odame, I.; Little, J. A.; Gurkan, U. A. Emerging Point-of-Care Technologies for Sickle Cell Disease Screening and Monitoring. *Expert Rev. Med. Devices* **2016**, *13*, 1073–1093,https://doi.org/10.1080/17434440.2016.1254038.
54. Alenzi, F. Q.; AlShaya, D. S. Biochemical and Molecular Analysis of the Beta-Globin Gene on Saudi Sickle Cell Anemia. *Saudi J. Biol. Sci.* **2019**, *26*, 1377–1384, https://doi.org/10.1016/j.sjbs.2019.03.003.
55. Steinberg, M. H. Pathophysiologically Based Drug Treatment of Sickle Cell Disease. **2006**, *27*. https://doi.org/10.1016/j.tips.2006.02.007.
56. Power-Hays, A.; Ware, R. E. Effective Use of Hydroxyurea for Sickle Cell Anemia in Low-Resource Countries. *Curr. Opin. Hematol.* **2020**, *27*, 172–180, https://doi.org/10.1097/MOH.0000000000000582.
57. Cartron, J.; Elion, J. Erythroid Adhesion Molecules in Sickle Cell Disease : Effect of Hydroxyurea ´ Cules D ' Adhe ´ Rence Dans La Dre ´ Panocytose : Mole ´ E Effet de L ' Hydroxyure. **2008**, *15*, 39–50,https://doi.org/10.1016/j.tracli.2008.05.001.
58. Johnson, CT; elen, MJ. Adhesion molecules and hydroxyurea in the pathophysiology of sickle cell disease. Haematologica. 2008, 93, 481-5, https://doi.org/10.3324/haematol.12734.
59. Steinberg, M. H.; Barton, F.; Castro, O.; Pegelow, C. H.; Ballas, S. K.; Kutlar, A.; Orringer, E.; Bellevue, R.; Olivieri, N.; Eckman, J.; Varma, M.; Ramirez, G.; Adler, B.; Smith, W.; Carlos, T.; Ataga, K.; DeCastro, L.; Bigelow, C.; Saunthararajah, Y.; Telfer, M.; Vichinsky, E.; Claster, S.; Shurin, S.; Bridges, K.; Waclawiw, M.; Bonds, D.; Terrin, M. Effect of Hydroxyurea on Mortality and Morbidity in Adult Sickle Cell Anemia: Risks and Benefits Up to 9 Years of Treatment. *J. Am. Med. Assoc.* **2003**, *289*, 1645–1651,https://doi.org/10.1001/jama.289.13.1645.
60. Charache, S.; Terrin, M. L.; Moore, R. D.; Dover, G. J.; Barton, F. B.; Eckert, S. V.; McMahon, R. P.; Bonds, D. R. Effect of Hydroxyurea on the Frequency of Painful Crises in Sickle Cell Anemia. *N. Engl. J. Med.* **1995**, *332*, 1317–1322,https://doi.org/10.1056/nejm199505183322001.
61. Lanzkron, S.; Strouse, J. J.; Wilson, R.; Beach, M. C.; Haywood, C.; Park, H.; Witkop, C.; Bass, E. B.; Segal, J. B. Annals of Internal Medicine NIH Conference Systematic Review : Hydroxyurea for the Treatment of Adults with Sickle Cell Disease. *Ann. Intern. Med.* **2008**, 939–956.
62. McGann, P. T.; Ware, R. E. Hydroxyurea Therapy for Sickle Cell Anemia. *Expert Opin. Drug Saf.* **2015**, *14*, 1749–1758,https://doi.org/10.1517/14740338.2015.1088827.
63. Ware, R. E. How I Use Hydroxyurea to Treat Young Patients with Sickle Cell Anemia. *Blood* **2010**, *115* (26), 5300–5311. https://doi.org/10.1182/blood-2009-04-146852.
64. Wang, W. C.; Wynn, L. W.; Rogers, Z. R.; Scott, J. P.; Lane, P. A.; Ware, R. E. A Two-Year Pilot Trial of Hydroxyurea in Very Young Children with Sickle-Cell Anemia. *J. Pediatr.* **2001**, *139*, 790–796, https://doi.org/10.1067/mpd.2001.119590.
65. Hankins, JS; Helton, KJ; McCarville, MB; Li, CS; Wang, WC; Ware, RE. Preservation of spleen and brain function in children with sickle cell anemia treated with hydroxyurea. *Pediatr Blood Cancer*. **2008**,50,293-7.
66. Papadopoulou, E.; Teli, A.; Theodoridou, S.; Gompakis, N.; Economou, M. Safety and Efficacy of Hydroxyurea in Children and Adolescents with Sickle/betathalassemia: Two-Year Experience. *Hippokratia* **2015**, *19*, 172–175.
67. Niihara, Y.; Zerez, C. R.; Akiyama, D. S.; Tanaka, K. R. Oral L-Glutamine Therapy for Sickle Cell Anemia: I. Subjective Clinical Improvement and Favorable Change in Red Cell NAD Redox Potential. *Am. J. Hematol.* **1998**, *58*, 117–121,https://doi.org/10.1002/(SICI)1096-8652(199806)58:2<117::AID-AJH5>3.0.CO;2-V.

68. Niihara, Y. L-Glutamine Therapy Reduces Hospitalization for Sickle Cell Anemia and Sickle β°-Thalassemia Patients at Six Months – A Phase II Randomized Trial. *Clin. Pharmacol. Biopharm.* **2014**, *3*, 1–5. https://doi.org/10.4172/2167-065x.1000116.
69. Niihara, Y.; Miller, S. T.; Kanter, J.; Lanzkron, S.; Smith, W. R.; Hsu, L. L.; Gordeuk, V. R.; Viswanathan, K.; Sarnaik, S.; Osunkwo, I.; Guillaume, E.; Sadanandan, S.; Sieger, L.; Lasky, J. L.; Panosyan, E. H.; Blake, O. A.; New, T. N.; Bellevue, R.; Tran, L. T.; Razon, R. L.; Stark, C. W.; Neumayr, L. D.; Vichinsky, E. P. A Phase 3 Trial of L -Glutamine in Sickle Cell Disease. *N. Engl. J. Med.* **2018**, *379*, 226–235. https://doi.org/10.1056/nejmoa1715971.
70. Gardner, R. V. Sickle Cell Disease: Advances in Treatment. *Ochsner J.* **2018**, *18*, 377–389, https://doi.org/10.31486/toj.18.0076.
71. Zaidi, A. U.; Heeney, M. M. A Scientific Renaissance: Novel Drugs in Sickle Cell Disease. *Pediatr. Clin. North Am.* **2018**, *65*, 445–464,https://doi.org/10.1016/j.pcl.2018.01.006.
72. Xu, J.; Peng, C.; Sankaran, V. G.; Shao, Z.; Esrick, E. B.; Chong, B. G.; Ippolito, G. C.; Fujiwara, Y.; Ebert, B. L.; Tucker, P. W.; Orkin, S. H. Correction of Sickle Cell Disease in Adult Mice by Interference with Fetal Hemoglobin Silencing. *Science (80-.).* **2011**, *334*, 993–996, https://doi.org/10.1126/science.1211053.
73. Ginder, G. D. Epigenetic Regulation of Fetal Globin Gene Expression in Adult Erythroid Cells. *Transl. Res.* **2015**, *165*, 115–125,https://doi.org/10.1016/j.trsl.2014.05.002.
74. Basak, A.; Sankaran, V. G. Regulation of the Fetal Hemoglobin Silencing Factor BCL11A. *Ann. N. Y. Acad. Sci.* **2016**, *1368*, 25–30,https://doi.org/10.1111/nyas.13024.
75. Molokie, R.; Lavelle, D.; Gowhari, M.; Pacini, M.; Krauz, L.; Hassan, J.; Ibanez, V.; Ruiz, M. A.; Ng, K. P.; Woost, P.; Radivoyevitch, T.; Pacelli, D.; Fada, S.; Rump, M.; Hsieh, M.; Tisdale, J. F.; Jacobberger, J.; Phelps, M.; Engel, J. D.; Saraf, S.; Hsu, L. L.; Gordeuk, V.; DeSimone, J.; Saunthararajah, Y. Oral Tetrahydrouridine and Decitabine for Non-Cytotoxic Epigenetic Gene Regulation in Sickle Cell Disease: A Randomized Phase 1 Study. *PLoS Med.* **2017**, *14*, 1–28, https://doi.org/10.1371/journal.pmed.1002382.
76. DeSimone, J.; Koshy, M.; Dorn, L.; Lavelle, D.; Bressler, L.; Molokie, R.; Talischy, N. Maintenance of Elevated Fetal Hemoglobin Levels by Decitabine during Dose Interval Treatment of Sickle Cell Anemia. *Blood* **2002**, *99*, 3905–3908,https://doi.org/10.1182/blood.V99.11.3905.
77. Saunthararajah, Y ; Molokie, R ; Saraf, S ; et al. Clinical effectiveness of decitabine in severe sickle cell disease. Br J Haematol. **2008**, 141,126-9, https://doi:10.1111/j.1365-2141.2008.07027.x.
78. Ebrahem, Q.; Mahfouz, R.; Ng, K. P.; Saunthararajah, Y. High Cytidine Deaminase Expression in the Liver Provides Sanctuary for Cancer Cells from Decitabine Treatment Effects. *Oncotarget* **2012**, *3*, 1137–1145,https://doi.org/10.18632/oncotarget.597.
79. Ataga, K. I.; Desai, P. C. Advances in New Drug Therapies for the Management of Sickle Cell Disease. *Expert Opin. Orphan Drugs* **2018**, *6*, 329–343,https://doi.org/10.1080/21678707.2018.1471983.
80. Manwani, D.; Frenette, P. S. Vaso-Occlusion in Sickle Cell Disease: Pathophysiology and Novel Targeted Therapies. *Blood* **2013**, *122*, 3892–3898,https://doi.org/10.1182/blood-2013-05-498311.
81. Shiu, Y. T.; Udden, M. M.; McIntire, L. V. Perfusion with Sickle Erythrocytes up-Regulates ICAM-1 and VCAM-1 Gene Expression in Cultured Human Endothelial Cells. *Blood* **2000**, *95*, 3232–3241,https://doi.org/10.1182/blood.v95.10.3232.010k16_3232_3241.
82. Zennadi, R.; Chien, A.; Xu, K.; Batchvarova, M.; Telen, M. J. Sickle Red Cells Induce Adhesion of Lymphocytes and Monocytes to Endothelium. *Blood* **2008**, *112*, 3474–3483, https://doi.org/10.1182/blood-2008-01-134346.
83. Matsui, N. M.; Borsig, L.; Rosen, S. D.; Yaghmai, M.; Varki, A.; Embury, S. H. P-Selectin Mediates the Adhesion of Sickle Erythrocytes to the Endothelium. *Blood* **2001**, *98*, 1955–1962, https://doi.org/10.1182/blood.V98.6.1955.

84. Embury, S. H.; Matsui, N. M.; Ramanujam, S.; Mayadas, T. N.; Noguchi, C. T.; Diwan, B. A.; Mohandas, N.; Cheung, A. T. W. The Contribution of Endothelial Cell P-Selectin to the Microvascular Flow of Mouse Sickle Erythrocytes in Vivo. *Blood* **2004**, *104*, 3378–3385, https://doi.org/10.1182/blood-2004-02-0713.
85. Field, J. J.; Lin, G.; Okam, M. M.; Majerus, E.; Keefer, J.; Onyekwere, O.; Ross, A.; Campigotto, F.; Neuberg, D.; Linden, J.; Nathan, D. G. Sickle Cell Vaso-Occlusion Causes Activation of iNKT Cells That Is Decreased by the Adenosine A2A Receptor Agonist Regadenoson. *Blood* **2013**, *121* (17), 3329–3334, https://doi.org/10.1182/blood-2012-11-465963.
86. Ataga, K. I.; Kutlar, A.; Kanter, J.; Liles, D.; Cancado, R.; Friedrisch, J.; Guthrie, T. H.; Knight-Madden, J.; Alvarez, O. A.; Gordeuk, V. R.; Gualandro, S.; Colella, M. P.; Smith, W. R.; Rollins, S. A.; Stocker, J. W.; Rother, R. P. Crizanlizumab for the Prevention of Pain Crises in Sickle Cell Disease. *N. Engl. J. Med.* **2017**, *376*, 429–439,https://doi.org/10.1056/nejmoa1611770.
87. Kutlar, A.; Kanter, J.; Liles, D. K.; Alvarez, O. A.; Cançado, R. D.; Friedrisch, J. R.; Knight-Madden, J. M.; Bruederle, A.; Shi, M.; Zhu, Z.; Ataga, K. I. Effect of Crizanlizumab on Pain Crises in Subgroups of Patients with Sickle Cell Disease: A SUSTAIN Study Analysis. *Am. J. Hematol.* **2019**, *94*, 55–61, https://doi.org/10.1002/ajh.25308.
88. Chang, J.; Patton, J. T.; Sarkar, A.; Ernst, B.; Magnani, J. L.; Frenette, P. S. GMI-1070, a Novel Pan-Selectin Antagonist, Reverses Acute Vascular Occlusions in Sickle Cell Mice. *Blood* **2010**, *116*, 1779–1786,https://doi.org/10.1182/blood-2009-12-260513.
89. Wun, T.; Styles, L.; DeCastro, L.; Telen, M. J.; Kuypers, F.; Cheung, A.; Kramer, W.; Flanner, H.; Rhee, S.; Magnani, J. L.; Thackray, H. Phase 1 Study of the E-Selectin Inhibitor GMI 1070 in Patients with Sickle Cell Anemia. *PLoS One* **2014**, *9*, 1–12,https://doi.org/10.1371/journal.pone.0101301.
90. Telen, M. J.; Wun, T.; McCavit, T. L.; De Castro, L. M.; Krishnamurti, L.; Lanzkron, S.; Hsu, L. L.; Smith, W. R.; Rhee, S.; Magnani, J. L.; Thackray, H. Randomized Phase 2 Study of GMI-1070 in SCD: Reduction in Time to Resolution of Vaso-Occlusive Events and Decreased Opioid Use. *Blood* **2015**, *125*, 2656–2664,https://doi.org/10.1182/blood-2014-06-583351.
91. Öztaş, Y.; Boşgelmez, İ. İ. Oxidative Stress in Sickle Cell Disease and Emerging Roles for Antioxidants in Treatment Strategies. *Pathology* **2020**, 65–75,https://doi.org/10.1016/b978-0-12-815972-9.00006-8.
92. Gizi, A.; Papassotiriou, I.; Apostolakou, F.; Lazaropoulou, C.; Papastamataki, M.; Kanavaki, I.; Kalotychou, V.; Goussetis, E.; Kattamis, A.; Rombos, I.; Kanavakis, E. Assessment of Oxidative Stress in Patients with Sickle Cell Disease: The Glutathione System and the Oxidant-Antioxidant Status. *Blood Cells, Mol. Dis.* **2011**, *46*, 220–225,https://doi.org/10.1016/j.bcmd.2011.01.002.
93. Daak, A.; Rabinowicz, A.; Ghebremeskel, K. Omega-3 Fatty Acids Are a Potential Therapy for Patients with Sickle Cell Disease. *Nat. Rev. Dis. Prim.* **2018**, *4*, 2973360. https://doi.org/10.1038/s41572-018-0012-9.
94. Tomer, A.; Kasey, S.; Connor, W. E.; Clark, S.; Harker, L. A.; Eckman, J. R. Reduction of Pain Episodes and Prothrombotic Activity in Sickle Cell Disease by Dietary N-3 Fatty Acids. *Thromb. Haemost.* **2001**, *85*, 966–974,https://doi.org/10.1055/s-0037-1615948.
95. Daak, A. A.; Ghebremeskel, K.; Hassan, Z.; Attallah, B.; Azan, H. H.; Elbashir, M. I.; Crawford, M. Effect of Omega-3 (n-3) Fatty Acid Supplementation in Patients with Sickle Cell Anemia: Randomized, Double-Blind, Placebo-Controlled Trial. *Am. J. Clin. Nutr.* **2013**, *97*, 37–44, https://doi.org/10.3945/ajcn.112.036319.
96. Pace, B. S.; Shartava, A.; Pack-Mabien, A.; Mulekar, M.; Ardia, A.; Goodman, S. R. Effects of N-Acetylcysteine on Dense Cell Formation in Sickle Cell Disease. *Am. J. Hematol.* **2003**, *73*, 26–32, https://doi.org/10.1002/ajh.10321.
97. Oniyangi, O., & Cohall, D. H. Phytomedicines (medicines derived from plants) for sickle cell disease. *Cochrane Database of Systematic Reviews*, 2020, *9*. https://doi.org/10.1002/14651858.CD004448.pub7

98. Cotoraci, C., Ciceu, A., Sasu, A., & Hermenean, A. (2021). Natural Antioxidants in Anemia Treatment. *International Journal of Molecular Sciences* , Vol. 22. https://doi.org/10.3390/ijms22041883
99. Mohan, J. S.; Lip, G. Y. H.; Wright, J.; Bareford, D.; Blann, A. D. Plasma Levels of Tissue Factor and Soluble E-Selectin in Sickle Cell Disease: Relationship to Genotype and to Inflammation. *Blood Coagul. Fibrinolysis* **2005**, *16*, 209–214,https://doi.org/10.1097/01.mbc.0000164431.98169.8f.
100. Lee, S. P.; Ataga, K. I.; Orringer, E. P.; Phillips, D. R.; Parise, L. V. Biologically Active CD40 Ligand Is Elevated in Sickle Cell Anemia: Potential Role for Platelet-Mediated Inflammation. *Arterioscler. Thromb. Vasc. Biol.* **2006**, *26*, 1626–1631, https://doi.org/10.1161/01.ATV.0000220374.00602.a2.
101. Sparkenbaugh, E.; Pawlinski, R. Interplay between Coagulation and Vascular Inflammation in Sickle Cell Disease. *Br. J. Haematol.* **2013**, *162*, 3–14,https://doi.org/10.1111/bjh.12336.
102. Qari, M. H.; Aljaouni, S. K.; Alardawi, M. S.; Fatani, H.; Alsayes, F. M.; Zografos, P.; Alsaigh, M.; Alalfi, A.; Alamin, M.; Gadi, A.; Mousa, S. A. Reduction of Painful Vaso-Occlusive Crisis of Sickle Cell Anaemia by Tinzaparin in a Double-Blind Randomized Trial. *Thromb. Haemost.* **2007**, *98*, 392–396, https://doi.org/10.1160/TH06-12-0718.
103. van Zuuren, E. J.; Fedorowicz, Z. Low-Molecular-Weight Heparins for Managing Vaso-Occlusive Crises in People with Sickle Cell Disease. *Cochrane Database Syst. Rev.* **2015**, *2015*, https://doi.org/10.1002/14651858.CD010155.pub3.
104. White, J.; Lindgren, M.; Liu, K.; Gao, X.; Jendeberg, L.; Hines, P. Sevuparin Blocks Sickle Blood Cell Adhesion and Sickle-Leucocyte Rolling on Immobilized L-Selectin in a Dose Dependent Manner. *Br. J. Haematol.* **2019**, *184*, 873–876,https://doi.org/10.1111/bjh.15188.
105. Heeney, M. M.; Hoppe, C. C.; Abboud, M. R.; Inusa, B.; Kanter, J.; Ogutu, B.; Brown, P. B.; Heath, L. E.; Jakubowski, J. A.; Zhou, C.; Zamoryakhin, D.; Agbenyega, T.; Colombatti, R.; Hassab, H. M.; Nduba, V. N.; Oyieko, J. N.; Robitaille, N.; Segbefia, C. I.; Rees, D. C. A Multinational Trial of Prasugrel for Sickle Cell Vaso-Occlusive Events. *N. Engl. J. Med.* **2016**, *374*, 625–635,https://doi.org/10.1056/nejmoa1512021.
106. Wun, T.; Soulieres, D.; Frelinger, A. L.; Krishnamurti, L.; Novelli, E. M.; Kutlar, A.; Ataga, K. I.; Knupp, C. L.; McMahon, L. E.; Strouse, J. J.; Zhou, C.; Heath, L. E.; Nwachuku, C. E.; Jakubowski, J. A.; Riesmeyer, J. S.; Winters, K. J. A Double-Blind, Randomized, Multicenter Phase 2 Study of Prasugrel versus Placebo in Adult Patients with Sickle Cell Disease. *J. Hematol. Oncol.* **2013**, *6*, 1–10. https://doi.org/10.1186/1756-8722-6-17.
107. Zhang, D.; Xu, C.; Manwani, D.; Frenette, P. S. Neutrophils, Platelets, and Inflammatory Pathways at the Nexus of Sickle Cell Disease Pathophysiology. *Blood* **2016**, *127*, 801–809, https://doi.org/10.1182/blood-2015-09-618538.
108. Qari, M. H.; Dier, U.; Mousa, S. A. Biomarkers of Inflammation, Growth Factor, and Coagulation Activation in Patients with Sickle Cell Disease. *Clin. Appl. Thromb.* **2012**, *18*, 195–200,https://doi.org/10.1177/1076029611420992.
109. Field, J. J.; Lin, G.; Okam, M. M.; Majerus, E.; Keefer, J.; Onyekwere, O.; Ross, A.; Campigotto, F.; Neuberg, D.; Linden, J.; Nathan, D. G. Sickle Cell Vaso-Occlusion Causes Activation of iNKT Cells That Is Decreased by the Adenosine A2A Receptor Agonist Regadenoson. *Blood* **2013**, *121*, 3329–3334,https://doi.org/10.1182/blood-2012-11-465963.
110. Field, J. J.; Majerus, E.; Gordeuk, V. R.; Gowhari, M.; Hoppe, C.; Heeney, M. M.; Achebe, M.; George, A.; Chu, H.; Sheehan, B.; Puligandla, M.; Neuberg, D.; Lin, G.; Linden, J.; Nathan, D. G. Randomized Phase 2 Trial of Regadenoson for Treatment of Acute Vaso-Occlusive Crises in Sickle Cell Disease. *Blood Adv.* **2017**, *1*, 1645–1649, https://doi.org/10.1182/bloodadvances.2017009613.
111. Ataga, K. I. Novel Therapies in Sickle Cell Disease. *Hematology Am. Soc. Hematol. Educ. Program* **2009**, 54–61,https://doi.org/10.1182/asheducation-2009.1.54.
112. Marouf, R. Blood Transfusion in Sickle Cell Disease. *Hemoglobin* **2011**, *35*, 495–502, https://doi.org/10.3109/03630269.2011.596984.

113. Howard, J. The Role of Blood Transfusion in Sickle Cell Disease. *ISBT Sci. Ser.* **2013**, *8*, 225–228. https://doi.org/10.1111/voxs.12047.
114. Howard, J. Sickle Cell Disease: When and How to Transfuse. *Hematology* **2016**, *2016*, 625–631. https://doi.org/10.1182/asheducation-2016.1.625.
115. DeBaun, M. R.; Gordon, M.; McKinstry, R. C.; Noetzel, M. J.; White, D. A.; Sarnaik, S. A.; Meier, E. R.; Howard, T. H.; Majumdar, S.; Inusa, B. P. D.; Telfer, P. T.; Kirby-Allen, M.; McCavit, T. L.; Kamdem, A.; Airewele, G.; Woods, G. M.; Berman, B.; Panepinto, J. A.; Fuh, B. R.; Kwiatkowski, J. L.; King, A. A.; Fixler, J. M.; Rhodes, M. M.; Thompson, A. A.; Heiny, M. E.; Redding-Lallinger, R. C.; Kirkham, F. J.; Dixon, N.; Gonzalez, C. E.; Kalinyak, K. A.; Quinn, C. T.; Strouse, J. J.; Miller, J. P.; Lehmann, H.; Kraut, M. A.; Ball, W. S.; Hirtz, D.; Casella, J. F. Controlled Trial of Transfusions for Silent Cerebral Infarcts in Sickle Cell Anemia. *N. Engl. J. Med.* **2014**, *371*, 699–710, https://doi.org/10.1056/nejmoa1401731.
116. Styles, L. A.; Abboud, M.; Larkin, S.; Lo, M.; Kuypers, F. A. Transfusion Prevents Acute Chest Syndrome Predicted by Elevated Secretory Phospholipase A2. *Br. J. Haematol.* **2007**, *136* (2), 343–344, https://doi.org/10.1111/j.1365-2141.2006.06409.x.
117. Howard, J.; Malfroy, M.; Llewelyn, C.; Choo, L.; Hodge, R.; Johnson, T.; Purohit, S.; Rees, D. C.; Tillyer, L.; Walker, I.; Fijnvandraat, K.; Kirby-Allen, M.; Spackman, E.; Davies, S. C.; Williamson, L. M. The Transfusion Alternatives Preoperatively in Sickle Cell Disease (TAPS) Study: A Randomised, Controlled, Multicentre Clinical Trial. *Lancet* **2013**, *381* , 930–938. https://doi.org/10.1016/S0140-6736(12)61726-7.
118. Files, B.; Brambilla, D.; Kutlar, A.; Miller, S.; Vichinsky, E.; Wang, W.; Granger, S.; Adams, R. J. Longitudinal Changes in Ferritin during Chronic Transfusion: A Report from the Stroke Prevention Trial in Sickle Cell Anemia (STOP). *J. Pediatr. Hematol. Oncol.* **2002**, *24*, 284–290, https://doi.org/10.1097/00043426-200205000-00013.
119. Chou, S. T.; Jackson, T.; Vege, S.; Smith-Whitley, K.; Friedman, D. F.; Westhoff, C. M. High Prevalence of Red Blood Cell Alloimmunization in Sickle Cell Disease despite Transfusion from Rh-Matched Minority Donors. *Blood* **2013**, *122*, 1062–1071,https://doi.org/10.1182/blood-2013-03-490623.
120. Chou, S. T. Transfusion Therapy for Sickle Cell Disease: A Balancing Act. *Hematology Am. Soc. Hematol. Educ. Program* **2013**, *2013*, 439–446,https://doi.org/10.1182/asheducation-2013.1.439.
121. Breuer, W.; Hershko, C.; Cabantchik, Z. I. The Importance of Non-Transferrin Bound Iron in Disorders of Iron Metabolism. *Transfus. Sci.* **2000**, *23*, 185–192,https://doi.org/10.1016/S0955-3886(00)00087-4.
122. Pennell, D. J.; Berdoukas, V.; Karagiorga, M.; Ladis, V.; Piga, A.; Aessopos, A.; Gotsis, E. D.; Tanner, M. A.; Smith, G. C.; Westwood, M. A.; Wonke, B.; Galanello, R. Randomized Controlled Trial of Deferiprone or Deferoxamine in Beta-Thalassemia Major Patients with Asymptomatic Myocardial Siderosis. *Blood* **2006**, *107*, 3738–3744,https://doi.org/10.1182/blood-2005-07-2948.
123. Vichinsky, E.; Onyekwere, O.; Porter, J.; Swerdlow, P.; Eckman, J.; Lane, P.; Files, B.; Hassell, K.; Kelly, P.; Wilson, F.; Bernaudin, F.; Forni, G. L.; Okpala, I.; Ressayre-Djaffer, C.; Alberti, D.; Holland, J.; Marks, P.; Fung, E.; Fischer, R.; Mueller, B. U.; Coates, T. A Randomised Comparison of Deferasirox versus Deferoxamine for the Treatment of Transfusional Iron Overload in Sickle Cell Disease. *Br. J. Haematol.* **2007**, *136*, 501–508,https://doi.org/10.1111/j.1365-2141.2006.06455.x.
124. Tanner, M. A.; Galanello, R.; Dessi, C.; Smith, G. C.; Westwood, M. A.; Agus, A.; Roughton, M.; Assomull, R.; Nair, S. V.; Walker, J. M.; Pennell, D. J. A Randomized, Placebo-Controlled, Double-Blind Trial of the Effect of Combined Therapy with Deferoxamine and Deferiprone on Myocardial Iron in Thalassemia Major Using Cardiovascular Magnetic Resonance. *Circulation* **2007**, *115*, 1876–1884,https://doi.org/10.1161/CIRCULATIONAHA.106.648790.

125. Whitley, R. J. The New England Journal of Medicine Downloaded from Nejm.org at UNIVERSITY OF LIVERPOOL on July 21, 2014. For Personal Use Only. No Other Uses without Permission. From the NEJM Archive. Copyright © 2009 Massachusetts Medical Society. All Rights Reserved. *New Engl. J. Med.* **1986**, *314* (3), 144–149.
126. Chan, Y. L.; Pang, L. M.; Chik, K. W.; Cheng, J. C. Y.; Li, C. K. Patterns of Bone Diseases in Transfusion-Dependent Homozygous Thalassaemia Major: Predominance of Osteoporosis and Desferrioxamine-Induced Bone Dysplasia. *Pediatr. Radiol.* **2002**, *32*, 492–497, https://doi.org/10.1007/s00247-002-0664-0.
127. De Sanctis, V.; Roos, M.; Gasser, T.; Fortini, M.; Raiola, G.; Galati, M. C.; Nicoletti, M. C.; Ponzi, G.; Gamberini, M. R.; Pedretti, S.; Corciulo, N.; Forni, G. L.; Cilla, V.; Meo, A.; Malizia, R.; D'Ascola, G.; Ciaccio, C.; Gerardi, C.; Mangiagli, A.; Pintor, C. Impact of Long-Term Iron Chelation Therapy on Growth and Endocrine Functions in Thalassaemia. *J. Pediatr. Endocrinol. Metab.* **2006**, *19*, 471–480,https://doi.org/10.5167/uzh-18427.
128. Sins, J. W. R.; Biemond, B. J.; van den Bersselaar, S. M.; Heijboer, H.; Rijneveld, A. W.; Cnossen, M. H.; Kerkhoffs, J. L. H.; van Meurs, A. H.; von Ronnen, F. B.; Zalpuri, S.; de Rijke, Y. B.; Ellen van der Schoot, C.; de Haas, M.; van der Bom, J. G.; Fijnvandraat, K. Early Occurrence of Red Blood Cell Alloimmunization in Patients with Sickle Cell Disease. *Am. J. Hematol.* **2016**, *91*, 763–769, https://doi.org/10.1002/ajh.24397.
129. Johnson, F. L.; Look, A. T.; Gockerman, J.; Ruggiero, M. R.; Dalla-Pozza, L.; Billings, F. T. Bone-Marrow Transplantation in a Patient with Sickle-Cell Anemia. *N. Engl. J. Med.* **1984**, *311*, 780–783, https://doi.org/10.1056/nejm198409203111207.
130. Gluckman, E.; Cappelli, B.; Bernaudin F., Labopin M.; Volt, F.; Carreras J. et al. Sickle Cell Disease: An International Survey of Results of HLA-Identical Sibling Hematopoietic Stem Cell Transplantation. *Blood* **2017**, *129*, 1548–1556, https://doi.org/10.1182/blood-2016-10-745711.There.
131. Hsieh, M. M.; Fitzhugh, C. D.; Weitzel, R. P.; Link, M. E.; Coles, W. A.; Zhao, X.; Rodgers, G. P.; Powell, J. D.; Tisdale, J. F. Nonmyeloablative HLA-Matched Sibling Allogeneic Hematopoietic Stem Cell Transplantation for Severe Sickle Cell Phenotype. *JAMA - J. Am. Med. Assoc.* **2014**, *312*, 48–56, https://doi.org/10.1001/jama.2014.7192.
132. Lucarelli, G. Bone Marrow Transplantation for Thalassaemia. *J. Intern. Med. Suppl.* **1997**, *242* , 49–52. https://doi.org/10.1111/joim.1997.242.s740.49.
133. Mahesri, M.; Schneeweiss, S.; Globe, D.; Mutebi, A.; Bohn, R.; Achebe, M.; Levin, R.; Desai, R. J. Clinical Outcomes Following Bone Marrow Transplantation in Patients with Sickle Cell Disease: A Cohort Study of US Medicaid Enrollees. *Eur. J. Haematol.* **2020**, 0–2, https://doi.org/10.1111/ejh.13546.
134. Kogel, F.; Hakimeh, D.; Sodani, P.; Lang, P.; Kühl, J. S.; Hundsdoerfer, P.; Künkele, A.; Eggert, A.; Oevermann, L.; Schulte, J. H. Allogeneic Hematopoietic Stem Cell Transplantation from Sibling and Unrelated Donors in Pediatric Patients with Sickle Cell disease—A Single Center Experience. *Pediatr. Transplant.* **2020**, 1–8, https://doi.org/10.1111/petr.13892.
135. Williams, T. N.; Thein, S. L. Sickle Cell Anemia and Its Phenotypes. *Annu. Rev. Genomics Hum. Genet.* **2018**, *19*, 113–147,https://doi.org/10.1146/annurev-genom-083117-021320.
136. Stuart, MJ; Nagel, RL. Sickle-cell disease. The Lancet. **2004** , 364,1343-60, DOI: 10.1016/S0140-6736(04)17192-4
137. Bolaños-Meade, J.; Fuchs, E. J.; Luznik, L.; Lanzkron, S. M.; Gamper, C. J.; Jones, R. J.; Brodsky, R. A. HLA-Haploidentical Bone Marrow Transplantation with Posttransplant Cyclophosphamide Expands the Donor Pool for Patients with Sickle Cell Disease. *Blood* **2012**, *120*, 4285–4291,https://doi.org/10.1182/blood-2012-07-438408.

138. Shenoy, S. Hematopoietic Stem-Cell Transplantation for Sickle Cell Disease: Current Evidence and Opinions. *Ther. Adv. Hematol.* **2013**, *4*, 335–344,https://doi.org/10.1177/2040620713483063.
139. Fitzhugh, C. D.; Abraham, A. A.; Tisdale, J. F.; Hsieh, M. M. Hematopoietic Stem Cell Transplantation for Patients with Sickle Cell Disease. Progress and Future Directions. *Hematol. Oncol. Clin. North Am.* **2014**, *28*, 1171–1185,https://doi.org/10.1016/j.hoc.2014.08.014.
140. Bhatia, M.; Sheth, S. Hematopoietic Stem Cell Transplantation in Sickle Cell Disease: Patient Selection and Special Considerations. *J. Blood Med.* **2015**, *6*, 229–238, https://doi.org/10.2147/JBM.S60515.
141. Arnold, S. D.; Brazauskas, R.; He, N.; Li, Y.; Aplenc, R.; Jin, Z.; Hall, M.; Atsuta, Y.; Dalal, J.; Hahn, T.; Khera, N.; Bonfim, C.; Majhail, N. S. et al. Clinical Risks and Healthcare Utilization of Hematopoietic Cell Transplantation for Sickle Cell Disease in the USA Using Merged Databases. *Haematologica* **2017**, *102*, 1823–1832, https://doi.org/10.3324/haematol.2017.169581.
142. Romero, Z.; Urbinati, F.; Geiger, S.; Cooper, A. R.; Wherley, J.; Kaufman, M. L. et al. B-Globin Gene Transfer To Human Bone Marrow for Sickle Cell Disease. *J. Clin. Invest.* **2013**, *123*, 3317–3330,https://doi.org/10.1172/JCI67930.
143. Olowoyeye, A.; Okwundu, C. I. Gene Therapy for Sickle Cell Disease. *Cochrane Database Syst. Rev.* **2018**, *2018* ,11,https://doi.org/10.1002/14651858.CD007652.pub6.
144. Pawliuk, R.; Westerman, K. A.; Fabry, M. E.; Payen, E.; Tighe, R.; Bouhassira, E. E.; Acharya, S. A.; Ellis, J.; London, I. M.; Eaves, C. J.; Humphries, R. K.; Beuzard, Y.; Nagel, R. L.; Leboulch, P. Correction of Sickle Cell Disease in Transgenic Mouse Models by Gene Therapy. *Science.* **2001**, *294*, 2368–2371,https://doi.org/10.1126/science.1065806.
145. Ribeil, J.-A.; Hacein-Bey-Abina, S.; Payen, E.; Magnani, A.; Semeraro, M.; Magrin, E.; Caccavelli, L.; Neven, B.; Bourget, P.; El Nemer, W.; Bartolucci, P.; Weber, L.; Puy, H.; Meritet, J.-F.; Grevent, D.; Beuzard, Y.; Chrétien, S.; Lefebvre, T.; Ross, R. W.; Negre, O.; Veres, G.; Sandler, L.; Soni, S.; de Montalembert, M.; Blanche, S.; Leboulch, P.; Cavazzana, M. Gene Therapy in a Patient with Sickle Cell Disease. *N. Engl. J. Med.* **2017**, *376*, 848–855. https://doi.org/10.1056/nejmoa1609677.
146. Hoban, M. D.; Lumaquin, D.; Kuo, C. Y.; Romero, Z.; Long, J.; Ho, M.; Young, C. S.; Mojadidi, M.; Fitz-Gibbon, S.; Cooper, A. R.; Lill, G. R.; Urbinati, F.; Campo-Fernandez, B.; Bjurstrom, C. F.; Pellegrini, M.; Hollis, R. P.; Kohn, D. B. CRISPR/Cas9-Mediated Correction of the Sickle Mutation in Human CD34+ Cells. *Mol. Ther.* **2016**, *24* (9), 1561–1569,https://doi.org/10.1038/mt.2016.148.
147. Drugbank online Home Page. Available online https://go.drugbank.com/drugs/DB06280 (Assessed on 12 November 2021).
148. Stocker, J. W.; De Franceschi, L.; McNaughton-Smith, G. A.; Corrocher, R.; Beuzard, Y.; Brugnara, C. ICA-17043, a Novel Gardos Channel Blocker, Prevents Sickled Red Blood Cell Dehydration in Vitro and in Vivo in SAD Mice. *Blood* **2003**, *101*, 2412–2418,https://doi.org/10.1182/blood-2002-05-1433.
149. McNaughton-Smith, G. A.; Burns, J. F.; Stocker, J. W.; Rigdon, G. C.; Creech, C.; Arlington, S.; Shelton, T.; De Franceschi, L. Novel Inhibitors of the Gardos Channel for the Treatment of Sickle Cell Disease. *J. Med. Chem.* **2008**, *51*, 976–982, https://doi.org/10.1021/jm070663s.
150. Ataga, K. I.; Stocker, J. Senicapoc (ICA-17043): A Potential Therapy for the Prevention and Treatment of Hemolysis-Associated Complications in Sickle Cell Anemia. *Expert Opinion on Investigational Drugs.* **2009**, 18, 231–239. https://doi.org/10.1517/13543780802708011.
151. Stocker, JW; Bergman, KL; Ridgon, GC. Pharmacokinetics (PK) and Pharmacodynamics (PD) of ICA-17043 (ICA), a Novel Gardos Channel Inhibitor for the Treatment of Sickle Cell Disease, Following Single, Ascending Doses in Healthy, Male Subjects. American College of Clinical Pharmacology Meeting, Vienna, VA; **2001.**

152. Ataga, K. I. ; Orringer, E.P.; Styles, L. ; et al. Dose-Escalation Study of ICA-17043 in Patients with Sickle Cell Disease. *Pharmacotherapy*. **2006**, 26, 1557-64, DOI: 10.1592/phco.26.11.1557
153. Ataga, K. I.; Smith, W. R.; De Castro, L. M.; Swerdlow, P.; Saunthararajah, Y.; Castro, O.; Vichinsky, E.; Kutlar, A.; Orringer, E. P.; Rigdon, G. C.; Stacker, J. W. Efficacy and Safety of the Gardos Channel Blocker, Senicapoc (ICA-17043), in Patients with Sickle Cell Anemia. *Blood* **2008**, *111*, 3991–3997, https://doi.org/10.1182/blood-2007-08-110098.
154. Ataga, K. I.; Reid, M.; Ballas, S. K.; Yasin, Z.; Bigelow, C.; James, L. S.; Smith, W. R.; Galacteros, F.; Kutlar, A.; Hull, J. H.; Stocker, J. W. Improvements in Haemolysis and Indicators of Erythrocyte Survival Do Not Correlate with Acute Vaso-Occlusive Crises in Patients with Sickle Cell Disease: A Phase III Randomized, Placebo-Controlled, Double-Blind Study of the Gardos Channel Blocker Senicapo. *Br. J. Haematol.* **2011**, *153* (1), 92–104. https://doi.org/10.1111/j.1365-2141.2010.08520.x.
155. US Food and Drug Adminstration Home Page. Available online : https://www.accessdata.fda.gov/drugsatfda_docs/label/2019/213137s000lbl.pdf Assessed on 30 October 2021)
156. Metcalf, B.; Chuang, C.; Dufu, K.; Patel, M. P.; Silva-Garcia, A.; Johnson, C.; Lu, Q.; Partridge, J. R.; Patskovska, L.; Patskovsky, Y.; Almo, S. C.; Jacobson, M. P.; Hua, L.; Xu, Q.; Gwaltney, S. L.; Yee, C.; Harris, J.; Morgan, B. P.; James, J.; Xu, D.; Hutchaleelaha, A.; Paulvannan, K.; Oksenberg, D.; Li, Z. Discovery of GBT440, an Orally Bioavailable R-State Stabilizer of Sickle Cell Hemoglobin. *ACS Med. Chem. Lett.* **2017**, *8*, 321–326. https://doi.org/10.1021/acsmedchemlett.6b00491.
157. Dufu, K.; Patel, M.; Oksenberg, D.; Cabrales, P. GBT440 Improves Red Blood Cell Deformability and Reduces Viscosity of Sickle Cell Blood under Deoxygenated Conditions. *Clin. Hemorheol. Microcirc.* **2018**, *70*, 95–105,https://doi.org/10.3233/CH-170340.
158. Dufu, K.; Oksenberg, D. GBT440 Reverses Sickling of Sickled Red Blood Cells under Hypoxic Conditions in Vitro. *Hematol. Rep.* **2018**, *10*, 1–9. https://doi.org/10.4081/hr.2018.7419.
159. Hutchaleelaha, A.; Patel, M.; Washington, C.; Siu, V.; Allen, E.; Oksenberg, D.; Gretler, D. D.; Mant, T.; Lehrer-Graiwer, J. Pharmacokinetics and Pharmacodynamics of Voxelotor (GBT440) in Healthy Adults and Patients with Sickle Cell Disease. *Br. J. Clin. Pharmacol.* **2019**, *85*, 1290–1302, https://doi.org/10.1111/bcp.13896.
160. Lehrer-Graiwer J.; Howard J.; Hemmaway C.J.; et al. GBT440, a potent anti-sickling hemoglobin modifier reduces hemolysis, improves anemia and nearly eliminates sickle cells in peripheral blood of patients with sickle cell disease. Blood. **2015**, 126,542, https://doi.org/10.1182/blood.V126.23.542.542.
161. Rademacher, P.; Hutchaleelaha A.; Washington C.; Lehrer J.; Ramos E. Absorption, metabolism and excretion of GBT440, a novel hemoglobin S (HbS) polymerization inhibitor for the treatment of sickle cell disease (SCD), in healthy male subjects. Blood. **2016**,128,2487, https://doi.org/10.1182/blood.V128.22.2487.2487
162. Vichinsky, E.; Hoppe, C. C.; Ataga, K. I.; Ware, R. E.; Nduba, V.; El-Beshlawy, A.; Hassab, H.; Achebe, M. M.; Alkindi, S.; Brown, R. C.; Diuguid, D. L.; Telfer, P.; Tsitsikas, D. A.; Elghandour, A.; Gordeuk, V. R.; Kanter, J.; Abboud, M. R.; Lehrer-Graiwer, J.; Tonda, M.; Intondi, A.; Tong, B.; Howard, J. A Phase 3 Randomized Trial of Voxelotor in Sickle Cell Disease. *N. Engl. J. Med.* **2019**, *381*, 509–519. https://doi.org/10.1056/nejmoa1903212.
163. Shah, M.K.; Khatri, P.; Vora, N.; Patel, N.K.; Jain, S.; Lin, S. Lipid Nanocarriers: Preparation, Characterization and Absorption Mechanism and Applications to Improve Oral Bioavailability of Poorly Water-Soluble Drugs. In *Biomedical Applications of Nanoparticles*; William Andrew Publisher, Norwich, NY, USA,2019; pp. 117–147, ISBN 9780128165065.
164. Vasconcelos, T.; Sarmento, B.; Costa, P. Solid Dispersions as Strategy to Improve Oral Bioavailability of Poor Water Soluble Drugs. *Drug Discov. Today* **2007**, *12* (23), 1068–1075. https://doi.org/https://doi.org/10.1016/j.drudis.2007.09.005

165. Attari, Z.; Kalvakuntla, S.; Reddy, M. S.; Deshpande, M.; Rao, C. M.; Koteshwara, K. B. Formulation and Characterisation of Nanosuspensions of BCS Class II and IV Drugs by Combinative Method. *J. Exp. Nanosci.* **2016**, *11* (4), 276–288. https://doi.org/10.1080/17458080.2015.1055841.
166. Albetawi, S.; Abdalhafez, A.; Abu-Zaid, A.; Matrouk, A.; Alhourani, N. Recent Solubility and Dissolution Enhancement Techniques for Repaglinide a BCS Class II Drug: A Review. *Pharmacia* , *68* (3), 573–583.
167. Loftsson, T.; Brewster, M. E. Cyclodextrins as Functional Excipients: Methods to Enhance Complexation Efficiency. *J. Pharm. Sci.* **2012**, *101* (9), 3019–3032. https://doi.org/https://doi.org/10.1002/jps.23077.
168. Gao, P.; Morozowich, W. Development of Supersaturatable Self-Emulsifying Drug Delivery System Formulations for Improving the Oral Absorption of Poorly Soluble Drugs. *Expert Opin. Drug Deliv.* **2006**, *3*, 97–110, doi:10.1517/17425247.3.1.97.
169. Mandal, S., & Mandal, S. S. Microemulsion Drug Delivery System: A Platform for Improving Dissolution Rate of Poorly Water-Soluble Drug. *International Journal of Pharmaceutical Sciences and Nanotechnology*, **2011**, 3(4 SE - Research Articles). https://doi.org/10.37285/ijpsn.2010.3.4.6.
170. Porter, C.J.H.; Charman, W.N. Transport and Absorption of Drugs via the Lymphatic System. *Adv. Drug Deliv. Rev.* **2001**, *50*, 1–2, doi:10.1016/S0169-409X(01)00146-6.
171. Williams, H.D.; Ford, L.; Igonin, A.; Shan, Z.; Botti, P.; Morgen, M.M.; Hu, G.; Pouton, C.W.; Scammells, P.J.; Porter, C.J.H.; et al. Unlocking the Full Potential of Lipid-Based Formulations Using Lipophilic Salt/ionic Liquid Forms. *Adv. Drug Deliv. Rev.* **2019**, *142*, 75–90, doi:10.1016/j.addr.2019.05.008.
172. Siqueira Jørgensen, S.D.; Al Sawaf, M.; Graeser, K.; Mu, H.; Müllertz, A.; Rades, T. The Ability of Two in vitro Lipolysis Models Reflecting the Human and Rat Gastro-Intestinal Conditions to Predict the in vivo Performance of SNEDDS Dosing Regimens. *Eur. J. Pharm. Biopharm.* **2018**, *124*, 116–124, doi:10.1016/j.ejpb.2017.12.014.
173. Pouton, C.W. Lipid Formulations for Oral Administration of Drugs: Non-Emulsifying, Self-Emulsifying and "Self-Microemulsifying" Drug Delivery Systems. *Eur. J. Pharm. Sci.* **2000**, *11*, 93–98, doi:10.1016/S0928-0987(00)00167-6.
174. Ujhelyi, Z.; Vecsernyés, M.; Fehér, P.; Kósa, D.; Arany, P.; Nemes, D.; Sinka, D.; Vasvári, G.; Fenyvesi, F.; Váradi, J.; et al. Physico-Chemical Characterization of Self-Emulsifying Drug Delivery Systems. *Drug Discov. Today Technol.* **2018**, *27*, 81–86, doi:10.1016/j.ddtec.2018.06.005.
175. Li, Z.; Xu, D.; Yuan, Y.; Wu, H.; Hou, J.; Kang, W.; Bai, B. Advances of Spontaneous Emulsification and Its Important Applications in Enhanced Oil Recovery Process. *Adv. Colloid Interface Sci.* **2020**, *277*, 102119, doi:10.1016/j.cis.2020.102119.
176. Rachmawati, H.; Rasaputri, D.H.; Susilowidodo, R.A.; Darijanto, S.T.; Sumirtapura, Y.C. The Influence of Oils and Surfactants on the Formation of Self-Nanoemulsifying Drug Delivery Systems (SNEDDS) Containing Therapeutic Protein. *Proc. Int. Conf. Mater. Sci. Technol.* **2011**, 247, 3-9.
177. Ding, W.; Hou, X.; Cong, S.; Zhang, Y.; Chen, M.; Lei, J.; Meng, Y.; Li, X.; Li, G. Co-Delivery of Honokiol, a Constituent of Magnolia Species, in a Self-Microemulsifying Drug Delivery System for Improved Oral Transport of Lipophilic Sirolimus. *Drug Deliv.* **2016**, *23*, 2513–2523, doi:10.3109/10717544.2015.1020119.
178. Hetényi, G.; Griesser, J.; Moser, M.; Demarne, F.; Jannin, V.; Bernkop-Schnürch, A. Comparison of the Protective Effect of Self-Emulsifying Peptide Drug Delivery Systems towards Intestinal Proteases and Glutathione. *Int. J. Pharm.* **2017**, *523*, 357–365, doi:10.1016/j.ijpharm.2017.03.027.
179. Mahmood, A.; Bernkop-Schnürch, A. SEDDS: A Game Changing Approach for the Oral Administration of Hydrophilic Macromolecular Drugs. *Adv. Drug Deliv. Rev.* **2019**, *142*, 91–101, doi:10.1016/j.addr.2018.07.001.

180. Gursoy, R.N.; Benita, S. Self-Emulsifying Drug Delivery Systems (SEDDS) for Improved Oral Delivery of Lipophilic Drugs. *Biomed. Pharmacother.* **2004**, *58*, 173–182, doi:10.1016/j.biopha.2004.02.001.
181. Larsen, A.T.; Åkesson, P.; Juréus, A.; Saaby, L.; Abu-Rmaileh, R.; Abrahamsson, B.; Østergaard, J.; Müllertz, A. Bioavailability of Cinnarizine in Dogs: Effect of SNEDDS Loading Level and Correlation with Cinnarizine Solubilization during in Vitro Lipolysis. *Pharm. Res.* **2013**, *30*, 3101–3113, doi:10.1007/s11095-013-1145-x.
182. Pouton, C.W.; Porter, C.J.H. Formulation of Lipid-Based Delivery Systems for Oral Administration: Materials, Methods and Strategies. *Adv. Drug Deliv. Rev.* **2008**, *60*, 625–637, doi:10.1016/j.addr.2007.10.010.
183. Date, A.A.; Desai, N.; Dixit, R.; Nagarsenker, M. Self-Nanoemulsifying Drug Delivery Systems: Formulation Insights, Applications and Advances. *Nanomedicine* **2010**, 1595–1616, doi:10.2217/nnm.10.126.
184. Singh, B.; Bandopadhyay, S.; Kapil, R.; Singh, R.; Katare, O.P. Self-Emulsifying Drug Delivery Systems (SEDDS): Formulation Development, Characterization, and Applications. *Crit. Rev. Ther. Drug Carrier Syst.* **2009**, *26*, 427–521, doi:10.1615/critrevtherdrugcarriersyst.v26.i5.10.
185. Kollipara, S.; Gandhi, R.K. Pharmacokinetic Aspects and in Vitro–in Vivo Correlation Potential for Lipid-Based Formulations. *Acta Pharm. Sin. B* **2014**, *4*, 333–349, doi:10.1016/j.apsb.2014.09.001.
186. Mu, H.; Holm, R.; Mullertz, A. Lipid-Based Formulations for Oral Administration of Poorly Water-Soluble Drugs. *Int. J. Pharm.* **2013**, *453*, 215–224. https://doi.org/10.1016/j.ijpharm.2013.03.054.
187. Rajpoot, K.; Tekade, M.; Pandey, V.; Nagaraja, S.H.; Youngren-Ortiz, S.R.; Tekade, R.K. *Self-Microemulsifying Drug-Delivery System: Ongoing Challenges and Future Ahead*; Tekade, R.K., Ed.; Drug Delivery Systems: Academic Press, Cambridge, MA, USA, 2020; pp. 393–454, doi:10.1016/B978-0-12-814487-9.00009-0.
188. Qian, J.; Meng, H.; Xin, L.; Xia, M.; Shen, H.; Li, G.; Xie, Y. Self-Nanoemulsifying Drug Delivery Systems of Myricetin: Formulation Development, Characterization, and in Vitro and in Vivo Evaluation. *Colloids Surfaces B Biointerfaces* **2017**, *160*, 101–109, doi:10.1016/j.colsurfb.2017.09.020.
189. Maher, S.; Brayden, D.J. Overcoming Poor Permeability: Translating Permeation Enhancers for Oral Peptide Delivery. *Drug Discov. Today Technol.* **2012**, *9*, 113–119, doi:10.1016/j.ddtec.2011.11.006.
190. Chatterjee, B.; Hamed Almurisi, S.; Ahmed Mahdi Dukhan, A.; Mandal, U.K.; Sengupta, P. Controversies with Self-Emulsifying Drug Delivery System from Pharmacokinetic Point of View. *Drug Deliv.* **2016**, *23*, 3639–3652, doi:10.1080/10717544.2016.1214990.
191. Izgelov, D.; Shmoeli, E.; Domb, A.J.; Hoffman, A. The Effect of Medium Chain and Long Chain Triglycerides Incorporated in Self-Nano Emulsifying Drug Delivery Systems on Oral Absorption of Cannabinoids in Rats. *Int. J. Pharm.* **2020**, *580*, 119201, doi:10.1016/j.ijpharm.2020.119201.
192. Gracia, G.; Cao, E.; Johnston, A.P.R.; Porter, C.J.H.; Trevaskis, N.L. Organ-Specific Lymphatics Play Distinct Roles in Regulating HDL Trafficking and Composition. *Am. J. Physiol. Gastrointest. Liver Physiol.* **2020**, *318*, G725–G735, doi:10.1152/ajpgi.00340.2019.
193. Chen, M.L. Lipid Excipients and Delivery Systems for Pharmaceutical Development: A Regulatory Perspective. *Adv. Drug Deliv. Rev.* **2008**, *60*, 768–777, doi:10.1016/j.addr.2007.09.010.
194. Li, L.; Zhou, C.H.; Xu, Z.P. Self-Nanoemulsifying Drug-Delivery System and Solidified Self-Nanoemulsifying Drug-Delivery System. In *Nanocarriers for Drug Delivery*; Elsevier: Amsterdam, The Netherlands, 2019; pp. 421–449, doi:10.1016/b978-0-12-814033-8.00014-x.
195. Gupta, S.; Kesarla, R.; Omri, A. Formulation Strategies to Improve the Bioavailability of Poorly Absorbed Drugs with Special Emphasis on Self-Emulsifying Systems. *ISRN Pharm.* **2013**, *2013*, doi:10.1155/2013/848043.
196. Zupančič, O.; Grießinger, J.A.; Rohrer, J.; Pereira de Sousa, I.; Danninger, L.; Partenhauser, A.; Sündermann, N.E.; Laffleur, F.; Bernkop-Schnürch, A. Development, in Vitro and in Vivo

Evaluation of a Self-Emulsifying Drug Delivery System (SEDDS) for Oral Enoxaparin Administration. *Eur. J. Pharm. Biopharm.* **2016**, *109*, 113–121, doi:10.1016/j.ejpb.2016.09.013.

197. Yin, Y.M.; Cui, F.D.; Mu, C.F.; Choi, M.K.; Kim, J.S.; Chung, S.J.; Shim, C.K.; Kim, D.D. Docetaxel Microemulsion for Enhanced Oral Bioavailability: Preparation and in Vitro and in Vivo Evaluation. *J. Control. Release* **2009**, *140*, 86–94, doi:10.1016/j.jconrel.2009.08.015.
198. Mountfield, R.J.; Senepin, S.; Schleimer, M.; Walter, I.; Bittner, B. Potential Inhibitory Effects of Formulation Ingredients on Intestinal Cytochrome P450. *Int. J. Pharm.* **2000**, *211*, 89–92, doi:10.1016/S0378-5173(00)00586-X.
199. Rege, B.D.; Kao, J.P.Y.; Polli, J.E. Effects of Nonionic Surfactants on Membrane Transporters in Caco-2 Cell Monolayers. *Eur. J. Pharm. Sci.* **2002**, *16*, 237–246, doi:10.1016/S0928-0987(02)00055-6.
200. Čerpnjak, K.; Zvonar, A.; Gašperlin, M.; Vrečer, F. Lipid-Based Systems as a Promising Approach for Enhancing the Bioavailability of Poorly Water-Soluble Drugs. *Acta Pharm.* **2013**, *63*, 427–445, doi:10.2478/acph-2013-0040.
201. Pouton, C.W. Formulation of Poorly Water-Soluble Drugs for Oral Administration: Physicochemical and Physiological Issues and the Lipid Formulation Classification System. *Eur. J. Pharm. Sci.* **2006**, *29*, 278–287, doi:10.1016/j.ejps.2006.04.016.
202. Hua, L.; Weisan, P.; Jiayu, L.; Ying, Z. Preparation, Evaluation, and NMR Characterization of Vinpocetine Microemulsion for Transdermal Delivery. *Drug Dev. Ind. Pharm.* **2004**, *30*, 657–666, doi:10.1081/DDC-120039183.
203. Borhade, V.; Pathak, S.; Sharma, S.; Patravale, V. Clotrimazole Nanoemulsion for Malaria Chemotherapy. Part I: Preformulation Studies, Formulation Design and Physicochemical Evaluation. *Int. J. Pharm.* **2012**, *431*, 138–148, doi:10.1016/j.ijpharm.2011.12.040.
204. Kale, A.A.; Patravale, V.B. Design and Evaluation of Self-Emulsifying Drug Delivery Systems (SEDDS) of Nimodipine. *AAPS Pharmscitech* **2008**, *9*, 191–196, doi:10.1208/s12249-008-9037-9.
205. Nepal, P.R.; Han, H.K.; Choi, H.K. Preparation and in Vitro-in Vivo Evaluation of Witepsol®® H35 Based Self-Nanoemulsifying Drug Delivery Systems (SNEDDS) of Coenzyme Q10. *Eur. J. Pharm. Sci.* **2010**, *39*, 224–232, doi:10.1016/j.ejps.2009.12.004.
206. Memvanga, P.B.; Coco, R.; Préat, V. An Oral Malaria Therapy: Curcumin-Loaded Lipid-Based Drug Delivery Systems Combined with β-Arteether. *J. Control. Release* **2013**, *172*, 904–913, doi:10.1016/j.jconrel.2013.09.001.
207. Memvanga, P.B.; Préat, V. Formulation Design and in Vivo Antimalarial Evaluation of Lipid-Based Drug Delivery Systems for Oral Delivery of β-Arteether. *Eur. J. Pharm. Biopharm.* **2012**, *82*, 112–119, doi:10.1016/j.ejpb.2012.05.004.
208. Jain, S.; Garg, T.; Kushwah, V.; Thanki, K.; Agrawal, A.K.; Dora, C.P. α-Tocopherol as Functional Excipient for Resveratrol and Coenzyme Q10-Loaded SNEDDS for Improved Bioavailability and Prophylaxis of Breast Cancer. *J. Drug Target.* **2017**, *25*, 554–565, doi:10.1080/1061186X.2017.1298603.
209. Yanfei, M.; Guoguang, C.; Lili, R.; Pingkai, O. Controlled Release of Glaucocalyxin—A Self-Nanoemulsifying System from Osmotic Pump Tablets with Enhanced Bioavailability. *Pharm. Dev. Technol.* **2017**, *22*, 148–155, doi:10.3109/10837450.2015.1089901.
210. Hosny, K.M.; Aldawsari, H.M.; Bahmdan, R.H.; Sindi, A.M.; Kurakula, M.; Alrobaian, M.M.; Aldryhim, A.Y.; Alkhalidi, H.M.; Bahmdan, H.H.; Khallaf, R.A.; et al. Preparation, Optimization, and Evaluation of Hyaluronic Acid-Based Hydrogel Loaded with Miconazole Self-Nanoemulsion for the Treatment of Oral Thrush. *AAPS Pharmscitech* **2019**, *20*, 297, doi:10.1208/s12249-019-1496-7.
211. Batool, A.; Arshad, R.; Razzaq, S.; Nousheen, K.; Kiani, M.H.; Shahnaz, G. Formulation and Evaluation of Hyaluronic Acid-Based Mucoadhesive Self Nanoemulsifying Drug Delivery System

(SNEDDS) of Tamoxifen for Targeting Breast Cancer. *Int. J. Biol. Macromol.* **2020**, *152*, 503–515, doi:10.1016/j.ijbiomac.2020.02.275.

212. Zhang, L.; Zhang, L.; Zhang, M.; Pang, Y.; Li, Z.; Zhao, A.; Feng, J. Self-Emulsifying Drug Delivery System and the Applications in Herbal Drugs. *Drug Deliv.* **2015**, *22*, 475–486, doi:10.3109/10717544.2013.861659.
213. Yoo, J.; Baskaran, R.; Yoo, B.K. Self-Nanoemulsifying Drug Delivery System of Lutein: Physicochemical Properties and Effect on Bioavailability of Warfarin. *Biomol. Ther.* **2013**, *21*, 173–179, doi:10.4062/biomolther.2013.011.
214. Date, A.A.; Nagarsenker, M.S. Design and Evaluation of Self-Nanoemulsifying Drug Delivery Systems (SNEDDS) for Cefpodoxime Proxetil. *Int. J. Pharm.* **2007**, *329*, 166–172, doi:10.1016/j.ijpharm.2006.08.038.
215. Khattab, A.; Mohamed, M.; Basalious, E.B. Design of Self-Nanoemulsifying System to Enhance Absorption and Bioavailability of Poorly Permeable Aliskiren Hemi-Fumarate. *J. Drug Deliv. Sci. Technol.* **2020**, *57*, 101646, doi:10.1016/j.jddst.2020.101646.
216. Shah, M.K.; Madan, P.; Lin, S. Elucidation of Intestinal Absorption Mechanism of Carvedilol-Loaded Solid Lipid Nanoparticles Using Caco-2 Cell Line as an in-Vitro Model. *Pharm. Dev. Technol.* **2015**, *20*, 877–885, doi:10.3109/10837450.2014.938857.
217. Shukla, M.; Jaiswal, S.; Sharma, A.; Srivastava, P.K.; Arya, A.; Dwivedi, A.K.; Lal, J. A Combination of Complexation and Self-Nanoemulsifying Drug Delivery System for Enhancing Oral Bioavailability and Anticancer Efficacy of Curcumin. *Drug Dev. Ind. Pharm.* **2017**, *43*, 847–861, doi:10.1080/03639045.2016.1239732.
218. Yadav, P.; Rastogi, V.; Verma, A. Application of Box–Behnken Design and Desirability Function in the Development and Optimization of Self-Nanoemulsifying Drug Delivery System for Enhanced Dissolution of Ezetimibe. *Futur. J. Pharm. Sci.* **2020**, *6*, 7, doi:10.1186/s43094-020-00023-3.
219. Panigrahi, K.C.; Jena, J.; Jena, G.K.; Patra, C.N.; Rao, M.E.B. QBD-Based Systematic Development of BosentanSNEDDS: Formulation, Characterization and Pharmacokinetic Assessment. *J. Drug Deliv. Sci. Technol.* **2018**, *47*, 31–42, doi:10.1016/j.jddst.2018.06.021.
220. Sanka, K.; Suda, D.; Bakshi, V. Optimization of Solid-Self Nanoemulsifying Drug Delivery System for Solubility and Release Profile of Clonazepam Using Simplex Lattice Design. *J. Drug Deliv. Sci. Technol.* **2016**, *33*, 114–124, doi:10.1016/j.jddst.2016.04.003.
221. El-Zahaby, S.A.; AbouGhaly, M.H.H.; Abdelbary, G.A.; El-Gazayerly, O.N. Zero-Order Release and Bioavailability Enhancement of Poorly Water Soluble Vinpocetine from Self-Nanoemulsifying Osmotic Pump Tablet. *Pharm. Dev. Technol.* **2018**, *23*, 900–910, doi:10.1080/10837450.2017.1335321.
222. Ujilestari, T.; Martien, R.; Ariyadi, B.; Dono, N.D. Zuprizal. Self-Nanoemulsifying Drug Delivery System (SNEDDS) of Amomum Compactum Essential Oil: Design, Formulation, and Characterization. *J. Appl. Pharm. Sci.* **2018**, *8*, 14–21, doi:10.7324/JAPS.2018.8603.
223. Das, S.S.; Singh, A.; Kar, S.; Ghosh, R.; Pal, M.; Fatima, M.; Singh, N.; Singh, S.K. Application of QbD Framework for Development of Self-Emulsifying Drug Delivery Systems. In *Pharmaceutical Quality by Design*; Academic Press, Cambridge, MA, USA, 2019; pp. 297–350, doi:10.1016/b978-0-12-815799-2.00015-0.
224. Garg, V.; Kaur, P.; Singh, S.K.; Kumar, B.; Bawa, P.; Gulati, M.; Yadav, A.K. Solid Self-Nanoemulsifying Drug Delivery Systems for Oral Delivery of Polypeptide-K: Formulation, Optimization, in-Vitro and in-Vivo Antidiabetic Evaluation. *Eur. J. Pharm. Sci.* **2017**, *109*, 297–315, doi:10.1016/j.ejps.2017.08.022.
225. Gündoğdu, T.K.; Deniz, I.; Çalişkan, G.; Şahin, E.S.; Azbar, N. Experimental Design Methods for Bioengineering Applications. *Crit. Rev. Biotechnol.* **2016**, *36*, 368–388, doi:10.3109/07388551.2014.973014.

226. Rad, A.H.; Pirouzian, H.R.; Toker, O.S.; Konar, N. Application of Simplex Lattice Mixture Design for Optimization of Sucrose-Free Milk Chocolate Produced in a Ball Mill. *Lwt* **2019**, *115*, 108435, doi:10.1016/j.lwt.2019.108435.
227. Astuti, I.Y.; Marchaban, M.; Martien, R.; Nugroho, A.E. Design and Optimization of Self Nano-Emulsifying Drug Delivery System Containing a New Anti-Inflammatory Agent Pentagamavunon-0. *Indones. J. Chem.* **2017**, *17*, 365–375, doi:10.22146/ijc.22640.
228. Antony, J. Full Factorial Designs. In *Design of Experiments for Engineers and Scientists (Second Edi)*; Elsevier: Amsterdam, The Netherlands, 2014; pp. 63–85, ISBN 9780080994178, doi:10.1016/B978-0-08-099417-8.00006-7.
229. Karamanidou, T.; Karidi, K.; Bourganis, V.; Kontonikola, K.; Kammona, O.; Kiparissides, C. Effective Incorporation of Insulin in Mucus Permeating Self-Nanoemulsifying Drug Delivery Systems. *Eur. J. Pharm. Biopharm.* **2015**, *97*, 223–229, doi:10.1016/j.ejpb.2015.04.013.
230. de Aguiar, P.F.; Bourguignon, B.; Khots, M.S.; Massart, D.L.; Phan-Than-Luu, R. D-Optimal Designs. *Chemom. Intell. Lab. Syst.* **1995**, *30*, 199–210, doi:10.1016/0169-7439(94)00076-X.
231. Talekar, S.D.; Haware, R.V.; Dave, R.H. Evaluation of Self-Nanoemulsifying Drug Delivery Systems Using Multivariate Methods to Optimize Permeability of Captopril Oral Films. *Eur. J. Pharm. Sci.* **2019**, *130*, 215–224, doi:10.1016/j.ejps.2019.01.039.
232. Cunha, S.; Costa, C.P.; Moreira, J.N.; Lobo, J.M.S.; Silva, A.C. Using the Quality by Design (QbD) Approach to Optimize Formulations of Lipid Nanoparticles and Nanoemulsions: A Review. *Nanomed. Nanotechnol. Biol. Med.* **2020**, 102206, doi:10.1016/j.nano.2020.102206.
233. Phan, S.; Salentinig, S.; Prestidge, C.A.; Boyd, B.J. Self-Assembled Structures Formed during Lipid Digestion: Characterization and Implications for Oral Lipid-Based Drug Delivery Systems. *Drug Deliv. Transl. Res.* **2014**, *4*, 275–294, doi:10.1007/s13346-013-0168-5.
234. Franzen, U.; Vermehren, C.; Jensen, H.; Østergaard, J. Physicochemical Characterization of a PEGylated Liposomal Drug Formulation Using Capillary Electrophoresis. *Electrophoresis* **2011**, *32*, 738–748, doi:10.1002/elps.201000552.
235. Fischer, K.; Schmidt, M. Pitfalls and Novel Applications of Particle Sizing by Dynamic Light Scattering. *Biomaterials* **2016**, *98*, 79–91, doi:10.1016/j.biomaterials.2016.05.003.
236. Phillies, G.D.J. Interpretation of Fluorescence Correlation Spectra of Biopolymer Solutions. *Biopolymers* **2016**, *105*, 260–266, doi:10.1002/bip.22802.
237. Piñeiro, L.; Novo, M.; Al-Soufi, W. Fluorescence Emission of Pyrene in Surfactant Solutions. *Adv. Colloid Interface Sci.* **2015**, *215*, 1–12, doi:10.1016/j.cis.2014.10.010.
238. Khan, M.F.; Singh, M.K.; Sen, S. Measuring Size, Size Distribution, and Polydispersity of Water-in-Oil Microemulsion Droplets Using Fluorescence Correlation Spectroscopy: Comparison to Dynamic Light Scattering. *J. Phys. Chem. B* **2016**, *120*, 1008–1020, doi:10.1021/acs.jpcb.5b09920.
239. Chamieh, J.; Merdassi, H.; Rossi, J.C.; Jannin, V.; Demarne, F.; Cottet, H. Size Characterization of Lipid-Based Self-Emulsifying Pharmaceutical Excipients during Lipolysis Using Taylor Dispersion Analysis with Fluorescence Detection. *Int. J. Pharm.* **2018**, *537*, 94–101, doi:10.1016/j.ijpharm.2017.12.032.
240. Vithani, K.; Jannin, V.; Pouton, C.W.; Boyd, B.J. Colloidal Aspects of Dispersion and Digestion of Self-Dispersing Lipid-Based Formulations for Poorly Water-Soluble Drugs. *Adv. Drug Deliv. Rev.* **2019**, *142*, 16–34, doi:10.1016/j.addr.2019.01.008.
241. Chamieh, J.; Jannin, V.; Demarne, F.; Cottet, H. Hydrodynamic Size Characterization of a Self-Emulsifying Lipid Pharmaceutical Excipient by Taylor Dispersion Analysis with Fluorescent Detection. *Int. J. Pharm.* **2016**, *513*, 262–269, doi:10.1016/j.ijpharm.2016.09.016.
242. Tominaga, T.; Nishinaka, M. Tracer Diffusion of Ionic Micelles: Effects of Size and Interactions. *J. Chem. Soc. Faraday Trans.* **1993**, *89*, 3459–3464, doi:10.1039/FT9938903459.

243. Chamieh, J.; Davanier, F.; Jannin, V.; Demarne, F.; Cottet, H. Size Characterization of Commercial Micelles and Microemulsions by Taylor Dispersion Analysis. *Int. J. Pharm.* **2015**, *492*, 46–54, doi:10.1016/j.ijpharm.2015.06.037.
244. Yi, T.; Wan, J.; Xu, H.; Yang, X. A New Solid Self-Microemulsifying Formulation Prepared by Spray-Drying to Improve the Oral Bioavailability of Poorly Water Soluble Drugs. *Eur. J. Pharm. Biopharm.* **2008**, *70*, 439–444, doi:10.1016/j.ejpb.2008.05.001.
245. Kamal, M.M.; Nazzal, S. Novel Sulforaphane-Enabled Self-Microemulsifying Delivery Systems (SFN-SMEDDS) of Taxanes: Formulation Development and in Vitro Cytotoxicity against Breast Cancer Cells. *Int. J. Pharm.* **2018**, *536*, 187–198, doi:10.1016/j.ijpharm.2017.11.063.
246. Zhu, J.X.; Tang, D.; Feng, L.; Zheng, Z.G.; Wang, R.S.; Wu, A.G.; Duan, T.T.; He, B.; Zhu, Q. Development of Self-Microemulsifying Drug Delivery System for Oral Bioavailability Enhancement of Berberine Hydrochloride. *Drug Dev. Ind. Pharm.* **2013**, *39*, 499–506, doi:10.3109/03639045.2012.683875.
247. Li, F.; Song, S.; Guo, Y.; Zhao, Q.; Zhang, X.; Pan, W.; Yang, X. Preparation and Pharmacokinetics Evaluation of Oral Self-Emulsifying System for Poorly Water-Soluble Drug Lornoxicam. *Drug Deliv.* **2015**, *22*, 487–498, doi:10.3109/10717544.2014.885615.
248. Yap, S.P.; Yuen, K.H. Influence of Lipolysis and Droplet Size on Tocotrienol Absorption from Self-Emulsifying Formulations. *Int. J. Pharm.* **2004**, *281*, 67–78, doi:10.1016/j.ijpharm.2004.05.015.
249. Kovarik, J.M.; Mueller, E.A.; van Bree, J.B.; Tetzloff, W.; Kutz, K. Reduced Inter- and Intraindividual Variability in Cyclosporine Pharmacokinetics from a Microemulsion Formulation. *J. Pharm. Sci.* **1994**, *83*, 444–446, doi:10.1002/jps.2600830336.
250. Nielsen, F.S.; Petersen, K.B.; Müllertz, A. Bioavailability of Probucol from Lipid and Surfactant Based Formulations in Minipigs: Influence of Droplet Size and Dietary State. *Eur. J. Pharm. Biopharm.* **2008**, *69*, 553–562, doi:10.1016/j.ejpb.2007.12.020.
251. Feeney, O.M.; Crum, M.F.; McEvoy, C.L.; Trevaskis, N.L.; Williams, H.D.; Pouton, C.W.; Charman, W.N.; Bergström, C.A.S.; Porter, C.J.H. 50 Years of Oral Lipid-Based Formulations: Provenance, Progress and Future Perspectives. *Adv. Drug Deliv. Rev.* **2016**, *101*, 167–194, doi:10.1016/j.addr.2016.04.007.
252. Cherniakov, I.; Domb, A.J.; Hoffman, A. Self-Nano-Emulsifying Drug Delivery Systems: An Update of the Biopharmaceutical Aspects. *Expert Opin. Drug Deliv.* **2015**, *12*, 1121–1133, doi:10.1517/17425247.2015.999038.
253. de Sousa, I.P.; Steiner, C.; Schmutzler, M.; Wilcox, M.D.; Veldhuis, G.J.; Pearson, J.P.; Huck, C.W.; Salvenmoser, W.; Bernkop-Schnürch, A. Mucus Permeating Carriers: Formulation and Characterization of Highly Densely Charged Nanoparticles. *Eur. J. Pharm. Biopharm.* **2015**, *97*, 273–279, doi:10.1016/j.ejpb.2014.12.024.
254. Netsomboon, K.; Bernkop-Schnürch, A. Mucoadhesive vs. Mucopenetrating Particulate Drug Delivery. *Eur. J. Pharm. Biopharm.* **2016**, *98*, 76–89, doi:10.1016/j.ejpb.2015.11.003.
255. Corbo, D.C.; Liu, J.-C.; Chienx, Y.W. Characterization of the Barrier Properties of Mucosal Membranes. *J. Pharm. Sci.* **1990**, *79*, 202–206, doi:10.1002/jps.2600790304.
256. Gershanik, T.; Benita, S. Positively Charged Self-Emulsifying Oil Formulation for Improving Oral Bioavailability of Progesterone. *Pharm. Dev. Technol.* **1996**, *1*, 147–157, doi:10.3109/10837459609029889.
257. Salimi, E.; Le-Vinh, B.; Zahir-Jouzdani, F.; Matuszczak, B.; Ghaee, A.; Bernkop-Schnürch, A. Self-Emulsifying Drug Delivery Systems Changing Their Zeta Potential via a Flip-Flop Mechanism. *Int. J. Pharm.* **2018**, *550*, 200–206, doi:10.1016/j.ijpharm.2018.08.046.
258. Basalious, E.B.; Shawky, N.; Badr-Eldin, S.M. SNEDDS Containing Bioenhancers for Improvement of Dissolution and Oral Absorption of Lacidipine. I: Development and Optimization. *Int. J. Pharm.* **2010**, *391*, 203–211, doi:10.1016/j.ijpharm.2010.03.008.

259. Wang, L.; Dong, J.; Chen, J.; Eastoe, J.; Li, X. Design and Optimization of a New Self-Nanoemulsifying Drug Delivery System. *J. Colloid Interface Sci.* **2009**, *330*, 443–448, doi:10.1016/j.jcis.2008.10.077.
260. Czajkowska-Kośnik, A.; Szekalska, M.; Amelian, A.; Szymańska, E.; Winnicka, K. Development and Evaluation of Liquid and Solid Self-Emulsifying Drug Delivery Systems for Atorvastatin. *Molecules* **2015**, *20*, 21010–21022, doi:10.3390/molecules201219745.
261. Mandal, S.; Mandal, S.S. Microemulsion Drug Delivery System: A Platform for Improving Dissolution Rate of Poorly Water Soluble Drug. *Int. J. Pharm. Sci. Nanotechnol.* **2011**, *3*, 1214–1219, doi:10.37285/ijpsn.2010.3.4.6.
262. Patel, J.; Dhingani, A.; Garala, K.; Raval, M.; Sheth, N. Quality by Design Approach for Oral Bioavailability Enhancement of Irbesartan by Self-Nanoemulsifying Tablets. *Drug Deliv.* **2014**, *21*, 412–435, doi:10.3109/10717544.2013.853709.
263. Nazzal, S.; Smalyukh, I.I.; Lavrentovich, O.D.; Khan, M.A. Preparation and in Vitro Characterization of a Eutectic Based Semisolid Self-Nanoemulsified Drug Delivery System (SNEDDS) of Ubiquinone: Mechanism and Progress of Emulsion Formation. *Int. J. Pharm.* **2002**, *235*, 247–265, doi:10.1016/S0378-5173(02)00003-0.
264. Bali, V.; Ali, M.; Ali, J. Study of Surfactant Combinations and Development of a Novel Nanoemulsion for Minimising Variations in Bioavailability of Ezetimibe. *Colloids Surfaces B Biointerfaces* **2010**, *76*, 410–420, doi:10.1016/j.colsurfb.2009.11.021.
265. Parikh, K.J.; Sawant, K.K. Solubilization of Vardenafil HCl in Lipid-Based Formulations Enhances Its Oral Bioavailability in Vivo: A Comparative Study Using Tween®—20 and Cremophor®—EL. *J. Mol. Liq.* **2019**, *277*, 189–199, doi:10.1016/j.molliq.2018.12.079.
266. Bandyopadhyay, S.; Katare, O.P.; Singh, B. Optimized Self Nano-Emulsifying Systems of Ezetimibe with Enhanced Bioavailability Potential Using Long Chain and Medium Chain Triglycerides. *Colloids Surfaces B Biointerfaces* **2012**, *100*, 50–61, doi:10.1016/j.colsurfb.2012.05.019.
267. Gupta, S.; Chavhan, S.; Sawant, K.K. Self-Nanoemulsifying Drug Delivery System for Adefovir Dipivoxil: Design, Characterization, in Vitro and Ex Vivo Evaluation. *Colloids Surfaces A Physicochem. Eng. Asp.* **2011**, *392*, 145–155, doi:10.1016/j.colsurfa.2011.09.048.
268. Elsheikh, M.A.; Elnaggar, Y.S.R.; Gohar, E.Y.; Abdallah, O.Y. Nanoemulsion Liquid Preconcentrates for Raloxifene Hydrochloride: Optimization and in Vivo Appraisal. *Int. J. Nanomed.* **2012**, *7*, 3787–3802, doi:10.2147/IJN.S33186.
269. Elnaggar, Y.S.R.; El-Massik, M.A.; Abdallah, O.Y. Self-Nanoemulsifying Drug Delivery Systems of Tamoxifen Citrate: Design and Optimization. *Int. J. Pharm.* **2009**, *380*, 133–141, doi:10.1016/j.ijpharm.2009.07.015.
270. Shafiq, S.; Shakeel, F.; Talegaonkar, S.; Ahmad, F.J.; Khar, R.K.; Ali, M. Development and Bioavailability Assessment of Ramipril Nanoemulsion Formulation. *Eur. J. Pharm. Biopharm.* **2007**, *66*, 227–243, doi:10.1016/j.ejpb.2006.10.014.
271. Zhuang, X.; Tian, X.; Zheng, Y.; Lan, N.; Liu, L.; Zhang, R.; Liu, Y. Formulation and Physicochemical Characterisation of a Novel Self-Microemulsifying Delivery System as Hydrotropic and Solubilising Agent for Penfluridol. *Procedia Eng.* **2011**, *18*, 59–65, doi:10.1016/j.proeng.2011.11.010.
272. Hedge, O. J.; Bergström, C. A. S. Suitability of Artificial Membranes in Lipolysis-Permeation Assays of Oral Lipid-Based Formulations. *Pharm. Res.* **2020**, *37*,9, https://doi.org/10.1007/s11095-020-02833-9.
273. Alvebratt, C.; Keemink, J.; Edueng, K.; Cheung, O.; Strømme, M.; Bergström, C.A.S. An in Vitro Dissolution-digestion-permeation Assay for the Study of Advanced Drug Delivery Systems. *Eur. J. Pharm. Biopharm.* **2020**, *149*, 21–29, doi:10.1016/j.ejpb.2020.01.010.

274. Kohli, K.; Chopra, S.; Dhar, D.; Arora, S.; Khar, R.K. Self-Emulsifying Drug Delivery Systems: An Approach to Enhance Oral Bioavailability. *Drug Discov. Today* **2010**, *15*, 958–965, doi:10.1016/j.drudis.2010.08.007.
275. Dash, R.N.; Mohammed, H.; Humaira, T.; Ramesh, D. Design, Optimization and Evaluation of Glipizide Solid Self-Nanoemulsifying Drug Delivery for Enhanced Solubility and Dissolution. *Saudi Pharm. J.* **2015**, *23*, 528–540, doi:10.1016/j.jsps.2015.01.024.
276. Eleftheriadis, G.K.; Mantelou, P.; Karavasili, C.; Chatzopoulou, P.; Katsantonis, D.; Irakli, M.; Mygdalia, A.; Vizirianakis, I.S.; Fatouros, D.G. Development and Characterization of a Self-Nanoemulsifying Drug Delivery System Comprised of Rice Bran Oil for Poorly Soluble Drugs. *AAPS Pharmscitech* **2019**, *20*, doi:10.1208/s12249-018-1274-y.
277. Abouhussein, D.M.N.; Bahaa El Din Mahmoud, D.; Mohammad, F.E. Design of a Liquid Nano-Sized Drug Delivery System with Enhanced Solubility of Rivaroxaban for Venous Thromboembolism Management in Paediatric Patients and Emergency Cases. *J. Liposome Res.* **2019**, *29*, 399–412, doi:10.1080/08982104.2019.1576732.
278. Vertzoni, M.; Dressman, J.; Butler, J.; Hempenstall, J.; Reppas, C. Simulation of Fasting Gastric Conditions and Its Importance for the in Vivo Dissolution of Lipophilic Compounds. *Eur. J. Pharm. Biopharm.* **2005**, *60*, 413–417, doi:10.1016/j.ejpb.2005.03.002.
279. Kamboj, S.; Rana, V. Quality-by-Design Based Development of a Self-Microemulsifying Drug Delivery System to Reduce the Effect of Food on Nelfinavir Mesylate. *Int. J. Pharm.* **2016**, *501*, 311–325, doi:10.1016/j.ijpharm.2016.02.008.
280. Prajapat, M.D.; Patel, N.J.; Bariya, A.; Patel, S.S.; Butani, S.B. Formulation and Evaluation of Self-Emulsifying Drug Delivery System for Nimodipine, a BCS Class II Drug. *J. Drug Deliv. Sci. Technol.* **2017**, *39*, 59–68, doi:10.1016/j.jddst.2017.02.002.
281. Barba, A.A.; Dalmoro, A.; Bochicchio, S.; de Simone, V.; Caccavo, D.; Iannone, M.; Lamberti, G. Engineering Approaches for Drug Delivery Systems Production and Characterization. *Int. J. Pharm.* **2020**, *581*, 119267, doi:10.1016/j.ijpharm.2020.119267.
282. Jantratid, E.; Janssen, N.; Reppas, C.; Dressman, J.B. Dissolution Media Simulating Conditions in the Proximal Human Gastrointestinal Tract: An Update. *Pharm. Res.* **2008**, *25*, 1663–1676, doi:10.1007/s11095-008-9569-4.
283. Baxevanis, F.; Zarmpi, P.; Kuiper, J.; Fotaki, N. Investigation of Drug Partition Kinetics to Fat in Simulated Fed State Gastric Conditions Based on Drug Properties. *Eur. J. Pharm. Sci.* **2020**, *146*, 105263, doi:10.1016/j.ejps.2020.105263.
284. Dressman, J.B.; Reppas, C. In Vitro-in Vivo Correlations for Lipophilic, Poorly Water-Soluble Drugs. *Eur. J. Pharm. Sci.* **2000**, *11*, 73–80, doi:10.1016/S0928-0987(00)00181-0.
285. Nicolaides, E.; Symillides, M.; Dressman, J.B.; Reppas, C. Biorelevant Dissolution Testing to Predict the Plasma Profile of Lipophilic Drugs after Oral Administration. *Pharm. Res.* **2001**, *18*, 380–388, doi:10.1023/A:1011071401306.
286. van der Meer, J.W.M.; Keuning, J.J.; Scheijgrond, H.W.; Heykants, J.; van Cutsem, J.; Brugmans, J. The Influence of Gastric Acidity on the Bio-Availability of Ketoconazole. *J. Antimicrob. Chemother.* **1980**, *6*, 552–554, doi:10.1093/jac/6.4.552.
287. Galia, E.; Nicolaides, E.; Hörter, D.; Löbenberg, R.; Reppas, C.; Dressman, J.B. Evaluation of Various Dissolution Media for Predicting In Vivo Performance of Class I and II Drugs. *Pharm Res.* **1998**, *15*, 698–705, doi:10.1023/A:1011910801212.
288. Mendes, C.; Buttchevitz, A.; Kruger, J.H.; Caon, T.; de Oliveira Benedet, P.; Lemos-Senna, E.; Silva, M.A.S. Self-Nanoemulsified Drug Delivery System of Hydrochlorothiazide for Increasing Dissolution Rate and Diuretic Activity. *AAPS Pharmscitech* **2017**, *18*, 2494–2504, doi:10.1208/s12249-017-0735-z.
289. Khan, J.; Hawley, A.; Rades, T.; Boyd, B.J. In Situ Lipolysis and Synchrotron Small-Angle X-Ray Scattering for the Direct Determination of the Precipitation and Solid-State Form of a Poorly

Water-Soluble Drug During Digestion of a Lipid-Based Formulation. *J. Pharm. Sci.* **2016**, *105*, 2631–2639, doi:10.1002/jps.24634.

290. Williams, H.D.; Sassene, P.; Kleberg, K.; Bakala-N'Goma, J.C.; Calderone, M.; Jannin, V.; Igonin, A.; Partheil, A.; Marchaud, D.; Jule, E.; et al. Toward the Establishment of Standardized in Vitro Tests for Lipid-Based Formulations, Part 1: Method Parameterization and Comparison of in Vitro Digestion Profiles across a Range of Representative Formulations. *J. Pharm. Sci.* **2012**, *101*, 3360–3380, doi:10.1002/jps.23205.
291. Bakala-N'Goma, J.C.; Williams, H.D.; Sassene, P.J.; Kleberg, K.; Calderone, M.; Jannin, V.; Igonin, A.; Partheil, A.; Marchaud, D.; Jule, E.; et al. Toward the Establishment of Standardized in Vitro Tests for Lipid-Based Formulations. 5. Lipolysis of Representative Formulations by Gastric Lipase. *Pharm. Res.* **2015**, *32*, 1279–1287, doi:10.1007/s11095-014-1532-y.
292. Dahan, A.; Hoffman, A. Use of a Dynamic in Vitro Lipolysis Model to Rationalize Oral Formulation Development for Poor Water Soluble Drugs: Correlation with in Vivo Data and the Relationship to Intra-Enterocyte Processes in Rats. *Pharm. Res.* **2006**, *23*, 2165–2174, doi:10.1007/s11095-006-9054-x.
293. Dahan, A.; Hoffman, A. The Effect of Different Lipid Based Formulations on the Oral Absorption of Lipophilic Drugs: The Ability of in Vitro Lipolysis and Consecutive Ex Vivo Intestinal Permeability Data to Predict in Vivo Bioavailability in Rats. *Eur. J. Pharm. Biopharm.* **2007**, *67*, 96–105, doi:10.1016/j.ejpb.2007.01.017.
294. Crum, M.F.; Trevaskis, N.L.; Williams, H.D.; Pouton, C.W.; Porter, C.J.H. A New in Vitro Lipid Digestion—In Vivo Absorption Model to Evaluate the Mechanisms of Drug Absorption from Lipid-Based Formulations. *Pharm. Res.* **2016**, *33*, 970–982, doi:10.1007/s11095-015-1843-7.
295. Reis, P.; Miller, R.; Leser, M.; Watzke, H. Lipase-Catalyzed Reactions at Interfaces of Two-Phase Systems and Microemulsions. *Appl. Biochem. Biotechnol.* **2009**, *158*, 706–721, doi:10.1007/s12010-008-8354-5.
296. Porter, C.J.H.; Kaukonen, A.M.; Taillardat-Bertschinger, A.; Boyd, B.J.; O'Connor, J.M.; Edwards, G.A.; Charman, W.N. Use of in Vitro Lipid Digestion Data to Explain the in Vivo Performance of Triglyceride-Based Oral Lipid Formulations of Poorly Water-Soluble Drugs: Studies with Halofantrine. *J. Pharm. Sci.* **2004**, *93*, 1110–1121, doi:10.1002/jps.20039.
297. Fatouros, D.G.; Mullertz, A. In Vitro Lipid Digestion Models in Design of Drug Delivery Systems for Enhancing Oral Bioavailability. *Expert Opin. Drug Metab. Toxicol.* **2008**, *4*, 65–76, doi:10.1517/17425255.4.1.65.
298. Larsen, A.; Holm, R.; Pedersen, M.L.; Müllertz, A. Lipid-Based Formulations for Danazol Containing a Digestible Surfactant, Labrafil® M2125CS: In Vivo Bioavailability and Dynamic in Vitro Lipolysis. *Pharm. Res.* **2008**, *25*, 2769–2777, doi:10.1007/s11095-008-9641-0.
299. Christophersen, P.C.; Christiansen, M.L.; Holm, R.; Kristensen, J.; Jacobsen, J.; Abrahamsson, B.; Müllertz, A. Fed and Fasted State Gastro-Intestinal in Vitro Lipolysis: In Vitro in Vivo Relations of a Conventional Tablet, a SNEDDS and a Solidified SNEDDS. *Eur. J. Pharm. Sci.* **2014**, *57*, 232–239, doi:10.1016/j.ejps.2013.09.007.
300. Fei, Y.; Kostewicz, E.S.; Sheu, M.T.; Dressman, J.B. Analysis of the Enhanced Oral Bioavailability of Fenofibrate Lipid Formulations in Fasted Humans Using an in Vitro-in Silico-in Vivo Approach. *Eur. J. Pharm. Biopharm.* **2013**, *85*, 1274–1284, doi:10.1016/j.ejpb.2013.03.001.
301. Thomas, N.; Holm, R.; Müllertz, A.; Rades, T. In Vitro and in Vivo Performance of Novel Supersaturated Self-Nanoemulsifying Drug Delivery Systems (super-SNEDDS). *J. Control. Release* **2012**, *160*, 25–32, doi:10.1016/j.jconrel.2012.02.027.
302. Bibi, H.A.; Holm, R.; Bauer-Brandl, A. Simultaneous Lipolysis/permeation in Vitro Model, for the Estimation of Bioavailability of Lipid Based Drug Delivery Systems. *Eur. J. Pharm. Biopharm.* **2017**, *117*, 300–307, doi:10.1016/j.ejpb.2017.05.001.

303. Tung, N.T.; Tran, C.S.; Pham, T.M.H.; Nguyen, H.A.; Nguyen, T.L.; Chi, S.C.; Nguyen, D.D.; Bui, T.B.H. Development of Solidified Self-Microemulsifying Drug Delivery Systems Containing L-Tetrahydropalmatine: Design of Experiment Approach and Bioavailability Comparison. *Int. J. Pharm.* **2018**, *537*, 9–21, doi:10.1016/j.ijpharm.2017.12.027.
304. Stillhart, C.; Kuentz, M. Comparison of High-Resolution Ultrasonic Resonator Technology and Raman Spectroscopy as Novel Process Analytical Tools for Drug Quantification in Self-Emulsifying Drug Delivery Systems. *J. Pharm. Biomed. Anal.* **2012**, *59*, 29–37, doi:10.1016/j.jpba.2011.10.018.
305. Thomas, N.; Holm, R.; Rades, T.; Müllertz, A. Characterising Lipid Lipolysis and Its Implication in Lipid-Based Formulation Development. *AAPS J.* **2012**, *14*, 860–871, doi:10.1208/s12248-012-9398-6.
306. Stillhart, C.; Cavegn, M.; Kuentz, M. Study of Drug Supersaturation for Rational Early Formulation Screening of Surfactant/co-Solvent Drug Delivery Systems. *J. Pharm. Pharmacol.* **2013**, *65*, 181–192, doi:10.1111/j.2042-7158.2012.01586.x.
307. Stillhart, C.; Imanidis, G.; Kuentz, M. Insights into Drug Precipitation Kinetics during in Vitro Digestion of a Lipid-Based Drug Delivery System Using in-Line Raman Spectroscopy and Mathematical Modeling. *Pharm. Res.* **2013**, *30*, 3114–3130, doi:10.1007/s11095-013-0999-2.
308. Warren, D.B.; Anby, M.U.; Hawley, A.; Boyd, B.J. Real Time Evolution of Liquid Crystalline Nanostructure during the Digestion of Formulation Lipids Using Synchrotron Small-Angle X-ray Scattering. *Langmuir* **2011**, *27*, 9528–9534, doi:10.1021/la2011937.
309. Phan, S.; Hawley, A.; Mulet, X.; Waddington, L.; Prestidge, C.A.; Boyd, B.J. Structural Aspects of Digestion of Medium Chain Triglycerides Studied in Real Time Using sSAXS and Cryo-TEM. *Pharm. Res.* **2013**, *30*, 3088–3100, doi:10.1007/s11095-013-1108-2.
310. Vithani, K.; Hawley, A.; Jannin, V.; Pouton, C.; Boyd, B.J. Solubilisation Behaviour of Poorly Water-Soluble Drugs during Digestion of Solid SMEDDS. *Eur. J. Pharm. Biopharm.* **2018**, *130*, 236–246, doi:10.1016/j.ejpb.2018.07.006.
311. Psimadas, D.; Georgoulias, P.; Valotassiou, V.; Loudos, G. Molecular Nanomedicine Towards Cancer. *J. Pharm. Sci.* **2012**, *101*, 2271–2280, doi:10.1002/jps.
312. Heshmati, N.; Cheng, X.; Dapat, E.; Sassene, P.; Eisenbrand, G.; Fricker, G.; Müllertz, A. In Vitro and in Vivo Evaluations of the Performance of an Indirubin Derivative, Formulated in Four Different Self-Emulsifying Drug Delivery Systems. *J. Pharm. Pharmacol.* **2014**, *66*, 1567–1575, doi:10.1111/jphp.12286.
313. Berthelsen, R.; Holm, R.; Jacobsen, J.; Kristensen, J.; Abrahamsson, B.; Müllertz, A. Kolliphor Surfactants Affect Solubilization and Bioavailability of Fenofibrate. Studies of in Vitro Digestion and Absorption in Rats. *Mol. Pharm.* **2015**, *12*, 1062–1071, doi:10.1021/mp500545k.
314. Do, T.T.; Van Speybroeck, M.; Mols, R.; Annaert, P.; Martens, J.; Van Humbeeck, J.; Vermant, J.; Augustijns, P.; van den Mooter, G. The Conflict between in Vitro Release Studies in Human Biorelevant Media and the in Vivo Exposure in Rats of the Lipophilic Compound Fenofibrate. *Int. J. Pharm.* **2011**, *414*, 118–124, doi:10.1016/j.ijpharm.2011.05.009.
315. Griffin, B.T.; Kuentz, M.; Vertzoni, M.; Kostewicz, E.S.; Fei, Y.; Faisal, W.; Stillhart, C.; O'Driscoll, C.M.; Reppas, C.; Dressman, J.B. Comparison of in Vitro Tests at Various Levels of Complexity for the Prediction of in Vivo Performance of Lipid-Based Formulations: Case Studies with Fenofibrate. *Eur. J. Pharm. Biopharm.* **2014**, *86*, 427–437, doi:10.1016/j.ejpb.2013.10.016.
316. Mosgaard, M.D.; Sassene, P.; Mu, H.; Rades, T.; Müllertz, A. Development of a High-Throughput in Vitro Intestinal Lipolysis Model for Rapid Screening of Lipid-Based Drug Delivery Systems. *Eur. J. Pharm. Biopharm.* **2015**, *94*, 493–500, doi:10.1016/j.ejpb.2015.06.028.

317. Mosgaard, M.D.; Sassene, P.J.; Mu, H.; Rades, T.; Müllertz, A. High-Throughput Lipolysis in 96-Well Plates for Rapid Screening of Lipid-Based Drug Delivery Systems. *J. Pharm. Sci.* **2017**, *106*, 1183–1186, doi:10.1016/j.xphs.2016.12.026.
318. Keemink, J.; Mårtensson, E.; Bergström, C.A.S. Lipolysis-permeation setup for simultaneous study of digestion and absorption in vitro. *Mol. Pharm.* **2019**, *16*, 921–930, doi:10.1021/acs.molpharmaceut.8b00811.
319. Alskär, L.C.; Parrow, A.; Keemink, J.; Johansson, P.; Abrahamsson, B.; Bergström, C.A.S. Effect of Lipids on Absorption of Carvedilol in Dogs: Is Coadministration of Lipids as Efficient as a Lipid-Based Formulation? *J. Control. Release* **2019**, *304*, 90–100, doi:10.1016/j.jconrel.2019.04.038.
320. Ciappellano, S.G.; Tedesco, E.; Venturini, M.; Benetti, F. In Vitro Toxicity Assessment of Oral Nanocarriers. *Adv. Drug Deliv. Rev.* **2016**, *106*, 381–401, doi:10.1016/j.addr.2016.08.007.
321. Avdeef, A. The Rise of PAMPA. *Expert Opin. Drug Metab. Toxicol.* **2005**, *1*, 325–342, doi:10.1517/17425255.1.2.325.
322. Cabrera-Pérez, M.Á.; Sanz, M.B.; Sanjuan, V.M.; González-Álvarez, M.; Álvarez, I.G. Importance and Applications of Cell-and Tissue-Based in Vitro Models for Drug Permeability Screening in Early Stages of Drug Development. *Concepts Model. Drug Permeability Stud. Cell Tissue Based Vitr. Cult. Model.* **2016**, 3–29, doi:10.1016/B978-0-08-100094-6.00002-X.
323. Hiremath, P.S.; Soppimath, K.S.; Betageri, G.V. Proliposomes of Exemestane for Improved Oral Delivery: Formulation and in Vitro Evaluation Using PAMPA, Caco-2 and Rat Intestine. *Int. J. Pharm.* **2009**, *380*, 96–104, doi:10.1016/j.ijpharm.2009.07.008.
324. Berben, P.; Bauer-Brandl, A.; Brandl, M.; Faller, B.; Flaten, G.E.; Jacobsen, A.C.; Brouwers, J.; Augustijns, P. Drug Permeability Profiling Using Cell-Free Permeation Tools: Overview and Applications. *Eur. J. Pharm. Sci.* **2018**, *119*, 219–233, doi:10.1016/j.ejps.2018.04.016.
325. Sugano, K. Artificial Membrane Technologies to Assess Transfer and Permeation of Drugs in Drug Discovery. *Compr. Med. Chem. II* **2006**, *5*, 453–487, doi:10.1016/b0-08-045044-x/00136-x.
326. Diukendjieva, A.; Tsakovska, I.; Alov, P.; Pencheva, T.; Pajeva, I.; Worth, A.P.; Madden, J.C.; Cronin, M.T.D. Advances in the Prediction of Gastrointestinal Absorption: Quantitative Structure-Activity Relationship (QSAR) Modelling of PAMPA Permeability. *Comput. Toxicol.* **2019**, *10*, 51–59, doi:10.1016/j.comtox.2018.12.008.
327. Nekkanti, V.; Wang, Z.; Betageri, G.V. Pharmacokinetic Evaluation of Improved Oral Bioavailability of Valsartan: Proliposomes Versus Self-Nanoemulsifying Drug Delivery System. *AAPS Pharmscitech* **2016**, *17*, 851–862, doi:10.1208/s12249-015-0388-8.
328. Dumont, C.; Bourgeois, S.; Fessi, H.; Jannin, V. Lipid-Based Nanosuspensions for Oral Delivery of Peptides, a Critical Review. *Int. J. Pharm.* **2018**, *541*, 117–135, doi:10.1016/j.ijpharm.2018.02.038.
329. Sambuy, Y.; de Angelis, I.; Ranaldi, G.; Scarino, M.L.; Stammati, A.; Zucco, F. The Caco-2 Cell Line as a Model of the Intestinal Barrier: Influence of Cell and Culture-Related Factors on Caco-2 Cell Functional Characteristics. *Cell Biol. Toxicol.* **2005**, *21*, 1–26, doi:10.1007/s10565-005-0085-6.
330. Föger, F.; Kopf, A.; Loretz, B.; Albrecht, K.; Bernkop-Schnürch, A. Correlation of in Vitro and in Vivo Models for the Oral Absorption of Peptide Drugs. *Amino Acids* **2008**, *35*, 233–241, doi:10.1007/s00726-007-0581-5.
331. Artursson, P.; Palm, K.; Luthman, K. Caco-2 Monolayers in Experimental and Theoretical Predictions of Drug Transport. *Adv. Drug Deliv. Rev.* **2012**, *64*, 280–289, doi:10.1016/j.addr.2012.09.005.
332. Buya, A.B.; Ucakar, B.; Beloqui, A.; Memvanga, P.B.; Préat, V. Design and Evaluation of Self-Nanoemulsifying Drug Delivery Systems (SNEDDSs) for Senicapoc. *Int. J. Pharm.* **2020**, *580*, 119180, doi:10.1016/j.ijpharm.2020.119180.
333. Dantzig, A.H.; Bergin, L. Uptake of the Cephalosporin, Cephalexin, by a Dipeptide Transport Carrier in the Human Intestinal Cell Line, Caco-2. *BBA Biomembr.* **1990**, *1027*, 211–217, doi:10.1016/0005-2736(90)90309-C.

334. Yamashita, S.; Furubayashi, T.; Kataoka, M.; Sakane, T.; Sezaki, H.; Tokuda, H. Optimized Conditions for Prediction of Intestinal Drug Permeability Using Caco-2 Cells. *Eur. J. Pharm. Sci.* **2000**, *10*, 195–204, doi:10.1016/S0928-0987(00)00076-2.
335. Obringer, C.; Manwaring, J.; Goebel, C.; Hewitt, N.J.; Rothe, H. Suitability of the in Vitro Caco-2 Assay to Predict the Oral Absorption of Aromatic Amine Hair Dyes. *Toxicol. Vitr.* **2016**, *32*, 1–7, doi:10.1016/j.tiv.2015.11.007.
336. Love, S.A.; Maurer-Jones, M.A.; Thompson, J.W.; Lin, Y.-S.; Haynes, C.L. Assessing Nanoparticle Toxicity. *Annu. Rev. Anal. Chem.* **2012**, *5*, 181–205, doi:10.1146/annurev-anchem-062011-143134.
337. Rathod, D.; Fu, Y.; Patel, K. BRD4 PROTAC as a Novel Therapeutic Approach for the Treatment of Vemurafenib Resistant Melanoma: Preformulation Studies, Formulation Development and in Vitro Evaluation. *Eur. J. Pharm. Sci.* **2019**, *138*, 105039, doi:10.1016/j.ejps.2019.105039.
338. Li, J.; Yang, L.; Shen, R.; Gong, L.; Tian, Z.; Qiu, H.; Shi, Z.; Gao, L.; Sun, H.; Zhang, G. Self-Nanoemulsifying System Improves Oral Absorption and Enhances Anti-Acute Myeloid Leukemia Activity of Berberine. *J. Nanobiotechnol.* **2018**, *16*, 1–13, doi:10.1186/s12951-018-0402-x.
339. Beg, S.; Alam, M.N.; Ahmad, F.J.; Singh, B. Chylomicron Mimicking Nanocolloidal Carriers of Rosuvastatin Calcium for Lymphatic Drug Targeting and Management of Hyperlipidemia. *Colloids Surfaces B Biointerfaces* **2019**, *177*, 541–549, doi:10.1016/j.colsurfb.2019.02.039.
340. Tong, Y.; Zhang, Q.; Shi, W.; Wang, J. Mechanisms of Oral Absorption Improvement for Insoluble Drugs by the Combination of Phospholipid Complex and SNEDDS. *Drug Deliv.* **2019**, *26*, 1155–1166, doi:10.1080/10717544.2019.1686086.
341. Aktas, Y.; Celik Tekeli, M.; Celebi, N. Development and Characterization of Exendin-4 Loaded Self-Nanoemulsifying System and in Vitro Evaluation on Caco-2 Cell Line. *J. Microencapsul.* **2020**, *37*, 41–51, doi:10.1080/02652048.2019.1692945.
342. Kontogiannidou, E.; Meikopoulos, T.; Virgiliou, C.; Bouropoulos, N.; Gika, H.; Vizirianakis, I.S.; Müllertz, A.; Fatouros, D.G. Towards the Development of Self-Nano-Emulsifying Drug Delivery Systems (SNEDDS) Containing Trimethyl Chitosan for the Oral Delivery of Amphotericin B: In Vitro Assessment and Cytocompatibility Studies. *J. Drug Deliv. Sci. Technol.* **2020**, *56*, 101524, doi:10.1016/j.jddst.2020.101524.
343. Jones, C.F.; Grainger, D.W. In Vitro Assessments of Nanomaterial Toxicity. *Adv. Drug Deliv. Rev.* **2009**, *61*, 438–456, doi:10.1016/j.addr.2009.03.005.
344. Marquis, B.J.; Love, S.A.; Braun, K.L.; Haynes, C.L. Analytical Methods to Assess Nanoparticle Toxicity. *Analyst* **2009**, *134*, 425–439, doi:10.1039/b818082b.
345. Monteiro-Riviere, N.A.; Inman, A.O.; Zhang, L.W. Limitations and Relative Utility of Screening Assays to Assess Engineered Nanoparticle Toxicity in a Human Cell Line. *Toxicol. Appl. Pharmacol.* **2009**, *234*, 222–235, doi:10.1016/j.taap.2008.09.030.
346. Botha, N.; Gehringer, M.M.; Downing, T.G.; van de Venter, M.; Shephard, E.G. The Role of Microcystin-LR in the Induction of Apoptosis and Oxidative Stress in $CaCo_2$ Cells. *Toxicon* **2004**, *43*, 85–92, doi:10.1016/j.toxicon.2003.10.025.
347. Fisichella, M.; Bérenguer, F.; Steinmetz, G.; Auffan, M.; Rose, J.; Prat, O. Reply to Comment on Fisichella et al. (2012), "Intestinal Toxicity Evaluation of TiO_2 Degraded Surface-Treated Nanoparticles: A Combined Physico-Chemical and Toxicogenomics Approach in Caco-2 Cells" by Faust et al. *Part. Fibre Toxicol.* **2012**, *9*, 1–2, doi:10.1186/1743-8977-9-39.
348. Holder, A.L.; Goth-Goldstein, R.; Lucas, D.; Koshland, C.P. Particle-Induced Artifacts in the MTT and LDH Viability Assays. *Chem. Res. Toxicol.* **2012**, *25*, 1885–1892, doi:10.1021/tx3001708.
349. Alvi, M.M.; Chatterjee, P. A Prospective Analysis of Co-Processed Non-Ionic Surfactants in Enhancing Permeability of a Model Hydrophilic Drug. *AAPS Pharmscitech* **2014**, *15*, 339–353, doi:10.1208/s12249-013-0065-8.
350. Riss, T.L.; Moravec, R.A.; Niles, A.L.; Duellman, S.; Benink, H.A.; Worzella, T.J.; Minor, L. Cell Viability Assays. Assay Guidance Manual, Eli Lilly & Company and the National Center for

Advancing Translational Sciences, Bethesda, MD, USA, **2004**; pp 1-31, PMID: 23805433. Available online: http://www.ncbi.nlm.nih.gov/pubmed/23805433 (Accessed on 17 April 2020).

351. Desai, H.H.; Bu, P.; Shah, A.V.; Cheng, X.; Serajuddin, A.T.M. Evaluation of Cytotoxicity of Self-Emulsifying Formulations Containing Long-Chain Lipids Using Caco-2 Cell Model: Superior Safety Profile Compared to Medium-Chain Lipids. *J. Pharm. Sci.* **2020**, *109*, 1752–1764, doi:10.1016/j.xphs.2020.01.031.
352. Grassi, M.; Cadelli, G. Theoretical Considerations on the in Vivo Intestinal Permeability Determination by Means of the Single Pass and Recirculating Techniques. *Int. J. Pharm.* **2001**, *229*, 95–105, doi:10.1016/S0378-5173(01)00848-1.
353. Prajapati, S.T.; Joshi, H.A.; Patel, C.N. Preparation and Characterization of Self-Microemulsifying Drug Delivery System of Olmesartan Medoxomil for Bioavailability Improvement. *J. Pharm.* **2013**, *2013*, 1–9, doi:10.1155/2013/728425.
354. Dezani, T.M.; Dezani, A.B.; Junior, J.B.D.S.; Serra, C.H.D.R. Single-Pass Intestinal Perfusion (SPIP) and Prediction of Fraction Absorbed and Permeability in Humans: A Study with Antiretroviral Drugs. *Eur. J. Pharm. Biopharm.* **2016**, *104*, 131–139, doi:10.1016/j.ejpb.2016.04.020.
355. Luo, Z.; Liu, Y.; Zhao, B.; Tang, M.; Dong, H.; Zhang, L.; Lv, B.; Wei, L. Ex Vivo and in Situ Approaches Used to Study Intestinal Absorption. *J. Pharmacol. Toxicol. Methods* **2013**, *68*, 208–216, doi:10.1016/j.vascn.2013.06.001.
356. Zhou, P.; Li, L.P.; Luo, S.Q.; Jiang, H.D.; Zeng, S. Intestinal Absorption of Luteolin from Peanut Hull Extract Is More Efficient than That from Individual Pure Luteolin. *J. Agric. Food Chem.* **2008**, *56*, 296–300, doi:10.1021/jf072612+.
357. Singh, B.; Singh, R.; Bandyopadhyay, S.; Kapil, R.; Garg, B. Optimized Nanoemulsifying Systems with Enhanced Bioavailability of Carvedilol. *Colloids Surfaces B Biointerfaces* **2013**, *101*, 465–474, doi:10.1016/j.colsurfb.2012.07.017.
358. Kazi, M.; Al-Swairi, M.; Ahmad, A.; Raish, M.; Alanazi, F.K.; Badran, M.M.; Khan, A.A.; Alanazi, A.M.; Hussain, M.D. Evaluation of Self-Nanoemulsifying Drug Delivery Systems (SNEDDS) for Poorly Water-Soluble Talinolol: Preparation, in Vitroand in vivoAssessment. *Front. Pharmacol.* **2019**, *10*, 1–13, doi:10.3389/fphar.2019.00459.
359. Beg, S.; Kaur, R.; Khurana, R.K.; Rana, V.; Sharma, T.; Singh, B. QbD-Based Development of Cationic Self-Nanoemulsifying Drug Delivery Systems of Paclitaxel with Improved Biopharmaceutical Attributes. *AAPS Pharmscitech* **2019**, *20*, 1–13, doi:10.1208/s12249-019-1319-x.
360. Sandhu, P.S.; Beg, S.; Mehta, F.; Singh, B.; Trivedi, P. Novel Dietary Lipid-Based Self-Nanoemulsifying Drug Delivery Systems of Paclitaxel with P-Gp Inhibitor: Implications on Cytotoxicity and Biopharmaceutical Performance. *Expert Opin. Drug Deliv.* **2015**, *12*, 1809–1822, doi:10.1517/17425247.2015.1060219.
361. Zhang, H.; Yao, M.; Morrison, R.A.; Chong, S. Commonly Used Surfactant, Tween® 80, Improves Absorption of P-Glycoprotein Substrate, Digoxin, in Rats. *Arch. Pharm. Res.* **2003**, *26*, 768–772, doi:10.1007/BF02976689.
362. Seo, Y.G.; Kim, D.H.; Ramasamy, T.; Kim, J.H.; Marasini, N.; Oh, Y.K.; Kim, D.W.; Kim, J.K.; Yong, C.S.; Kim, J.O.; et al. Development of Docetaxel-Loaded Solid Self-Nanoemulsifying Drug Delivery System (SNEDDS) for Enhanced Chemotherapeutic Effect. *Int. J. Pharm.* **2013**, *452*, 412–420, doi:10.1016/j.ijpharm.2013.05.034.
363. Truong, D.H.; Tran, T.H.; Ramasamy, T.; Choi, J.Y.; Lee, H.H.; Moon, C.; Choi, H.G.; Yong, C.S.; Kim, J.O. Development of Solid Self-Emulsifying Formulation for Improving the Oral Bioavailability of Erlotinib. *AAPS Pharmscitech* **2016**, *17*, 466–473, doi:10.1208/s12249-015-0370-5.
364. Faisal, W.; Ruane-O'Hora, T.; O'Driscoll, C.M.; Griffin, B.T. A Novel Lipid-Based Solid Dispersion for Enhancing Oral Bioavailability of Lycopene - In Vivo Evaluation Using a Pig Model. *Int. J. Pharm.* **2013**, *453*, 307–314, doi:10.1016/j.ijpharm.2013.06.027.

365. Bourkaib, N.; Zhou, J.; Yao, J.; Fang, Z.; Mezghrani, O. Combination of β-Cyclodextrin Inclusion Complex and Self-Microemulsifying Drug Delivery System for Photostability and Enhanced Oral Bioavailability of Methotrexate: Novel Technique. *Drug Dev. Ind. Pharm.* **2013**, *39*, 918–927, doi:10.3109/03639045.2012.718785.
366. Negi, L.M.; Tariq, M.; Talegaonkar, S. Nano Scale Self-Emulsifying Oil Based Carrier System for Improved Oral Bioavailability of Camptothecin Derivative by P-Glycoprotein Modulation. *Colloids Surfaces B Biointerfaces* **2013**, *111*, 346–353, doi:10.1016/j.colsurfb.2013.06.001.
367. Wei, L.; Sun, P.; Nie, S.; Pan, W. Preparation and Evaluation of SEDDS and SMEDDS Containing Carvedilol. *Drug Dev. Ind. Pharm.* **2005**, *31*, 785–794, doi:10.1080/03639040500216428.
368. Jing, B.; Wang, Z.; Yang, R.; Zheng, X.; Zhao, J.; Tang, S.; He, Z. Enhanced Oral Bioavailability of Felodipine by Novel Solid Self-Microemulsifying Tablets. *Drug Dev. Ind. Pharm.* **2016**, *42*, 506–512, doi:10.3109/03639045.2015.1058816.
369. Bakhle, S.S.; Avari, J.G. Development and Characterization of Solid Self-Emulsifying Drug Delivery System of Cilnidipine. *Chem. Pharm. Bull.* **2015**, *63*, 408–417, doi:10.1248/cpb.c14-00326.
370. Chopra, M.; Nayak, U.Y.; Kumar Gurram, A.; Sreenivasa Reddy, M.; Koteshwara, K.B. Formulation, Characterization and In Vivo Evaluation of Self-Nanoemulsifying Drug Delivery System for Oral Delivery of Valsartan. *Curr. Nanosci.* **2013**, *10*, 263–270, doi:10.2174/15734137113096660107.
371. Bhattacharjee, A.; Verma, S.; Verma, P.R.P.; Singh, S.K.; Chakraborty, A. Fabrication of Liquid and Solid Self-Double Emulsifying Drug Delivery System of Atenolol by Response Surface Methodology. *J. Drug Deliv. Sci. Technol.* **2017**, *41*, 45–57, doi:10.1016/j.jddst.2017.06.014.
372. Li, P.; Tan, A.; Prestidge, C.A.; Nielsen, H.M.; Müllertz, A. Self-Nanoemulsifying Drug Delivery Systems for Oral Insulin Delivery: In Vitro and in Vivo Evaluations of Enteric Coating and Drug Loading. *Int. J. Pharm.* **2014**, *477*, 390–398, doi:10.1016/j.ijpharm.2014.10.039.
373. Bari, A.; Chella, N.; Sanka, K.; Shastri, N.R.; Diwan, P.V. Improved Anti-Diabetic Activity of Glibenclamide Using Oral Self Nano Emulsifying Powder. *J. Microencapsul.* **2015**, *32*, 54–60, doi:10.3109/02652048.2014.944950.
374. Wang, H.; Li, Q.; Deng, W.; Omari-Siaw, E.; Wang, Q.; Wang, S.; Wang, S.; Cao, X.; Xu, X.; Yu, J. Self-Nanoemulsifying Drug Delivery System of Trans-Cinnamic Acid: Formulation Development and Pharmacodynamic Evaluation in Alloxan-Induced Type 2 Diabetic Rat Model. *Drug Dev. Res.* **2015**, *76*, 82–93, doi:10.1002/ddr.21244.
375. Wankhade, V.P.; Atram, S.C.; Bobade, N.N.; Pande, S.D.; Tapar, K.K. Formulation and Optimization of SNEDDS of Gliclazide Using Response Surface Methodology. *Asian J. Pharm.* **2012**, *6*, 289–294, doi:10.4103/0973-8398.107565.
376. Menzel, C.; Holzeisen, T.; Laffleur, F.; Zaichik, S.; Abdulkarim, M.; Gumbleton, M.; Bernkop-Schnürch, A. In Vivo Evaluation of an Oral Self-Emulsifying Drug Delivery System (SEDDS) for Exenatide. *J. Control. Release* **2018**, *277*, 165–172, doi:10.1016/j.jconrel.2018.03.018.
377. Jain, S.; Jain, A.K.; Pohekar, M.; Thanki, K. Novel Self-Emulsifying Formulation of Quercetin for Improved in Vivo Antioxidant Potential: Implications for Drug-Induced Cardiotoxicity and Nephrotoxicity. *Free Radic. Biol. Med.* **2013**, *65*, 117–130, doi:10.1016/j.freeradbiomed.2013.05.041.
378. Mamadou, G.; Charrueau, C.; Dairou, J.; Limas Nzouzi, N.; Eto, B.; Ponchel, G. Increased Intestinal Permeation and Modulation of Presystemic Metabolism of Resveratrol Formulated into Self-Emulsifying Drug Delivery Systems. *Int. J. Pharm.* **2017**, *521*, 150–155, doi:10.1016/j.ijpharm.2017.02.036.
379. Zhu, S.; Hong, M.; Liu, C.; Pei, Y. Application of Box-Behnken Design in Understanding the Quality of Genistein Self-Nanoemulsified Drug Delivery Systems and Optimizing Its Formulation. *Pharm. Dev. Technol.* **2009**, *14*, 642–649, doi:10.3109/10837450902882385.

380. Taha, E.I.; Al-Saidan, S.; Samy, A.M.; Khan, M.A. Preparation and in Vitro Characterization of Self-Nanoemulsified Drug Delivery System (SNEDDS) of All-Trans-Retinol Acetate. *Int. J. Pharm.* **2004**, *285*, 109–119, doi:10.1016/j.ijpharm.2004.03.034.
381. Garg, B.; Beg, S.; Kaur, R.; Kumar, R.; Katare, O.P.; Singh, B. Long-Chain Triglycerides-Based Self-Nanoemulsifying Oily Formulations (SNEOFs) of Darunavir with Improved Lymphatic Targeting Potential. *J. Drug Target.* **2018**, *26*, 252–266, doi:10.1080/1061186X.2017.1365875.
382. Garg, B.; Katare, O.P.; Beg, S.; Lohan, S.; Singh, B. Systematic Development of Solid Self-Nanoemulsifying Oily Formulations (S-SNEOFs) for Enhancing the Oral Bioavailability and Intestinal Lymphatic Uptake of Lopinavir. *Colloids Surfaces B Biointerfaces* **2016**, *141*, 611–622, doi:10.1016/j.colsurfb.2016.02.012.
383. Patel, D.; Sawant, K.K. Oral Bioavailability Enhancement of Acyclovir by Self-Microemulsifying Drug Delivery Systems (SMEDDS). *Drug Dev. Ind. Pharm.* **2007**, *33*, 1318–1326, doi:10.1080/03639040701385527.
384. Hussain, A.; Kumar Singh, S.; Ranjan Prasad Verma, P.; Singh, N.; Jalees Ahmad, F. Experimental Design-Based Optimization of Lipid Nanocarrier as Delivery System against Mycobacterium Species: In Vitro and in Vivo Evaluation. *Pharm. Dev. Technol.* **2017**, *22*, 910–927, doi:10.1080/10837450.2016.1212879.
385. Wasan, E.K.; Bartlett, K.; Gershkovich, P.; Sivak, O.; Banno, B.; Wong, Z.; Gagnon, J.; Gates, B.; Leon, C.G.; Wasan, K.M. Development and Characterization of Oral Lipid-Based Amphotericin B Formulations with Enhanced Drug Solubility, Stability and Antifungal Activity in Rats Infected with Aspergillus Fumigatus or Candida Albicans. *Int. J. Pharm.* **2009**, *372*, 76–84, doi:10.1016/j.ijpharm.2009.01.003.
386. Gurav, N.P.; Dandagi, P.M.; Gadad, A.P.; Masthiholimath, V.S. Solubility Enhancement of Satranidazole Using Self Emulsified Drug Delivery Systems. *Indian J. Pharm. Educ. Res.* **2016**, *50*, S68–S75, doi:10.5530/ijper.50.2.20.
387. Perlman, M.E.; Murdande, S.B.; Gumkowski, M.J.; Shah, T.S.; Rodricks, C.M.; Thornton-Manning, J.; Freel, D.; Erhart, L.C. Development of a Self-Emulsifying Formulation That Reduces the Food Effect for Torcetrapib. *Int. J. Pharm.* **2008**, *351*, 15–22, doi:10.1016/j.ijpharm.2007.09.015.
388. El-Say, K.M.; Ahmed, T.A.; Ahmed, O.A.A.; Hosny, K.M.; Abd-Allah, F.I. Self-Nanoemulsifying Lyophilized Tablets for Flash Oral Transmucosal Delivery of Vitamin K: Development and Clinical Evaluation. *J. Pharm. Sci.* **2017**, *106*, 2447–2456, doi:10.1016/j.xphs.2017.01.001.
389. Julianto, T.; Yuen, K.H.; Noor, A.M. Improved Bioavailability of Vitamin E with a Self Emulsifying Formulation. *Int. J. Pharm.* **2000**, *200*, 53–57, doi:10.1016/S0378-5173(00)00337-9.
390. Postolache, P.; Petrescu, O.; Dorneanu, V.; Zanini, A.C. Cyclosporine Bioavailability of Two Physically Different Oral Formulations. *Eur. Rev. Med. Pharmacol. Sci.* **2002**, *6*, 127–131, PMID 12776806.
391. Abdelbary, G.; Amin, M.; Salah, S. Self Nano-Emulsifying Simvastatin Based Tablets: Design and in Vitro/in Vivo Evaluation. *Pharm. Dev. Technol.* **2013**, *18*, 1294–1304, doi:10.3109/10837450.2012.672989.
392. Roche Laboratoiries Home Page. Available online: http://www.pharmatimes.com/news/roche_to_pull_Fortovase®_hiv_drug_998246 (accessed on 18 May 2020).
393. Mohsin, K.; Alamri, R.; Ahmad, A.; Raish, M.; Alanazi, F.K.; Hussain, M.D. Development of Self-Nanoemulsifying Drug Delivery Systems for the Enhancement of Solubility and Oral Bioavailability of Fenofibrate, A Poorly Water-Soluble Drug. *Int. J. Nanomed.* **2016**, *11*, 2829–2838, doi:10.2147/IJN.S104187.
394. Park, H.; Ha, E.; Kim, M. Current Status of Supersaturable Self-Emulsifying Drug Delivery Systems. *Pharmaceutics* **2020**, *12*, 365, doi:10.3390/pharmaceutics12040365.

395. Porter, C.J.H.; Trevaskis, N.L.; Charman, W.N. Lipids and Lipid-Based Formulations: Optimizing the Oral Delivery of Lipophilic Drugs. *Nat. Rev. Drug Discov.* **2007**, *6*, 231–248, doi:10.1038/nrd2197.
396. Christensen, J.Ø.; Schultz, K.; Mollgaard, B.; Kristensen, H.G.; Mullertz, A. Solubilisation of Poorly Water-Soluble Drugs during in Vitro Lipolysis of Medium- and Long-Chain Triacylglycerols. *Eur. J. Pharm. Sci.* **2004**, *23*, 287–296, doi:10.1016/j.ejps.2004.08.003.
397. Kaukonen, A.M.; Boyd, B.J.; Porter, C.J.H.; Charman, W.N. Drug Solubilization Behavior during in Vitro Digestion of Simple Triglyceride Lipid Solution Formulations. *Pharm. Res.* **2004**, *21*, 245–253, doi:10.1023/B:PHAM.0000016282.77887.1f.
398. Thomas, N.; Holm, R.; Garmer, M.; Karlsson, J.J.; Müllertz, A.; Rades, T. Supersaturated Self-Nanoemulsifying Drug Delivery Systems (Super-SNEDDS) Enhance the Bioavailability of the Poorly Water-Soluble Drug Simvastatin in Dogs. *AAPS J.* **2013**, *15*, 219–227, doi:10.1208/s12248-012-9433-7.
399. Mukherjee, T.; Plakogiannis, F.M. Development and Oral Bioavailability Assessment of a Supersaturated Self-Microemulsifying Drug Delivery System (SMEDDS) of Albendazole. *J. Pharm. Pharmacol.* **2010**, *62*, 1112–1120, doi:10.1111/j.2042-7158.2010.01149.x.
400. Bandyopadhyay, S.; Katare, O.; Singh, B. Development of Optimized Supersaturable Self-Nanoemulsifying Systems of Ezetimibe: Effect of Polymers and Efflux Transporters. *Expert Opin. Drug Deliv.* **2014**, *11*, 479–492, doi:10.1517/17425247.2014.877885.
401. Strindberg, S.; Plum, J.; Stie, M.B.; Christiansen, M.L.; Hagner Nielsen, L.; Rades, T.; Müllertz, A. Effect of Supersaturation on Absorption of Indomethacin and Tadalafil in a Single Pass Intestinal Perfusion Rat Model, in the Absence and Presence of a Precipitation Inhibitor. *Eur. J. Pharm. Biopharm.* **2020**, *151*, 108–115, doi:10.1016/j.ejpb.2020.03.019.
402. van Speybroeck, M.; Mellaerts, R.; Mols, R.; Do Thi, T.; Martens, J.A.; Van Humbeeck, J.; Annaert, P.; van den Mooter, G.; Augustijns, P. Enhanced Absorption of the Poorly Soluble Drug Fenofibrate by Tuning Its Release Rate from Ordered Mesoporous Silica. *Eur. J. Pharm. Sci.* **2010**, *41*, 623–630, doi:10.1016/j.ejps.2010.09.002.
403. Bannow, J.; Yorulmaz, Y.; Löbmann, K.; Müllertz, A.; Rades, T. Improving the Drug Load and in Vitro Performance of Supersaturated Self-Nanoemulsifying Drug Delivery Systems (super-SNEDDS) Using Polymeric Precipitation Inhibitors. *Int. J. Pharm.* **2020**, *575*, 118960, doi:10.1016/j.ijpharm.2019.118960.
404. Quan, G.; Niu, B.; Singh, V.; Zhou, Y.; Wu, C.Y.; Pan, X.; Wu, C. Supersaturable Solid Self-Microemulsifying Drug Delivery System: Precipitation Inhibition and Bioavailability Enhancement. *Int. J. Nanomed.* **2017**, *12*, 8801–8811, doi:10.2147/IJN.S149717.
405. Hansson, G.C. Role of Mucus Layers in Gut Infection and Inflammation. *Curr. Opin. Microbiol.* **2012**, *15*, 57–62, doi:10.1016/j.mib.2011.11.002.
406. Zaichik, S.; Steinbring, C.; Jelkmann, M.; Bernkop-Schnürch, A. Zeta Potential Changing Nanoemulsions: Impact of PEG-Corona on Phosphate Cleavage. *Int. J. Pharm.* **2020**, *581*, 119299, doi:10.1016/j.ijpharm.2020.119299.
407. Hintzen, F.; Perera, G.; Hauptstein, S.; Müller, C.; Laffleur, F.; Bernkop-Schnürch, A. In Vivo Evaluation of an Oral Self-Microemulsifying Drug Delivery System (SMEDDS) for Leuprorelin. *Int. J. Pharm.* **2014**, *472*, 20–26, doi:10.1016/j.ijpharm.2014.05.047.
408. Dünnhaupt, S.; Kammona, O.; Waldner, C.; Kiparissides, C.; Bernkop-Schnürch, A. Nano-Carrier Systems: Strategies to Overcome the Mucus Gel Barrier. *Eur. J. Pharm. Biopharm.* **2015**, *96*, 447–453, doi:10.1016/j.ejpb.2015.01.022.
409. Griesser, J.; Hetényi, G.; Kadas, H.; Demarne, F.; Jannin, V.; Bernkop-Schnürch, A. Self-Emulsifying Peptide Drug Delivery Systems: How to Make Them Highly Mucus Permeating. *Int. J. Pharm.* **2018**, *538*, 159–166, doi:10.1016/j.ijpharm.2018.01.018.

410. Friedl, H.; Dünnhaupt, S.; Hintzen, F.; Waldner, C.; Parikh, S.; Pearson, J.P.; Wilcox, M.D.; Bernkop-Schnürch, A. Development and Evaluation of a Novel Mucus Diffusion Test System Approved by Self-Nanoemulsifying Drug Delivery Systems. *J. Pharm. Sci.* **2013**, *102*, 4406–4413, doi:10.1002/jps.23757.
411. Suchaoin, W.; Pereira de Sousa, I.; Netsomboon, K.; Lam, H.T.; Laffleur, F.; Bernkop-Schnürch, A. Development and in Vitro Evaluation of Zeta Potential Changing Self-Emulsifying Drug Delivery Systems for Enhanced Mucus Permeation. *Int. J. Pharm.* **2016**, *510*, 255–262, doi:10.1016/j.ijpharm.2016.06.045.
412. Griesser, J.; Hetényi, G.; Moser, M.; Demarne, F.; Jannin, V.; Bernkop-Schnürch, A. Hydrophobic Ion Pairing: Key to Highly Payloaded Self-Emulsifying Peptide Drug Delivery Systems. *Int. J. Pharm.* **2017**, *520*, 267–274, doi:10.1016/j.ijpharm.2017.02.019.
413. Nazir, I.; Fürst, A.; Lupo, N.; Hupfauf, A.; Gust, R.; Bernkop-Schnürch, A. Zeta Potential Changing Self-Emulsifying Drug Delivery Systems: A Promising Strategy to Sequentially Overcome Mucus and Epithelial Barrier. *Eur. J. Pharm. Biopharm.* **2019**, *144*, 40–49, doi:10.1016/j.ejpb.2019.09.007.
414. Prüfert, F.; Fischer, F.; Leichner, C.; Zaichik, S.; Bernkop-Schnürch, A. Development and In Vitro Evaluation of Stearic Acid Phosphotyrosine Amide as New Excipient for Zeta Potential Changing Self-Emulsifying Drug Delivery Systems. *Pharm. Res.* **2020**, *37*, 79, doi:10.1007/s11095-020-02802-2.
415. Bernkop-Schnürch, A. Thiomers: A New Generation of Mucoadhesive Polymers. *Adv. Drug Deliv. Rev.* **2005**, *57*, 1569–1582, doi:10.1016/j.addr.2005.07.002.
416. Barthelmes, J.; Dnnhaupt, S.; Hombach, J.; Bernkop-Schnrch, A. Thiomer Nanoparticles: Stabilization via Covalent Cross-Linking. *Drug Deliv.* **2011**, *18*, 613–619, doi:10.3109/10717544.2011.621986.
417. Rohrer, J.; Partenhauser, A.; Hauptstein, S.; Gallati, C.M.; Matuszczak, B.; Abdulkarim, M.; Gumbleton, M.; Bernkop-Schnürch, A. Mucus Permeating Thiolated Self-Emulsifying Drug Delivery Systems. *Eur. J. Pharm. Biopharm.* **2016**, *98*, 90–97, doi:10.1016/j.ejpb.2015.11.004.
418. Efiana, N.A.; Phan, T.N.Q.; Wicaksono, A.J.; Bernkop-Schnürch, A. Mucus Permeating Self-Emulsifying Drug Delivery Systems (SEDDS): About the Impact of Mucolytic Enzymes. *Colloids Surfaces B Biointerfaces* **2018**, *161*, 228–235, doi:10.1016/j.colsurfb.2017.10.032.
419. Bonengel, S.; Haupstein, S.; Perera, G.; Bernkop-Schnürch, A. Thiolated and S-Protected Hydrophobically Modified Cross-Linked Poly(acrylic Acid)—A New Generation of Multifunctional Polymers. *Eur. J. Pharm. Biopharm.* **2014**, *88*, 390–396, doi:10.1016/j.ejpb.2014.06.009.
420. Leonaviciute, G.; Adamovic, N.T.; Lam, H.T.; Rohrer, J.; Partenhauser, A.; Bernkop-Schnürch, A. Self-Emulsifying Drug Delivery Systems (SEDDS): Proof-of-Concept How to Make Them Mucoadhesive. *Eur. J. Pharm. Biopharm.* **2017**, *112*, 51–57, doi:10.1016/j.ejpb.2016.11.019.
421. Abdulkarim, M.; Sharma, P.K.; Gumbleton, M. Self-Emulsifying Drug Delivery System: Mucus Permeation and Innovative Quantification Technologies. *Adv. Drug Deliv. Rev.* **2019**, *142*, 62–74, doi:10.1016/j.addr.2019.04.001.
422. Leichner, C.; Menzel, C.; Laffleur, F.; Bernkop-Schnürch, A. Development and in Vitro Characterization of a Papain Loaded Mucolytic Self-Emulsifying Drug Delivery System (SEDDS). *Int. J. Pharm.* **2017**, *530*, 346–353, doi:10.1016/j.ijpharm.2017.08.059.
423. Balakrishnan, P.; Lee, B.J.; Oh, D.H.; Kim, J.O.; Lee, Y.I.; Kim, D.D.; Jee, J.P.; Lee, Y.B.; Woo, J.S.; Yong, C.S.; et al. Enhanced Oral Bioavailability of Coenzyme Q10 by Self-Emulsifying Drug Delivery Systems. *Int. J. Pharm.* **2009**, *374*, 66–72, doi:10.1016/j.ijpharm.2009.03.008.
424. Milović, M.; Simović, S.; Lošić, D.; Dashevskiy, A.; Ibrić, S. Solid Self-Emulsifying Phospholipid Suspension (SSEPS) with Diatom as a Drug Carrier. *Eur. J. Pharm. Sci.* **2014**, *63*, 226–232, doi:10.1016/j.ejps.2014.07.010.

425. Chavan, R.B.; Modi, S.R.; Bansal, A.K. Role of Solid Carriers in Pharmaceutical Performance of Solid Supersaturable SEDDS of Celecoxib. *Int. J. Pharm.* **2015**, *495*, 374–384, doi:10.1016/j.ijpharm.2015.09.011.
426. Soliman, K.A.B.; Ibrahim, H.K.; Ghorab, M.M. Formulation of Avanafil in a Solid Self-Nanoemulsifying Drug Delivery System for Enhanced Oral Delivery. *Eur. J. Pharm. Sci.* **2016**, *93*, 447–455, doi:10.1016/j.ejps.2016.08.050.
427. Aleksovski, A.; van Bockstal, P.J.; Roškar, R.; Sovány, T.; Regdon, G.; de Beer, T.; Vervaet, C.; Dreu, R. Comparison of Metoprolol Tartrate Multiple-Unit Lipid Matrix Systems Produced by Different Technologies. *Eur. J. Pharm. Sci.* **2016**, *88*, 233–245, doi:10.1016/j.ejps.2016.03.011.
428. Beg, S.; Katare, O.P.; Saini, S.; Garg, B.; Khurana, R.K.; Singh, B. Solid Self-Nanoemulsifying Systems of Olmesartan Medoxomil: Formulation Development, Micromeritic Characterization, in Vitro and in Vivo Evaluation. *Powder Technol.* **2016**, *294*, 93–104, doi:10.1016/j.powtec.2016.02.023.
429. Vohra, A.M.; Patel, C.V.; Kumar, P.; Thakkar, H.P. Development of Dual Drug Loaded Solid Self Microemulsifying Drug Delivery System: Exploring Interfacial Interactions Using QbD Coupled Risk Based Approach. *J. Mol. Liq.* **2017**, *242*, 1156–1168, doi:10.1016/j.molliq.2017.08.002.
430. Yan, Y.D.; Kim, J.A.; Kwak, M.K.; Yoo, B.K.; Yong, C.S.; Choi, H.G. Enhanced Oral Bioavailability of Curcumin via a Solid Lipid-Based Self-Emulsifying Drug Delivery System Using a Spray-Drying Technique. *Biol. Pharm. Bull.* **2011**, *34*, 1179–1186, doi:10.1248/bpb.34.1179.
431. Kang, J.H.; Oh, D.H.; Oh, Y.K.; Yong, C.S.; Choi, H.G. Effects of Solid Carriers on the Crystalline Properties, Dissolution and Bioavailability of Flurbiprofen in Solid Self-Nanoemulsifying Drug Delivery System (solid SNEDDS). *Eur. J. Pharm. Biopharm.* **2012**, *80*, 289–297, doi:10.1016/j.ejpb.2011.11.005.
432. Tang, B.; Cheng, G.; Gu, J.C.; Xu, C.H. Development of Solid Self-Emulsifying Drug Delivery Systems: Preparation Techniques and Dosage Forms. *Drug Discov. Today* **2008**, *13*, 606–612, doi:10.1016/j.drudis.2008.04.006.
433. Nanda Kishore, R.; Yalavarthi, P.R.; Vadlamudi, H.C.; Vandana, K.R.; Rasheed, A.; Sushma, M. Solid Self Microemulsification of Atorvastatin Using Hydrophilic Carriers: A Design. *Drug Dev. Ind. Pharm.* **2015**, *41*, 1213–1222, doi:10.3109/03639045.2014.938655.
434. Tarate, B.; Chavan, R.; Bansal, A. Oral Solid Self-Emulsifying Formulations: A Patent Review. *Recent Pat. Drug Deliv. Formul.* **2014**, *8*, 126–143, doi:10.2174/1872211308666140313145836.
435. Tan, A.; Rao, S.; Prestidge, C.A. Transforming Lipid-Based Oral Drug Delivery Systems into Solid Dosage Forms: An Overview of Solid Carriers, Physicochemical Properties, and Biopharmaceutical Performance. *Pharm. Res.* **2013**, *30*, 2993–3017, doi:10.1007/s11095-013-1107-3.
436. Krupa, A.; Szlęk, J.; Jany, B.R.; Jachowicz, R. Preformulation Studies on Solid Self-Emulsifying Systems in Powder Form Containing Magnesium Aluminometasilicate as Porous Carrier. *AAPS Pharmscitech* **2015**, *16*, 623–635, doi:10.1208/s12249-014-0247-z.
437. Ito, Y.; Kusawake, T.; Ishida, M.; Tawa, R.; Shibata, N.; Takada, K. Oral Solid Gentamicin Preparation Using Emulsifier and Adsorbent. *J. Control. Release* **2005**, *105*, 23–31, doi:10.1016/j.jconrel.2005.03.017.
438. Mandić, J.; Zvonar Pobirk, A.; Vrečer, F.; Gašperlin, M. Overview of Solidification Techniques for Self-Emulsifying Drug Delivery Systems from Industrial Perspective. *Int. J. Pharm.* **2017**, *533*, 335–345, doi:10.1016/j.ijpharm.2017.05.036.
439. Li, L.; Yi, T.; Lam, C.W.K. Effects of Spray-Drying and Choice of Solid Carriers on Concentrations of Labrasol®® and Transcutol®® in Solid Self-Microemulsifying Drug Delivery Systems (SMEDDS). *Molecules* **2013**, *18*, 545–560, doi:10.3390/molecules18010545.
440. Baek, I.H.; Ha, E.S.; Yoo, J.W.; Jung, Y.; Kim, M.S. Design of a Gelatin Microparticle-Containing Self-Microemulsifying Formulation for Enhanced Oral Bioavailability of Dutasteride. *Drug Des. Dev. Ther.* **2015**, *9*, 3231–3238, doi:10.2147/DDDT.S86458.

441. Čerpnjak, K.; Pobirk, A.Z.; Vrečer, F.; Gašperlin, M. Tablets and Minitablets Prepared from Spray-Dried SMEDDS Containing Naproxen. *Int. J. Pharm.* **2015**, *495*, 336–346, doi:10.1016/j.ijpharm.2015.08.099.
442. Kalepu, S.; Manthina, M.; Padavala, V. Oral Lipid-Based Drug Delivery Systems—An Overview. *Acta Pharm. Sin. B* **2013**, *3*, 361–372, doi:10.1016/j.apsb.2013.10.001.
443. Seo, A.; Schæfer, T. Melt Agglomeration with Polyethylene Glycol Beads at a Low Impeller Speed in a High Shear Mixer. *Eur. J. Pharm. Biopharm.* **2001**, *52*, 315–325, doi:10.1016/S0939-6411(01)00183-7.
444. Rani, S.; Rana, R.; Saraogi, G.K.; Kumar, V.; Gupta, U. Self-Emulsifying Oral Lipid Drug Delivery Systems: Advances and Challenges. *AAPS Pharmscitech* **2019**, *20*, 129, doi:10.1208/s12249-019-1335-x.
445. Breitenbach, J. Melt Extrusion: From Process to Drug Delivery Technology. *Eur. J. Pharm. Biopharm.* **2002**, *54*, 107–117, doi:10.1016/S0939-6411(02)00061-9.
446. GlattGmbH Home Page. Available online: https://www.glatt.com/en/processes/%20pelletizing/extrusion-spheronization/ (accessed on 5 February 2020).
447. Abdalla, A.; Mäder, K. Preparation and Characterization of a Self-Emulsifying Pellet Formulation. *Eur. J. Pharm. Biopharm.* **2007**, *66*, 220–226, doi:10.1016/j.ejpb.2006.11.015.
448. Wang, Z.; Sun, J.; Wang, Y.; Liu, X.; Liu, Y.; Fu, Q.; Meng, P.; He, Z. Solid Self-Emulsifying Nitrendipine Pellets: Preparation and in Vitro/in Vivo Evaluation. *Int. J. Pharm.* **2010**, *383*, 1–6, doi:10.1016/j.ijpharm.2009.08.014.
449. Kumar, R. Chapter 8—Lipid-Based Nanoparticles for Drug-Delivery Systems. *Nanocarriers Drug Deliv.* **2019**, 249–284, doi:10.1016/B978-0-12-814033-8.00008-4.
450. Dorset, D.L. X-ray Diffraction: A Practical Approach. *Microsc. Microanal.* **1998**, *4*, 513–515, doi:10.1017/S143192769800049X.
451. Martin-Gonzalez, M.F.S. Solid Lipid Nanoparticles and Applications. *Nanotechnol. Funct. Foods Eff. Deliv. Bioact. Ingred.* **2015**, *47*, 214–223, doi:10.1002/9781118462157.ch13.
452. Silva, C.O.; Reis, C.P. Drug Nanocarriers Based on Biomacromolecules: How Far We've Come? *Nanotechnology* **2014**, *11*, 484.
453. Westbrook, J.D.; Burley, S.K. How Structural Biologists and the Protein Data Bank Contributed to Recent FDA New Drug Approvals. *Structure* **2019**, *27*, 211–217, doi:10.1016/j.str.2018.11.007.
454. Roskoski, R. Properties of FDA-Approved Small Molecule Protein Kinase Inhibitors: A 2020 Update. *Pharmacol. Res.* **2020**, *152*, 104609, doi:10.1016/j.phrs.2019.104609.
455. Leonaviciute, G.; Bernkop-Schnürch, A. Self-Emulsifying Drug Delivery Systems in Oral (poly)peptide Drug Delivery. *Expert Opin. Drug Deliv.* **2015**, *12*, 1703–1716, doi:10.1517/17425247.2015.1068287.
456. Hauptstein, S.; Prüfert, F.; Bernkop-Schnürch, A. Self-Nanoemulsifying Drug Delivery Systems as Novel Approach for pDNA Drug Delivery. *Int. J. Pharm.* **2015**, *487*, 25–31, doi:10.1016/j.ijpharm.2015.03.064.
457. Mahmood, A.; Prüfert, F.; Efiana, N.A.; Ashraf, M.I.; Hermann, M.; Hussain, S.; Bernkop-Schnürch, A. Cell-Penetrating Self-Nanoemulsifying Drug Delivery Systems (SNEDDS) for Oral Gene Delivery. *Expert Opin. Drug Deliv.* **2016**, *13*, 1503–1512, doi:10.1080/17425247.2016.1213236.
458. Li, P.; Nielsen, H.M.; Müllertz, A. Impact of Lipid-Based Drug Delivery Systems on the Transport and Uptake of Insulin Across Caco-2 Cell Monolayers. *J. Pharm. Sci.* **2016**, *105*, 2743–2751, doi:10.1016/j.xphs.2016.01.006.
459. Bravo-Alfaro, D.A.; Muñoz-Correa, M.O.F.; Santos-Luna, D.; Toro-Vazquez, J.F.; Cano-Sarmiento, C.; García-Varela, R.; García, H.S. Encapsulation of an Insulin-Modified Phosphatidylcholine Complex in a Self-Nanoemulsifying Drug Delivery System (SNEDDS) for Oral Insulin Delivery. *J. Drug Deliv. Sci. Technol.* **2020**, *57*, 101622, doi:10.1016/j.jddst.2020.101622.

460. AboulFotouh, K.; Allam, A.A.; El-Badry, M.; El-Sayed, A.M. Role of Self-Emulsifying Drug Delivery Systems in Optimizing the Oral Delivery of Hydrophilic Macromolecules and Reducing Interindividual Variability. *Colloids Surfaces B Biointerfaces* **2018**, *167*, 82–92, doi:10.1016/j.colsurfb.2018.03.034.
461. O'Driscoll, C.M.; Bernkop-Schnürch, A.; Friedl, J.D.; Préat, V.; Jannin, V. Oral Delivery of Non-Viral Nucleic Acid-Based Therapeutics - Do We Have the Guts for This? *Eur. J. Pharm. Sci.* **2019**, *133*, 190–204, doi:10.1016/j.ejps.2019.03.027.
462. Rao, S.V.R.; Shao, J. Self-Nanoemulsifying Drug Delivery Systems (SNEDDS) for Oral Delivery of Protein Drugs. I. Formulation Development. *Int. J. Pharm.* **2008**, *362*, 2–9, doi:10.1016/j.ijpharm.2008.05.018.
463. Meyer, J.D.; Manning, M.C. Altering Properties of Biomolecules.Pdf. *Pharm. Res.* **1998**, *15*, 188–192, doi:10.1080/17425247.2017.1266329.
464. Zhang, Q.; He, N.; Zhang, L.; Zhu, F.; Chen, Q.; Qin, Y.; Zhang, Z.; Zhang, Q.; Wang, S.; He, Q. The in Vitro and in Vivo Study on Self-Nanoemulsifying Drug Delivery System (SNEDDS) Based on Insulin-Phospholipid Complex. *J. Biomed. Nanotechnol.* **2012**, *8*, 90–97, doi:10.1166/jbn.2012.1371.
465. Mahjub, R.; Dorkoosh, F.A.; Rafiee-Tehrani, M.; Bernkop Schnürch, A. Oral Self-Nanoemulsifying Peptide Drug Delivery Systems: Impact of Lipase on Drug Release. *J. Microencapsul.* **2015**, *32*, 401–407, doi:10.3109/02652048.2015.1035685.
466. Ijaz, M.; Bonengel, S.; Zupančič, O.; Yaqoob, M.; Hartl, M.; Hussain, S.; Huck, C.W.; Bernkop-Schnürch, A. Development of Oral Self Nano-Emulsifying Delivery System(s) of Lanreotide with Improved Stability against Presystemic Thiol-Disulfide Exchange Reactions. *Expert Opin. Drug Deliv.* **2016**, *13*, 923–929, doi:10.1517/17425247.2016.1167034.
467. Soltani, Y.; Goodarzi, N.; Mahjub, R. Preparation and Characterization of Self Nano-Emulsifying Drug Delivery System (SNEDDS) for Oral Delivery of Heparin Using Hydrophobic Complexation by Cationic Polymer of β-Cyclodextrin. *Drug Dev. Ind. Pharm.* **2017**, *43*, 1899–1907, doi:10.1080/03639045.2017.1353522.
468. Qi, X.; Wang, L.; Zhu, J.; Hu, Z.; Zhang, J. Self-Double-Emulsifying Drug Delivery System (SDEDDS): A New Way for Oral Delivery of Drugs with High Solubility and Low Permeability. *Int. J. Pharm.* **2011**, *409*, 245–251, doi:10.1016/j.ijpharm.2011.02.047.
469. Wang, X.; Jiang, S.; Wang, X.; Liao, J.; Yin, Z. Preparation and Evaluation of Nattokinase-Loaded Self-Double-Emulsifying Drug Delivery System. *Asian J. Pharm. Sci.* **2015**, *10*, 386–395, doi:10.1016/j.ajps.2015.04.005.
470. Shima, M.; Tanaka, M.; Fujii, T.; Egawa, K.; Kimura, Y.; Adachi, S.; Matsuno, R. Oral Administration of Insulin Included in Fine W/O/W Emulsions to Rats. *Food Hydrocoll.* **2006**, *20*, 523–531, doi:10.1016/j.foodhyd.2005.05.002.
471. Siddhartha, T.; Senthil, V.; Kishan, I.; Khatwal, R.; Madhunapantula, S. Design and Development of Oral Nanoparticulated Insulin in Multiple Emulsion. *Curr. Drug Deliv.* **2014**, *11*, 472–485, doi:10.2174/1567201811666140414115259.
472. Winarti, L.; Suwaldi; Martien, R.; Hakim, L. Formulation of Self-Nanoemulsifying Drug Delivery System of Bovine Serum Albumin Using HLB (Hydrophilic-Lypophilic Balance) Approach. *Indones. J. Pharm.* **2016**, *27*, 117–127, doi:10.14499/indonesianjpharm27iss3pp117.
473. Cole, E.T.; Cadé, D.; Benameur, H. Challenges and Opportunities in the Encapsulation of Liquid and Semi-Solid Formulations into Capsules for Oral Administration. *Adv. Drug Deliv. Rev.* **2008**, *60*, 747–756, doi:10.1016/j.addr.2007.09.009.
474. Wang, J.; Wu, D.; Shen, W.C. Structure-Activity Relationship of Reversibly Lipidized Peptides: Studies of Fatty Acid-Desmopressin Conjugates. *Pharm. Res.* **2002**, *19*, 609–614, doi:10.1023/A:1015397811161.

475. Wang, J.; Chow, D.; Heiati, H.; Shen, W.C. Reversible Lipidization for the Oral Delivery of Salmon Calcitonin. *J. Control. Release* **2003**, *88*, 369–380, doi:10.1016/S0168-3659(03)00008-7.
476. Wang, J.; Shen, W.C. Gastric Retention and Stability of Lipidized Bowman-Birk Protease Inhibitor in Mice. *Int. J. Pharm.* **2000**, *204*, 111–116, doi:10.1016/S0378-5173(00)00489-0.
477. Ekrami, H.M.; Kennedy, A.R.; Shen, W.C. Water-Soluble Fatty Acid Derivatives as Acylating Agents for Reversible Lipidization of Polypeptides. *FEBS Lett.* **1995**, *371*, 283–286, doi:10.1016/0014-5793(95)00910-2.
478. Zupančič, O.; Rohrer, J.; Thanh Lam, H.; Grießinger, J.A.; Bernkop-Schnürch, A. Development and in Vitro Characterization of Self-Emulsifying Drug Delivery System (SEDDS) for Oral Opioid Peptide Delivery. *Drug Dev. Ind. Pharm.* **2017**, *43*, 1694–1702, doi:10.1080/03639045.2017.1338722.
479. Park, J.H.; Saravanakumar, G.; Kim, K.; Kwon, I.C. Targeted Delivery of Low Molecular Drugs Using Chitosan and Its Derivatives. *Adv. Drug Deliv. Rev.* **2010**, *62*, 28–41, doi:10.1016/j.addr.2009.10.003.
480. Stout, D.B.; Suckow, C.E. MicroCT Liver Contrast Agent Enhancement over Time, Dose, and Mouse Strain. *Mol. Imaging Biol.* **2008**, *10*, 114–120, doi:10.1007/s11307-007-0128-x.
481. Hallouard, F.; Anton, N.; Choquet, P.; Constantinesco, A.; Vandamme, T. Iodinated Blood Pool Contrast Media for Preclinical X-ray Imaging Applications—A Review. *Biomaterials* **2010**, *31*, 6249–6268, doi:10.1016/j.biomaterials.2010.04.066.
482. Dierling, A.M.; Cui, Z. Targeting Primaquine into Liver Using Chylomicron Emulsions for Potential Vivax Malaria Therapy. *Int. J. Pharm.* **2005**, *303*, 143–152, doi:10.1016/j.ijpharm.2005.07.015.
483. Jang, J.H.; Kim, C.K.; Choi, H.G.; Sung, J.H. Preparation and Evaluation of 2-(allylthio)pyrazine-Loaded Lipid Emulsion with Enhanced Stability and Liver Targeting. *Drug Dev. Ind. Pharm.* **2009**, *35*, 363–368, doi:10.1080/03639040802363696.
484. Nikonenko, B.; Reddy, V.M.; Bogatcheva, E.; Protopopova, M.; Einck, L.; Nacy, C.A. Therapeutic Efficacy of SQ641-NE against Mycobacterium Tuberculosis. *Antimicrob. Agents Chemother.* **2014**, *58*, 587–589, doi:10.1128/AAC.01254-13.
485. Shegokar, R.; Singh, K.K. Stavudine Entrapped Lipid Nanoparticles for Targeting Lymphatic HIV Reservoirs. *Pharmazie* **2011**, *66*, 264–271, doi:10.1691/ph.2011.0149.
486. Shahnaz, G.; Hartl, M.; Barthelmes, J.; Leithner, K.; Sarti, F.; Hintzen, F.; Rahmat, D.; Salvenmoser, W.; Bernkop-Schnürch, A. Uptake of Phenothiazines by the Harvested Chylomicrons Ex Vivo Model: Influence of Self-Nanoemulsifying Formulation Design. *Eur. J. Pharm. Biopharm.* **2011**, *79*, 171–180, doi:10.1016/j.ejpb.2011.01.025.
487. Padera, T.P.; Meijer, E.F.J.; Munn, L.L. The Lymphatic System in Disease Processes and Cancer Progression. *Annu. Rev. Biomed. Eng.* **2016**, *18*, 125–158, doi:10.1146/annurev-bioeng-112315-031200.
488. Ohya, Y.; Shiratani, M.; Kobayashi, H.; Ouchi, T. Release Behavior of 5-Fluorouracil from Chitosan-Gel Nanospheres Immobilizing 5-Fluorouracil Coated with Polysaccharides and Their Cell Specific Cytotoxicity. *J. Macromol. Sci. Part A* **1994**, *31*, 629–642, doi:10.1080/10601329409349743.
489. Anton, N.; Vandamme, T.F. The Universality of Low-Energy Nano-Emulsification. *Int. J. Pharm.* **2009**, *377*, 142–147, doi:10.1016/j.ijpharm.2009.05.014.
490. Rehman, J.; Dillow, J.M.; Carter, S.M.; Chou, J.; Le, B.; Maisel, A.S. Increased Production of Antigen-Specific Immunoglobulins G and M Following in Vivo Treatment with the Medicinal Plants Echinacea Angustifolia and Hydrastis Canadensis. *Immunol. Lett.* **1999**, *68*,391–395, doi:10.1016/S0165-2478(99)00085-1.
491. Wiseman, N. Traditional Chinese Medicine: A Brief Outline. *J. Chem. Inf. Comput. Sci.* **2002**, *42*, 445–455, doi:10.1021/ci010107l.

492. Rivera, E.; Hu, S.; Concha, C. Ginseng and Aluminium Hydroxide Act Synergistically as Vaccine Adjuvants. *Vaccine* **2003**, *21*, 1149–1157, doi:10.1016/S0264-410X(02)00518-2.
493. Borchers, A.T.; Hackman, R.M.; Keen, C.L.; Stern, J.S.; Gershwin, M.E. Complementary Medicine: A Review of Immunomodulatory Effects of Chinese Herbal Medicines. *Am. J. Clin. Nutr.* **1997**, *66*, 1303–1312, doi:10.1093/ajcn/66.6.1303.
494. Cragg, G.M. Natural Product Drug Discovery and Development: The United States National Cancer Institute Role. *P. R. Health Sci. J.* **2002**, *21*, 97–111, doi:10.1007/978-1-4615-1455-8_3.
495. Jang, M.H.; Piao, X.L.; Kim, J.M.; Kwon, S.W.; Park, J.H. Inhibition of Cholinesterase and Amyloid-beta Aggregation by Resveratrol Oligomers from Vitis Amurensis. *Phyther. Res.* **2008**, *22*, 544–549, doi:10.1002/ptr.
496. Licciardi, P.V.; Underwood, J.R. Plant-Derived Medicines: A Novel Class of Immunological Adjuvants. *Int. Immunopharmacol.* **2011**, *11*, 390–398, doi:10.1016/j.intimp.2010.10.014.
497. Atul Bhattaram, V.; Graefe, U.; Kohlert, C.; Veit, M.; Derendorf, H. Pharmacokinetics and Bioavailability of Herbal Medicinal Products. *Phytomedicine* **2002**, *9*, 1–33, doi:10.1078/1433-187X-00210.
498. Byeon, J. C.; Ahn, J. Bin; Jang, W. S.; Lee, S. E.; Choi, J. S.; Park, J. S. Recent Formulation Approaches to Oral Delivery of Herbal Medicines. *J. Pharm. Investig.* **2019**, *49*, 17–26. https://doi.org/10.1007/s40005-018-0394-4.
499. Lagoa, R.; Silva, J.; Rodrigues, J.R.; Bishayee, A. Advances in Phytochemical Delivery Systems for Improved Anticancer Activity. *Biotechnol. Adv.* **2020**, *38*, 1–22, doi:10.1016/j.biotechadv.2019.04.004.
500. Dou, Y.X.; Zhou, J.T.; Wang, T.T.; Huang, Y.F.; Chen, V.P.; Xie, Y.L.; Lin, Z.X.; Gao, J.S.; Su, Z.R.; Zeng, H.F. Self-Nanoemulsifying Drug Delivery System of Bruceine D: A New Approach for Anti-Ulcerative Colitis. *Int. J. Nanomed.* **2018**, *13*, 5887–5907, doi:10.2147/IJN.S174146.
501. Tung, N.T.; Tran, C.S.; Nguyen, H.A.; Nguyen, T.D.; Chi, S.C.; Pham, D.V.; Bui, Q.D.; Ho, X.H. Formulation and Biopharmaceutical Evaluation of Supersaturatable Self-Nanoemulsifying Drug Delivery Systems Containing Silymarin. *Int. J. Pharm.* **2019**, *555*, 63–76, doi:10.1016/j.ijpharm.2018.11.036.
502. Shanmugam, S.; Baskaran, R.; Balakrishnan, P.; Thapa, P.; Yong, C.S.; Yoo, B.K. Solid Self-Nanoemulsifying Drug Delivery System (S-SNEDDS) Containing Phosphatidylcholine for Enhanced Bioavailability of Highly Lipophilic Bioactive Carotenoid Lutein. *Eur. J. Pharm. Biopharm.* **2011**, *79*, 250–257, doi:10.1016/j.ejpb.2011.04.012.
503. Kazi, M.; Shahba, A.A.; Alrashoud, S.; Alwadei, M.; Sherif, A.Y.; Alanazi, F.K. Bioactive Self-Nanoemulsifying Drug Delivery Systems (Bio-SNEDDS) for Combined Oral Delivery of Curcumin and Piperine. *Molecules* **2020**, *25*, 1703, doi:10.3390/molecules25071703.
504. Shao, B.; Tang, J.; Ji, H.; Liu, H.; Liu, Y.; Zhu, D.; Wu, L. Enhanced Oral Bioavailability of Wurenchun (Fructus Schisandrae Chinensis Extracts) by Self-Emulsifying Drug Delivery Systems. *Drug Dev. Ind. Pharm.* **2010**, *36*, 1356–1363, doi:10.3109/03639045.2010.480975.
505. Setthacheewakul, S.; Kedjinda, W.; Maneenuan, D.; Wiwattanapatapee, R. Controlled Release of Oral Tetrahydrocurcumin from a Novel Self-Emulsifying Floating Drug Delivery System (SEFDDS). *AAPS Pharmscitech* **2011**, *12*, 152–164, doi:10.1208/s12249-010-9568-8.
506. Ma, H.; Zhao, Q.; Wang, Y.; Guo, T.; An, Y.; Shi, G. Design and Evaluation of Self-Emulsifying Drug Delivery Systems of Rhizoma Corydalis Decumbentis Extracts. *Drug Dev. Ind. Pharm.* **2012**, *38*, 1200–1206, doi:10.3109/03639045.2011.643897.
507. Shen, J.; Bi, J.; Tian, H.; Jin, Y.; Wang, Y.; Yang, X.; Yang, Z.; Kou, J.; Li, F. Preparation and Evaluation of a Self-Nanoemulsifying Drug Delivery System Loaded with Akebia Saponin D-Phospholipid Complex. *Int. J. Nanomed.* **2016**, *11*, 4919–4929, doi:10.2147/IJN.S108765.

508. Kalantari, A.; Kósa, D.; Nemes, D.; Ujhelyi, Z.; Fehér, P.; Vecsernyés, M.; Váradi, J.; Fenyvesi, F.; Kuki, Á.; Gonda, S.; et al. Self-Nanoemulsifying Drug Delivery Systems Containing Plantago Lanceolata—An Assessment of Their Antioxidant and Antiinflammatory Effects. *Molecules* **2017**, *22*, 1773, doi:10.3390/molecules22101773.
509. Wang, Y.; Shen, J.; Yang, X.; Jin, Y.; Yang, Z.; Wang, R.; Zhang, F.; Linhardt, R.J. Mechanism of Enhanced Oral Absorption of Akebia Saponin D by a Self-Nanoemulsifying Drug Delivery System Loaded with Phospholipid Complex. *Drug Dev. Ind. Pharm.* **2019**, *45*, 124–129, doi:10.1080/03639045.2018.1526183.
510. Chairuk, P.; Tubtimsri, S.; Jansakul, C.; Sriamornsak, P.; Weerapol, Y. Enhancing Oral Absorption of Poorly Water-Soluble Herb (Kaempferia Parviflora) Extract Using Self-Nanoemulsifying Formulation. *Pharm. Dev. Technol.* **2020**, *25*,340–350, doi:10.1080/10837450.2019.1703134.
511. Mohsin, K.; Alanazi, F. The Fate of Paclitaxel during in Vitro Dispersion Testing of Different Lipid-Based Formulations. *J. Drug Deliv. Sci. Technol.* **2012**, *22*, 197–204, doi:10.1016/S1773-2247(12)50026-2.
512. Shahba, A.A.W.; Mohsin, K.; Alanazi, F.K. Novel Self-Nanoemulsifying Drug Delivery Systems (SNEDDS) for Oral Delivery of Cinnarizine: Design, Optimization, and in-Vitro Assessment. *AAPS Pharmscitech* **2012**, *13*, 967–977, doi:10.1208/s12249-012-9821-4.
513. Kuentz, M. Drug Supersaturation during Formulation Digestion, Including Real-Time Analytical Approaches. *Adv. Drug Deliv. Rev.* **2019**, *142*, 50–61, doi:10.1016/j.addr.2018.11.003.
514. Cserháti, T.; Forgács, E.; Oros, G. Biological Activity and Environmental Impact of Anionic Surfactants. *Environ. Int.* **2002**, *28*, 337–348, doi:10.1016/S0160-4120(02)00032-6.
515. Bandopadhyay, S.; Manchanda, S.; Chandra, A.; Ali, J.; Deb, P.K. *Overview of Different Carrier Systems for Advanced Drug Delivery*; Drug Delivery Systems: Academic Press, Cambridge, MA, USA, 2020; pp. 179–233, ISBN 9780128144879, doi:10.1016/B978-0-12-814487-9.00005-3.
516. Halbaut, L.; Barbé, C.; Aróztegui, M.; De La Torre, C. Oxidative Stability of Semi-Solid Excipient Mixtures with Corn Oil and Its Implication in the Degradation of Vitamin A. *Int. J. Pharm.* **1997**, *147*, 31–40, doi:10.1016/S0378-5173(96)04789-8.
517. Wasylaschuk, W.R.; Harmon, P.A.; Wagner, G.; Amy, B.H.; Allen, C.T.; Huix, X.; Robert, A.A. Evaluation of hydroperoxides in common pharmaceutical excipients. *J. Pharm. Sci.* **2007**, *96*, 106–116, doi:10.1002/jps.20726.
518. Chambin, O.; Jannin, V.; Champion, D.; Chevalier, C.; Rochat-Gonthier, M.H.; Pourcelot, Y. Influence of Cryogenic Grinding on Properties of a Self-Emulsifying Formulation. *Int. J. Pharm.* **2004**, *278*, 79–89, doi:10.1016/j.ijpharm.2004.02.033.
519. Zhang, P.; Liu, Y.; Feng, N.; Xu, J. Preparation and Evaluation of Self-Microemulsifying Drug Delivery System of Oridonin. *Int. J. Pharm.* **2008**, *355*, 269–276, doi:10.1016/j.ijpharm.2007.12.026.
520. Sunesen, V.H.; Pedersen, B.L.; Kristensen, H.G.; Müllertz, A. In Vivo in Vitro Correlations for a Poorly Soluble Drug, Danazol, Using the Flow-through Dissolution Method with Biorelevant Dissolution Media. *Eur. J. Pharm. Sci.* **2005**, *24*, 305–313, doi:10.1016/j.ejps.2004.11.007.
521. Stillhart, C.; Kuentz, M. Trends in the Assessment of Drug Supersaturation and Precipitation In Vitro Using Lipid-Based Delivery Systems. *J. Pharm. Sci.* **2016**, *105*, 2468–2476, doi:10.1016/j.xphs.2016.01.010.
522. Li, Y.; Mcclements, D.J. New Mathematical Model for Interpreting Ph-Stat Digestion Profiles: Impact of Lipid Droplet Characteristics on in Vitro Digestibility. *J. Agric. Food Chem.* **2010**, *58*, 8085–8092, doi:10.1021/jf101325m.
523. Buyukozturk, F.; Di Maio, S.; Budil, D.E.; Carrier, R.L. Effect of Ingested Lipids on Drug Dissolution and Release with Concurrent Digestion: A Modeling Approach. *Pharm. Res.* **2013**, *30*, 3131–3144, doi:10.1007/s11095-013-1238-6.

524. Berthelsen, R.; Klitgaard, M.; Rades, T.; Müllertz, A. In Vitro Digestion Models to Evaluate Lipid Based Drug Delivery Systems; Present Status and Current Trends. *Adv. Drug Deliv. Rev.* **2019**, *142*, 35–49, doi:10.1016/j.addr.2019.06.010.
525. Crommelin, J.A.D.; Metselaar, M.J.; Storm, G. *Non-Biological Complex Drugs: The Science and the Regulatory Landscape*; Springer: Cham, Switzerland, 2015; pp. 77–185, ISBN978-3-319-16241-6, doi:10.1007/978-3-319-16241-6.
526. Ragelle, H.; Danhier, F.; Préat, V.; Langer, R.; Anderson, D.G. Nanoparticle-Based Drug Delivery Systems: A Commercial and Regulatory Outlook as the Field Matures. *Expert Opin. Drug Deliv.* **2017**, *14*, 851–864, doi:10.1080/17425247.2016.1244187.
527. Nardin, I.; Köllner, S. Successful Development of Oral SEDDS: Screening of Excipients from the Industrial Point of View. *Adv. Drug Deliv. Rev.* **2019**, *142*, 128–140, doi:10.1016/j.addr.2018.10.014.
528. Williams, H. D.; Trevaskis, N. L.; Charman, S. A.; Shanker, R. M.; Charman, W. N.; Pouton, C. W.; Porter, C. J. H. Strategies to Address Low Drug Solubility in Discovery and Development. *Pharmacol. Rev.* **2013**, *65*, 315–499, https://doi.org/10.1124/pr.112.005660.
529. US Food and Drug Administration Home Page. Available online: https://www.fda.gov/drugs/drug-approvals-and-databases/approved-drug-products-therapeutic-equivalence-evaluations-orange-book (accessed on 12 May 2020).
530. US Food and Drug Administration Home Page. Available online: https://www.fda.gov/media/70837/ download (accessed on 12 May 2020).
531. US Food and Drug Administration Home Page. Available online: http://home.att.ne.jp/red/akihiro/fda/ 2635fnl.pdf (accessed on 20 May 2020).
532. Eifler, A.C.; Thaxton, C.S. Nanoparticle therapeutics: FDA approval, clinical trials, regulatory pathways, and case study. *Methods Mol. Biol.* **2011**, *726*, 325–338, doi:10.1007/978-1-61779-052-2_21.
533. Bobo, D.; Robinson, K.J.; Islam, J.; Thurecht, K.J.; Corrie, S.R. Nanoparticle-Based Medicines: A Review of FDA-Approved Materials and Clinical Trials to Date. *Pharm. Res.* **2016**, *33*, 2373–2387, doi:10.1007/s11095-016-1958-5.
534. US Food and Drug Administration Home Page. Available online: http://www.fda.gov/downloads/Drugs/ GuidanceComplianceRegulatoryInformation/Guidances/ucm070570.pdf (accessed on 17 May 2020).
535. Committee for Medicinal Products for Human Use; European Medicine Agency. Joint MHLW/EMA Reflection Paper on the Development of Block Copolymer Micelle Medicinal Products. *Ema/Chmp/13099/2013* **2013**, *44*, 1–18.
536. European Medicine Agency Home Page. Available online: http://www.euronanoforum2015.eu/wpcontent/ uploads/2015/06/2_NanomedicinesEMA-experienceperspective_DoloresHernan_10042015.pdf (accessed on 9 May 2020).

CHAPTER II
AIM OF THE THESIS

Sickle cell disease is an increasing global health problem. Estimates suggest that every year approximately 300.000 infants are born with sickle cell disease [1]. Most of these births occur in Democratic Republic of the Congo, Nigeria and India, where half of the world's affected SCD individuals lives [2,3].

Despite an improved understanding of the pathophysiology of SCD, available drugs remain limited. Although SCD is referred as the first molecular disease [22], today, current approved drugs include hydroxyurea [4], L-glutamine [5] and Crizanlizumab [6]. Hydroxyurea is not effective in some patients and has significant safety concerns, including potential embryofetal toxicity and myelosuppression [7]. L-glutamine demonstrated only a modest effect in prevention of vaso-occlusive crisis without improvement in haematologic parameters [8] and does not target the pathophysiologic mechanism of the disease. Crizanlizumab, the latest approved is given intravenously, that could possibly be a drawback to its long-term use [9]. Also, studies assessing appropriate dosing and safety of crizanlizumab in pediatric population are not yet available.

Because HbS polymerization and red blood cell hemolysis have long been recognized to be the main pathophysiological process of SCD, several compounds have been investigated for their ability to inhibit HbS polymerization or erythrocyte hemolysis. Among these compounds, there are Senicapoc (ICA-17043) and Voxelotor (GBT440), two drugs for oral SCD therapy. Senicapoc was well tolerated when administered to SCD patients and produced a dose-dependent increase in hemoglobin and a decrease in markers of hemolysis [10,11]. Voxelotor has been shown to improve *in vitro* red blood cell flexibility and survival [12]. Clinical studies in healthy volunteers and SCD patients showed tolerability and safety of voxelotor associated with an increase in HbS-oxygen affinity [13]. Based on its favorable properties, OXBRYTA®, a specialty of voxelotor, has been given accelerated approval by the FDA for patients aged 12 and older [14].

Despite these promising pharmacological activities, senicapoc and voxelotor have some limitations. They are hydrophobic compounds with poor aqueous solubility and moderate oral bioavailability [13,15]. The experimentally measured solubilities of senicapoc and voxelotor in water were 6,2 μg/mL and 31 μg/mL, respectively. Furthermore, absorption of senicapoc and voxelotor from the GI tract showed considerable subject variability [14,15].

In recent years, much attention has been focused on lipid-based formulations to increase the aqueous solubility and oral bioavailability of poorly water-soluble compounds [16]. The development of self-nanoemulsifying drug delivery systems (SNEDDSs) is one of the approaches commonly adopted toward this direction. SNEDDSs have been described as a blend of oils, surfactants, and cosurfactants or cosolvents [17, 18]. Following aqueous dispersion and mild agitation (such in GI tract), SNEDDSs spontaneously form fine oil-in-water nanoemulsions with droplet size of 200 nm or below [19]. SNEDDSs have gained wide attention owing to their properties to enhance aqueous solubility and oral bioavailability of lipophilic compounds. More recently, however, the development of marketed SEDDSs formulations, such as Norvir® (ritonavir), Sandimmune® (cyclosporine), Fortavase® (saquinavir) and Neoral® (cyclosporine), has stimulated a growing interest in the use of SNEDDSs to improve the drug solubility and oral bioavailability. Ease of scaling up, presence of biodegradable excipients, and drug-targeting facilities

give SNEDDSs a clear distinction over other solubility and oral bioavailability enhancement strategies [20, 21].

The literature reports that SNEDDS are suitable for drugs with the following profile: LogP ≥ 2; relatively low melting point and good chemical stability. Senicapoc and Voxelotor comply with these requirements [22,23]. SNEDDSs could be a plausible drug delivery system for the oral delivery of senicapoc and voxelotor. However, to the best of our knowledge, the use of SNEDDSs for senicapoc and voxelotor oral delivery has not yet been exploited.

Therefore, **the aim of this thesis is to develop self-nanoemulsifying drug delivery systems for the oral delivery of senicapoc and voxelotor. The project is based on the hypothesis that SNEDDSs formulations may improve aqueous solubility and oral bioavailability of senicapoc and voxelotor.**

Hence, four SNEDDSs formulations were developed. They were optimized (ternary diagrams and quality-by-design approaches) and characterized in terms of emulsification time, transmittance percentage, particle size, zeta potential and morphology. Afterward, the *in vitro* dissolution, *in vitro* lipolysis, cytotoxicity and intestinal permeability of the optimized SNEDDSs were assessed. Finally, the in *vivo* pharmacokinetic studies of voxelotor-SNEDDSs were conducted in rats.

To summarize, the thesis project was conducted in five steps as shown in scheme 1.

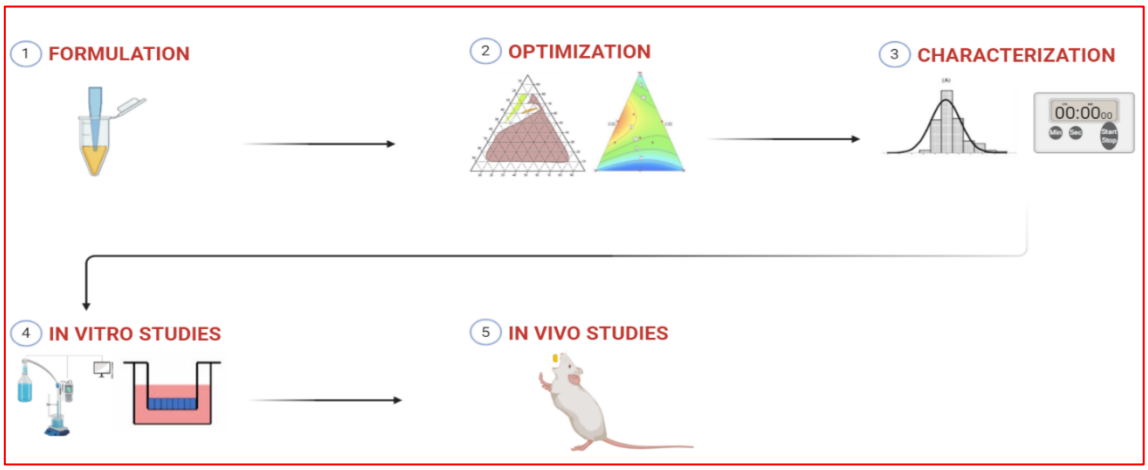

Scheme 1. The major objectives of this PhD thesis

REFERENCES

1. Palomo, M.; Diaz-Ricart, M.; Carreras, E. Is Sickle Cell Disease-Related Neurotoxicity a Systemic Endotheliopathy? *Hematol. Oncol. Stem Cell Ther.* **2020**, *13*, 111–115, https://doi.org/10.1016/j.hemonc.2019.12.005
2. Piel, F. B.; Steinberg, M. H.; Rees, D. C. Sickle Cell Disease. *N. Engl. J. Med.* **2017**, *376*, 1561–1573,https://doi.org/10.1056/NEJMra1510865.
3. Houwing, M. E.; de Pagter, P. J.; van Beers, E. J.; Biemond, B. J.; Rettenbacher, E.; Rijneveld, A. W.; Schols, E. M.; Philipsen, J. N. J.; Tamminga, R. Y. J.; van Draat, K. F.; Nur, E.; Cnossen, M. H. Sickle Cell Disease: Clinical Presentation and Management of a Global Health Challenge. *Blood Rev.* **2019**, *37*, 100580,https://doi.org/10.1016/j.blre.2019.05.004.
4. Brandow, A. M.; Panepinto, J. A. Hydroxyurea Use in Sickle Cell Disease: The Battle with Low Prescription Rates, Poor Patient Compliance and Fears of Toxicities. *Expert Rev. Hematol.* **2010**, *3* , 255–260,https://doi.org/10.1586/ehm.10.22.
5. Niihara, Y.; Zerez, C. R.; Akiyama, D. S.; Tanaka, K. R. Oral L-Glutamine Therapy for Sickle Cell Anemia: I. Subjective Clinical Improvement and Favorable Change in Red Cell NAD Redox Potential. *Am. J. Hematol.* **1998**, *58*, 117–121,https://doi.org/10.1002/(SICI)1096-8652(199806)58:2<117::AID-AJH5>3.0.CO;2-V.
6. ASH Clinical News Home Page. Available online: https://www.ashclinicalnews.org/news/latest-and-greatest/fda-approves-crizanlizumab-tmca-sickle-cell-disease (accessed on 16 December 2020).
7. Steinberg, M. H. Pathophysiologically Based Drug Treatment of Sickle Cell Disease. **2006**, *27*. https://doi.org/10.1016/j.tips.2006.02.007.
8. Niihara, Y.; Miller, S. T.; Kanter, J.; Lanzkron, S.; Smith, W. R.; Hsu, L. L.; Gordeuk, V. R.; Viswanathan, K.; Sarnaik, S.; Osunkwo, I.; Guillaume, E.; Sadanandan, S.; Sieger, L.; Lasky, J. L.; Panosyan, E. H.; Blake, O. A.; New, T. N.; Bellevue, R.; Tran, L. T.; Razon, R. L.; Stark, C. W.; Neumayr, L. D.; Vichinsky, E. P. A Phase 3 Trial of L -Glutamine in Sickle Cell Disease. *N. Engl. J. Med.* **2018**, *379*, 226–235. https://doi.org/10.1056/nejmoa1715971
9. Kutlar, A.; Kanter, J.; Liles, D. K.; Alvarez, O. A.; Cançado, R. D.; Friedrisch, J. R.; Knight-Madden, J. M.; Bruederle, A.; Shi, M.; Zhu, Z.; Ataga, K. I. Effect of Crizanlizumab on Pain Crises in Subgroups of Patients with Sickle Cell Disease: A SUSTAIN Study Analysis. *Am. J. Hematol.* **2019**, *94*, 55–61, https://doi.org/10.1002/ajh.25308.
10. Ataga, K. I.; Reid, M.; Ballas, S. K.; Yasin, Z.; Bigelow, C.; James, L. S.; Smith, W. R.; Galacteros, F.; Kutlar, A.; Hull, J. H.; Stocker, J. W. Improvements in Haemolysis and Indicators of Erythrocyte Survival Do Not Correlate with Acute Vaso-Occlusive Crises in Patients with Sickle Cell Disease: A Phase III Randomized, Placebo-Controlled, Double-Blind Study of the Gardos Channel Blocker Senicapo. *Br. J. Haematol.* **2011**, *153*, 92–104, https://doi.org/10.1111/j.1365-2141.2010.08520.x.
11. Ataga, K. I.; Stocker, J. Senicapoc (ICA-17043): A Potential Therapy for the Prevention and Treatment of Hemolysis-Associated Complications in Sickle Cell Anemia. *Expert Opinion on Investigational Drugs*. **2009**, 18, 231–239,https://doi.org/10.1517/13543780802708011.
12. Dufu, K.; Oksenberg, D. GBT440 Reverses Sickling of Sickled Red Blood Cells under Hypoxic Conditions in Vitro. *Hematol. Rep.* **2018**, *10*, 1–9,https://doi.org/10.4081/hr.2018.7419.
13. Hutchaleelaha, A.; Patel, M.; Washington, C.; Siu, V.; Allen, E.; Oksenberg, D.; Gretler, D. D.; Mant, T.; Lehrer-Graiwer, J. Pharmacokinetics and Pharmacodynamics of Voxelotor (GBT440) in Healthy Adults and Patients with Sickle Cell Disease. *Br. J. Clin. Pharmacol.* **2019**, *85*, 1290–1302, https://doi.org/10.1111/bcp.13896.
14. US Food and Drug Administration Home Page. Available online: https://www.accessdata.fda.gov/drugsatfda_docs/label/2019/213137s000lbl.pdf (accessed on 10 December 2020).

15. McNaughton-Smith, G. A.; Burns, J. F.; Stocker, J. W.; Rigdon, G. C.; Creech, C.; Arlington, S.; Shelton, T.; De Franceschi, L. Novel Inhibitors of the Gardos Channel for the Treatment of Sickle Cell Disease. *J. Med. Chem.* **2008**, *51*, 976–982,https://doi.org/10.1021/jm070663s.
16. Qian, J.; Meng, H.; Xin, L.; Xia, M.; Shen, H.; Li, G.; Xie, Y. Self-Nanoemulsifying Drug Delivery Systems of Myricetin: Formulation Development, Characterization, and in Vitro and in Vivo Evaluation. *Colloids Surfaces B Biointerfaces* **2017**, *160*, 101–109, https://doi.org/10.1016/j.colsurfb.2017.09.020.
17. Siqueira Jørgensen, S.D.; Al Sawaf, M.; Graeser, K.; Mu, H.; Müllertz, A.; Rades, T. The Ability of Two in vitro Lipolysis Models Reflecting the Human and Rat Gastro-Intestinal Conditions to Predict the in vivo Performance of SNEDDS Dosing Regimens. *Eur. J. Pharm. Biopharm.* **2018**, *124*, 116–124, doi:10.1016/j.ejpb.2017.12.014.
18. Buya A.B; Beloqui A.; Memvanga P.B.; Préat V. Self-Nano-Emulsifying Drug-Delivery Systems: From the Development to the Current Applications and Challenges in Oral Drug Delivery. Pharmaceutics. 2020; 12, 1194, https://doi.org/10.3390/pharmaceutics12121194.
19. Pouton, C.W. Lipid Formulations for Oral Administration of Drugs: Non-Emulsifying, Self-Emulsifying and "Self-Microemulsifying" Drug Delivery Systems. *Eur. J. Pharm. Sci.* **2000**, *11*, 93–98, doi:10.1016/S0928-0987(00)00167-6.
20. Rani, S.; Rana, R.; Saraogi, G. K.; Kumar, V.; Gupta, U. Self-Emulsifying Oral Lipid Drug Delivery Systems: Advances and Challenges. *AAPS PharmSciTech.* **2019**, 20, 129, https://doi.org/10.1208/s12249-019-1335-x.
21. Rehman, F. U.; Shah, K. U.; Shah, S. U.; Khan, I. U.; Khan, G. M.; Khan, A. From Nanoemulsions to Self-Nanoemulsions, with Recent Advances in Self-Nanoemulsifying Drug Delivery Systems (SNEDDS). *Expert Opin. Drug Deliv.* **2017**, *14*, 1325–1340, https://doi.org/10.1080/17425247.2016.1218462.
22. Rani, S.; Rana, R.; Saraogi, G. K.; Kumar, V.; Gupta, U. Self-Emulsifying Oral Lipid Drug Delivery Systems: Advances and Challenges. *AAPS PharmSciTech*. Springer New York LLC April 1, **2019**. https://doi.org/10.1208/s12249-019-1335-x.
23. Poovi, G.; Damodharan, N. Lipid Nanoparticles: A Challenging Approach for Oral Delivery of BCS Class-II Drugs. *Futur. J. Pharm. Sci.* **2018**, *4* (2), 191–205. https://doi.org/https://doi.org/10.1016/j.fjps.2018.04.001.

CHAPTER III
DESIGN AND EVALUATION OF SELF-NANOEMULSIFYING DRUG DELIVERY SYSTEMS (SNEDDSS) FOR SENICAPOC

Aristote B. Buya, Bernard Ucakar, Ana Beloqui, Patrick B. Memvanga, Véronique Préat

Adapted from International Journal of Pharmaceutics 2020, 58, 119180

TABLE OF CONTENTS

ABSTRACT

Senicapoc (SEN), a potent antisickling agent, shows poor water solubility and moderate oral bioavailability. To improve the solubility and cell permeation of SEN, self-nanoemulsifying drug delivery systems (SNEDDSs) were developed. Capryol PGMC®, which showed the highest solubilization capacity, was selected as the oil. The self-emulsification ability of two surfactants, viz., Cremophor-EL® and Tween® 80, was compared. Based on a solubility study and ternary phase diagrams, three optimized nanoemulsions with droplet sizes less than 200 nm were prepared. An *in vitro* dissolution study demonstrated the superior performance of the SNEDDS over the free drug. During *in vitro* lipolysis, 80% of SEN loaded in the SNEDDS remained solubilized. An *in vitro* cytotoxicity study using the Caco-2 cell line indicated the safety of the formulations at 1 mg/mL. The transport of SEN-SNEDDSs across Caco-2 monolayers was enhanced 115-fold ($p < 0.01$) compared to that of the free drug. According to these results, SNEDDS formulations could be promising tools for the oral delivery of SEN.

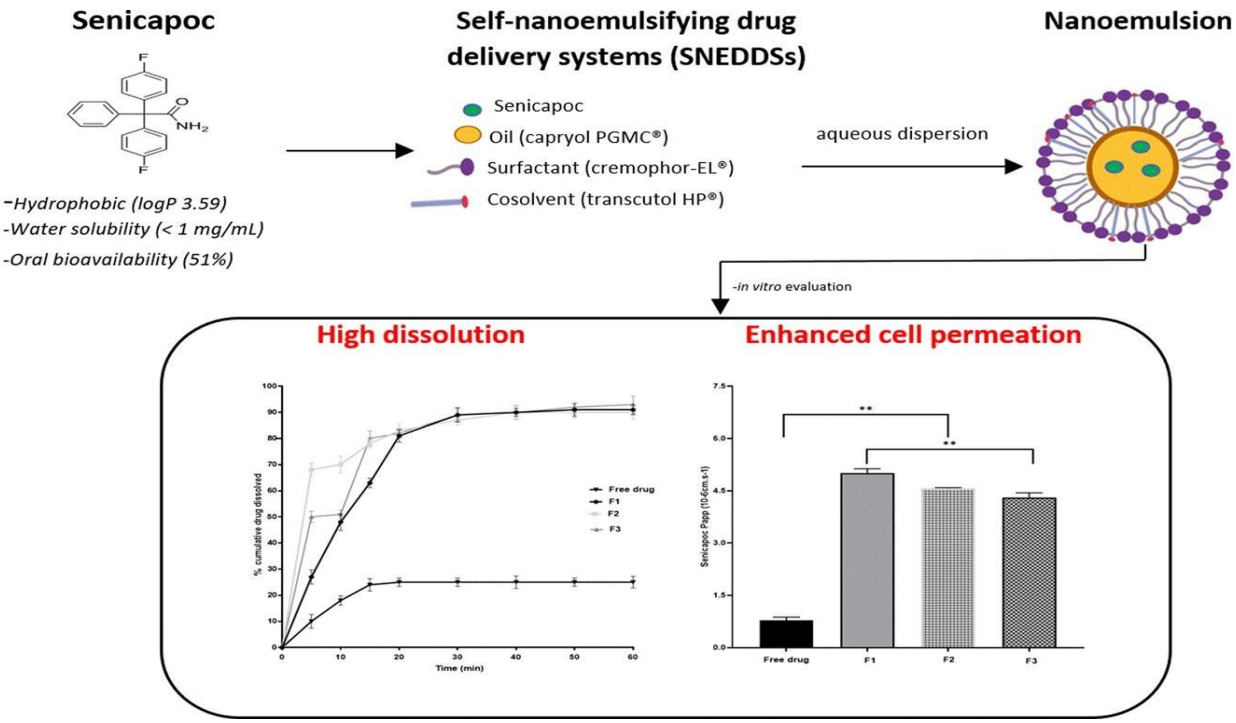

I. INTRODUCTION

Senicapoc (SEN), also identified as ICA-17043, is an ion-channel blocker that selectively blocks potassium efflux through the Gardos channel in red blood cells (RBCs) [1]. Preclinical studies and studies in transgenic models of sickle cell disease have shown that SEN increases hemoglobin levels and decreases the density of cells and hemolysis. SEN is well tolerated when administered at a dose of 10 mg to sickle cell disease patients, producing a dose-dependent increase in hemoglobin and a decrease in markers of hemolysis [2]. Additionally, due to Gardos channel inhibition, SEN has demonstrated pharmacological activity against malaria [3], chronic asthma [4], liver disease [5] and cancer [6].

Despite these promising pharmacological activities, SEN has some limitations. SEN is a very hydrophobic drug (logP 3.59) with poor aqueous solubility (975 ng/mL) and moderate oral bioavailability (51%). It has been reported that SEN has a half-life of 1 h in rats, with a maximum concentration attained after 4 h when administered orally [7].

In recent years, much attention has been focused on lipid-based formulations to increase the solubility and oral bioavailability of poorly water-soluble compounds [8]. One of the most popular approaches is the incorporation of drug compounds into inert lipid vehicles such as surfactant dispersions [9], solid lipid nanoparticles [10], nanoemulsions [11], microemulsions [12], self-nanoemulsifying drug delivery systems [13] and liposomes [14]. To enhance the ocular bioavailability of SEN, Phua and coworkers prepared novel topical nanoliposomes that improved the residence time by up to 12-fold that of the free drug [15]. However, when applied to oral delivery, liposomes are characterized by several limitations, such as high cost, limited drug loading, poor scaling up and the use of organic solvents [16, 17].

To overcome these drawbacks, self-nanoemulsifying drug delivery systems (SNEDDSs) appear to be an effective and suitable alternative. SNEDDSs are isotropic mixtures of oils, surfactants and cosurfactants that form oil-in-water nanoemulsions upon mild agitation in aqueous media, such as gastro-intestinal (GI) fluid [18]. Due to their anhydrous nature, SNEDDSs can be orally administered in soft or hard gelatin capsules. They can produce nanoemulsions with droplet sizes less than 200 nm upon dilution [19]. SNEDDSs have generated tremendous interest owing to their capability to increase drug solubilization and the oral bioavailability of poorly water-soluble compounds [16]. Many poorly water-soluble drugs such as docetaxel, resveratrol, quercetin, and amphotericin B have been encapsulated into SNEDDSs, leading to improved oral bioavailability [20].

SNEDDSs seem to be a plausible drug delivery system for the oral delivery of SEN. However, to the best of our knowledge, the use of a SNEDDS for SEN oral delivery has not yet been exploited.

Therefore, the aim of this study was to develop self-nanoemulsifying drug delivery systems of SEN to enhance its aqueous solubility and oral bioavailability. The developed SEN-SNEDDS formulations were characterized in terms of emulsification time, percentage of transmittance, particle size, and zeta potential. Afterward, the *in vitro* dissolution, *in vitro* lipolysis, cytotoxicity and intestinal permeability of the optimized SEN-SNEDDS were assessed.

II. MATERIALS AND METHODS

II.1. MATERIALS

Senicapoc with a purity greater than 98% was purchased from Ark Pharma, Inc. (Arlington Hts, USA). Cremophor- EL® (polyoxyl -35 castor oil) and polyethylene glycol 400 (PEG 400) were kindly provided by BASF (Ludwigshafen, Germany). Labrafil M® 1944 CS (oleoyl polyoxyl-6-glycerides), Labrafil M® 2125 CS (linoleoyl polyoxyl-6-glycerides), Labrasol AFL® (caprylocaproyl polyoxyl-8-glycerides), Transcutol HP® (diethylene glycol monoethyl), Capryol®90 (propylene glycol monocaprylate type II)**,** Capryol PGMC® (propylene glycol monocaprylate type I), Labrafac lipophile WL® 1349 (triglycerides medium-chain), Lauroglycol®90 (propylene glycol monolaurate) and Maisine® 35-1 (glycerol monolinoleate) were kind gifts from Gattefossé (Saint-Priest, France). Tween® 80 (polysorbate 80), Tween® 20 (polysorbate 20), sodium taurodeoxycholate (NaTDC), L-α-phosphatidylcholine (TLC), 4-bromophenylboronic acid, Triton X-100, thiazolyl blue tetrazolium bromide (MTT) and porcine pancreatin extract (P7545, 8x USP specification activity) were all purchased from Sigma-Aldrich (St. Louis, MO, USA). Propylene glycol and oleic acid were purchased from Fagron (Colombes, France). HPLC grade solvents such as acetonitrile (Thermo Fisher Scientific, MA, USA), formic acid (VWR chemicals, Leuven, Belgium), and dimethylsulfoxide (Carl Roth, Karlsruhe, Germany) were used for chromatography studies.

II.2. DEVELOPMENT OF SNEDDS FORMULATIONS

II.2.1. Screening of formulation components based on saturation solubility studies

An excess amount of SEN was added to 1 g of each vehicle, followed by mixing (100 rpm) in a shaking incubator (Infors AG, Bottmingen, Switzerland) at 37 °C for 48 h. Afterward, the equilibrated samples were centrifuged (Eppendorf centrifuge 5804 R, Hamburg, Germany) at 4000 x g for 30 min (37°C) to remove the insoluble drug. The concentration of SEN in supernatants was measured by HPLC-UV (Shimadzu C 204353, Kyoto, Japan) after dilution with acetonitrile.

II.2.2. Screening of surfactants and cosurfactants for emulsifying ability

The emulsification ability of various surfactants was screened as described by Date et al. [21] with minor modifications. In brief, selected oils and surfactants were mixed 1:1 (w/w), heated at 40-45 °C and mixed to homogenize the components. The mixture (500 mg) was accurately weighed and dispersed into 10 mL of deionized water under gentle stirring. Visual evaluation was used to assess the relative turbidity. The resulting dispersions were allowed to stand for 2 h, and their transmittance values were measured at a wavelength of 550 nm using a NanoDrop™ 2000 spectrophotometer (Thermo Fisher Scientific) against deionized water as a control.

Various cosurfactants were screened by mixing the surfactant with each selected cosurfactant in a 2:1 (w/w) ratio. The oily phase was added to this mixture in a 1:3 ratio and homogenized with the aid of gentle stirring and heat (40-45°C). The resulting dispersions were accessed for different parameters as mentioned for the surfactant screening.

II.2.3. Ternary phase diagrams

Different surfactants (Cremophor-EL® and Tween® 80) and cosurfactants (Transcutol HP® and PEG 400) were mixed in various weight ratios (1:1, 2:1, 3:1, 3:2) to form Smix. Oil and Smix were mixed thoroughly in different weight ratios from 0:10 to 10:0 (0:10, 1:9, 2:8, 3:7, 4:6, 5:5, 6:4, 7:3, 8:2, 9:1 and 10:0) for the four Smix ratios. To determine the feasibility of the self-(nano)emulsification, 1 g of the mixture (oil + Smix) was slowly titrated with deionized water (100 mL, 37°C), gently stirred and visually examined for transparency. The droplet size and its distribution (polydispersity index, PDI) were determined at 37°C by DLS using a Nano ZS system (Malvern Instruments Ltd, UK). Ternary plots were then constructed using Chemix School vers. 3.60 software (Arne Standnes, Norway).

II.2.4. Preparation of SEN-loaded SNEDDSs and maximum drug content determination

The blank SNEDDSs were prepared by mixing the appropriate quantities of oil, surfactant and cosurfactant under agitation (100 rpm, 35 min). Then, 10 mg of SEN was added to 600 mg of each blank SNEDDS and mixed under agitation (100 rpm, 35 min) for dissolution until a transparent preparation was obtained. To determine the maximum loading content of SEN in each formulation, an excess amount of SEN was added to 1 g of each blank SNEDDS formulation by mixing (100 rpm) in a shaking incubator at 37°C for 48 h. The equilibrated samples were centrifuged at 4000 x g for 30 min to remove the excess SEN, and the concentration of SEN in the supernatant was determined by HPLC-UV after appropriate dilution with acetonitrile.

II.3. CHARACTERIZATION OF OPTIMIZED FORMULATIONS

II.3.1. Transmittance percentage

The percentage transmittance was evaluated as described by Shakeel et al. [22]. Briefly, the SNEDDS formulations (1 g) were nanoemulsified in 100 mL of deionized water and allowed to stabilize for an hour. The transmittance percentage of samples was measured at 550 nm wavelength using a Nanodrop UV spectrophotometer (Thermo Fisher Scientific Inc., Waltham, MA, USA) against deionized water as a control.

II.3.2. Viscosity measurement

Viscosities of formulations were determined with the aid of a modular compact rheometer (MCR 102, Anton Paar Instruments Ltd, Graz, Australia) equipped with a temperature control system. A parallel plate (50 mm) was used for the measurements. The gap size was set at 500 μm, and 4 μL of each preconcentrated SNEDDS was used. The shear stress was measured at varying rates from 0.1 to 100 s^{-1} for 5 min. All rheological measurements were made at 25°C, and data were analyzed with Rheocompass software (version 1.13.44-release, Anton Paar Instruments Ltd, Graz, Australia).

II.3.3. Emulsification time

One gram of each formulation was added to 500 mL of 0.1 HCl and maintained at 37 ± 0.5 °C under gentle agitation (100 rpm). The time required in seconds to obtain a clear dispersion was recorded as the emulsification time [23].

II.3.4. Determination of size and zeta potential

The average globule size and polydispersity index (PDI) of formulations were determined by dynamic light scattering (DLS) at 37°C using a Nano ZS system (Malvern Instruments Ltd, UK). To prepare samples, 600 mg of each formulation was dispersed in 200 mL of deionized water, PBS pH 6.8, FaSSGF pH 1.6 and FaSSIF pH 6.8. The droplet size and PDI of the resulting emulsions were directly measured.

Zeta potential was measured by electrophoretic mobility (PCS) using a Zetasizer Nano ZS system (Malvern Instruments Ltd, UK). After diluting the SNEDDS formulation (600 mg) with 200 mL of deionized water, the samples were directly measured.

II.3.5. Thermodynamic stability studies

The formulations were subjected to heating-cooling cycles. Six cycles between 4°C and 40°C were applied with storage at each temperature for not less than 48h. Those formulations, which were stable (no phase separation) were subjected to freeze-thaw cycles involved three cycles between -21°C and 20°C with storage at each temperature for not less than 48h. Further, centrifugation was performed at 4000 x g for 30 min to observe phase separation.

II.3.6. HPLC analysis of senicapoc

Reversed-phase HPLC-UV was used for the analysis of SEN [15]. The HPLC (Shimadzu C 204353, Kyoto, Japan) consisted of an LC-20A pump equipped with an SPD-20A intelligent UV/VIS detector and a SIL-20A autosampler. Chromatographic separation was performed on a CC 250-4.6 Nucleosil 100-5, C18 HD HPLC column (Macherey-Nagel, Germany). A mixture of 80% (acetonitrile + 0.1% formic acid) and 20% (water + 0.1% formic acid) was used as the mobile phase. All samples were analyzed under isocratic elution at a flow rate of 1.0 mL/min, and the effluent was monitored at 261 nm [15]. A 10 µL sample was injected into the Rheodyne and analyzed at 25°C. The method was linear (r^2=0.99) in the concentration range of 0.7-100 µg/mL, and the retention time of SEN was approximately 4.31 ± 0.71 min. The limit of detection (LOD) and limit of quantification (LOQ) were 1.3 µg/mL and 4 µg/mL, respectively.

II.4. IN VITRO DISSOLUTION PROFILE

Dissolution studies were performed using a drug dissolution tester (Sotax AT7, CH-4008 Basel, Switzerland) according to US Apparatus II (paddle method). Pure SEN and SEN-SNEDDS formulations (600 mg) equivalent to 10 mg filled in size "0" hard gelatin capsules (Capsugel Inc., Morristown, NJ, USA) were placed in 500 mL of USP buffer (pH 1.2) used as dissolution media. A paddle rotation speed of 100 rpm and a temperature of 37 ± 0.5 °C were used. At predefined

time intervals (5, 10, 20, 30, 40, 50 and 60 min), a 2 mL aliquot was withdrawn and replenished with a similar volume of fresh blank media. The withdrawal samples were filtered through 0.22 μm hydrophylic Rotilabo® syringe filters (Carl Roth, Karlsruhe, Germany) and transferred into glass vials. Then, 10 μL of the resulting filtrate was quantified by HPLC-UV to measure the concentration of SEN.

II.5. IN VITRO LIPOLYSIS

Lipolysis experiments were carried out according to the procedure described by Crum et al. [24] with minor adjustments. The experimental setup consisted of a T5 Mettler Toledo pH-stat titration unit (Greifensee, Switzerland) comprising a combined pH Ag/AgCl electrode (DGI 115-SC) and coupled to a 30 mL DV 1020 Mettler Toledo autoburette (Greifensee, Switzerland), an IKA C-MAG HS7 thermostat-jacketed glass reaction vessel (Staufen, Germany) and a compact stirrer (Mettler Toledo).

The SEN-SNEDDS formulations were gently dispersed into 40 mL of digestion buffer (comprising 1.4 mM $CaCl_2.2H_2O$, 2 mM Tris-maleate, 150 mM NaCl, 3 mM NaTDC, and 0.75 mM TLC). After 15 min, the pH was automatically adjusted to 6.5 ± 0.05 with 0.5 M NaOH. The *in vitro* lipolysis was initiated by the addition of 4 mL of pancreatin extract containing lipase (lipase activity equivalent to 8X USP specifications) and other pancreatic enzymes (amylase, protease and ribonuclease). The pancreatin extract was freshly prepared before each experiment by mixing 1 g of pancreatic powder with 5 mL of digestion buffer and 20 μL of 0.5 M NaOH solution to reach the target pH 6.5. The resulting enzyme suspension was centrifuged (4000 x g, 4°C, Eppendorf centrifuge 5804 R, Hamburg, Germany) for 15 min.

During the experiment, the released fatty acids were automatically titrated with 0.5 M NaOH to maintain pH 6.5. Two milliliters of digestion medium was withdrawn in 5 min intervals up to 60 min. The lipase activity was inhibited by the addition of 10 μL of 1.0 M 4-bromophenylboronic acid (in methanol). The samples were vortexed and centrifuged (6700 x g, 4°C MiniSpin, Eppendorf AG, Hamburg, Germany) for 15 min, resulting in the separation of the digestion content in a clear supernatant and off-white pellet. The drug content in the supernatant was quantified by HPLC-UV following appropriate dilution with acetonitrile. Lipolysis was also performed with blank digestion medium containing no SNEDDS.

II.6. TRANSPORT OF SENICAPOC THROUGH THE CACO-2 CELL MONOLAYER

II.6.1. Cytotoxicity assessment of the SNEDDS formulations

The viability of Caco-2 cells against blank SNEDDS formulations was evaluated as described by Memvanga et al. [25]. Briefly, Caco-2 cells were seeded on 96-well plates (2x 10^4 cells/well; 100 μL per well) in culture medium consisting of Dulbecco's modified Eagle's minimal essential medium (DMEM) supplemented with 10% (v/v) heat-inactivated fetal bovine serum (HyClone®, Thermo Scientific, UK), 1% (v/v) L-glutamine, 1% (v/v) nonessential amino acids and penicillin/streptomycin solution (10 units/ 10 μg/mL) and were incubated at 37 °C in a 10% CO_2 humidified incubator for 24 h. Once the cells were confluent, they were washed with phosphate-buffered saline (PBS) at 37 °C and treated with 100 μL of free SEN, unloaded-SNEDDS or SEN-

SNEDDS dispersed in Hank's salt balanced solution (HBSS). Samples were prepared at concentrations varying from 0.3 mg/mL to 6 mg/mL. HBSS served as a negative control, and 1% (v/v) Triton X-100 served as a positive control. After 2 h of incubation, cells were washed with HBSS at 37°C, treated with 100 µl of MTT solution (0.5 mg/mL in DMEM) and further incubated for 3 h. Next, 200 µL of DMSO was added to solubilize the formazan crystals formed during the incubation, and the product of the reaction was measured at 545 nm using a Multiskan Spectrum microplate reader (Thermo Fisher Scientific Inc., Waltham, MA, USA). Cell viability rates of the samples were calculated according to equation (1): Cell viability (%) = A_s/A_c x 100 where A_s is the sample absorbance and A_c is the absorbance measured after treatment of cells with HBSS.

II.6.2. Cell culture for transport studies

The *in vitro* transport studies were carried out as described by Memvanga et al. [25]. Caco-2 cells ($5x10^5$ cells/well) were seeded on 12-well cell culture inserts with a 1 µm pore diameter and 0.9 cm^2 surface area (Corning Costar®, NY, USA) and were grown in culture medium at 37 °C in an atmosphere of 10% CO_2. Cell culture medium was added to the apical (0.5 mL) and basolateral (1.2 mL) sides, and the medium was replaced every 2 days. After 21 days of incubation, only Caco-2 cell monolayers with initial transepithelial electrical resistance (TEER) values between 300 and 600 ohm/cm^2 were selected.

Before the transport study, the culture medium was replaced with preheated (37°C) HBSS. After the cell monolayer was equilibrated for 30 min at 37°C, TEER values of monolayers were determined in triplicate. The apical to basolateral transport experiments across Caco-2 cell monolayers were conducted by adding 0.5 mL of SEN free drug (1 mg/mL SEN in HBSS) or 0.5 mL of dispersed formulations in HBSS (1 mg/mL SEN-SNEDDS, i.e., 16.6 µg/mL SEN) on the apical side of the inserts and 1.2 mL of HBSS on the basolateral side. After 2 h, samples from the basolateral compartment were withdrawn to determine the permeation of free SEN or SEN loaded in the SNEDDSs. The amount of SEN that crossed the Caco-2 cell monolayers was determined by HPLC-UV. The apparent permeability coefficient (P_{app}) was determined using the following equation (2): $P_{app=} = \frac{dQ}{dt} * \frac{1}{CoA}$

where dQ/dt (transport rate) is the amount of SEN (µg) appearing per time unit (s) in the receiver compartment, C_o is the initial concentration in the donor compartment (µg/mL) and A is the surface area of the monolayer (A = 0.9 cm^2).

II.7. STATISTICAL ANALYSIS

Student's t-test and analysis of variance (ANOVA) were used to compare different groups. A P-value less than 0.05 was considered statistically significant. GraphPad Prism version 8 (San Diego, CA, USA) was used for statistical analysis of the data. Unless otherwise stated, the data are the mean ± SD for n=3.

III. RESULTS AND DISCUSSION

III.1. DEVELOPMENT OF SNEDDS FORMULATIONS

III.1.1. Selection of components

The selection of an appropriate oil is crucial for the preparation of SNEDDSs. Two important factors to be considered are the ability of an oil to solubilize the drug and its ease of emulsification. The oil with the maximum drug solubilizing capacity is typically selected due to its key influence in achieving optimal drug loading [8, 26]. This property in turn is important in avoiding drug precipitation during the emulsification process. The results of solubility studies in oily phases are depicted in Fig. 1. Among all oils screened, the maximum solubilization capacity was exhibited by Lauroglycol®90 (14.8 ± 0.3 mg/mL) and Capryol PGMC® (14.5 ± 1.6 mg/mL); hence, they were selected as the oily phases for further studies.

The solubility of SEN in various surfactants and cosurfactants is graphically represented in Fig. 1. Labrasol AFL® showed the highest solubility (37.4 ± 2.8 mg/mL), followed by Cremophor-EL® (27.2 ± 0.7 mg/mL) and Tween® 80 (22.1 ± 1.5 mg/mL). These three nonionic surfactants are known to be less toxic than ionic surfactants (Rani et al., 2019). Among the tested cosurfactants and cosolvents, Transcutol HP® yielded the highest solubility for SEN (16.5 ± 2.2 mg/mL), followed by PEG 400 (14.2 ± 1.2 mg/mL).

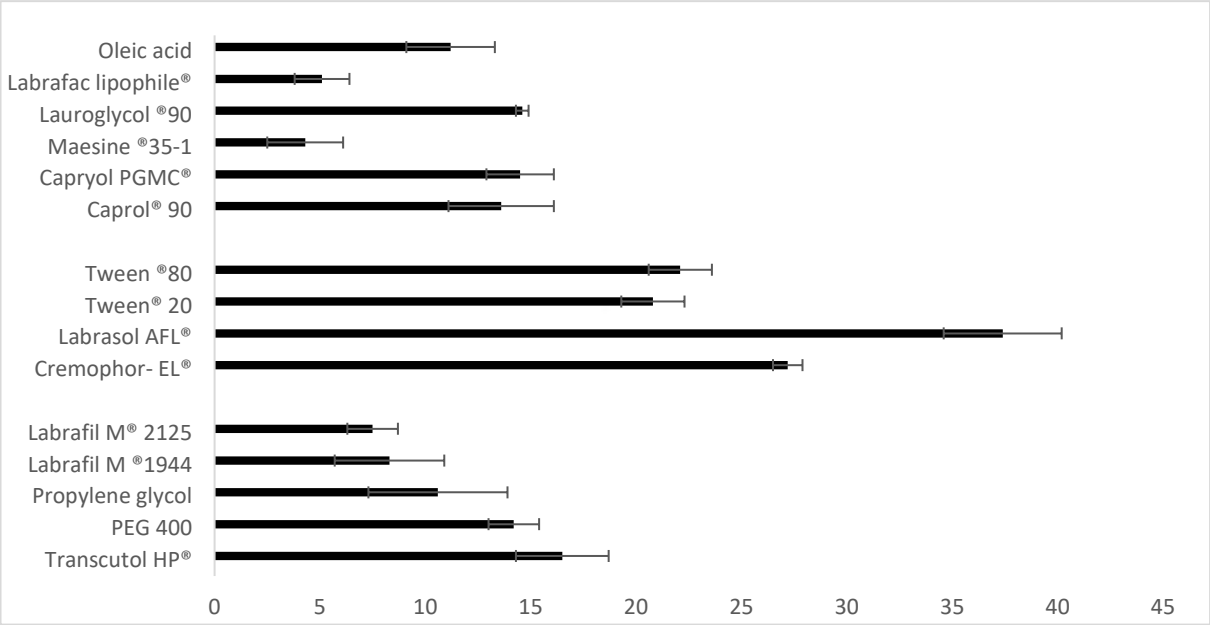

Figure 1. Solubility of SEN (mg/mL) in various oils, surfactants and cosurfactants at 37°C. Data are expressed as the mean ± SD, n=3.

Surfactant screening was based on their emulsification abilities toward the selected oils. Lauroglycol® 90 and Capryol PGMC® were screened against Labrasol ALF®, Cremophor-EL® and Tween® 80. The percentage transmittance values of various dispersions were measured (table 1) and clearly distinguished the ability of various surfactants to emulsify Lauroglycol® 90 and Capryol PGMC®. It can be observed that Cremophor-EL® (HLB =13) had a very good ability to emulsify Capryol PGMC®, followed by Tween® 80 (HLB= 15), whereas Labrasol ALF® (HLB = 14) was a poor emulsifier for Capryol PGMC®. The emulsification ability of a surfactant is typically influenced by its structure and HLB. The HLB values of selected surfactants were above 12, and the considerable differences in their ability to emulsify Capryol PGMC® could be explained by their structural differences [23].

Table 1. Emulsification study of surfactants for oils

Surfactant	**HLB**	**% Transmittance**	
		CapryolPGMC®	Lauroglycol® 90
Tween® 20	16	94.4 ±0.55	64.7 ± 0.42
Tween® 80	15	95.1 ±0.79	63.4 ± 0.49
Labrasol ALF®	14	60.5 ± 0.86	55.0± 0.36
Cremophor-EL®	14	99.3 ± 0.69	73.6 ± 0.15

None of the selected surfactants could effectively emulsify Lauroglycol® 90. Chemically, Lauroglycol®90 and Capryol PGMC® are propylene glycol monolaurate (C12) and propylene glycol monocaprylate (C8), respectively. Borhade and coworkers reported that the emulsification of oil and its amount incorporated into the nanoemulsion are affected by its molecular volume [27].

The increase in the number and length of hydrophobic alkyl chains increases the molecular volume, which renders emulsification of the oil difficult. This fact could explain the poor emulsification of Lauroglycol® 90 (C12) compared to Capryol PGMC® (C8). Therefore, Capryol PGMC® was selected as the oily phase for further studies due to its ease of emulsification.

In SNEDDS development, the role of the surfactant is to lower the interfacial tension, which ultimately eases the dispersion process during nanoemulsion formation. Reducing the interfacial tension to zero results in a negative free energy that makes the system stable and favors spontaneous emulsification [28]. However, surfactant alone may not be able to sufficiently lower the interfacial tension to form nanoemulsions [29]. Hence, the use of cosurfactants or cosolvents is important in the preparation of SNEDDSs. The cosolvent is used to cooperate with the surfactant in reducing the interfacial tension, increasing the drug solubility and enhancing the dispersibility of surfactant in the oily phase, thus promoting formulation homogeneity and stability [30]. All the hydrophilic cosolvents improved the emulsifying ability of Cremophor-EL®, whereas some of them (PEG 400 and propylene glycol) were less effective as a cosolvent for Tween® 80 (Supplementary table S1). Lipophilic cosurfactants were less effective because they could not improve the emulsification of the selected surfactants. In general, cosurfactants increase the interfacial fluidity by penetrating the surfactant film, creating void spaces between the surfactant molecules. Their performance is affected by their structure and chain length [31,32], which might explain the lower effectiveness of lipophilic cosurfactants compared to hydrophilic cosurfactants. Paradoxically, Labrafil M® 1944 CS did not follow this behavior. Labrafil M® 1944 CS, which has an oleic acid backbone, showed a good ability to improve the emulsification of selected surfactants, probably owing to its better hydrophilicity and surfactant-like properties than those of other cosurfactants. These observations are in line with studies reported by Date et al. [21]. Therefore, Transcutol HP® and PEG 400 were selected as cosurfactants due to their superior solubilizing potential for SEN and ability to improve the emulsification of the selected surfactants.

III.1.2. Ternary phase diagram study

Based on the solubility and emulsification ability studies (Fig. 1, S1), ternary diagrams were constructed to identify the self-(nano)emulsification regions and to select a suitable ratio of oil, surfactant and cosurfactant for SNEDDS development. The phase diagrams were studied for the following combinations: Capryol PGMC®-Cremophor-EL®-Transcutol HP® (F1), Capryol PGMC®-Cremophor-EL®PEG 400 (F2) and Capryol PGMC®-Tween® 80-Transcutol HP® (F3). The area where the ternary mixture showed a clear dispersion with a low droplet size (< 200 nm) was selected for further optimization studies. As shown in Fig. 2 (A-C), all three diagrams possessed a (nano)emulsification area, and these areas decreased as the ratio of cosurfactant increased. Furthermore, the sizes of the nanoemulsion regions were compared; the larger the size is, the greater the self-(nano)emulsification efficiency is. The largest nanoemulsion area was observed with a Smix ratio of 2:1 compared to 1:1, 3:1 and 3:2.

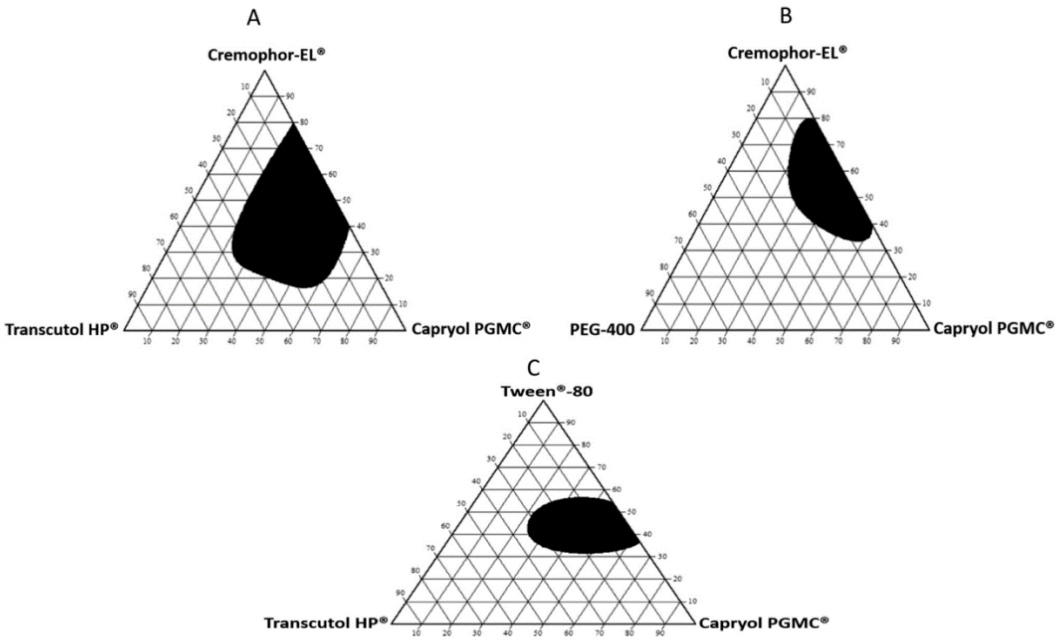

Figure 2. Phase diagrams of (A) Capryol PGMC®-Cremophor EL®-Transcutol HP® (F1), (B) Capryol PGMC®-Cremophor EL®-PEG 400 (F2), Capryol PGMC®-Tween® 80-Transcutol HP® (F3).

Cremophor-EL®-based systems with Transcutol HP® had larger nanoemulsification areas than those with PEG 400. This result could be attributed to the high aqueous partition of PEG 400, limiting its cosolvent efficacy compared to that of Transcutol HP® [25].

The nanoemulsion area of the Tween® 80-based system was small compared to that of the CremophorEL®-based systems, and there was no increase in the cosolvent used (data not shown). Moreover, Cremophor-EL®-based systems could form nanoemulsions for the compositions that had surfactant concentrations as high as 75% (w/w), compared 55% for the Tween® 80-based systems.

In view of the current investigations, F1, F2 and F3 (table 2 and Fig. 2) were chosen because of their resulting nanoemulsion droplet size and polydispersity index (PDI). With these components and proportions of oil/Smix, stable nanoemulsions could be formed spontaneously by gentle agitation following water dilution, and the preconcentrated SNEDDSs could be used for further studies by filling them into capsules.

III.1.3. Maximum drug content determination

The saturation solubility of SEN in the preconcentrated SNEDDS formulations was 20 ± 1 mg/g, 24 ± 0 mg/g and 28 ± 0 mg/g for F1, F2 and F3, respectively. The oil, surfactants and cosurfactants used along with their amounts could have contributed to the significant ($p<0.05$) difference in solubility. For a more direct comparison among the three formulations, and following SEN pharmacokinetics studies [2], 10 mg of SEN was loaded into 600 mg of each SNEDDS formulation.

III.2. CHARACTERIZATION OF THE OPTIMIZED FORMULATIONS

III.2.1. Transmittance percentage

Since SNEDDSs are defined as mixtures of oils, surfactants, cosurfactants and drugs that form oil-in water optically isotropic and kinetically stable nanoemulsions upon mild agitation, the transmittance percentage is a useful tool to assess the isotropic properties of the resulting nanoemulsions. As presented in table 2, all the selected formulations exhibited high transmittance values (≥ 95%), suggesting the clarity of the dispersions.

III.2.2. Viscosity measurement

Preconcentrated liquid SNEDDSs are generally filled into capsules. Low-viscosity SNEDDSs face leakage issues, whereas more high viscous formulations are difficult to fill into gelatin capsules owing to pourability issues [33]. The viscosity was found to be 41.6 ± 1.4 mPa, 67.8 ± 2.4 mPa and 27.3 ± 1.7 mPa for F1, F2 and F3, respectively. The high viscosity of the Cremophor-EL®-based systems compared to the Tween® 80-based systems was expected and was previously reported by Li et al. [30]. Moreover, the rheogram for the three formulations showed newtonian systems (data not shown), indicating that a change in shear stress will not induce a variation in viscosity during capsule machine filling operation [33].

III.2.3. Emulsification time

The emulsification time is an important parameter for assessing the spontaneity of the self(nano)emulsification of formulations without the aid of any external thermal or mechanical energy [34]. The emulsification time was less than 80 s for the three optimized formulations, which indicated their ability to disperse completely and quickly when subjected to aqueous dilution under mild agitation [23]. The quick emulsification process was correlated with the ease of water penetration into the complex colloidal structure formed on the surface of the droplets [34]. As shown in table 2, the Tween® 80-based system showed a lower emulsification time (27 s) than that of the Cremophor®-EL-based systems. This result could be correlated with a lower amount of oil and a higher amount of cosurfactant, which resulted in a lower viscosity of the Tween®80 -based system.

III.2.4. Droplet size analysis

The pH of the dispersion medium and drug incorporation may have a considerable impact on the behavior of SNEDDS formulations. Thus, the pH effect of the dispersion medium on the self-nanoemulsifying formulations was investigated (table 3). The mean droplet size of the diluted blank (F1 and F2) SNEDDS was < 60 nm, with a narrow distribution (PDI <0.4). However, the diluted blank F3 showed a mean droplet size > 100 nm with a distribution (PDI) >0.4. The high particle size could be attributed to the high aqueous partition of Tween® 80, probably owing to its high HLB value (HLB=15), whereas the high observed PDI appears to correlate with a higher amount (>65%) of relatively hydrophilic components (Tween® 80 and Transcutol® HP) and lower (<35%) amount of the oily phase (Capryol PGMC®). It was reported that the droplet size and the PDI of the nanoemulsion formed upon SNEDDS dispersion in aqueous environments depend on the type

and amount of components (surfactant and cosurfactant) used. This observation is in agreement with studies reported by Zupančičet al. [35].

The incorporation of SEN into SNEDDSs led to an increase in the droplet size of nanoemulsions compared to drug-free compositions, indicating its successful incorporation into the SNEDDS droplet [36]. The increased globule size of nanoemulsions could be attributed to the alteration of surfactant-oil interactions at the interface in the presence of SEN molecules.

Furthermore, the assessment of the *in vitro* precipitation was very important to eliminate the formulations that could potentially precipitate SEN at this development step. Even after storage for 48 h at 37°C in deionized water or buffers, SEN-SNEDDSs were clear in appearance and did not show any signs of flocculation, phase separation or drug precipitation.

Table 2. Composition and characterization of SNEDDS formulations. Data are expressed as the mean ± SD, n=3.

Fx	Sample composition (mg)			Emulsification time (s)	Zeta potential (mV)	Senicapoc solubility (mg/g)	% transmittance
	Oil	SA	Co-SA				
F1	260[a]	240[b]	100[d]	58 ± 2	-7.6± 3	20 ± 1	99 ± 0
F2	300[a]	240[b]	60[e]	64 ± 3	-7.4± 0	24 ± 0	96 ± 1
F3	180[a]	240[c]	180[d]	27 ± 6	-6.8 ± 2	28 ± 0	95 ± 1

a Capryol PGMC® b Cremophor-EL® c Tween®-80 d Transcutol HP® e PEG 400

Table 3. Globule size and polydispersity index of formulations before and after SEN incorporation diluted with various buffers as dispersion medium. Data are expressed as the mean ± SD, n=3.

	Hydrochloric acid buffer pH 1.2		Deionized water		PBS pH 6.8		FaSSGF pH 1.6		FaSSIF pH 6.8	
	Globule size (nm)	PDI	Globule size (nm)	PDI	Globule size (nm)	PDI	Globule size (nm)	PDI	Globule size (nm)	PDI
F1[a]	41 ± 1	0.19	28 ± 0	0.17	31 ± 0	0.13	60 ± 2	0.13	39 ± 0	0.27
[b]	62 ± 1	0.24	41 ± 1	0.22	63 ± 0	0.25	78 ± 1	0.33	57 ± 1	0.18
F2 [a]	33 ± 1	0.32	38 ± 2	0.39	60 ± 2	0.36	33 ± 0	0.36	34 ± 2	0.38
[b]	41 ± 0	0.25	52 ± 1	0.15	81 ± 1	0.44	48 ± 1	0.40	86 ± 2	0.33
F3 [a]	111 ± 2	0.58	123 ±3	0.45	105± 2	0.48	125 ± 2	0.41	130 ± 3	0.42
[b]	136 ± 0	0.44	152 ±1	0.33	111 ± 4	0.46	130 ± 4	0.23	145 ± 3	0.38

a Before SEN incorporation **b** After SEN incorporation

The zeta potential is responsible for repulsion between adjacent, similarly charged and dispersed droplets. As shown in table 2, all formulations exhibited zeta potential values of approximately -7

mV, which complies with the zeta potential requirement and indicates the stability of SNEDDS formulations [37].

III.2.5. Thermodynamic stability studies

To check the stability, formulations were subjected to heating and cooling cycles, freeze-thawing cycles and centrifugation. As shown in supplementary table S2, all the SNEDDSs remained stable and no phase separation was observed.

III.3. IN VITRO DISSOLUTION PROFILE

The *in vitro* dissolution profile of SEN from SNEDDSs is presented in Fig. 3. The pure drug showed a maximum drug release of up to 26.2% in 20 min. The amount of SEN released from the three SENSNEDDSs filled in hard gelatin capsules was over 80% within 20 min. Interestingly, F3 provided the highest release among all formulations (> 92%). It is obvious that SEN release from SNEDDSs was primarily governed by its solubility because SEN release was independent of the SNEDDS droplet size. SEN was released from the SNEDDS formulations in 60 min (F3>F2>F1) ($p< 0.05$), which was consistent with the increased solubility of SEN in the SNEDDS formulations (F3>F2>F1) ($p< 0.05$), indicating a good correlation between SEN solubility and its release. The solubility-dependent dissolution has also been reported earlier by Qian et al.[8].

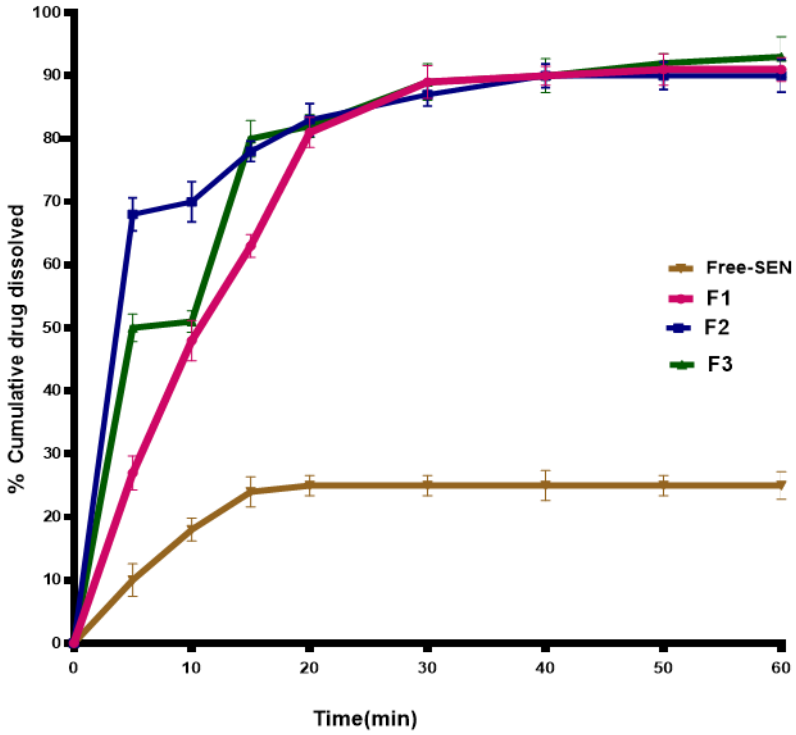

Figure 3. Dissolution profile of formulations in USP buffer pH 1.2 using paddle apparatus at 37± 0.5 °C. Data are expressed as the mean ± SD, n=3.

III.4. IN VITRO LIPOLYSIS

When administered orally, SNEDDSs are prone to digestion by pancreatic lipase. It has been reported that SNEDDS digestion in the GI tract is crucial for drug dissolution and absorption: it can be beneficial (drug solubilization) or deleterious (drug precipitation after digestion of the oil phase). The *in vitro* lipolysis of formulations was studied to understand the impact of the formulations on the lipolysis process. The consumption of NaOH during the experiment, reflecting the progress of lipolysis, is depicted in Fig. 4A. As presented in Fig. 4B, F1 and F2 show high SEN solubilization in the aqueous phase after 60 min of *in vitro* lipolysis. The larger quantities of lipids in those formulations could explain the higher SEN solubilization compared to that in F3 ($p < 0.05$). In agreement with previous studies [38], increasing the quantity of lipid in the formulation reduced drug precipitation during digestion.

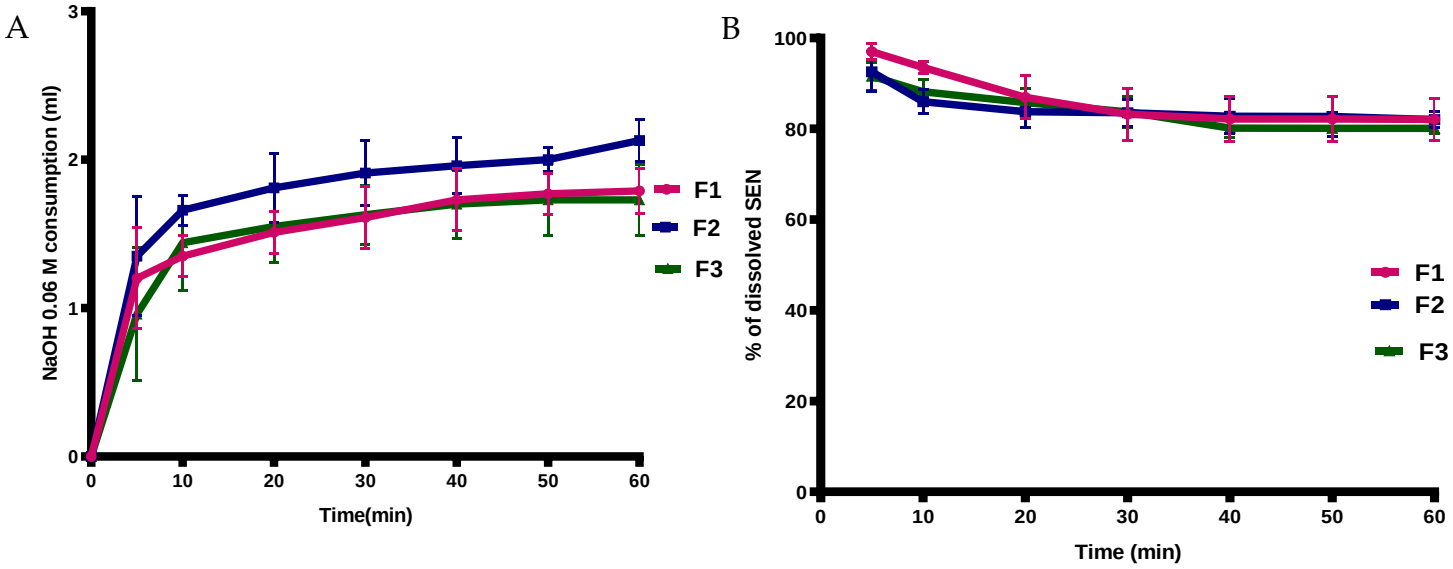

Figure 4A. NaOH consumption of SNEDDSS formulations during *in vitro* lipolysis. Data are expressed as the mean ± SD, n=3.

Figure 4B. SEN content in the aqueous phase during *in vitro* lipolysis. Data are expressed as the mean ± SD, n=3.

III.5. TRANSPORT STUDY THROUGH THE CACO-2 CELL MONOLAYERS

III.5.1. Cytotoxic assessment of the SNEDDS formulations

The potential cytotoxicity of SNEDDS formulations to Caco-2 cells was tested to find the highest no/low toxic concentration to be used in transport experiments. Fig. 5 presents the concentration versus percent viability data of cells incubated with free SEN and unloaded-SNEDDS. Caco-2 cell viability exceeded 80% following exposure to all SNEDDS formulations (from 0.3 mg/mL to 1.25 mg/mL). The literature reports that a SNEDDS with a cell viability of 80% or more is considered

non-toxic [16]. Moreover, the IC50 values of F1, F2 and F3 were 1.6 mg/mL, 1.7 mg/mL and 2.9 mg/mL, respectively.

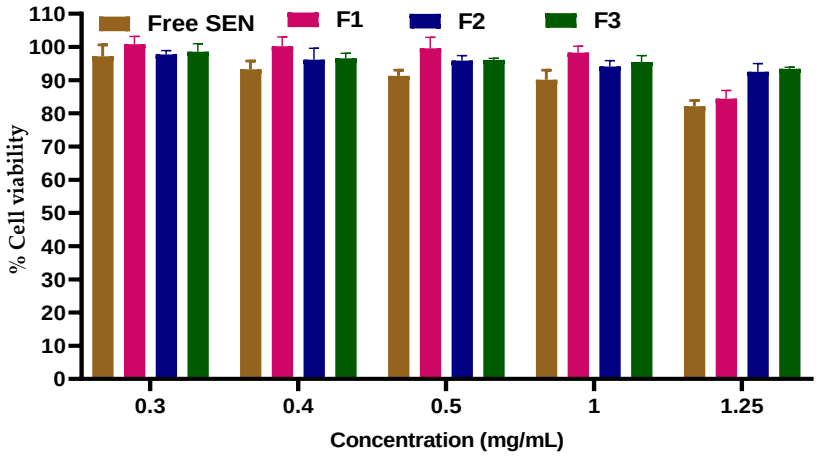

Figure 5. Cytotoxicity of the three formulations without SEN after 2 h incubation in concentrations of 0.3 mg/mL, 0.4 mg/mL, 0.5 mg/mL, 1 mg/mL and 1.25 mg/mL. Each data point shows the mean ± SD (n= 6).

III.5.2. The transport of senicapoc across Caco-2 cell monolayers

Based on the cytotoxicity studies, Caco-2 monolayers were ncubated for 120 min at 37°C with 1 mg/mL of each SEN-SNEDDS corresponding to 16.6 µg/mL SEN. No significant change in TEER values before and after incubation with the formulations was observed ($p > 0.05$). The apical to basolateral transport of SEN from each formulation was in the following order: F1>F2>F3>control group (Fig. 6). The quantity of SEN transported across the Caco-2 monolayers ranged between 2.2 and 2.6% (0.57 to 0.66 µg) of the donor SEN-SNEDDS. The P_{app} values of SEN from F1, F2 and F3 were 115- ($p < 0.01$), 105- ($p < 0.01$) and 99-fold ($p < 0.01$) higher than those for the free drug, respectively, demonstrating that the P_{app} of SEN could be significantly enhanced using SNEDDS formulations. Compared to the Tween® 80-based system, the Cremophor-EL®-based systems yielded the highest P_{app} ($p < 0.01$). It was previously reported that Cremophor-EL® could affect membrane fluidity and increase the permeation of lipophilic drugs (Yin et al., 2009). Compared to that for F2, the significantly high P_{app} observed for F1 ($p < 0.01$) could come from the incorporation of Transcutol HP®. As reported in the literature [39], the P_{app} values of several poorly water-soluble model compounds were improved by Transcutol, and its permeation-enhancing effect on Caco-2 monolayers was much stronger than that of PEG 400. Thus, Transcutol HP® present in F1 showed a higher SEN absorption enhancing effect than did PEG 400 in F2.

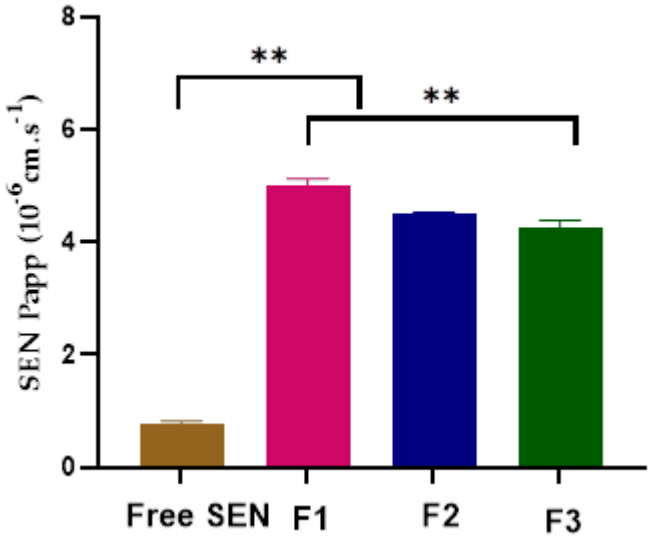

Figure 6. The apparent permeability (Papp) values of SEN across the Caco-2 cell monolayer for each formulation after 2 h of the A to B transport study. Each value is the mean ± of three separate determinations. **p < 0.01

IV. CONCLUSION

In this study, three optimized SNEDDS formulations were prepared and evaluated to improve the solubility and cell permeation of SEN. The screening of surfactants and cosurfactants helped to identify the most suitable components, whereas the ternary phase diagrams gave an idea about the ratio of SNEDDS excipients that should be used to achieve optimized formulations. The formulated SNEDDSs showed a high release profile, and at least 80% of SEN remained solubilized after the *in vitro* lipolysis of the SNEDDS formulations. Additionally, the *in vitro* transport study across Caco-2 cell monolayers revealed that the SNEDDSs could significantly enhance the permeation of SEN. Overall, the present and previous investigations showed the potential of SNEDDSs to enhance the solubility and permeation of insoluble drugs such as SEN, although further preclinical studies are required before clinical trials can be conducted.

Supplementary tables

Table S1. Emulsification study of surfactant/co-surfactant combinations

Cosurfactant/cosolvent	% Transmittance	
	Cremophor-EL®	Tween® 80
Transcutol HP®	99.8 ± 0.85	95.5 ± 0.67
Propylene glycol	99.4 ± 0.45	88.2 ± 0.76
Polyethylene glycol 400	99.6 ± 1.62	85.4 ± 0.89
Labrafil M® 1944 CS	98.3 ± 0.65	94.4 ± 0.25
Labrafil M® 2125 CS	89.4 ± 0.15	78.4 ± 0.60

Table S2. Thermodynamic stability studies

Formulation	Heating-cooling cycles	Freeze-thaw stress cycles	Centrifugation
F1	No phase separation	No phase separation	No phase separation
F2	No phase separation	No phase separation	No phase separation
F3	No phase separation	No phase separation	No phase separation

REFERENCES

1. Ataga, K. I.; Reid, M.; Ballas, S. K.; Yasin, Z.; Bigelow, C.; James, L. S.; Smith, W. R.; Galacteros, F.; Kutlar, A.; Hull, J. H.; Stocker, J. W. Improvements in Haemolysis and Indicators of Erythrocyte Survival Do Not Correlate with Acute Vaso-Occlusive Crises in Patients with Sickle Cell Disease: A Phase III Randomized, Placebo-Controlled, Double-Blind Study of the Gardos Channel Blocker Senicapo. *Br. J. Haematol.* **2011**, *153*, 92–104, https://doi.org/10.1111/j.1365-2141.2010.08520.x.
2. Ataga, K. I.; Stocker, J. Senicapoc (ICA-17043): A Potential Therapy for the Prevention and Treatment of Hemolysis-Associated Complications in Sickle Cell Anemia. *Expert Opinion on Investigational Drugs*. **2009**, 18, 231–239,https://doi.org/10.1517/13543780802708011.
3. Tubman, V. N.; Mejia, P.; Shmukler, B. E.; Bei, A. K.; Alper, S. L.; Mitchell, J. R.; Brugnara, C.; Duraisingh, M. T. The Clinically Tested Gardos Channel Inhibitor Senicapoc Exhibits Antimalarial Activity. *Antimicrob. Agents Chemother.* **2016**, *60* , 613–616,https://doi.org/10.1128/AAC.01668-15.
4. Van Der Velden, J.; Sum, G.; Barker, D.; Koumoundouros, E.; Barcham, G.; Wulff, H.; Castle, N.; Bradding, P.; Snibson, K. K Ca 3.1 Channel-Blockade Attenuates Airway Pathophysiology in a Sheep Model of Chronic Asthma. *PLoS One* **2013**, *8*,https://doi.org/10.1371/journal.pone.0066886.
5. Paka, L.; Smith, D. E.; Jung, D.; McCormack, S.; Zhou, P.; Duan, B.; Li, J. S.; Shi, J.; Hao, Y. J.; Jiang, K.; Yamin, M.; Goldberg, I. D.; Narayan, P. Anti-Steatotic and Anti-Fibrotic Effects of the KCa3.1 Channel Inhibitor, Senicapoc, in Non-Alcoholic Liver Disease. *World J. Gastroenterol.* **2017**, *23*, 4181–4190,https://doi.org/10.3748/wjg.v23.i23.4181.
6. Mohr, C. J.; Steudel, F. A.; Gross, D.; Ruth, P.; Lo, W. Y.; Hoppe, R.; Schroth, W.; Brauch, H.; Huber, S. M.; Lukowski, R. Cancer-Associated Intermediate Conductance Ca 2+ -Activated K + Channel K Ca 3.1. *Cancers (Basel).* **2019**, *11*, 1–22, https://doi.org/10.3390/cancers11010109.
7. McNaughton-Smith, G. A.; Burns, J. F.; Stocker, J. W.; Rigdon, G. C.; Creech, C.; Arlington, S.; Shelton, T.; De Franceschi, L. Novel Inhibitors of the Gardos Channel for the Treatment of Sickle Cell Disease. *J. Med. Chem.* **2008**, *51*, 976–982,https://doi.org/10.1021/jm070663s.
8. Qian, J.; Meng, H.; Xin, L.; Xia, M.; Shen, H.; Li, G.; Xie, Y. Self-Nanoemulsifying Drug Delivery Systems of Myricetin: Formulation Development, Characterization, and in Vitro and in Vivo Evaluation. *Colloids Surfaces B Biointerfaces* **2017**, *160*, 101–109, https://doi.org/10.1016/j.colsurfb.2017.09.020.
9. Park, S. H.; Choi, H. K. The Effects of Surfactants on the Dissolution Profiles of Poorly Water-Soluble Acidic Drugs. *Int. J. Pharm.* **2006**, *321*, 35–41,https://doi.org/10.1016/j.ijpharm.2006.05.004.
10. Kushwaha A.K.; Vuddanda P.R.; Karunanidhi P.; Singh S.K.; Singh S. Development and evaluation of solid lipid nanoparticles of raloxifene hydrochloride for enhanced bioavailability. Biomed Res Int. **2013**, 2013,584549, https://doi.org/10.1155/2013/584549
11. Piazzini, V.; Monteforte, E.; Luceri, C.; Bigagli, E.; Bilia, A. R.; Bergonzi, M. C. Nanoemulsion for Improving Solubility and Permeability of Vitex Agnus-Castus Extract: Formulation and in Vitro Evaluation Using PAMPA and Caco-2 Approaches. *Drug Deliv.* **2017**, *24*, 380–390, https://doi.org/10.1080/10717544.2016.1256002.
12. Yin, Y. M.; Cui, F. De; Mu, C. F.; Choi, M. K.; Kim, J. S.; Chung, S. J.; Shim, C. K.; Kim, D. D. Docetaxel Microemulsion for Enhanced Oral Bioavailability: Preparation and in Vitro and in Vivo Evaluation. *J. Control. Release* **2009**, *140*, 86–94,https://doi.org/10.1016/j.jconrel.2009.08.015.
13. Dou, Y. X.; Zhou, J. T.; Wang, T. T.; Huang, Y. F.; Chen, V. P.; Xie, Y. L.; Lin, Z. X.; Gao, J. S.; Su, Z. R.; Zeng, H. F. Self-Nanoemulsifying Drug Delivery System of Bruceine D: A New Approach for Anti-Ulcerative Colitis. *Int. J. Nanomedicine* **2018**, *13*,5887–5907,https://doi.org/10.2147/IJN.S174146.
14. Pereira, S.; Egbu, R.; Jannati, G.; Al-Jamal, W. T. Docetaxel-Loaded Liposomes: The Effect of Lipid Composition and Purification on Drug Encapsulation and in Vitro Toxicity. *Int. J. Pharm.* **2016**, *514* , 150–159,https://doi.org/10.1016/j.ijpharm.2016.06.057.
15. Phua, J. L.; Hou, A.; Lui, Y. S.; Bose, T.; Chandy, G. K.; Tong, L.; Venkatraman, S.; Huang, Y. Topical Delivery of Senicapoc Nanoliposomal Formulation for Ocular Surface Treatments. *Int. J. Mol. Sci.* **2018**, *19*, 2977,https://doi.org/10.3390/ijms19102977.
16. Cardona, M. I.; Nguyen Le, N. M.; Zaichik, S.; Aragón, D. M.; Bernkop-Schnürch, A. Development and in Vitro Characterization of an Oral Self-Emulsifying Delivery System (SEDDS) for Rutin Fatty Ester with High Mucus Permeating Properties. *Int. J. Pharm.* **2019**, *562*, 180–186, https://doi.org/10.1016/j.ijpharm.2019.03.036.

17. Zaichik, S.; Steinbring, C.; Caliskan, C.; Bernkop-Schnürch, A. Development and in Vitro Evaluation of a Self-Emulsifying Drug Delivery System (SEDDS) for Oral Vancomycin Administration. *Int. J. Pharm.* **2019**, *554*, 125–133,https://doi.org/10.1016/j.ijpharm.2018.11.010.
18. Mou, D.; Chen, H.; Du, D.; Mao, C.; Wan, J.; Xu, H.; Yang, X. Hydrogel-Thickened Nanoemulsion System for Topical Delivery of Lipophilic Drugs. *Int. J. Pharm.* **2008**, *353*, 270–276, https://doi.org/10.1016/j.ijpharm.2007.11.051.
19. Date, A. A.; Desai, N.; Dixit, R.; Nagarsenker, M. Self-Nanoemulsifying Drug Delivery Systems: Formulation Insights, Applications and Advances. *Nanomedicine*. **2010**, 5 ,1595–1616, https://doi.org/10.2217/nnm.10.126.
20. Rani, S.; Rana, R.; Saraogi, G. K.; Kumar, V.; Gupta, U. Self-Emulsifying Oral Lipid Drug Delivery Systems: Advances and Challenges. *AAPS PharmSciTech*. **2019**, 20, 129, https://doi.org/10.1208/s12249-019-1335-x.
21. Date, A. A.; Nagarsenker, M. S. Design and Evaluation of Self-Nanoemulsifying Drug Delivery Systems (SNEDDS) for Cefpodoxime Proxetil. *Int. J. Pharm.* **2007**, *329*, 166–172, https://doi.org/10.1016/j.ijpharm.2006.08.038.
22. Shakeel, F.; Haq, N.; Alanazi, F. K.; Alsarra, I. A. Impact of Various Nonionic Surfactants on Self-Nanoemulsification Efficiency of Two Grades of Capryol (Capryol-90 and Capryol-PGMC). *J. Mol. Liq.* **2013**, *182*, 57–63,https://doi.org/10.1016/j.molliq.2013.03.011.
23. Basalious, E. B.; Shawky, N.; Badr-Eldin, S. M. SNEDDS Containing Bioenhancers for Improvement of Dissolution and Oral Absorption of Lacidipine. I: Development and Optimization. *Int. J. Pharm.* **2010**, *391*, 203–211, https://doi.org/10.1016/j.ijpharm.2010.03.008.
24. Crum, M. F.; Trevaskis, N. L.; Williams, H. D.; Pouton, C. W.; Porter, C. J. H. A New in Vitro Lipid Digestion - In Vivo Absorption Model to Evaluate the Mechanisms of Drug Absorption from Lipid-Based Formulations. *Pharm. Res.* **2016**, *33*, 970–982,https://doi.org/10.1007/s11095-015-1843-7.
25. Memvanga, P. B.; Coco, R.; Préat, V. An Oral Malaria Therapy: Curcumin-Loaded Lipid-Based Drug Delivery Systems Combined with β-Arteether. *J. Control. Release* **2013**, *172*, 904–913, https://doi.org/10.1016/j.jconrel.2013.09.001.
26. Elsheikh, M. A.; Elnaggar, Y. S. R.; Gohar, E. Y.; Abdallah, O. Y. Nanoemulsion Liquid Preconcentrates for Raloxifene Hydrochloride: Optimization and in Vivo Appraisal. *Int. J. Nanomedicine* **2012**, *7*, 3787–3802,https://doi.org/10.2147/IJN.S33186.
27. Borhade, V.; Pathak, S.; Sharma, S.; Patravale, V. Clotrimazole Nanoemulsion for Malaria Chemotherapy. Part I: Preformulation Studies, Formulation Design and Physicochemical Evaluation. *Int. J. Pharm.* **2012**, *431*, 138–148,https://doi.org/10.1016/j.ijpharm.2011.12.040.
28. Patki, M.; Patel, K. Development of a Solid Supersaturated Self-Nanoemulsifying Preconcentrate (S-superSNEP) of Fenofibrate Using Dimethylacetamide and a Novel Co-Processed Excipient. *Drug Dev. Ind. Pharm.* **2019**, *45* , 405–414,https://doi.org/10.1080/03639045.2018.1546311.
29. Rajesh, S. Y.; Singh, S. K.; Pandey, N. K.; Sharma, P.; Bawa, P.; Kumar, B.; Gulati, M.; Jain, S. K.; Gowthamarajan, K.; Singh, S. Impact of Various Solid Carriers and Spray Drying on Pre/post Compression Properties of Solid SNEDDS Loaded with Glimepiride: In Vitro-Ex Vivo Evaluation and Cytotoxicity Assessment. *Drug Dev. Ind. Pharm.* **2018**, *44*, 1056–1069, https://doi.org/10.1080/03639045.2018.1431656.
30. Li, L.; Zhou, C.H.; Xu, Z.P. Self-Nanoemulsifying Drug-Delivery System and Solidified Self-Nanoemulsifying Drug-Delivery System. In *Nanocarriers for Drug Delivery*; Elsevier: Amsterdam, The Netherlands, 2019; pp. 421–449, doi:10.1016/b978-0-12-814033-8.00014-x.
31. Malcolmson, C.; Satra, C.; Kantaria, S.; Sidhu, A.; Lawrence, M. J. Effect of Oil on the Level of Solubilization of Testosterone Propionate into Nonionic Oil-in-Water Microemulsions. *J. Pharm. Sci.* **1998**, *87*, 109–116. https://doi.org/10.1021/js9700863.
32. Warisnoicharoen, W.; Lansley, A. B.; Lawrence, M. J. Nonionic Oil-in-Water Microemulsions: The Effect of Oil Type on Phase Behaviour. *Int. J. Pharm.* **2000**, *198*,7–27,https://doi.org/10.1016/S0378-5173(99)00406-8.
33. Parikh, K. J.; Sawant, K. K. Solubilization of Vardenafil HCl in Lipid-Based Formulations Enhances Its Oral Bioavailability in Vivo: A Comparative Study Using Tween - 20 and Cremophor - EL. *J. Mol. Liq.* **2019**, *277*, 189–199,https://doi.org/10.1016/j.molliq.2018.12.079.
34. Parmar, N.; Singla, N.; Amin, S.; Kohli, K. Study of Cosurfactant Effect on Nanoemulsifying Area and Development of Lercanidipine Loaded (SNEDDS) Self Nanoemulsifying Drug Delivery System. *Colloids Surfaces B Biointerfaces* **2011**, *86*, 327–338, https://doi.org/10.1016/j.colsurfb.2011.04.016.

35. Zupančič, O.; Grießinger, J. A.; Rohrer, J.; Pereira de Sousa, I.; Danninger, L.; Partenhauser, A.; Sündermann, N. E.; Laffleur, F.; Bernkop-Schnürch, A. Development, in Vitro and in Vivo Evaluation of a Self-Emulsifying Drug Delivery System (SEDDS) for Oral Enoxaparin Administration. *Eur. J. Pharm. Biopharm.* **2016**, *109*, 113–121,https://doi.org/10.1016/j.ejpb.2016.09.013.
36. Menzel, C.; Holzeisen, T.; Laffleur, F.; Zaichik, S.; Abdulkarim, M.; Gumbleton, M.; Bernkop-Schnürch, A. In Vivo Evaluation of an Oral Self-Emulsifying Drug Delivery System (SEDDS) for Exenatide. *J. Control. Release* **2018**, *277*, 165–172,https://doi.org/10.1016/j.jconrel.2018.03.018.
37. Xue, X.; Cao, M.; Ren, L.; Qian, Y.; Chen, G. Preparation and Optimization of Rivaroxaban by Self-Nanoemulsifying Drug Delivery System (SNEDDS) for Enhanced Oral Bioavailability and No Food Effect. *AAPS PharmSciTech* **2018**, *19*, 1847–1859,https://doi.org/10.1208/s12249-018-0991-6.
38. Alayoubi, A.; Aqueel, M. S.; Cruz, C. N.; Ashraf, M.; Zidan, A. S. Application of in Vitro Lipolysis for the Development of Oral Self-Emulsified Delivery System of Nimodipine. *Int. J. Pharm.* **2018**, *553* , 441–453,https://doi.org/10.1016/j.ijpharm.2018.10.066.
39. Alvi, M. M.; Chatterjee, P. A Prospective Analysis of Co-Processed Non-Ionic Surfactants in Enhancing Permeability of a Model Hydrophilic Drug. *AAPS PharmSciTech* **2014**, *15*, 339–353, https://doi.org/10.1208/s12249-013-0065-8.

CHAPTER IV
QUALITY-BY-DESIGN BASED DEVELOPMENT OF SELF-NANOEMULSIFYING DRUG DELIVERY SYSTEMS OF VOXELOTOR WITH IMPROVED BIOPHARMACEUTICAL ATTRIBUTES

Aristote B. Buya, Romano Terrasi, Jérémie K. Mbinze, Giulio G. Muccioli, Ana Beloqui, Patrick B. Memvanga and Véronique Préat

Adapted from Pharmaceutics 2021, 13, 1388

TABLE OF CONTENTS

ABSTRACT

Low aqueous solubility and poor oral bioavailability are limiting factors in the oral delivery of voxelotor, an antisickling agent. To overcome these limitations, a voxelotor self-nanoemulsifying drug delivery system was developed. Various oils, surfactants, and cosurfactants were screened for their solubilization potential for the drug. The area of nanoemulsification was identified using a ternary phase diagram. An experimental mixture design and a desirability function were applied to select SNEDDSs that contain a maximum amount of lipids and a minimum amount of surfactant, and that possess optimal emulsification properties (i.e., droplet sizes, polydispersity index (PDI), emulsification time, and transmittance percentage). The optimized SNEDDS formulation was evaluated for the self-emulsifying time (32 s), droplet size (35 nm), and zeta potential (−8 mV). In vitro dissolution studies indicated a 3.1-fold improvement in drug solubility from the optimized SNEDDS over pure drug powder. After 60 min of in vitro lipolysis, 88% of the voxelotor loaded in the SNEDDS remained in the aqueous phase. Cytotoxicity evaluation using Caco-2 cells indicated the safety of the formulation at 0.9 mg/mL. The transport of the voxelotor SNEDDS across Caco-2 monolayers was significantly enhanced compared to that of the free drug. Compared to the drug suspension, the developed SNEDDS enhanced the oral bioavailability (1.7-fold) of voxelotor in rats. The results suggest that further development of SNEDDSs for the oral delivery of voxelotor is needed.

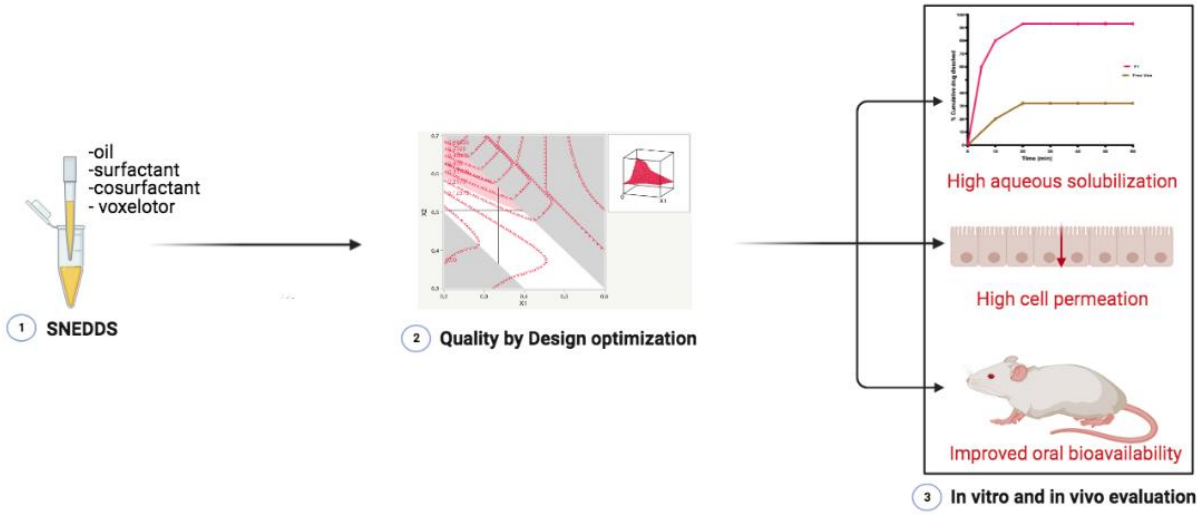

I. INTRODUCTION

During recent decades, the number of sickle cell disease (SCD) patients has increased significantly, making it the most common genetic disorder affecting millions of people worldwide, particularly in sub-Saharan Africa [1]. Several strategies have been applied in the treatment of this pathology, characterized by red blood cell sickling, vaso-occlusion, haemolytic anaemia, and vasculopathy leading to progressive organ damage [2]. The cellular sickling process can be reduced by increasing the oxygen affinity of haemoglobin S (HbS). The literature has reported that increasing the concentration of oxygenated HbS, without compromising oxygen delivery, is a promising approach to prevent red blood cell sickling and, subsequently, achieve long-term disease improvement [3].

Voxelotor (Vox), also known as GBT-440, is a small compound that binds to HbS and increases its affinity for oxygen. Vox improves the in vitro red blood cell flexibility and survival [4]. In a rat model, Vox prevented ex vivo red blood cell sickling [3]. The first-in-human studies in healthy volunteers and SCD patients showed that the tolerability and safety of Vox was associated with an increase in HbS oxygen affinity [5]. OXBRYTA®(tablets), a form of Vox, has been given accelerated approval by the U.S. Food and Drug Administration for patients aged 12 years and older [6]. However, the oral delivery of Vox has been thwarted because of its lipophilicity (log 3.54) and poor aqueous solubility (31 μg/mL) [5]. This aqueous solubility not only provides low oral bioavailability (36%), but also leads to considerable subject dose variability [5]. Furthermore, the absorption of Vox from the GI tract is affected by food intake [6]. When OXBRYTA® was orally given to healthy human volunteers with a high-fat meal, it showed a 42- and 45-fold enhancement in AUC and C_{max}, respectively, compared to the fasted state [6].

Lipid-based formulations have emerged as a promising strategy to improve the aqueous solubility and oral absorption of lipophilic drugs, and to decrease undesirable food effects [7]. The development of self-nanoemulsifying drug delivery systems (SNEDDSs) has provided one approach that is commonly adopted in this direction. SNEDDSs are anhydrous mixtures of oils, surfactants, and cosurfactants, that spontaneously form oil-in-water nanoemulsions with droplet sizes of less than 200 nm when exposed to GI fluids [8]. Compared to other lipid nanocarriers, SNEDDSs are easy to scale up and contain biodegradable excipients [9,10]. The food-associated effects of several lipophilic drugs, such as cinnarizine [11], torcetrapib [12], and itraconazole [13], have been nullified when encapsulated into SNEDDSs. Many SNEDDS formulations have been developed and optimized by taking into consideration the resulting emulsion droplet sizes after aqueous dispersion, through the use of empirical "trial and error" ternary diagram approaches, which consist of varying one factor at a time [14]. Unfortunately, such approaches are highly time consuming and require a number of experiments and resources. Furthermore, they often provide inadequate data to determine the impact of excipients on the performance of the formulation [10,15].

The use of the quality-by-design (Qbd) approach, applying the statistical design of experiments (DoE) for the systematic optimization of SNEDDSs has been reported to reduce expenditure in terms of time, resources, and developmental efforts. The Qbd approach provides an optimal amount of data and process understanding from a limited number of experiments [16]. A DoE applied during the component screening can provide more insight into excipient effects and

interactions in the SNEDDS performance [17,18]. The Qbd approach has been used in the optimization of a wide variety of lipid-based formulations, including itraconazole microemulsions [19], rivaroxaban self-nanoemulsifying drug delivery systems [20], doxorubicin and curcumin coloaded liposomes [21], and rosuvastatin calcium solid lipid nanoparticles [22].

Therefore, the present work aims to use the Qbd approach for the development and optimization of Vox-loaded SNEDDSs. An experimental mixture design and a desirability function were applied to select SNEDDSs that contain a maximum amount of lipids and a minimum amount of surfactant, and that possess optimal emulsification properties (i.e., droplet sizes, polydispersity index (PDI), emulsification time, and transmittance percentage). Further, this work endeavours to evaluate the biopharmaceutical performance of the optimized Vox-SNEDDS in terms of in vitro dissolution, lipolysis, cytotoxicity, transport studies, and in vivo pharmacokinetic studies.

II. MATERIALS AND METHODS

II.1. MATERIALS

Voxelotor with a purity greater than 98% was purchased from MedChemExpress (Monmouth, NJ, USA). Cremophor-EL® (polyoxyl-35 castor oil) was kindly provided by BASF (Ludwigshafen, Germany). Labrasol AFL® (caprylocaproyl polyoxyl-8- glycerides), Transcutol HP® (diethylene glycol monoethyl), Labrafil M® 1944 CS (oleoyl polyoxyl-6- glycerides), Labrafil M® 2125 CS (linoleoyl polyoxyl -6-glycerides), Capryol PGMC® (propylene glycol monocaprylate type I), Lauroglycol® 90 (propylene glycol monolaurate), and Maisine® 35-1 (glycerol monolinoleate) were kind gifts from Gattefossé (Saint-Priest, France). Tween® 80 (polysorbate 80), L-α-phosphatidylcholine (TLC), sodium taurodeoxycholate (NaTDC), 4-bromophenylboronic acid, porcine pancreatin extract (P7545, 8 × USP specification activity), and thiazolyl blue tetrazolium bromide (MTT) were all purchased from Sigma-Aldrich (St. Louis, MO, USA). Empty gelatine capsule shells (size "0") were purchased from Capsugel Inc. (Morristown, NJ, USA). Formic acid, acetonitrile, methanol, and dimethylsulfoxide (DMSO) (all HPLC grade) were purchased from VWR (Copenhagen, Denmark). Purified water was used in all experiments. All other reagents were of analytical grade and used as received.

II.2. ANALYTICAL METHODS

II.2.1. HPLC–UV Method

An HPLC-UV system was used to quantify voxelotor. The HPLC (Shimadzu C 204353, Kyoto, Japan) was equipped with of an LC-20A pump, an SIL-20A autosampler and SPD-20A intelligent UV/VIS detector. A CC 250-4.6 Nucleosil 100-5, C18 HD HPLC column (Macherey-Nagel, Düren, Germany) was used for chromatographic separation. The mobile phase consisted of 20% v/v (water + 0.1% formic acid) and 80% v/v (acetonitrile + 0.1% formic acid) under isocratic mode. The velocity of the flow, sample load and wavelength of the UV detector were set at 1.0 mL/min, 10 µL and 272 nm, respectively. The HPLC–UV method was validated according to the current international regulatory guidelines [23]. In particular, the linearity, accuracy, precision, reproducibility, and repeatability of the method were assessed and are presented in Supplementary Table S1 and Supplementary Figures S1and S2. Specificity was determined by comparing chromatograms of blank SNEDDS with voxelotor solution (in acetonitrile). SNEDDS blank did not interferer at the same retention time as the voxelotor (4.8 min), demonstrating that the method is specific to voxelotor. The limit of detection (LOD) and of quantification (LOQ) were 0.2 µg /mL and 0.7 µg /mL, respectively and were determined by the standard deviation of the response and the slope, using the calibration curve data as follows: LOD = 3.3 SD/S; LOQ = 10 SD/S, where SD is the standard deviation of y-intercepts and S is the average slope obtained from the calibration curves in the linearity test.

II.2.2. LC–MS Method

Voxelotor was extracted from rat serum samples (50 μL) in the presence of F21450908, which was used as an internal standard (30 pmol), by adding acetonitrile (400 μL) and hydrochloric acid (10 μL, 2 N). After an overnight incubation (−20 °C), the samples were centrifuged, and the supernatant was transferred to an injection vial. The samples were analysed using a Waters Xevo TQ-S tandem quadrupole mass spectrometer, coupled to an Acquity UPLC class H system (Waters, Milford, MA, USA). A Kinetex LC-18 (150 × 4.6 mm, 5 μm) column (Phenomenex) and a 10-min gradient between MeOH-water (75:25, *v*/*v*) (with 0.1% acetic acid) and MeOH (with 0.1% acetic acid) were used. Ionization (positive mode) was obtained using an ESI probe. The quantification transitions for voxelotor and F21450908 were 338.1 → 200.0 and 342.1 → 222.1, respectively. The ratio between the area under the curve (AUC) of voxelotor and of the internal standard was reported using a calibration curve (obtained under identical conditions). To establish the LOD and LOQ, plasma (50 μL) was spiked with voxelotor at several levels and analysed using the same protocol. The values were 337 × 10^{-5} and 1126 × 10^{-5} μg/mL, respectively.

II.3. OPTIMIZATION OF THE SNEDSS FORMULATION

II.3.1. Equilibrium Solubility of Vox

The solubility of Vox was studied in the selected excipients (oils, surfactants and cosurfactants). An excess amount of Vox was added to 500 mg of each excipient under stirring (100 rpm, 37 °C) in a shaking incubator (Infors AG, Bottmingen, Switzerland) for 48 h. The resultant samples were centrifuged at 4000 x g for 15 min (37 °C) using an Eppendorf centrifuge 5804 R (Hamburg, Germany). The supernatant was diluted with acetonitrile, and the concentration of Vox was determined by HPLC-UV.

II.3.2. Screening of Surfactants and Cosurfactants for Self-Emulsifying Ability

The self-emulsification capacity of the surfactants was studied as described by Date et al. [24], with minor modifications. In brief, mixture of the selected oil and surfactant at a ratio 1: 1 (w/w) was heated (40–45 °C) under gentle stirring. The resulting mixture (500 mg) was dispersed in 10 mL of deionized water under gentle stirring. Visual observation was carried out to assess the relative turbidity. The resulting dispersions were allowed to stand for 2h and the transmittance percentage values were determined at 550 nm using a NanoDropTM 2000 spectrophotometer (Thermo Fisher Scientific Inc., Waltham, MA, USA) with deionized water as a control.

To assess the emulsification ability of the cosurfactants and cosolvents, each of them was mixed with the selected surfactant at a 2:1 (w/w) ratio. The selected oil was addedto this mixture at a 1:3 ratio under stirring and heat (40–45 °C). The resulting dispersions were analyzed as mentioned for the surfactant screening.

II.3.3. Development of SNEDDSs Employing "Qbd"

Ternary Phase Diagram

A ternary phase diagram of the oil, surfactant, and cosurfactant was plotted, with each representing an apex on the triangle. Forty ternary mixtures (with varying compositions of oil, surfactant, and cosurfactant) chosen from the solubility studies were prepared. The mixture (500 mg) was accurately weighed and dispersed in 200 mL of deionized water (37 °C) under gentle agitation (50 rpm). Visual observation was carried out immediately to investigate the occurrence of self-nanoemulsification. Dispersions with measured particle sizes of less than 200 nm were used to draw the nanoemulsion area of the diagram [25]. Phase diagrams were constructed using Chemix School version 3.60 software (Arne Standnes, Bergen, Norway).

Preparation of SNEDDSs for the Experimental Design

The SNEDDSs were prepared by mixing (100 rpm, 20 ± 5 °C) the oil, surfactant, and cosurfactant at predetermined amounts, as per the design (Table 2). The final mixtures were stirred for dissolution until clear preparations were obtained and were then stored (20 ± 5 °C) for further studies.

Experimental Design

A 16-run custom design, using the Bayesian D-optimality quality criterion, was generated to estimate a full cubic model for the three critical formulation variables. The design was blocked on 4 days of 4 runs each. The experimental design and statistical analysis were executed using JMP Pro® 14.3.0 (SAS Institute, New York, NY, USA). The independent variables and their respective levels were selected based on solubility and ternary phase diagram studies. The proportions of oil (X_1, % *w/w*), surfactant (X_2, % *w/w*), and cosurfactant (X_3, % *w/w*) were considered independent variables (factors), whereas the dependent variables (responses) were emulsification time (Y_1, s), droplet size (Y_2, nm), PDI (Y_3), and transmittance percentage (Y_4, %). The amount of the components was held constant (1 g), while the ratio of the three was varied. Sixteen SNEDDS formulations were prepared and are presented in Table 2. The data obtained from the response measurements were analysed using a mixed model, with the day as a random variable, and a fixed full model on our explanatory variables. When possible, the model was simplified, taking into account the linear constraints between the factors, to raise the model power. The correlation of factors with response variables was then fitted into different mathematical models (quadratic, cubic, or special cubic). The model quality was estimated using the R-squared, adjusted R-squared, root mean square error, and *p*-value of the F-test associated with the contribution of the variables in the model (critical *p*-value = 5%). The models were reduced by removing nonsignificant higher-degree terms to make them cubic, then quadratic, and, finally, first-order. Next, a desirability function using JMP Pro® 14.3.0 was applied to optimize factors for desirable responses.

II.3.4. Evaluation of Dependent Variables

Emulsification Time (Y_1)

Each SNEDDS formulation (1 g) was dispersed in 250 mL of deionized water under gentle stirring (100 rpm, 37-±0.5 °C) [14]. The emulsification time was recorded as time in seconds required to obtain a clear dispersion [26].

Droplet Size and PDI (Y_2 and Y_3)

The droplet size and PDI were determined by dynamic light scattering (DLS) at 37 °C using a Nano ZS system (Malvern Instruments, Malvern, UK) with a water dispersant refractive index of 1.330. One gramm of the formulations were dispersed in 250 mL [14] of filtered deionized water and allowed to stand for 1h prior the analysis. The zeta potentials were determined via electrophoretic mobility using the same instrument. All measurements were done in triplicate using disposable polystyrene cuvettes (Malvern Instruments, UK).

Transmittance Percentage (Y_4)

One gram of the formulations were emulsified in 250 mL of deionized water and allowed to stand for 1h The transmittance percentage of resulting dispersions were mesuered at 550 nm [27,28] using a UV visible spectrophotometer (Thermo Fisher Scientific Inc.) with deionized water as a control.

II.3.5. Transmission Electron Microscopy (TEM)

The morphology of the optimized nanoemulsion droplet was examined using a transmission electron microscope (Tecnai 10 microscope, FEI, Hillsboro, OR, USA) with a 100 kV accelerating voltage. A 0.5-mL droplet of the reconstituted SNEDDS formulation was positioned on carbon-coated 300 mesh grids, followed by negative staining with a 0.2% aqueous solution of uranyl acetate.

II.4. IN VITRO CHARACTERIZATION OF VOX-LOADED SNEDDS

II.4.1. In Vitro Dissolution Studies

Dissolution studies were carried out using a USP Dissolution Tester (Apparatus II, Model Sotax AT7, CH-4008, Basel, Switzerland) with 500 mL hydrochloric acid USP buffer (pH 1.2), phosphate buffer (pH 6.8) [29], and biorelevant medium (FeSSGF and FeSSIF). The speed of the paddle and the temperature were adjusted to 100 rpm and 37 ± 0.5 °C, respectively. The FeSSGF (fed state simulated gastric fluid) and FeSSIF (fed state simulated intestinal fluid) were prepared as per the method reported by Jantratid and Dressman [30]. Hard gelatine capsules (size "0") were filled with 50 mg of pure Vox or 600 mg of Vox-loaded SNEDDS (equivalent to 50 mg of Vox), and placed in the dissolution tester. At predetermined time intervals, an aliquot (2 mL) was withdrawn and replenished with an equivalent volume of fresh and preheated (37 °C) medium. The withdrawn samples were centrifuged (4000 × *g*) for 10 min and filtered through 0.22-µm hydrophilic Rotilabo® syringe filters (Carl Roth, Karlsruhe, Germany). Appropriate dilutions in acetonitrile were performed prior to quantitative HPLC–UV analysis.

II.4.2. In Vitro Lipolysis

In vitro lipolysis study was performed as described previously [31], with minor modifications. The equipment consisted of a compact stirrer (Mettler Toledo, Greifensee, Switzerland), an IKA C-

MAG HS7 thermostat-jacketed glass reaction vessel (Staufen, Germany), a T5 Mettler Toledo pH-stat titration unit (Greifensee, Switzerland) containing a combined pH Ag/AgCl electrode (DGI 115-SC) and a 30-mL DV 1020 Mettler Toledo autoburette (Greifensee, Switzerland).

One gram of Vox-SNEDDS formulation was dispersed in 40 mL of lipolysis buffer (containing 1.4 mM CaCl2.2H2O, 0.75 mM TLC, 2 mM Tris-maleate, 3 mM NaTDC and 150 mM NaCl) for 20 min. Afterward, the pH was automatically set to 6.5, and in vitro lipolysis was started by adding 4 mL of pancreatin extract containing lipase (lipase activity equivalent to 8X USP specifications) and other pancreatic enzymes (ribonuclease, protease and amylase). The enzyme extract was prepared before each experiment by mixing 5 mL of lipolysis buffer with 1 g of pancreatic powder and 20 μL of NaOH solution (0.5 M) to reach the desired pH (6.5). The resulting enzyme dispersion was centrifuged (4000 x g) for 15 min.

The fatty acids released during in vitro lipolysis were automatically titrated with 0.05 M NaOH to maintain the pH at 6.5. Lipolysis medium (2 mL) was withdrawn in 5-min intervals up to 1h of the experiment, and 10 μL of 1.0 M 4-bromophenylboronic acid (in methanol) was added to inhibit the enzyme activity. This process was followed by ultracentrifugation (6700 x g, 4 °C MiniSpin, Eppendorf AG, Hamburg, Germany) for 20 min, resulting in the separation of the digestion content in a off-white pellet and clear supernatant. The supernatant was collected and Vox concentration was determined by HPLC-UV.

II.4.3. X-Ray Powder Diffraction (PXRD)

To elucidate the solid state of the precipitated Vox during in vitro lipolysis, the pellets retrieved at the end of the experiment were analysed by X-ray powder diffraction. An X-ray diffractometer (PXRD, Stoe Stadi P, Darmstadt, Germany), with CuKα as the radiation source (1.542 Å), was used. The radiation voltage and amperes were set to 40 kV and 40 mA, respectively. All PXRD profiles were obtained at room temperature in the angular range of 2θ = 5–60°, at a speed of 0.04° per second.

II.4.4. Stability of the Vox-SNEDDS Formulation

SNEDDS formulations were stored for 6 months at room temperature and evaluated for optical clarity, droplet size, zeta potential, emulsification time, and drug content.

II.5. IN VITRO CELL LINE STUDY

The in vitro experiments were performed with Caco-2 cells. The cells were cultured in medium containing Dulbecco's modified Eagle's minimal essential medium (DMEM) supplemented with 1% (*v/v*) L-glutamine, 10% (v/v) heat-inactivated foetal bovine serum (HyClone®, Thermo Fisher Scientific Inc.), penicillin/streptomycin solution (10 units/10 μg/mL) and 1% (*v/v*) nonessential amino acids. The cells incubation was done in a humidified atmosphere (37 °C) containing 10% CO2. The cells were subcultured weekly once they reach 80% confluence.

II.5.1. Cell Viability Assay

The cell viability against the optimized formulation was assessed as described by Memvanga et al. [32]. In brief, Caco-2 cells were seeded on 96-well culture plates (2 x 10^4 cells/well; 100 µL per well) and incubated in the culture media. After 24h, the cells were washed with phosphate-buffered saline (37 ° C) and treated with 100 µL of unloaded-SNEDDS or free Vox at various concentrations (from 0.3 to 4 mg/mL) diluted with Hank's salt balanced solution (HBSS). After 2h of incubation, the cell were washed and treated with 100 µL of MTT solution (0.5 mg/mL in DMEM) and were incubated for 3h (37 °C). To solubilize the formazan crystals formed during the incubation, 200 µL DMSO was added and the product of reaction was measured at 545 nm using a Multiskan Spectrum microplate reader (Thermo Fisher Scientific Inc.). The cell viability of the control cells (treated with HBSS) was defined as 100%. The cell viability rates of the samples were calculated according to the following equation:

$$\text{Cell viability (\%)} = A_s/A_c \times 100 \qquad (1)$$

where A_s is the sample absorbance, and A_c is the absorbance measured after treating the cells with HBSS.

II.5.2. Cell Culture for Transport Studies

The in vitro transport experiments were carried out as described by Memvanga et al. [32]. Caco-2 cells (5 x 10^5 cells/well) were seeded on 12-well cell culture inserts with a 0.9 cm^2 surface area (Corning Costar®, NY, USA) and 1 -µm pore diameter. Culture medium was replaced every two days and was added to the apical (0.5 mL) and basolateral (1.2 mL). The cells were incubated for 21 days to allow the differeciation until the measured transepithelial electrical resistance (TEER) increased to 400 ohm/cm^2. The TEER was measured using a voltmeter with a chopstick electrode (World Precision Instrument, Sarasota, USA). Thirty minutes before the experiments, the cells were incubated with HBSS (37 °C), and the TEER values of the monolayers were mesured in triplicate. Apical to basolateral (AB) transport experiments across Caco-2 cell monolayers were conducted by adding 0.5 mL of Vox suspension (0.9 mg/mL Vox in HBSS) or 0.5 mL of dispersed Vox-SNEDDS in HBSS (0.9 mg/mL Vox-SNEDDS, i.e., 75 µg/mL Vox) on the apical side of the inserts, and 1.2 mL HBSS on the basolateral side. For the basolateral to apical transport experiments (BA), 1.2 mL of Vox suspension (0.9 mg/mL Vox in HBSS), or 1.2 mL of dispersed Vox-SNEDDS in HBSS (0.9 mg/mL Vox-SNEDDS, i.e., 75 µg/mL Vox), was added to the basolateral side, while the apical side was filled with 0.5 mL HBSS. After 2h, TEER values of monolayers were determined in triplicate, and Vox content in acceptor compartments (basolateral for AB or apical for BA) was determined after appropriate dilutions by HPLC–UV. The apparent permeability coefficient (Papp) was determined using the following equation:

$$P_{app} = \frac{dQ}{dt} \times \frac{1}{CoA} \qquad (2)$$

where dQ/dt (transport rate) is the amount of Vox (µg) appearing per time unit (s) in the receiver compartment, C_o is the initial concentration in the donor compartment (µg/mL), and A is the surface area of the insert (A = 0.9 cm^2).

II.6. PHARMACOKINETIC STUDY

Male Sprague Dawley Fisher rats with a mean body weight of 300 g were obtained from Janvier Labs (Saint Berthevin, France). All rats were housed in a light-controlled room at a temperature of 20 ± 5 °C and a relative humidity of 25 ± 5%. All animal experiments were approved (March 2020) by, and performed in accordance with, the local animal committee (2020/UCL/MD/06).

Before the experiments, the rats were divided into three groups (n = 6) and fasted for 12h with free access to water. Group 1 animals were orally administered 1 mL of pure Vox suspension (in 0.5% sodium carboxyl methylcellulose) at a drug dose of 7.2 mg/kg, and group 2 animals were orally administered a Vox-loaded SNEDDS at a dose of 7.2 mg/kg. For intravenous administration, group 3 animals were administered 0.5 mL of Vox solution (in normal saline buffer containing 10% (w/v) Tween® 80) via the tail vein at a dose of 1.6 mg/kg [3]. Blood samples (0.25 mL) were withdrawn from the tail vein using heparinized capillaries at 0.5, 1, 2, 6, 10, 24, 36, 48, and 72h. The blood samples were centrifuged at 4000 × g (10 min) to separate the plasma. The samples were stored at −80 °C until analysis by LC–MS. A noncompartmental pharmacokinetic analysis was used to determine the pharmacokinetic behaviour of voxelotor. The pharmacokinetic parameters were computed using the PK solver programme (Microsoft Excel) with the trapezoidal rule. Statistical analysis of in vivo pharmacokinetic data was conducted using a two-tailed unpaired Student's t-test, with p values < 0.05 considered significant.

The absolute bioavailability (F) were calculated as follows:

$$F\ (\%) = \frac{\text{AUC o/dose o}}{\text{AUC i/dose i}} \times 100 \qquad (3)$$

where AUC o and AUC i are the areas under the curve of the oral groups (o) (SNEDDS and suspension) and the intravenous group (i), respectively.

III. RESULTS AND DISCUSSION

III.1. EXCIPIENT SCREENING

SNEDDS formulations are prepared to enhance the aqueous solubility and oral bioavailability of drugs. Excipient screening guides the right selection of components. The choice of the excipients was based on the literature. The screening of oils, surfactants, and cosurfactants was performed, based on emulsification and solubility studies. As presented in Figure 1, among the oils tested, Vox showed the highest solubility in Capryol PGMC® (16.6 ± 5.2 mg/mL). Therefore, Capryol PGMC® was selected as the oily phase for further studies. The solubility of Vox in various surfactants is presented in Figure 1. Only hydrophilic surfactants (HLB > 12) were tested, as they favour the occurrence of oil-in-water emulsions [33,34]. Labrasol AFL® yielded the highest solubility (37.4 ± 2.8 mg/mL), followed by Cremophor-EL® (27.2 ± 0.7 mg/mL). However, the selection of surfactants was primarily based on their emulsification efficiency, rather than their ability to solubilize the drug [34]. Good solubility of the drug in the surfactant was considered an additional advantage regarding avoiding drug precipitation [35].

The transmittance percentage values of various oil-surfactant dispersions were measured (Table 1), and clearly distinguished the ability of Labrasol ALF® and Cremophor-EL® to emulsify Capryol PGMC®. Cremophor-EL® exhibited a higher emulsification efficiency (99.3%), whereas Labrasol ALF® showed a lower emulsification efficiency, as indicated by the lower transmittance percentage value (60.5%). Thus, Cremophor-EL® was selected as the surfactant for further investigation.

Cosolvents and cosurfactants are used to cooperate with the surfactant to reduce the interfacial tension, increase the drug solubilization, and enhance the dispersibility, which resulted in improved emulsification and a reduced particle size. Among all the cosurfactants and cosolvents tested, Labrafil M® 1944 CS was selected, owing to its higher drug solubilization value (Figure 1) and better emulsification efficiency (Supplementary Table S2)

Table 1. Ability of the selected surfactants to emulsify the oil Capryol PGMC®.

Surfactant	% Transmittance
Labrasol ALF®	60.5 ± 0.86 *
Tween® 80	95.1 ± 0.79
Cremophor-EL®	99.3 ± 0.69

* $p < 0.05$ compared to Cremophor –EL® and Tween® 80

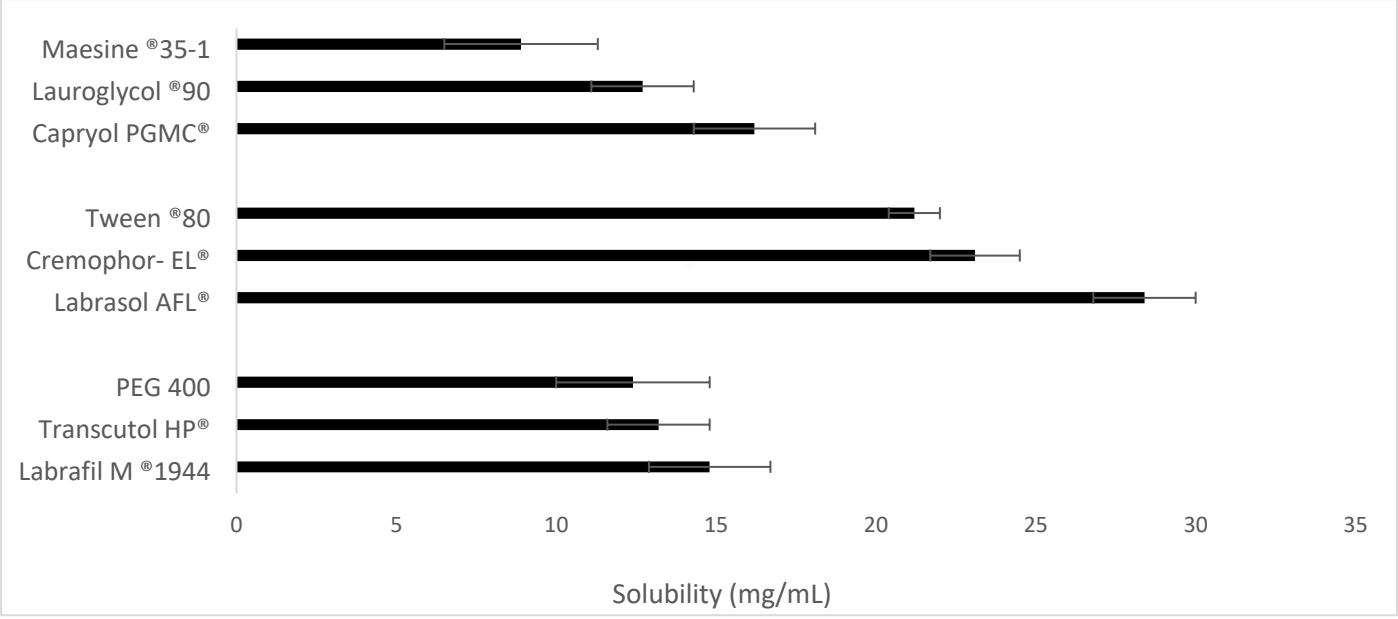

Figure 1. Solubility of Vox (mg/mL) in various oils, surfactants, and cosurfactants at 37 °C. Data are expressed as the mean ± SD, $n = 3$.

III.2. TERNARY PHASE DIAGRAM

Based on the emulsification and solubility studies, a ternary phase diagram was constructed in the absence of the drug to identify the self-nanoemulsifying region, as illustrated in Figure 2. The shaded area indicates the nanoemulsification region with a low droplet size (<200 nm). This study indicated that 20–60% (*w*/*w*) Capryol PGMC® (oil), 30–70% (*w*/*w*) Cremophor-EL® (surfactant), and 10–30% (*w*/*w*) Labrafil M® 1944 CS (cosurfactant) ternary mixture (total 100%) showed a clear area that could be used to optimize the SNEDDS formulations using the D-optimal mixture design approach.

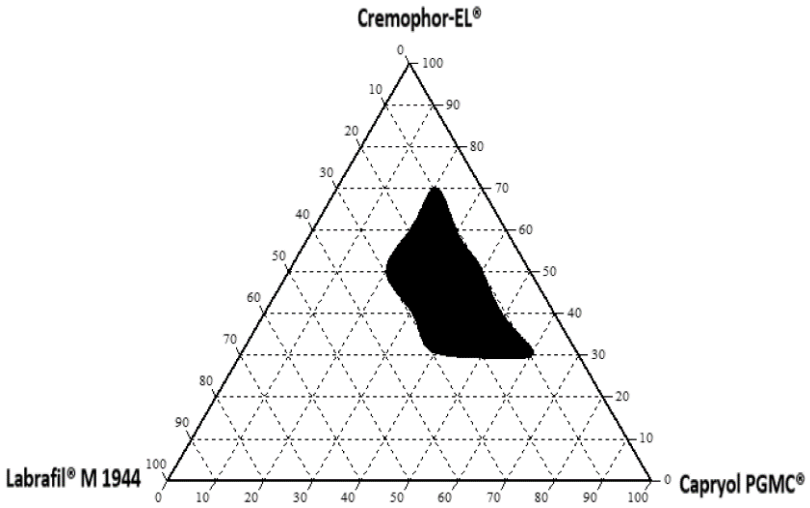

Figure 2. Phase diagram of oil (Capryol PGMC®), surfactant (Cremophor-EL®), and cosurfactant (Labrafil M® 1944 CS).

III.3. STATISTICAL ANALYSIS AND OPTIMIZATION OF SNEDDS FORMULATIONS

According to the results obtained from the ternary phase diagram, ranges of factors were fixed as follows: 20% ≤ Capryol PGMC® (X_1) ≤ 60%, 30% ≤ Cremophor-EL® (X_2) ≤ 70%, and 10% ≤ Labrafil M® 1944 CS (X_3) ≤ 30%. The response variables were taken as the emulsification time (Y_1, s), droplet size (Y_2, nm), PDI (Y_3), and transmittance percentage (Y_4, %), due to their impact on the SNEDDSs performance [16]. The 16 runs of the design and the measurements of the four responses are presented in Table 2. The statistical validity evaluation of the generated models (Table 3) confirmed that the mathematical models used for all the response variables were satisfactory and adequate (model p value > F < 0.05). Furthermore, model R-square and adjusted R-square values for each response variable indicated an excellent fit to the data.

Table 2. D-optimal mixture design and response data for the optimization of SNEDDSs.

	Oil(mg)	Surfactant(mg)	Cosurfactant(mg)	Y_1(s)	Y_2(nm)	Y_3	Y_4(%)
1	295	605	100	82	47	0.57	98
2	200	560	240	57	27	0.16	100
3	400	300	300	13	60	0.15	88
4	475	375	150	15	48	0.18	97
5	600	300	100	10	83	0.24	80
6	200	700	100	113	45	0.78	97
7	460	300	240	12	65	0.19	83
8	310	545	145	47	30	0.26	97
9	520	300	180	9.6	69	0.22	86
10	280	420	300	65	39	0.04	97
11	480	420	100	46	35	0.08	99
12	200	640	160	11	32	0.40	99
13	400	300	300	11	60	0.17	92
14	200	500	300	94	28	0.05	100
15	330	430	240	54	32	0.03	99
16	600	300	100	10	86	0.24	82

Y_1: emulsification time, Y_2: droplet size, Y_3: PDI, Y_4: transmittance percentage.

Table 3. Model fitting and statistical analysis.

Reponses	Model	R-Square	Adjusted R-Square	Root Mean Square Error	Prob ≥ F
Y_1	Quadratic	0.94	0.91	11.76	0.0036 *
Y_2	Cubic	0.98	0.96	3.61	0.0001 *
Y_3	Quadratic	0.90	0.86	0.07	0.0001 *
Y_4	Cubic	0.98	0.96	1.67	0.0018 *

* Significant.

III.3.1. Self-Emulsification Time (Y_1)

The self-emulsification ability of the SNEDDSs could effectively be estimated by determining the emulsification time. The correlation between the self-emulsification time and independent variables is presented in Table 4, Figure 3A, and Equation (4).

$$\mathbf{(Y_1, s)} = 11.9\ X_1 + 114.2\ X_2 + 144.9\ X_3 - 26.4\ X_1X_2 - 230.6\ X_1X_3 - 189.7\ X_2X_3\ \mathbf{r^2 = 0.945;\ model = quadratic} \quad (4)$$

Table 4. Summary of ANOVA for the response parameters.

	Term	Estimate	Std Error	DFDen	t Ratio	Prob>|t|
Y_1	$(X_1 - 0.2)/0.4$	11.92	8.82	9.97	1.35	0.2065
	$(X_2 - 0.3)/0.4$	114.21	11.15	9.94	10.24	<0.0001 *
	$(X_3 - 0.1)/0.4$	144.91	65.70	7.93	2.21	0.0588
	$X_1 \times X_2$	−26.47	45.32	7.80	−0.58	0.5756
	$X_1 \times X_3$	−230.62	123.98	7.79	−1.86	0.1009
	$X_2 \times X_3$	−189.73	120.93	7.46	−1.57	0.1580
Y_2	$(X_1 - 0.2)/0.4$	84.62	2.87	5.21	29.44	<0.0001 *
	$(X_2 - 0.3)/0.4$	46.44	4.00	4.86	11.61	<0.0001 *
	$(X_3 - 0.1)/0.4$	71.56	122.66	3.80	0.58	0.5924
	$X_1 \times X_2$	−125.69	19.64	4.75	−6.40	0.0017*
	$X_1 \times X_3$	−70.85	243.75	3.81	−0.29	0.7864
	$X_2 \times X_3$	−117.35	241.13	3.79	−0.49	0.6533
	$X_1 \times X_2 \times X_3$	23.12	336.43	3.83	0.07	0.9486
	$X_1 \times X_2 \times (X_1 - X_2)$	−114.32	29.26	3.97	−3.91	0.0177 *
	$X_1 \times X_3 \times (X_1 - X_3)$	6.80	164.64	3.90	0.04	0.9691
	$X_2 \times X_3 \times (X_2 - X_3)$	−46.16	160.42	3.88	−0.29	0.7882
Y_3	$(X_1 - 0.2)/0.4$	0.13	0.05	9.75	2.65	0.0248 *
	$(X_2 - 0.3)/0.4$	0.79	0.067	9.94	11.75	<0.0001 *
	$(X_3 - 0.1)/0.4$	0.08	0.42	8.38	0.20	0.8464
	$X_1 \times X_2$	−0.84	0.30	8.60	−2.81	0.0213*
	$X_1 \times X_3$	0.27	0.79	8.16	0.34	0.7407
	$X_2 \times X_3$	−1.73	0.77	7.36	−2.24	0.0586
Y_4	$(X_1 - 0.2)/0.4$	80.87	1.46	5.67	55.33	<0.0001 *
	$(X_2 - 0.3)/0.4$	97.96	1.92	4.72	50.81	<0.0001 *
	$(X_3 - 0.1)/0.4$	151.52	55.02	3.02	2.75	0.0698
	$X_1 \times X_2$	43.26	8.59	3.25	5.03	0.0124*
	$X_1 \times X_3$	−107.66	109.18	3.02	−0.99	0.3963
	$X_2 \times X_3$	−102.28	108.09	3.01	−0.95	0.4135
	$X_1 \times X_2 \times X_3$	161.85	149.42	3.01	1.08	0.3576
	$X_1 \times X_2 \times (X_1 - X_2)$	49.32	13.02	3.06	3.79	0.0311 *
	$X_1 \times X_3 \times (X_1 - X_3)$	74.99	73.50	3.04	1.02	0.3817
	$X_2 \times X_3 \times (X_2 - X_3)$	77.48	71.94	3.04	1.08	0.3592

* Significant.

A significant positive effect ($p < 0.05$) was observed for the surfactant concentration (X_2) on the time of emulsification. When the surfactant concentration increases, the emulsification time was found to increase. This phenomenon could be related to the high intrinsic viscosity of Cremophor-EL® (600–750 mPas), reducing water penetration into the complex colloidal structure formed on the surface of the droplets [36]. In addition, as reported by Croy et al. [37], Cremophor-EL® has a lower core polarity than other nonionic surfactants, which delays the penetration of water through the droplets during the emulsification process.

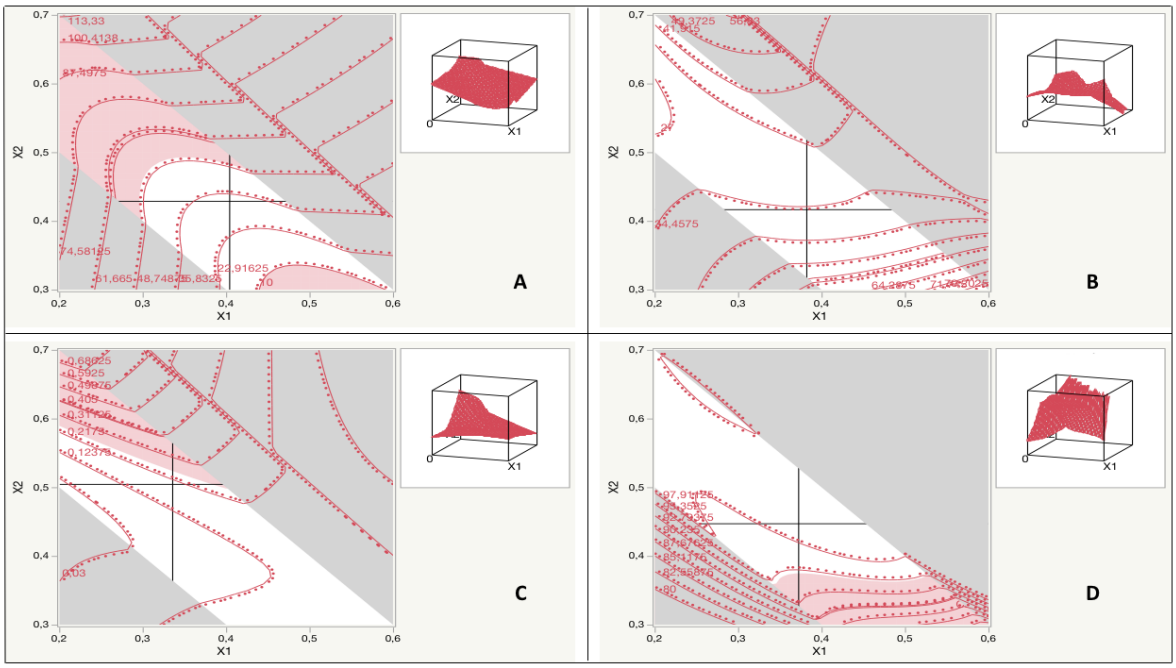

Figure 3. Contour profiler correlating independent variables with the (**A**) self-emulsification time (Y_1), (**B**) droplet size (Y_2), (**C**) PDI (Y_3), and (**D**) transmittance percentage (Y_4).

III.3.2. Droplet Size (Y_2) and PDI (Y_3)

The size of the globule and its distribution are crucial in self-emulsification, as they determine the rate and extent of drug release [16]. The correlation between globule size, or PDI, and the independent variables is shown in Table 4, Figure 3B,C, and Equation (5) and (6).

$$\mathbf{(Y_2, nm)} = 84.6\ X_1 + 46.4\ X_2 + 71.5\ X_3 - 125.6\ X_1X_2 - 70.8\ X_1X_3 - 117.3\ X_2X_3 + 23.1\ X_1X_2X_3 - 114.3\ X_1X_2(X_1 - X_2) + 6.8\ X_1X_3(X_1 - X_3) - 46.1\ X_2X_3(X_2 - X_3)\ \mathbf{r^2 = 0.985;\ model = cubic} \quad (5)$$

$$\mathbf{(Y_3)} = 0.1\ X_1 + 0.7\ X_2 + 0.0\ X_3 - 0.8\ X_1X_2 + 0.2\ X_1X_3 - 1.7\ X_2X_3\ \mathbf{r^2 = 0.905;\ model = quadratic} \quad (6)$$

The results demonstrate that the droplet size, and its distribution, were significantly ($p < 0.05$) influenced by the oil and surfactant concentrations. Increasing the Capryol PGMC® concentration up to, or above, 50% (*w*/*w*) induced a linear increase in the droplet size and PDI. This phenomenon could be attributed to an increase in hydrophobicity, owing to the lower amount of surfactant [38]. Conversely, there was a linear decrease in the globule size and PDI, with an increase in surfactant

concentration from 30 to 60% (*w*/*w*); a phenomenon that could be attributed to the surface-tension-lowering property of the surfactant at the oil-water interface, which reduces the energy that is free for emulsification [39]. However, above a surfactant concentration of 60% (*w*/*w*), there was a remarkable increase in droplet size and PDI, which could be explained by one or both of the following reasons: (1) excess water penetration into the oil droplets, causing massive interfacial disruption and the ejection of highly polydispersed droplets; (2) a possible condensation phenomenon and the multilayer formation of additional surfactant into the droplets. In accordance with previous studies [28,40], increasing the amount of hydrophilic components above 60% (*w*/*w*) promoted an increase in the droplet size and PDI of the nanoemulsion formed upon the SNEDDSs' dispersion in an aqueous environment. Furthermore, a negative effect of the interaction between the oil and surfactant concentrations on droplet size and PDI was observed. Simultaneously increasing the oil and surfactant concentrations significantly reduced the nanoemulsion droplet size and PDI. In agreement with previous studies [17], medium chain monoglycerides, such as Capryol PGMC®, were likely to increase the interfacial fluidity of the surfactant boundaries in the micelles. The entrapment of Capryol PGMC® in a high HLB surfactant (i.e., Cremophor-EL®) enhanced the emulsification process upon water dispersion, resulting in the narrow size distribution of the oil droplet. Accordingly, the oil and surfactant combination has a considerable impact on the droplet size, PDI, and the self-emulsification of the SNEDDSs upon dispersion in aqueous environments [34].

III.3.3. Transmittance Percentage

The transmittance percentage is a useful tool to meet the optical clarity of the diluted SNEDDSs with water. The correlation between the transmittance percentage and independent variables is presented in Table 4, Figure 3D, and Equation (7).

$$\mathbf{(Y_4, \%)} = 80.8\ X_1 + 97.9\ X_2 + 151.5\ X_3 + 43.2\ X_1X_2 - 107.6\ X_1X_3 - 102.2\ X_2X_3 + 161.8\ X_1X_2X_3 + 49.3\ X_1X_2(X_1 - X_2) + 74.9\ X_1X_3(X_1 - X_3) + 77.4\ X_2X_3(X_2 - X_3)\ \mathbf{r^2 = 0.985;\ model = cubic} \quad (7)$$

Initially, the transmittance percentage increased with an increasing oil amount (up to 40% *w*/*w*). However, the transmittance percentage decreased with a further increase in the oil concentration. This phenomenon might be attributed to an increase in globule size, owing to the decrease in the surfactant concentration, resulting in the coalescence of the oil globule [41]. Conversely, the increase in the surfactant content exhibited a significant positive effect on the transmittance percentage, which could be explained by the observation that more surfactant could sufficiently reduce the interfacial tension, stabilize the oil-water interface, and minimize the droplet size [35]. As for the droplet size, a significant ($p < 0.05$) positive interaction (an increase in the transmittance percentage) was observed between the oil and surfactant concentrations. Based on this result, it could be concluded that the transmittance percentage correlated with the droplet size, although in the opposite direction ($Y = 290 - 2.75X$, $r^2 = 0.896$, $p < 0.05$). As reported previously [42,43], the measurement of the transmittance percentage is a key parameter in a SNEDDSs' characterization and can serve as an alternative indicator of droplet size.

III.3.4. Optimization by Desirability Function

Emulsification time, droplet size, PDI, and transmittance percentage are each commonly studied response variables for a SNEDDSs' optimization [7,10,28]. A short emulsification (<50 s) contributes to the rapid release of the drug and a rapid onset of action [44]. A small particle size with a narrow distribution has a positive effect on the oral bioavailability of a drug encapsulated in a SNEDDS [45]. In addition, the generation of a smaller dispersion, after aqueous dilution or lipolysis, is generally necessary because it is known that the dose variability of these formulations can be minimized after oral ingestion [46,47]. The transmittance percentage is a useful tool for evaluating the isotropic properties of the resulting nanoemulsions. A high transmittance value (≥95 %) indicates clarity of the dispersion [10]. Thus, the targeted ranges of the responses were fixed as follows: Y_1 (≤50 s), Y_2 (≤100 nm), Y_3 (≤0.25 PDI), and Y_4 (≥95%) [16,27,48]. Under these conditions, the desirability function combines the four responses to determine an overall optimum region. Figure 4 shows the profiler desirability with the optimum region (in white). To maximize the drug loading capacity, only the SNEDDS formulations with a high oil content (>35%) were chosen for verification. The results suggest that a SNEDDS formulation comprised of Capryol PGMC® (40% *w/w*), Cremophor-EL® (43% *w/w*), and Labrafil M® 1944 CS (17% *w/w*) fulfilled the requirements for an optimum formulation, and was chosen for verification. To validate the predictability of the generated mathematical models, the optimum formulation (F1) was prepared according to the above values of factors and subjected to the response measurements (i.e., emulsification time (s), globule size (nm), PDI, transmittance percentage (%), and zeta potential (mV)). As presented in Table 5, values obtained from checking F1 were not significantly different (bias less than 5%) from the predicted values. Thus, the validity of the generated model was established. F1 was considered an optimum formulation and was used for further in vitro and in vivo evaluation.

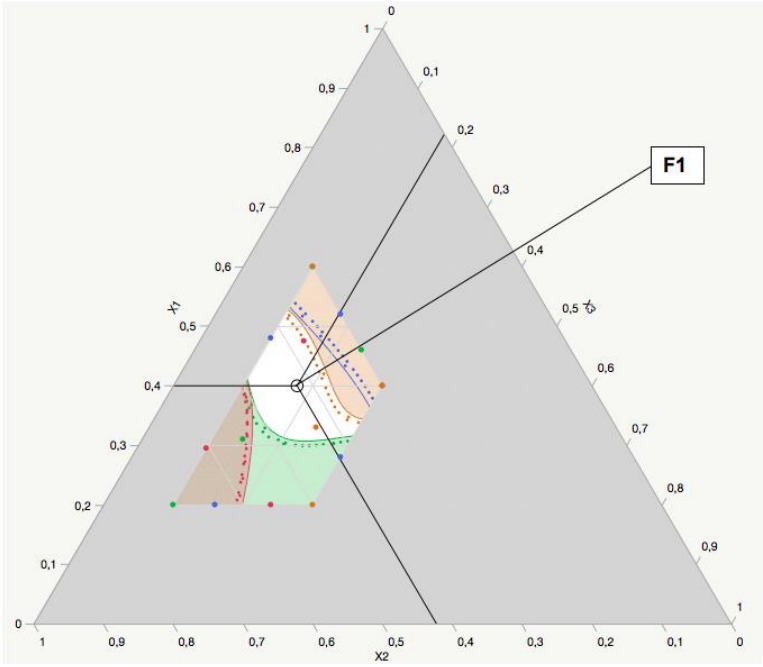

Figure 4. Mixture profiler of the isotropic blend prepared as per the D-optimal design. Prediction formula for the following: green, emulsification time (Y_1); blue, droplet size (Y_2); red, PDI (Y_3), brown, transmittance percentage (Y_4); white, optimum area.

Table 5. The predicted values and experimental results of F1 prepared under optimum conditions.

Response	Predicted Value	Experimental Value	Bias (%)
Y_1, emulsification time (s)	33.1	32.4 ± 0.4	2.1
Y_2, droplet size (nm)	33.8	34.9 ± 1.2	−3.2
Y_3, PDI	0.210	0.20 ± 0.0	2.9
Y_4, transmittance (%)	99.4	99.2 ± 0.6	0.2
Zeta potential (mV)	--	−8.4 ± 1.3	--

Bias (%) = (predicted value − observed value)/observed value × 100. −−: not determined.

III.4. TRANSMISSION ELECTRON MICROSCOPY

The morphology of the reconstituted F1 (as shown in Figure 5) was observed using TEM. The nanoemulsion droplets had spherical shapes and narrow size distributions.

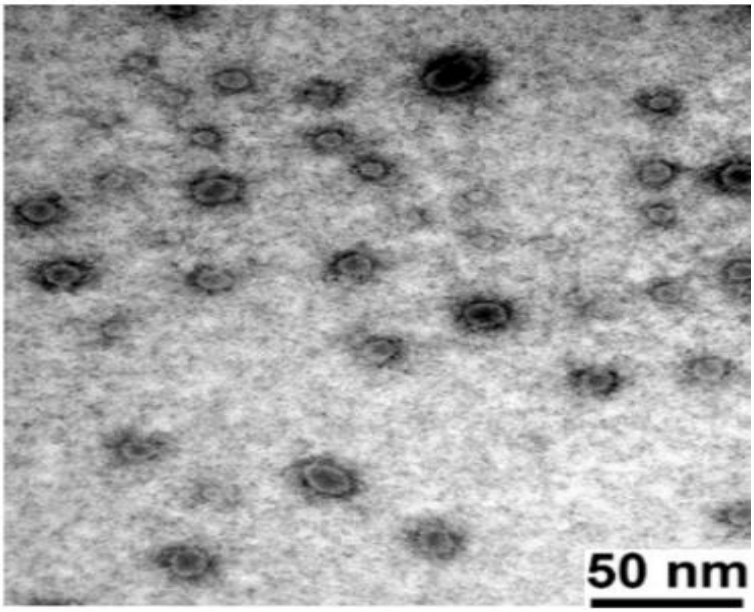

Figure 5. Transmission electron microphotography (TEM) of the reconstituted F1 formulation.

III.5. IN VITRO DISSOLUTION STUDIES

The in vitro dissolution of Vox in F1 was evaluated and compared to that of the pure drug in different dissolution media (pH 1.2 HCl, pH 6.8 phosphate buffer, FeSSGF and FeSSIF) (Figure 6). Compared to F1 (87%, 86.6 μg/mL), the pure drug showed relatively low dissolution in pH 1.2 HCl and pH 6.8 buffer, with approximately 28% (27.6 μg/mL) and 29% (28.8 μg/mL) of the dose being dissolved, respectively. The higher drug dissolution from the formulation could be attributed to the reduction in particle size and the increase in surface area and drug solubility [49]. The dissolution of Vox was enhanced in the simulated intestinal media (FeSSIF). Approximately 38% (37.7 μg/mL) and 93% (92. 6 μg/mL) of Vox were released from the pure drug and F1, respectively. Consistent with the previous study [50], micelles contained in the simulated intestinal media may increase drug solubility and dissolution.

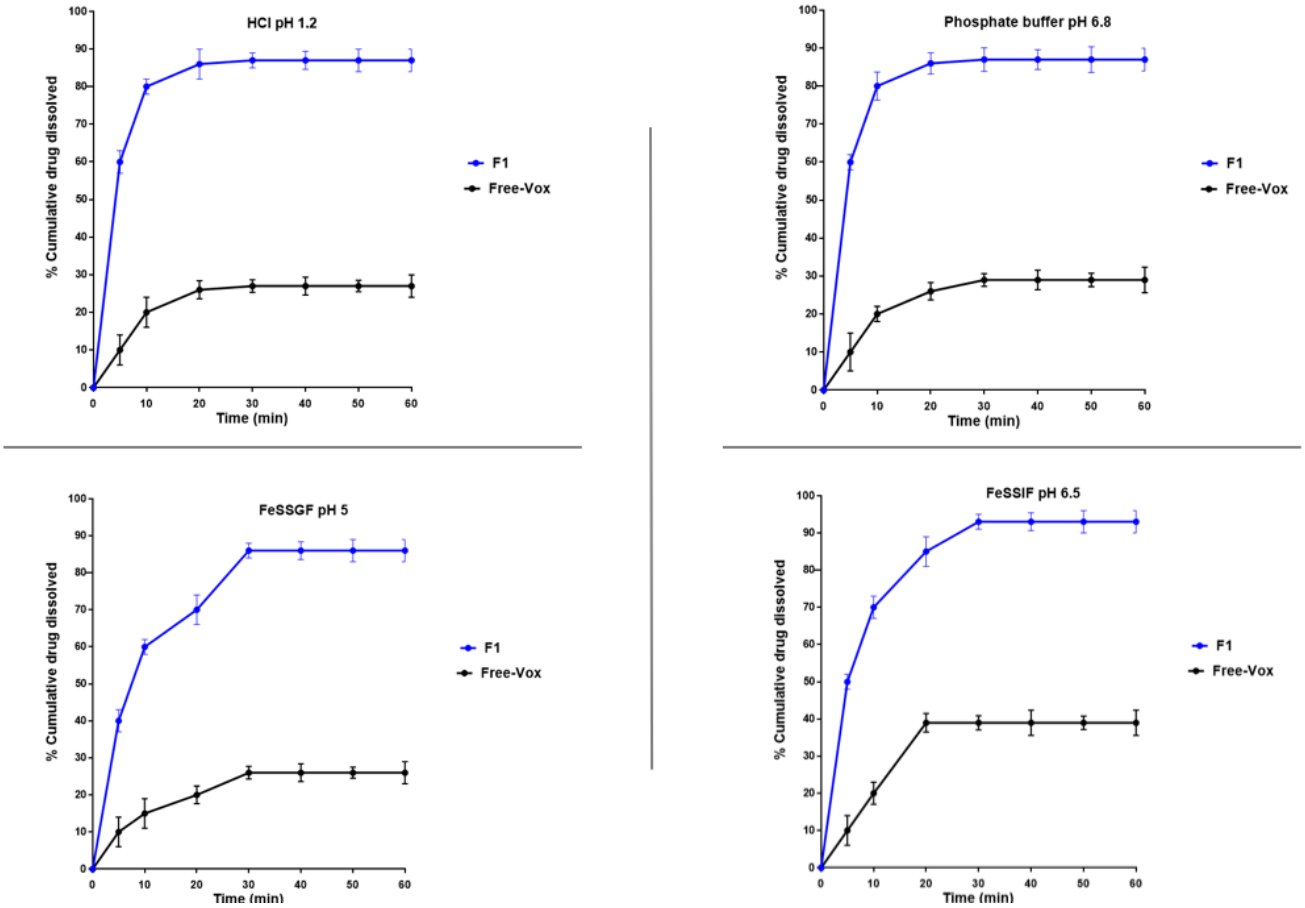

Figure 6. Dissolution profile of F1 and pure drug in various dissolution media using a paddle apparatus at 37± 0.5 °C. Data are expressed as the mean ± SD, *n* = 3. FeSSGF—fed state simulated gastric fluid; FeSSIF—fed state simulated intestinal fluid.

III.6. IN VITRO LIPOLYSIS AND X-RAY POWDER DIFFRACTION OF THE PRECIPITATES

When administered orally, SNEDDSs are prone to digestion by pancreatic lipase. The SNEDDS's digestion in the GI tract is crucial for drug dissolution and absorption. It can be beneficial (drug solubilization) or deleterious (drug precipitation after the digestion of the oil phase). An in vitro lipolysis test was used to study the impact of GI digestion on the in vitro performance of the SNEDDSs. The test aims to reveal the ability of the SNEDDSs to maintain drug solubilization after digestion [28,51]. The consumption of NaOH during the experiment, reflecting the progress of lipolysis, is depicted in Figure 7A. The results from this study show that 88% of Vox remained in the aqueous phase after 60 min of the experiment (Figure 7B). In the aqueous phase, the drug was clearly dissolved in the mixed micelles formed by the fatty acids and monoglycerides generated during the hydrolysis of lipids [25]. To investigate the physical state of the precipitated drug after the lipolysis, a powder X-ray diffractometry of the pure drug and the resulting pellets was performed. The results in Figure 8 show that pure Vox presented peaks in the range from 5-30°, providing proof of the crystalline state of the drug. However, the pellet-F1 diffractograms showed no peaks related to crystalline Vox, suggesting that the precipitates might be in an amorphous form

(or a molecular dispersed state), which could lead to rapid in vivo redissolution of the drug [52–54].

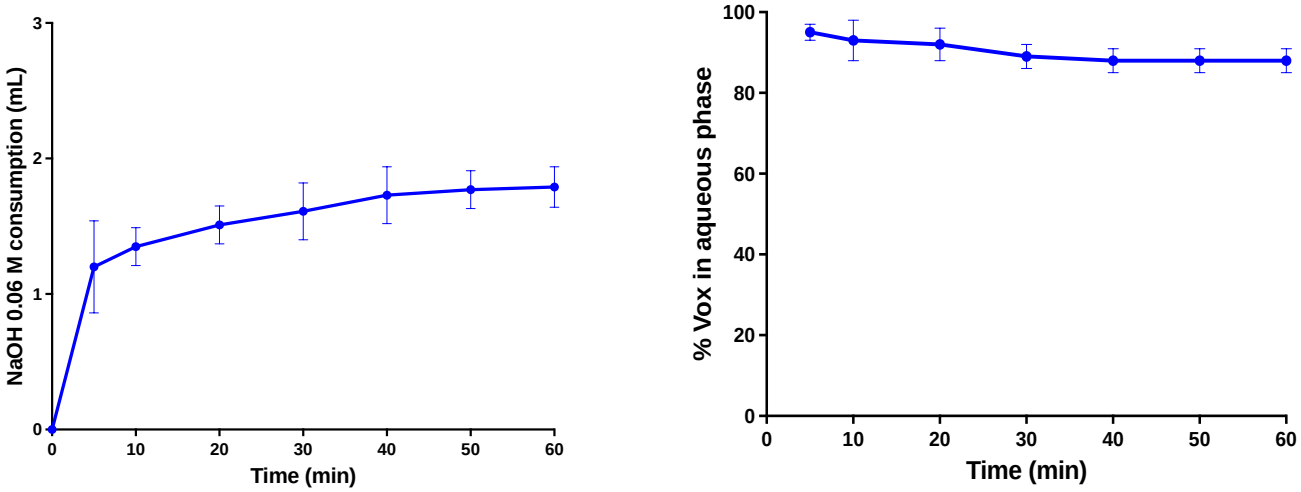

Figure 7. (**A**) NaOH consumption of SNEDDS during in vitro lipolysis. Data are expressed as the mean ± SD, n = 3. (**B**) VOX content in the aqueous phase during in vitro lipolysis. Data are expressed as the mean ± SD, n = 3.

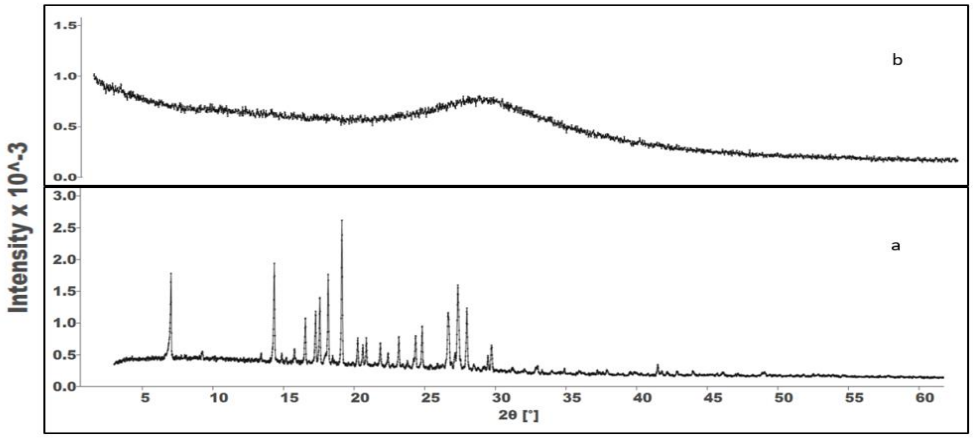

Figure 8. Powder X-ray diffractograms of pure Vox (a) and pellet-F1 (b).

III.7. STABILITY OF THE VOX-SNEDDSS FORMULATION

The SNEDDS showed no physical changes during the visual observation over six months. The droplet size, zeta potential, and emulsification time of the fresh SNEDDS vs. the stored SNEDDS were 32.4 ± 0.4 vs. 31.2 ± 0.7 (s ± SD, n = 3), -8.4 ± 1.3 vs. −8.2 ± 0.4 (mV ± SD, n = 3), and 34.9 ± 1.2 vs. 33.1 ± 2.4 (nm, SD, n = 3), respectively. The voxelotor content of the SNEDDS before the stability test was approximately 100%. At the end of the six months, the voxelotor content did not change significantly (>99%).

III.8. THE TRANSPORT OF VOX ACROSS CACO-2 CELL MONOLAYERS

To select the SNEDDS concentration to be used in the transport studies, the cytotoxicity of F1 was tested in Caco-2 cells. The Caco-2 cell viability was higher than 80% following the exposure to 0.9 mg/mL Vox suspension or unloaded F1 for up to 2h. A 0.9 mg/mL Vox suspension was used instead of 75 µg/mL to increase the chances of drug detection on the basolateral side. Based on these results, 2-h transport studies were conducted with 0.9 mg/mL free Vox dispersed in HBSS, or Vox-F1 (corresponding to 75 µg/mL Vox). The TEER values before and after the incubation period did not change ($p > 0.05$). The AB transport of Vox from the pure drug suspension and F1 is presented in Figure 9. The amounts of Vox transported from the drug suspension and F1 were 0.062 µg and 1.4 µg, respectively. The P_{app} values of Vox from F1 were 22-times ($p < 0.01$) higher than those of the free drug. This phenomenon could be explained by the observation that the Cremophor-EL® and Labrafil M® 1944 CS used in the F1 formulation could contribute to the enhancement of drug solubility and permeation across Caco-2 monolayers, by opening the tight junctions and increasing the membrane fluidity [55]. To investigate the potential existence of an active efflux during drug permeation, BA transport experiments were conducted. The P_{app} values of Vox from the BA transport are shown in Figure 9 and are compared to those of the AB transport. No significant difference was observed between the P_{app} values from the AB and BA transport of the free Vox or Vox-F1, indicating that Vox was not a substrate of P-gp. These observations are in line with studies reported by Metcalf et al. [56].

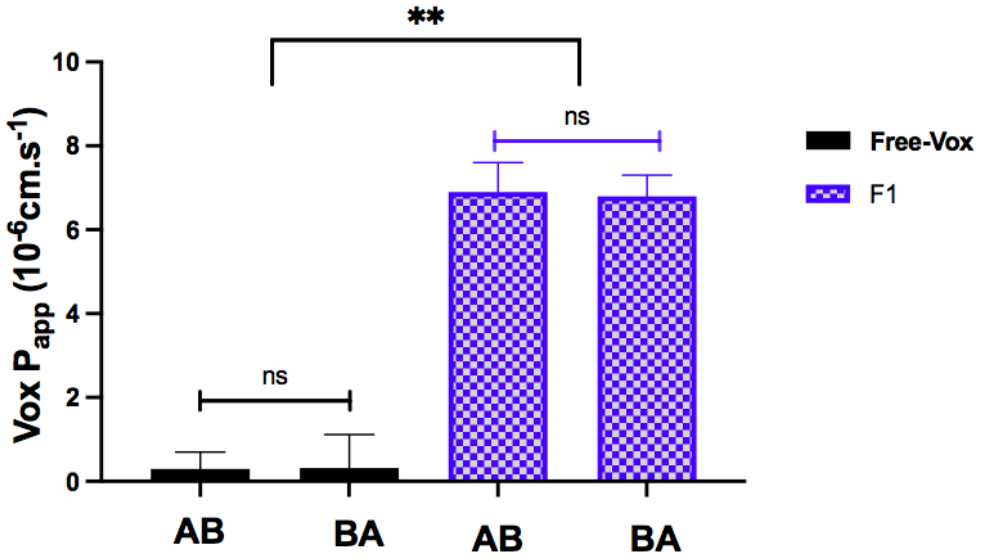

Figure 9. The apparent permeability (P_{app}) values of Vox across the Caco-2 cell monolayer-free drug and F1 after 2 h of the AB and BA transport studies. Each value is the mean of three separate determinations. ns $p > 0.01$, ** $p < 0.01$.

III.9. PHARMACOKINETICS STUDY

To assess whether the SNEDDS could enhance the oral bioavailability of Vox, the pharmacokinetic parameters of the Vox suspension, the SNEDDS, and the IV solution were evaluated in rats. The plasma concentration vs. the time profile of Vox after the administration of various formulations is shown in Figure 10, and their mean pharmacokinetic data are summarized in Table 6. The AUC of Vox in F1 increased 1.7-fold, compared to that of the drug suspension

(39469 ng·h/mL vs. 22530 ng·h/mL, $p < 0.01$). The T_{max} of the drug suspension and F-1 was found to be 2h and 0.5h, respectively. This result indicates a rapid absorption of Vox from the formulation. The C_{max} of the optimized formulation (1994 ng/mL) and the drug suspension (874 ng/mL) exhibited a nearly 2.3-fold enhancement ($p < 0.01$). Finally, the absolute oral bioavailability of Vox from the SNEDDS resulted in a 1.7-fold increase, compared to the drug in suspension. This increased bioavailability might be due to the improved drug solubility, the synergistic effect of the surfactant and oil as absorption enhancers, and the avoidance of the first pass metabolism via the lymphatic transport.

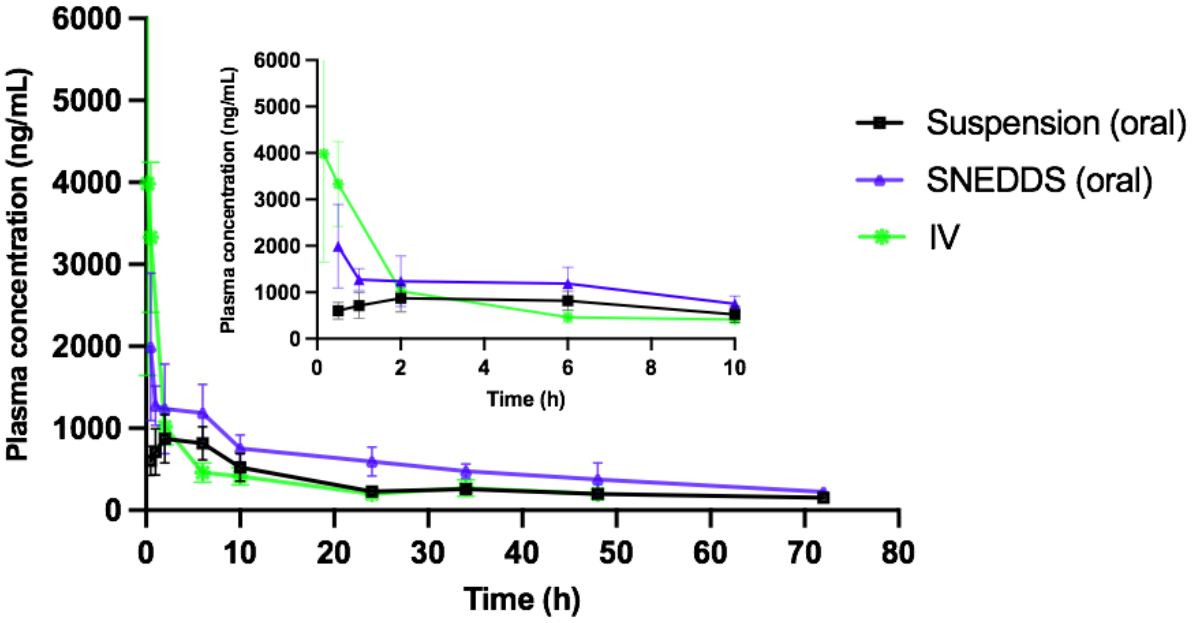

Figure 10. Plasma concentration time profiles of voxelotor after bolus intravenous injection (1.6 mg/kg) and oral administration of the suspension or SNEDDS (7.2 mg/kg) to rats. Data are expressed as the mean ± SD, $n = 6$.

Table 6. Pharmacokinetic parameters.

Parameters	Suspension	SNEDDS	IV
Dose (mg/kg)	7.2	7.2	1.6
$T_{1/2}$ (h)	50.5	32.6	24.6
T_{max} (h)	2	0.5	--
C_{max} (ng/mL)	873.8 ± 294.4	1993.9 ± 892.5 **	3984.5 ± 239.5
AUC_{0-72} (h.ng/mL)	22529.7 ± 146.1	39468.9 ± 580.2 **	19748.0 ± 420
F (%)	25.4	44.4	--

Each value is the mean ± SEM of six rats. ** $p < 0.01$ compared to Vox suspension.

IV. CONCLUSIONS

In this study, the Qbd approach was applied to develop Vox-SNEDDSs with improved aqueous solubility and oral bioavailability. Solubility and emulsification studies suggested the suitability of Capryol PGMC®, Cremophor-EL®, and Labrafil M® 1944 as oils, surfactants, and cosurfactants, respectively. Ternary diagram studies indicated the nanoemulsification region and range of factors that should be applied in the DoE. The D-optimal design suggested that the SNEDDSs' formulation comprised of Capryol PGMC® (40% *w/w*), Cremophor-EL® (43% *w/w*), and Labrafil M® 1944 CS (17% *w/w*). Thus, it fulfilled the maximum requirements of an optimum formulation and was chosen for further evaluation. The optimized formulation showed an emulsification time of 32.4 ± 0.4 s, globule size of 34.9 ± 1.2 nm, polydispersity index of 0.204 ± 0.0, zeta potential of −8.4 ± 1.3 mV, and transmittance percentage of 99.2 ± 0.6%. The spherical shape of the oil globules in the nanoemulsion was revealed using transmission electron microscopy. The optimized SNEDDS revealed a high drug dissolution, and at least 88% of the Vox remained solubilized after the in vitro lipolysis of the formulation. The in vitro transport study across Caco-2 cell monolayers revealed that the SNEDDSs could significantly enhance the permeation of Vox compared to the free drug. Thus, the developed SNEDDS resulted in a 1.7-fold higher oral bioavailability of Vox in rats, compared to the drug suspension. This new SNEDDS may be further developed as an alternative formulation of voxelotor.

Table S1. Validation results obtained for the quantification method of voxelotor

Validation criteria		Concentration levels (µg/mL) for voxelotor			
		2.5	10	25	75
Response function					
Trueness	Relative bias (%)	0.0018	-4.0894	1.5739	5.8087
Precision	Repeatability (RSD %)	0.5863	1.2562	0.6054	3.0666
	Intermediate precision (RSD %)	0.9519	2.7611	1.9830	2.5451
Accuracy (95% relative β-expectation lower and		-3.3838	-14.0593	-8.2013	-0.4523
Upper tolerance limits in %)		3.3875	5.8804	11.3492	12.0697
Uncertainty (µg/mL)		0.0265	0.3000	0.5769	2.0305
Expanded uncertainty (µg/mL)		0.053	0.0531	1.1538	4.0610
Relative expanded uncertainty (%)		2.1277	6.0093	4.6153	5.4147
Linearity	slope	1.0659			
	Intercept	-0.7684			
	R^2	0.9986			

Supplementary materials

Table S2. Emulsification study of surfactant/cosurfactant combinations.

Cosurfactant	% Transmittance
	Cremophor-EL®
Transcutol HP®	99.8 ± 0.85
Propylene glycol	99.4 ± 0.45
Polyethylene glycol 400	99.6 ± 1.62
Labrafil M® 1944 CS	98.3 ± 0.65
Labrafil M® 2125 CS	89.4 ± 0.15

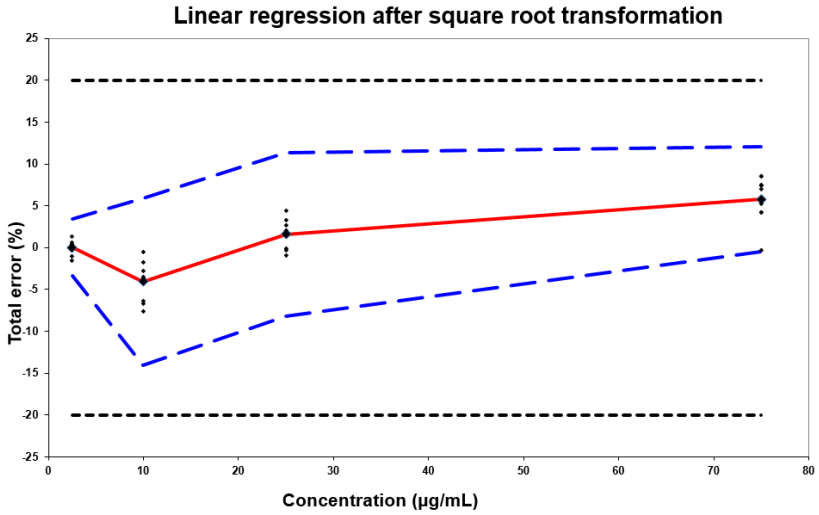

Figure S1. Accuracy profile of HPLC mathod obtained with four concentration levels of voxelotor. The plain line is the relative bias, dashed lines are the β-expectation tolerance limits (β=95%) and dotted lines represent the acceptance limits (±20%). The dots represent the relative back-calculated concentrations of the validation standards and are plotted according to their target concentration.

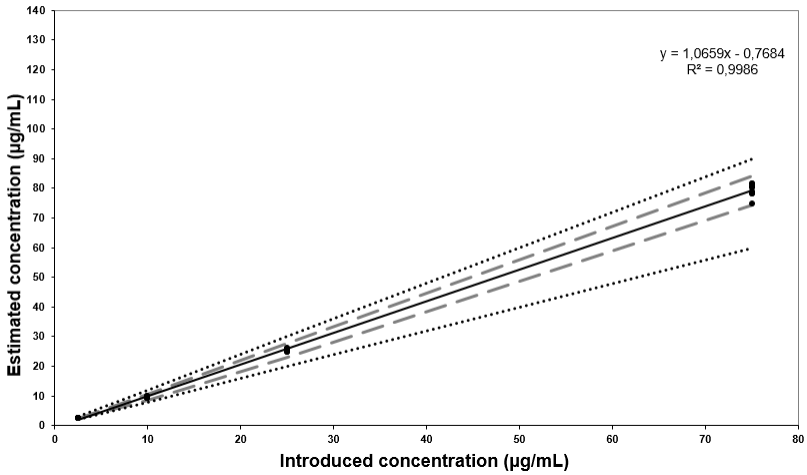

Figure S2. Linear profile of HPLC method obtained with four concentration levels of Voxelotor. The plain line is the identity line (y=x), the dashed line is the β-expectation tolerance limits (β=95%) and dotted lines represent the acceptance limits (±20%) [57].

REFERENCES

1. Gardner, R. V. Sickle Cell Disease: Advances in Treatment. *Ochsner J.* **2018**, *18*, 377–389, https://doi.org/10.31486/toj.18.0076.
2. Telen, M. J.; Malik, P.; Vercellotti, G. M. Therapeutic Strategies for Sickle Cell Disease: Towards a Multi-Agent Approach. *Nat. Rev. Drug Discov.* **2019**, *18*, 139–158, https://doi.org/10.1038/s41573-018-0003-2.
3. Oksenberg, D.; Dufu, K.; Patel, M. P.; Chuang, C.; Li, Z.; Xu, Q.; Silva-Garcia, A.; Zhou, C.; Hutchaleelaha, A.; Patskovska, L.; Patskovsky, Y.; Almo, S. C.; Sinha, U.; Metcalf, B. W.; Archer, D. R. GBT440 Increases Haemoglobin Oxygen Affinity, Reduces Sickling and Prolongs RBC Half-Life in a Murine Model of Sickle Cell Disease. *Br. J. Haematol.* **2016**, *175*, 141–153, https://doi.org/10.1111/bjh.14214.
4. Dufu, K.; Oksenberg, D. GBT440 Reverses Sickling of Sickled Red Blood Cells under Hypoxic Conditions in Vitro. *Hematol. Rep.* **2018**, *10*, 1–9,https://doi.org/10.4081/hr.2018.7419.
5. Hutchaleelaha, A.; Patel, M.; Washington, C.; Siu, V.; Allen, E.; Oksenberg, D.; Gretler, D. D.; Mant, T.; Lehrer-Graiwer, J. Pharmacokinetics and Pharmacodynamics of Voxelotor (GBT440) in Healthy Adults and Patients with Sickle Cell Disease. *Br. J. Clin. Pharmacol.* **2019**, *85*, 1290–1302, https://doi.org/10.1111/bcp.13896.
6. US Food and Drug Administration Home Page. Available online: https://www.accessdata.fda.gov/drugsatfda_docs/label/2019/213137s000lbl.pdf (accessed on 10 December 2020).
7. Qian, J.; Meng, H.; Xin, L.; Xia, M.; Shen, H.; Li, G.; Xie, Y. Self-Nanoemulsifying Drug Delivery Systems of Myricetin: Formulation Development, Characterization, and in Vitro and in Vivo Evaluation. *Colloids Surfaces B Biointerfaces* **2017**, *160*, 101–109, https://doi.org/10.1016/j.colsurfb.2017.09.020.
8. Siqueira Jørgensen, S. D.; Al Sawaf, M.; Graeser, K.; Mu, H.; Müllertz, A.; Rades, T. The Ability of Two in Vitro Lipolysis Models Reflecting the Human and Rat Gastro-Intestinal Conditions to Predict the in Vivo Performance of SNEDDS Dosing Regimens. *Eur. J. Pharm. Biopharm.* **2018**, *124*, 116–124,https://doi.org/10.1016/j.ejpb.2017.12.014.
9. Rehman, F. U.; Shah, K. U.; Shah, S. U.; Khan, I. U.; Khan, G. M.; Khan, A. From Nanoemulsions to Self-Nanoemulsions, with Recent Advances in Self-Nanoemulsifying Drug Delivery Systems (SNEDDS). *Expert Opin. Drug Deliv.* **2017**, *14*, 1325–1340, https://doi.org/10.1080/17425247.2016.1218462.
10. Buya A.B; Beloqui A.; Memvanga P.B.; Préat V. Self-Nano-Emulsifying Drug-Delivery Systems: From the Development to the Current Applications and Challenges in Oral Drug Delivery. Pharmaceutics. **2020;** 12, 1194, https://doi.org/10.3390/pharmaceutics12121194.
11. Christiansen, M. L.; Holm, R.; Kristensen, J.; Kreilgaard, M.; Jacobsen, J.; Abrahamsson, B.; Müllertz, A. Cinnarizine Food-Effects in Beagle Dogs Can Be Avoided by Administration in a Self Nano Emulsifying Drug Delivery System (SNEDDS). *Eur. J. Pharm. Sci.* **2014**, *57*, 164–172, https://doi.org/10.1016/j.ejps.2013.11.003.
12. Perlman, M. E.; Murdande, S. B.; Gumkowski, M. J.; Shah, T. S.; Rodricks, C. M.; Thornton-Manning, J.; Freel, D.; Erhart, L. C. Development of a Self-Emulsifying Formulation That Reduces the Food Effect for Torcetrapib. *Int. J. Pharm.* **2008**, *351*, 15–22, https://doi.org/10.1016/j.ijpharm.2007.09.015.

13. Woo, J. S.; Song, Y. K.; Hong, J. Y.; Lim, S. J.; Kim, C. K. Reduced Food-Effect and Enhanced Bioavailability of a Self-Microemulsifying Formulation of Itraconazole in Healthy Volunteers. *Eur. J. Pharm. Sci.* **2008**, *33*, 159–165,https://doi.org/10.1016/j.ejps.2007.11.001.
14. Bahloul, B.; Lassoued, M. A.; Sfar, S. A Novel Approach for the Development and Optimization of Self Emulsifying Drug Delivery System Using HLB and Response Surface Methodology: Application to Fenofibrate Encapsulation. *Int. J. Pharm.* **2014**, *466*, 341–348, https://doi.org/10.1016/j.ijpharm.2014.03.040.
15. Tran, T.; Rades, T.; Müllertz, A. Formulation of Self-Nanoemulsifying Drug Delivery Systems Containing Monoacyl Phosphatidylcholine and Kolliphor® RH40 Using Experimental Design. *Asian J. Pharm. Sci.* **2018**, *13*, 536–545,https://doi.org/10.1016/j.ajps.2017.09.006.
16. Vohra, A. M.; Patel, C. V.; Kumar, P.; Thakkar, H. P. Development of Dual Drug Loaded Solid Self Microemulsifying Drug Delivery System: Exploring Interfacial Interactions Using QbD Coupled Risk Based Approach. *J. Mol. Liq.* **2017**, *242*, 1156–1168,https://doi.org/10.1016/j.molliq.2017.08.002.
17. Patel, G.; Shelat, P.; Lalwani, A. Statistical Modeling, Optimization and Characterization of Solid Self-Nanoemulsifying Drug Delivery System of Lopinavir Using Design of Experiment. *Drug Deliv.* **2016**, *23*, 3027–3042,https://doi.org/10.3109/10717544.2016.1141260.
18. El-Say, K. M.; Ahmed, T. A.; Ahmed, O. A. A.; Hosny, K. M.; Abd-Allah, F. I. Self-Nanoemulsifying Lyophilized Tablets for Flash Oral Transmucosal Delivery of Vitamin K: Development and Clinical Evaluation. *J. Pharm. Sci.* **2017**, *106*, 2447–2456. https://doi.org/10.1016/j.xphs.2017.01.001.
19. Choi, D. H.; Kim, Y. S.; Kim, D. D.; Jeong, S. H. QbD Based Development and Evaluation of Topical Microemulsion-Based Hydrogel against Superficial Fungal Infections. *J. Pharm. Investig.* **2019**, *49* (1), 87–103. https://doi.org/10.1007/s40005-018-0386-4.
20. Xue, X.; Cao, M.; Ren, L.; Qian, Y.; Chen, G. Preparation and Optimization of Rivaroxaban by Self-Nanoemulsifying Drug Delivery System (SNEDDS) for Enhanced Oral Bioavailability and No Food Effect. *AAPS PharmSciTech* **2018**, *19*, 1847–1859,https://doi.org/10.1208/s12249-018-0991-6.
21. Tefas, L. R.; Sylvester, B.; Tomuta, I.; Sesarman, A.; Licarete, E.; Banciu, M.; Porfire, A. Development of Antiproliferative Long-Circulating Liposomes Co-Encapsulating Doxorubicin and Curcumin, through the Use of a Quality-by-Design Approach. *Drug Des. Devel. Ther.* **2017**, *11*, 1605–1621,https://doi.org/10.2147/DDDT.S129008.
22. Beniwal, A.; Choudhary, H. Rosuvastatin Calcium-Loaded Solid Lipid Nanoparticles (SLN) Using Design of Experiment Approach for Oral Delivery. *Int. J. Chem. Life Sci.* **2017**, *6*, 2029, https://doi.org/10.21746/ijcls.2017.5.1.
23. European Medicines Agency. (2012). EMA Guidelines, 44, 1–23
24. Date, A. A.; Nagarsenker, M. S. Design and Evaluation of Self-Nanoemulsifying Drug Delivery Systems (SNEDDS) for Cefpodoxime Proxetil. *Int. J. Pharm.* **2007**, *329*, 166–172, https://doi.org/10.1016/j.ijpharm.2006.08.038.
25. Alayoubi, A.; Aqueel, M. S.; Cruz, C. N.; Ashraf, M.; Zidan, A. S. Application of in Vitro Lipolysis for the Development of Oral Self-Emulsified Delivery System of Nimodipine. *Int. J. Pharm.* **2018**, *553*, 441–453. https://doi.org/10.1016/j.ijpharm.2018.10.066.
26. Basalious, E. B.; Shawky, N.; Badr-Eldin, S. M. SNEDDS Containing Bioenhancers for Improvement of Dissolution and Oral Absorption of Lacidipine. I: Development and Optimization. *Int. J. Pharm.* **2010**, *391*, 203–211. https://doi.org/10.1016/j.ijpharm.2010.03.008.
27. Shakeel, F.; Haq, N.; Alanazi, F. K.; Alsarra, I. A. Impact of Various Nonionic Surfactants on Self-Nanoemulsification Efficiency of Two Grades of Capryol (Capryol-90 and Capryol-PGMC). *J. Mol. Liq.* **2013**, *182*, 57–63. https://doi.org/10.1016/j.molliq.2013.03.011.
28. Buya, A. B.; Ucakar, B.; Beloqui, A.; Memvanga, P. B.; Préat, V. Design and Evaluation of Self-Nanoemulsifying Drug Delivery Systems (SNEDDSs) for Senicapoc. *Int. J. Pharm.* **2020**, *580*, 119180. https://doi.org/10.1016/j.ijpharm.2020.119180.
29. European Pharmacopoeia 7th ed., 2020. Strasbourg, France

30. Jantratid, E., Janssen, N., Reppas, C., & Dressman, J. B. (2008). Dissolution media simulating conditions in the proximal human gastrointestinal tract: An update. *Pharmaceutical Research*, *25*(7), 1663–1676. https://doi.org/10.1007/s11095-008-9569-4
31. Crum, M. F.; Trevaskis, N. L.; Williams, H. D.; Pouton, C. W.; Porter, C. J. H. A New in Vitro Lipid Digestion - In Vivo Absorption Model to Evaluate the Mechanisms of Drug Absorption from Lipid-Based Formulations. *Pharm. Res.* **2016**, *33* (4), 970–982. https://doi.org/10.1007/s11095-015-1843-7.
32. Memvanga, P. B.; Coco, R.; Préat, V. An Oral Malaria Therapy: Curcumin-Loaded Lipid-Based Drug Delivery Systems Combined with β-Arteether. *J. Control. Release* **2013**, *172* (3), 904–913. https://doi.org/10.1016/j.jconrel.2013.09.001.
33. Mohsin K. ; Long M.A. ; Pouton C.W. Design of lipid-based formulations for oral administration of poorly water-soluble drugs: precipitation of drug after dispersion of formulations in aqueous solution. J Pharm Sci. **2009**, 98, 3582-95, https://doi.org/10.1002/jps.21659.
34. Zhang, L.; Zhang, L.; Zhang, M.; Pang, Y.; Li, Z.; Zhao, A.; Feng, J. Self-Emulsifying Drug Delivery System and the Applications in Herbal Drugs. *Drug Deliv.* **2015**, *22*, 475–486, https://doi.org/10.3109/10717544.2013.861659.
35. Patel, J.; Dhingani, A.; Garala, K.; Raval, M.; Sheth, N. Quality by Design Approach for Oral Bioavailability Enhancement of Irbesartan by Self-Nanoemulsifying Tablets. *Drug Deliv.* **2014**, *21*, 412–435,https://doi.org/10.3109/10717544.2013.853709.
36. Gelderblom, H.; Verweij, J.; Nooter, K.; Sparreboom, A. Cremophor EL: The Drawbacks and Advantages of Vehicle Selection for Drug Formulation. *Eur. J. Cancer* **2001**, *37*, 1590–1598, https://doi.org/10.1016/S0959-8049(01)00171-X.
37. Croy, S. R.; Kwon, G. S. Polysorbate 80 and Cremophor EL Micelles Deaggregate and Solubilize Nystatin at the Core-Corona Interface. *J. Pharm. Sci.* **2005**, *94* (11), 2345–2354, https://doi.org/10.1002/jps.20301.
38. Zainol, S.; Basri, M.; Basri, H. Bin; Shamsuddin, A. F.; Abdul-Gani, S. S.; Karjiban, R. A.; Abdul-Malek, E. Formulation Optimization of a Palm-Based Nanoemulsion System Containing Levodopa. *Int. J. Mol. Sci.* **2012**, *13*, 13049–13064,https://doi.org/10.3390/ijms131013049.
39. Gursoy, R. N.; Benita, S. Self-Emulsifying Drug Delivery Systems (SEDDS) for Improved Oral Delivery of Lipophilic Drugs. *Biomed. Pharmacother.* **2004**, *58*, 173–182, https://doi.org/10.1016/j.biopha.2004.02.001.
40. Zupančič, O.; Grießinger, J. A.; Rohrer, J.; Pereira de Sousa, I.; Danninger, L.; Partenhauser, A.; Sündermann, N. E.; Laffleur, F.; Bernkop-Schnürch, A. Development, in Vitro and in Vivo Evaluation of a Self-Emulsifying Drug Delivery System (SEDDS) for Oral Enoxaparin Administration. *Eur. J. Pharm. Biopharm.* **2016**, *109*, 113–121,https://doi.org/10.1016/j.ejpb.2016.09.013.
41. Azeem, A.; Rizwan, M.; Ahmad, F. J.; Iqbal, Z.; Khar, R. K.; Aqil, M.; Talegaonkar, S. Nanoemulsion Components Screening and Selection: A Technical Note. *AAPS PharmSciTech* **2009**, *10*, 69–76, https://doi.org/10.1208/s12249-008-9178-x.
42. Bali, V.; Ali, M.; Ali, J. Study of Surfactant Combinations and Development of a Novel Nanoemulsion for Minimising Variations in Bioavailability of Ezetimibe. *Colloids Surfaces B Biointerfaces* **2010**, *76* , 410–420,https://doi.org/10.1016/j.colsurfb.2009.11.021.
43. Rahman, M. A.; Iqbal, Z.; Hussain, A. Formulation Optimization and in Vitro Characterization of Sertraline Loaded Self-Nanoemulsifying Drug Delivery System (SNEDDS) for Oral Administration. *J. Pharm. Investig.* **2012**, *42*, 191–202,https://doi.org/10.1007/s40005-012-0029-0.
44. Wang, L.; Dong, J.; Chen, J.; Eastoe, J.; Li, X. Design and Optimization of a New Self-Nanoemulsifying Drug Delivery System. *J. Colloid Interface Sci.* **2009**, *330*, 443–448, doi:10.1016/j.jcis.2008.10.077.
45. Li, F.; Song, S.; Guo, Y.; Zhao, Q.; Zhang, X.; Pan, W.; Yang, X. Preparation and Pharmacokinetics Evaluation of Oral Self-Emulsifying System for Poorly Water-Soluble Drug Lornoxicam. *Drug Deliv.* **2015**, *22*, 487–498, doi:10.3109/10717544.2014.885615

46. Kovarik, J.M.; Mueller, E.A.; van Bree, J.B.; Tetzloff, W.; Kutz, K. Reduced Inter- and Intraindividual Variability in Cyclosporine Pharmacokinetics from a Microemulsion Formulation. *J. Pharm. Sci.* **1994**, *83*, 444–446, doi:10.1002/jps.2600830336
47. Nielsen, F.S.; Petersen, K.B.; Müllertz, A. Bioavailability of Probucol from Lipid and Surfactant Based Formulations in Minipigs: Influence of Droplet Size and Dietary State. *Eur. J. Pharm. Biopharm.* **2008**, *69*, 553–562, doi:10.1016/j.ejpb.2007.12.020
48. Ujilestari, T.; Martien, R.; Ariyadi, B.; Dono, N. D.; Zuprizal. Self-Nanoemulsifying Drug Delivery System (SNEDDS) of Amomum Compactum Essential Oil: Design, Formulation, and Characterization. *J. Appl. Pharm. Sci.* **2018**, *8* (6), 14–21. https://doi.org/10.7324/JAPS.2018.8603.
49. Dash, R. N.; Mohammed, H.; Humaira, T.; Ramesh, D. Design, Optimization and Evaluation of Glipizide Solid Self-Nanoemulsifying Drug Delivery for Enhanced Solubility and Dissolution. *Saudi Pharm. J.* **2015**, *23* (5), 528–540. https://doi.org/10.1016/j.jsps.2015.01.024.
50. Van Speybroeck, M., Mellaerts, R., Mols, R., Thi, T. Do, Martens, J. A., Van Humbeeck, J., … Augustijns, P. (2010). Enhanced absorption of the poorly soluble drug fenofibrate by tuning its release rate from ordered mesoporous silica. *European Journal of Pharmaceutical Sciences*, *41*(5), 623–630. https://doi.org/10.1016/j.ejps.2010.09.002
51. Thomas, N.; Holm, R.; Müllertz, A.; Rades, T. In Vitro and in Vivo Performance of Novel Supersaturated Self-Nanoemulsifying Drug Delivery Systems (super-SNEDDS). *J. Control. Release* **2012**, *160*, 25–32,https://doi.org/10.1016/j.jconrel.2012.02.027.
52. Khan, J.; Hawley, A.; Rades, T.; Boyd, B. J. In Situ Lipolysis and Synchrotron Small-Angle X-Ray Scattering for the Direct Determination of the Precipitation and Solid-State Form of a Poorly Water-Soluble Drug During Digestion of a Lipid-Based Formulation. *J. Pharm. Sci.* **2016**, *105*, 2631–2639, https://doi.org/10.1002/jps.24634.
53. Bibi, H. A.; Holm, R.; Bauer-Brandl, A. Simultaneous Lipolysis/permeation in Vitro Model, for the Estimation of Bioavailability of Lipid Based Drug Delivery Systems. *Eur. J. Pharm. Biopharm.* **2017**, *117*, 300–307,https://doi.org/10.1016/j.ejpb.2017.05.001.
54. Tung, N. T.; Tran, C. S.; Pham, T. M. H.; Nguyen, H. A.; Nguyen, T. L.; Chi, S. C.; Nguyen, D. D.; Bui, T. B. H. Development of Solidified Self-Microemulsifying Drug Delivery Systems Containing L-Tetrahydropalmatine: Design of Experiment Approach and Bioavailability Comparison. *Int. J. Pharm.* **2018**, *537* (1-2), 9–21,https://doi.org/10.1016/j.ijpharm.2017.12.027.
55. Yin, Y. M.; Cui, F. De; Mu, C. F.; Choi, M. K.; Kim, J. S.; Chung, S. J.; Shim, C. K.; Kim, D. D. Docetaxel Microemulsion for Enhanced Oral Bioavailability: Preparation and in Vitro and in Vivo Evaluation. *J. Control. Release* **2009**, *140* (2), 86–94,https://doi.org/10.1016/j.jconrel.2009.08.015.
56. Metcalf, B.; Chuang, C.; Dufu, K.; Patel, M. P.; Silva-Garcia, A.; Johnson, C.; Lu, Q.; Partridge, J. R.; Patskovska, L.; Patskovsky, Y.; Almo, S. C.; Jacobson, M. P.; Hua, L.; Xu, Q.; Gwaltney, S. L.; Yee, C.; Harris, J.; Morgan, B. P.; James, J.; Xu, D.; Hutchaleelaha, A.; Paulvannan, K.; Oksenberg, D.; Li, Z. Discovery of GBT440, an Orally Bioavailable R-State Stabilizer of Sickle Cell Hemoglobin. *ACS Med. Chem. Lett.* **2017**, *8*, 321–326,https://doi.org/10.1021/acsmedchemlett.6b00491.
57. Biopharma International Home Page. Available online: https://www.biopharminternational.com/view/establishing-acceptance-criteria-analytical-methods (Assessed on 30 October 2021).

CHAPTER V
DISCUSSION AND PERSPECTIVES

TABLE OF CONTENTS

I. MAIN ACHIEVEMENTS

Sickle cell disease has become the most common monogenetic disorder affecting millions of people across all continents [1]. Estimates suggest that approximatively 300,000 babies per year are born with SCD [2, 3] and this number could rise to 400,000 by 2050 [4]. Therapeutic options for SCD patients are, however, still scarce. The clinically available and notably safe treatment modalities include hydroxyurea, L-glutamine, crizanlizumab and blood transfusions [5-8]. Safe, effective and affordable drug therapies are highly preferred. Many new drugs with various pharmacological targets have emerged [2,6]. Although the majority have failed to show benefit in clinical trials, some have produced encouraging results. Senicapoc and Voxelotor, two drug candidates for oral SCD therapy have shown promising results under preclinical and clinical trials. However, the oral delivery of senicapoc and voxelotor has been limited owing to many factors, including poor aqueous solubility, moderate oral bioavailability, food effect and subject dose variability [9-11].

When this project started, there was a need for developing formulations containing senicapoc and voxelotor. The formulations would need to be stable and provide optimum biopharmaceutical properties to the compounds (e.g., high solubility, suitable bioavailability, less dependency on food intake, etc.), and should be easily manufactured at commercially scalable. We assumed that lipid-based drug-delivery systems might improve biopharmaceutical properties of senicapoc and voxelotor based on previous studies conducted in our laboratory. Among the wide number of lipid-based drug-delivery systems, SNEDDSs have been chosen for our thesis project. SNEDDSs are defined as isotropic mixture of oils, surfactants, and cosurfactants or cosolvent, which can form a nanoemulsion with droplet size of 200 nm or below upon contact with GI fluids [12]. Why did we choose SNEDDSs as drug carrier for our project? Ease of manufacture and scale-up are the most important advantages that make SNEDDSs unique when compared to other drug delivery systems (solid dispersions, liposomes, nanoparticles, etc.). SNEDDSs require very simple and economical manufacturing facilities like a simple mixer with agitator and volumetric liquid filling equipment for large-scale manufacturing. This is particularly advantageous for low-income countries, where most of SCD patients are located.

We hypothesized that SNEDDSs formulations may improve the aqueous solubility and oral bioavailability of senicapoc and voxelotor. We strongly believe that by improving the biopharmaceutical properties of senicapoc and voxelotor, SNEDDSs will offer new hope in the treatment of SCD and help alleviate the drawbacks related to the efficacy and availability of SCD drugs. To undertake our objective, we firstly developed and optimized SNEDDSs loaded with senicapoc and voxelotor. Following *in vitro* evaluation, we have demonstrated that these SNEDDSs significantly increased drug solubility and cell permeation. Finally, voxelotor-loaded SNEDDSs achieved a high oral bioavailability in rats compared to the drug in suspension.

Our major findings can be summarized as follows:

SNEDDSs formulation and optimization

We developed and optimized four SNEDDSs formulations by mixing pre-selected excipients. Those formulations were encapsulated with 10 mg and 50 mg of senicapoc and voxelotor, respectively.

SNEDDSs characterization

The formulations have been characterized in terms of droplet size, PDI, zeta potential, time of emulsification, viscosity, transmittance percentage and morphology. Through these techniques, we have shown that the optimized formulations comply with SNEDDSs requirement and possess optimal emulsification properties.

Drug dissolution studies

The *in vitro* dissolution of senicapoc and voxelotor from SNEDDSs was characterized by fast release during the first 20 min as compared to the free drugs. A higher release of drug from SNEDDSs (> 80 %) was achieved after 60 min.

***In vitro* lipolysis**

The formulated SNEDDSs underwent lipolysis and maintained at least 80 % of the senicapoc and voxelotor dissolved after 60 min of *in vitro* lipolysis.

***In vitro* cytotoxicity**

We have shown that the formulations were not cytotoxic at 0.9 mg/mL (voxelotor-loaded SNEDDSs) and 1 mg/mL (senicapoc-loaded SNEDDSs), as 80 % of cell viability was observed after 2h of incubation.

Transport studies across CaCo-2 monolayers

The developed SNEDDSs significantly increased senicapoc (115-fold) and voxelotor (22-fold) permeation across Caco-2 monolayers in comparison to the drug suspensions.

***In vivo* pharmacokinetic studies**

Compared with the drug suspension, the developed SNEDDS enhanced the oral bioavailability (1.7-fold) of voxelotor in rats.

The major achievements of this PhD thesis are represented below.

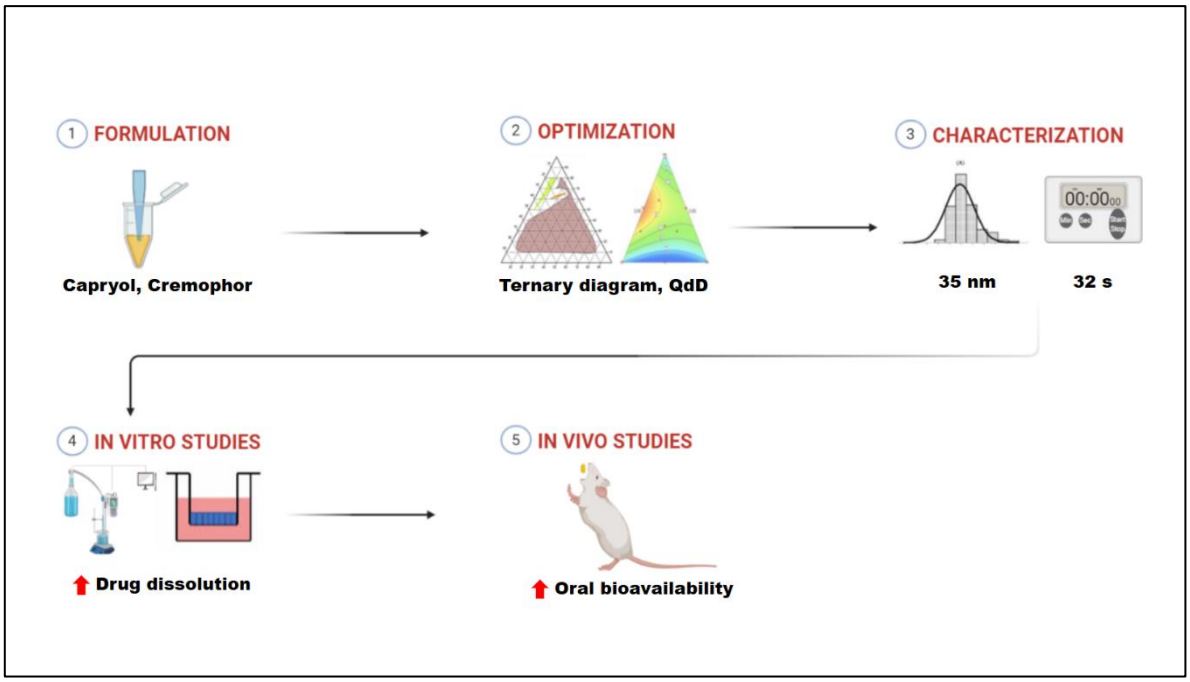

Scheme 2. The major achievements of this PhD thesis

II. DISCUSSION OF THE RESULTS

II.1. SNEDDSS FORMULATION AND CHARACTERIZATION

A successful formulation of a SNEDDS relies on the right selection of excipients. In this thesis, the selection of components was based on their safety, solubilization ability for drugs and compatibility. It is worth noting that we already considered the potential translation; therefore, we conceptually choose excipients listed by regulatory agencies (FDA, EMA) and *generally recognized as safe* (GRAS) that could be easily transferred to pharmaceutical market. Capryol PGMC®, a modified medium-chain triglyceride (C_8) was selected as oily phase regarding its solubilizing ability for senicapoc and voxelotor. Compared to long- chain triglycerides, medium-chain triglycerides are mostly used in the literature because of their better solubilizing ability and self-emulsification capacity [13]. After their oral administration, gastric and pancreatic lipases break down triglycerides into diglycerides, monoglycerides, and fatty acids. Once within the small intestine, those products stimulate the release of endogenous biliary lipids from the gall bladder, including bile salt, lipoprotein, phospholipid, and cholesterol, which enhance the solubilization and absorption ability of the intestinal tract via the formation of micelles [14-16].

Two non-ionic surfactants namely Cremophor®-EL and Tween®-80 were selected regarding their emulsification ability for Capryol PGMC® and better solubilization properties for senicapoc and voxelotor. Compared to ionic surfactants, non-ionic surfactants are generally preferred because of their lower toxicity and ability to stabilize emulsion over a wider range of nanoemulsion pH and ionic strength [17]. Furthermore, many non-ionic surfactants, such Tween® 80 and Cremophor®-EL possess the ability to increase membrane fluidity [18] and to inhibit efflux transporters [19, 20], which are contributing factors in enhancing drug bioavailability.

The literature reports that fluid interfacial film is rarely achieved by the use of a single surfactant; usually the addition of cosurfactant or cosolvent is needed [21]. These components decrease the bending stress of interface and provide sufficient flexibility to take up different curvatures required to form a nanoemulsion over a wide range of compositions [21]. Thus, Transcutol® HP, PEG 400 and Labrafil® M 1944 were chosen based on their ability to solubilize the drugs and to improve the oil emulsification.

The optimization studies are crucial in the development of SNEDDSs as they allow the selection of the best formulation(s), among others [22]. The ternary diagram approach is the most popular technique used to optimize SNEDDSs formulations [23, 24]. This approach was employed in the first part of this project and allows the selection of three optimized SNEDDSs, which were encapsulated with 10 mg of senicapoc. However, what criteria did we use to select those three SNEDDSs among others? and how did we select the dose (10 mg of senicapoc)? The selection of any SNEDDSs from the nanoemulsification regions was based on the following two criteria: 1) formulation droplet size after aqueous dispersion and 2) surfactant content of the formulation. Regarding formulation droplet size, the literature reports that smaller particle size with a narrow distribution has a positive effect on the oral bioavailability of a drug encapsulated into SNEDDSs [23, 25]. A plausible explanation for the improved oral bioavailability could be that the smaller the particle size, the larger interfacial area, which improves the drug solubilization and permeability.

Moreover, it is well-known that formulations with smaller droplet sizes following aqueous dispersion reduce dose variability after oral administration [26–28]. Regarding the amount of surfactant, it was reported that some surfactants (i.e., Cremophor®-EL) might cause irritation to the GI epithelium following oral administration [29]. Thus, the amount of surfactant in SNEDDSs must be maintained at a level as low as possible. In view of this, SNEDDSs which contain a minimal amount of surfactant and possess a smaller droplet size and PDI was selected among others. Ten milligrams of senicapoc were loaded into SNEDDSs following clinical studies with senicapoc as reported by Ataga et al. [30].

Although ternary diagram approach has been successful in the optimization of three senicapoc loaded SNEDDSs, this approach shows some limitations. The ternary diagram approach is an empirical "trial and error" approach, which consists on varying one factor at time. This approach is highly demanding in time, number of experiments and resources [31]. Furthermore, this approach often provides with insufficient data to determine the impact of excipients on the formulation performance [32, 33]. An alternative to ternary diagrams is the quality-by-design (QbD) approach. The QbD approach, applying statistical design of experiments (DoE) for systematic optimization of SNEDDSs has been reported to reduce expenditure in terms of time, resources and developmental efforts. The Qbd approach provides an optimal amount of data and process understanding from a limited number of experiments [33]. The QbD approach was successfully employed in the second part of this project for the optimization of voxelotor loaded SNEDDSs. The savings in terms of costs and time are the major benefits that motivate the translation of this approach to the industry. The QbD knowledge generated during this thesis can be translated into many efficient industrial dimensions, including higher operational flexibility, faster manufacture, fewer rejected batches and better product quality. The literature reports that QbD has been widely used for the development of different pharmaceutical dosage forms, either conventional (tablets, capsules, topical creams, etc.) or non-conventional (nano- suspensions, SNEDDSs, liposomes, etc.) [34].

Table 1. Composition and characterization of SNEDDSs formulations.

F-x	Sample composition (mg)			Optimization	Drug	Size (nm) PDI	Zeta potential (mV)	Emulsification Time (mV)	% transmittance
	Oil	SA	Co-SA						
F1	260[a]	240[b]	100[d]	Ternary diagram	SEN	28 ± 0 0.17	-7.6 ± 3	58 ± 2	99 ± 0
F2	300[a]	240[b]	60[e]	Ternary diagram	SEN	38 ± 2 0.39	-7.4 ± 0	64 ± 3	96 ± 1
F3	180[a]	240[c]	180[d]	Ternary diagram	SEN	123 ±3 0.45	-6.8 ± 2	27 ± 6	95 ± 1
F4	240 [a]	258 [b]	102 [f]	QbD	Vox	34.9 ± 1 0.2	-8.4 ± 1.3	32 ± 0	99.1 ± 0
a Capryol PGMC® b Cremophor®-EL c Tween®-80 d Transcutol® HP e PEG 400, f Labrafil® M 1499									

Size characterization is one of the most essential examinations for SNEDDSs development since the droplet size can affect not only the *in vitro* tested characteristics (i.e., dissolution, stability) but also the *in vivo* performance of a SNEDDS (i.e., drug absorption) [35,36]. Particle size can be measured using a number of methods, including photon correlation spectroscopy also known as dynamic light scattering, laser diffraction, transmission electron microscopy, scanning electron

microscopy and atomic force microscopy [31]. In the DLS technique, a single frequency laser is directed to the sample contained in a cuvette. If there are particles in the sample, the incident laser light gets scattered in all directions. The scattered light is detected at a certain angle over time and this signal is used to determine the diffusion coefficient and the particle size by the Stokes-Einstein equation. Dynamic light scattering technique was used in this project. As presented in table 1, all the formulations showed droplet size less than 200 nm, complying with the definition of SNEDDSs formulations. However, it should be noted that depending on the type of surfactant, different droplet sizes have been obtained. It was reported that the droplet size of the nanoemulsion formed upon SNEDDS dispersion in aqueous environments depended on the type and amount of components used [37, 38]. As stated above, the improved drug absorption is generally assumed associated with smaller droplet size. However, many examples exist in which drug absorption is not influenced by droplet size [39, 40]. It should be noted, however, that the cited studies utilized different lipids and surfactants, which can also influence on drug absorption, thus making difficult to draw conclusions on the impact of droplet size. For this project, it was difficult to determine the impact of the formulation droplet size on drug absorption since the *in vivo* studies were carried out only for one formulation (F4).

The zeta potential of SNEDDSs is another important property that should be assessed. The zeta potential provides information about the colloidal stability and is estimated by measuring the electrophoretic mobility of the droplets. Moreover, the zeta potential can affect the oral absorption of the drug encapsulated into SNEDDSs. Charge-dependent interaction with mucus and cell membrane barriers with respect to absorption enhancement has been reported [31]. As shown in table 1, all formulations exhibited zeta potential values of approximately -7 mV. These charges provide repulsive forces between particles, prevents aggregation, and increases systems stability [41,42].

The self-emulsification ability of SNEDDS is directly linked to the spontaneous formation of a nanoemulsion when in contact with an aqueous environment. The emulsification time was less than 70 s for all the optimized formulations, which indicated their ability to disperse quickly when subjected to aqueous dilution under mild agitation. A very low self- emulsification time (< 2 min) promoted the spontaneous emulsification upon dilution with aqueous media [43]. Moreover, this rapid emulsification could contribute to a fast drug release and a subsequently rapid onset of action [44, 45]. This is important for SCD patients, especially during VOC requiring urgent drug administration.

II.2. SNEDDSS EVALUATION

To verify that the newly developed formulations could increase aqueous solubility and oral bioavailability of the drugs, a series of *in vitro* tests are commonly used to simulate key processes related to drugs absorption. These processes are mainly evaluated in term of dissolution, digestion, and permeation.

The in *vitro* dissolution test is routinely employed as an indicator of the likely GI drug dissolution and, consequently, as a tool to predict the rate and extent of absorption for poorly water-soluble drugs [31]. Our results showed that formulated SNEDDSs significantly increased the dissolution

of the drugs (> 80 % in 60 min) in comparison to the free drug suspensions (< 30 % in 60 min). We have further demonstrated that senicapoc release from SNEDDSs was governed by its solubility because senicapoc release was independent of the SNEDDSs droplet size. Qian et al. [46] have also reported a solubility-dependent dissolution. In general, the *in vitro* dissolution from a SNEDDS formulation is faster compared with the native drug due to the reduction in particle size and increase in surface area [44, 47].

When administered orally, SNEDDSs are prone to digestion by pancreatic lipase. It is a known fact that SNEDDS digestion in the GI tract is crucial for drug dissolution and absorption: it can be beneficial (drug solubilization) or deleterious (drug precipitation after digestion of the oil phase). An *in vitro* lipolysis test is commonly used to study the impact of GI digestion on the *in vitro* performance of SNEDDSs. The test aims to reveal the ability of SNEDDSs to maintain the drug solubilized after being digested. Following an *in vitro* lipolysis test, we have demonstrated that firstly, the formulated SNEDDSs undergo lipolysis because they consume NaOH during the experiment, and secondly, they could maintain at least 80 % of the senicapoc and voxelotor dissolved 60 min after the end of the experiment. In aqueous phase, senicapoc and voxelotor were dissolved in mixed micelles formed by fatty acids and mono-glycerides generated during the hydrolysis of lipids. It is considered that a high *in vitro* drug solubilization equates to high oral absorption, thus the high percentage of drug dissolved in the aqueous phase during the *in vitro* lipolysis has been related to a high oral drug absorption [48]. Further, it was important to elucidate the solid-state characteristics of the precipitates formed during the *in vitro* lipolysis. A drug precipitation in amorphous form (or molecular dispersed state) is expected to lead to rapid *in vivo* drug re-dissolution in comparison to the precipitation in the crystalline form. Several techniques can be used to study the solid-state of the precipitates, including X-ray diffraction [49, 50]. The X-ray diffraction of the precipitates formed within the voxelotor loaded-SNEDDSs digestion study showed no peaks associated to the crystallization of the drug, suggesting that the precipitates might be in amorphous form (or molecular dispersed state), which could lead to a rapid *in vivo* re-dissolution of the drug [51-55].

All so far published, SNEDDSs show cell-toxic effects *in vitro* due to their high concentration of surfactants being able to penetrate and destroy the cell membrane. An *in vitro* cytotoxicity experiment was carried out to evaluate the toxicity of the formulations in Caco-2 cells. In addition, this test allowed us to select the dose of each SNEDDSs, which could be used for the transport studies. Our results showed that the developed SNEDDSs were not cytotoxic at 1 mg/mL, as 80% of cell viability was obtained after 2h of incubation. In the literature, no cytotoxic effect of SNEDDSs was observed for a concentration of 3 mg/mL and higher [38]. It is important to note that the *in vitro* cytotoxicity test does not reproduce the actual *in vivo* conditions. Physiological sink conditions reduce concentration and toxic effects over time. According to already published data, the liquid volume in the small intestine of humans ranges from 30 to 420 mL in fasted state and from 18 to 660 mL in the fed state, which can alleviate toxic effects of the formulations [56, 57]. Furthermore, unlike cells of the intestinal epithelium, Caco-2 cells are not protected by a mucus layer. Even enzyme containing and highly mucus penetrating nanocarriers do not destroy this protective barrier [58].

Following the results from cytotoxicity studies, transport studies were conducted to assess the ability of the formulations to increase drug transport across Caco-2 monolayers. We have shown

that SNEDDDSs increased significantly the transport of senicapoc (115-fold) and voxelotor (22-fold) compared to the corresponding drug suspensions. The enhanced transport across Caco-2 cells was explained by the increased drugs solubility and the fact that components (i.e., Cremophor-EL®, Tween®-80) used to formulate SNEDDSs could reversibly affect membrane fluidity and increase the permeation of senicapoc and voxelotor. Furthermore, by comparing the permeability coefficients from the two-way transport studies, we have demonstrated that voxelotor was not substrate of the P-gp.

Finally, we have demonstrated that developed SNEDDS resulted in a higher oral bioavailability of voxelotor (44%) in rats compared to the drug suspension (25%). This increase in bioavailability might be due to the improved drug solubility, the synergistic effect of the surfactant and oil as absorption enhancers and the avoidance of first pass metabolism via lymphatic transport.

By increasing aqueous solubility and oral bioavailability of voxelotor, my PhD work will help solve problems associated with its clinical use. Voxelotor is currently in the market under the name Oxbryta® and is administered daily at a dose of 1.5 g. This high dose was partly set based on its low aqueous solubility in order to achieve effective plasma concentrations. We believe that the increase in solubility, cell transport and oral bioavailability as demonstrated in this work could contribute to the reduction of the daily dose. In addition, the food effect observed in patients under Oxbryta® may be reduced because SNEEDSs have shown the ability to reverse the influence of food on drug absorption.

II.3. MY PHD: A STEP TAKEN TOWARDS PEDIATRIC FORMULATIONS OF SCD

SCD is a serious problem among the pediatric population. Estimates suggest that approximatively 300.000 babies per year are born with SCD and this number could rise to 400.000 by 2050 [2]. The vast majority (up to 90%) of children with SCD do not reach their fifth birthday [4]. Due to the physiological and biopharmaceutical differences that occur in pediatric population, ideal dosing should be based on body surface area calculations or body weight in relation to normal growth. In most cases, especially in resource-limited countries, these methods are not applicable, leading to sub-therapeutic dosing of hydroxyurea and voxelotor in children, mainly because the solid dosage forms available (gelules or tablets) must be divided for their administration. Ideal dosage forms would be liquids as they can be easily administrated and offer more flexible dosing for the prescribers. By encapsulating senicapoc and voxelotor in SNEEDSs, our PhD thesis opens a new path towards pediatric formulations. The developed SNEDDSs (preconcentrate) can be used for dosage adjustment. Using a graduated pipette, the required dose according to weight can be withdrawn and dispersed in a volume of water before administration. These liquid dosage forms will help improve drugs' availability and dosing for pediatric population.

II.4. LIMITS OF MY PHD

Although my thesis project demonstrated the ability of SNEDDSs to improve aqueous solubility and intestinal transport of senicapoc and voxelotor, it is important to note here some weak points associated to this PhD thesis.

As mentioned earlier, SNEDDSs can be easily scaled up by mixing components; however, SNEDDSs evaluation (i.e, characterization, *in vitro* and *in vivo* studies) requires sophisticated equipments that may limit access to this promising technology only to wealthy labs, scarce in low-incoming countries.

We recognize that the in *vitro* tests used to evaluate SNEDDSs do not completely simulate the *in vivo* conditions. In the GI tract, the interplay between dosage form, drug and intestinal physiology (fluid composition, enzymatic capacity, permeation through the gut wall, gastric emptying, and transit times) determine the *in vivo* absorption or precipitation. These conditions are difficult to reproduce through *in vitro* methods. Moreover, the *in vitro* tests were carried out separately in opposition to the dynamic environment of the GI tract, where successive steps are involved after formulation ingestion. Attempts have been made to combine artificial membranes or a cell-based permeation step with the current *in vitro* digestion model, but they were not be able to remove enough drug to mimic effective *in vivo* drug absorption [31]. We propose the introduction of models that incorporate a means to accurately monitor *in vitro* dissolution, lipolysis and to simultaneously assess lipids and drug absorption for better predicting *in vivo* behavior of drugs delivered in SNEDDSs. The suggested models should include the gastric lipolysis step, as it has been recognized critical for evaluating formulation digestion and drug absorption [33,60].

For voxelotor-SNEDDSs, only 50 mg of the drug was encapsulated in the formulations for its evaluation. However, the daily dose of voxelotor used clinically in SCD patients is of 1500 mg. The cost of voxelotor was a limiting factor for its use in this project. We believe that future studies encapsulating the increasing doses of voxelotor will be essential to fully exploit the results of this PhD thesis.

Despite the benefits provided by liquid SNEDDSs formulated in this project, certain drawbacks remain such as drug/components precipitation when stored, interactions between the filling and the capsule shell, and formulation stability during storage. We believe that the conversion of formulated liquid SNEDDSs to solid SNEDDSs would provide relatively lower production cost, better formulation stability, ease of handing and, consequently, better patient compliance.

III. PERSPECTIVES

III.1. SNEDDSs FOR SENICAPOC AND VOXELOTOR

This PhD thesis provides enough data to demonstrate the ability of SNEDDSs formulations to impove aqueous solubility and oral absorption of senicapoc and voxelotor, two oral SCD drugs. However, to exploit the full potential of SNEDDSs in SCD therapy, further studies could be conducted in the near future. Examples of studies recommended are the following:

III.1.1. Preclinical studies for Senicapoc-SNEDDSs

As for voxelotor-SNEDDSs, animal pharmacokinetics studies should be carried out for senicapoc-loaded SNEDDSs. An oral dose of senicapoc-loaded in SNEDDSs (10 mg/kg) and suspension (10 mg/kg) can be given to Male Sprague-Dawley Fisher rats as previously described in the chapter IV, section II.6. To analyze the absorbed drug in the plasma, liquid chromatography-mass spectrometry can be used. The pharmacokinetic parameters (i.e., $t^{1/2}$, $C_{max,}$ $T_{max,}$ AUC_{0-t}) of SNEDDSs and suspension can be calculated and compared.

III.1.2. Liquid SNEDDSs solidification

As mentioned above, it is believed that the conversion of liquid SNEDDSs to solid SNEDDSs could provide relatively lower production cost, better formulation stability, ease of handing and precise dosing. Several techniques, including adsorption onto inert carriers, spray drying, melt granulation and extrusion-spheronization can be used for solid-SNEDDSs preparation. We propose absorption onto inert carriers as it remains the most instigated technique and the simplest to implement. Thus, several solid porous carriers including Aerosil® 200, Aeroperl® 300 and Neusilin® US2 should be screened for their oil adsorption capacity. The carrier that required the least quantity to render the blend free flowing could be selected as solid adsorbent for the formulations. The solid-SNEDDSs obtained can further be characterized through several techniques, including differential scanning calorimetry (DSC), X-ray diffraction and Fourier-transform infrared spectroscopy (FTIR) to ensure the stability of the drugs and the compatibility of components. Finally, the obtained solid SNEDDS can directly be filled into gelatin capsules or, alternatively, mixed with appropriate ingredients (diluent, binder, etc.) prior compression into tablets.

III.1.3. Combination therapy strategies

The increased number of compounds under evaluation offers hope for the availability of more drugs for SCD treatment. With its complex pathophysiology, it is unlikely that individual drugs will ameliorate all the complications related to this disease. We believe that the availability of combination drug therapies based on different mechanisms of action and side effect profiles can improve the outcomes for patients with SCD. However, the following questions must be answered: Which drugs/drug ratios to use in such combinations? Which mechanisms should be targeted? At what age should this approach begin — infancy, childhood, adulthood or before organ damage? Can the toxicity of adding multiple drugs be tolerated? Would more complicated regimes

and greater 'pill burden' hamper compliance with therapy? Will host defences be dangerously compromised, leading to infections and autoimmunity? Should there be a separate combination for acute events versus chronic therapy? [61].

Senicapoc targets red blood cell hemolysis while voxelotor reduces cell vaso-occlusion. The combination of those two drugs could improve the complications of SCD patients since hemolysis and vaso-occlusion are the main complications of the disease. Importantly, this combination will give a new hope for clinical use of senicapoc. Indeed, Ataga et al. demonstrated that although being an anti-hemolytic agent, senicapoc could not reduce vaso-occlusive crisis in patients with SCD. These crises are the clinical hallmark of SCD, and the main reason for emergency care of SCD patients. As a result, senicapoc was completely removed from the list of candidate drugs for SCD. Currently, all the researchers agree on the association of senicapoc with another drugs in order to have a synergy of action and to reduce the vaso-occlusive crisis. Among these combinations, the most cited are senicapoc-voxelotor, senicapoc-hydroxyurea and senicapoc-L-glutamine [62]. The last two are challenging given the difference in physicochemical properties of the drugs (senicapoc: hydrophobic, hydroxyurea and L-glutamine: hydrophilic). However, the following possibilities can be tried for their oral administration:

1. Give two tablets/capsules, each containing one of the drugs: the first limit of this possibility will be the adherence to the treatment. SCD is a chronic disease; it is desirable to reduce the burden of treatment as much as possible. Another factor that can reduce treatment adherence is the size of the tablets. Finally, this approach will not solve the problem of low aqueous solubility and oral bioavailability of senicapoc.

2. Include the two molecules wihtin a single tablet/capsule: the long-term compatibility of these molecules as well as the low solubility of senicapoc could be limiting factors. This low solubility could create an imbalance in the absorption of drugs.

In view of this, a senicapoc-voxelotor combination could be an appropriate choice given the similar physicochemical properties of the drugs. It remains uncertain which carrier to use for their oral administration. So far, SNEEDSs have shown the potential to combine two compounds [63, 64]. We believe that a combined SNEDDS formulation of senicapoc and voxelotor could improve efficacy and ultimately reduce the cost of the therapy. However, before this combination becomes conceivable, two questions are worth asking: 1) what is the maximum amount of each compound to be included simultaneously in the formulation? and 2) what is the rational dosage of each drug to be used in the combination?

The maximum amount of a drug to be encapsulated in SNEDDSs depends on its solubility in the selected oil. Among the oils tested in this project, Capryol PGMC® was the best and was able to dissolve 14.5 mg/mL and 16.6 mg/mL of senicapoc and voxelotor, respectively. Obviously, the co-encapsulation of senicapoc and voxelotor is expected to reduce their solubility in the oil. This will be a challenge, especially for voxelotor, which needs to be given at a high dose.

Regarding the rational dosage of the drugs, we propose to study different combinations of senicapoc (5-10 mg) and voxelotor (100-1000 mg) on transgenic SCD mice or rats [65]. Several

blood parameters, including hemoglobin levels, hematocrit, erythrocyte density, mean corpuscular hemoglobin concentration, cell dehydration, erythrocytes sickling, and reticulocytes counts can be determined in order to select the optimal ratio. When different drugs are combined, the toxicity might increase; therefore, the necessity of recognizing and managing adverse events will be critical for the success of the treatment. The optimal combination should significantly reduce erythrocyte hemolysis and vaso-occlusion without showing any notable adverse side. Further, the combination can be encapsulated into SNEDDSs to improve biopharmaceutical properties.

III.2. TRANSLATIONAL PERSPECTIVE: TOWARDS THE CLINIC

A drug delivery system can only be successful when the technology can be transferred from a lab-scale to a large-scale. This PhD thesis demonstrated the ability of SNEDDSs to increase the aqueous solubility and oral absorption of senicapoc and voxelotor. Even though the formulated SNEDDSs were made of FDA and EMA approved components, from a regulatory point of view, they require going through the clinical trials, especially phase I study.

The aim of clinical study phase I is to assess the safety and bioavailabilty of SNEDDSs compared to the references, and to determine the dosage of the drug to be encapsulated towards further clinical use. The comparison of the reference and the new formulation should be assessed in terms of equivalence of drug content and physicochemical characteristics [65,66]. According to the regulatory guidance for generics, two formulations of the same drug are claimed to be "bioequivalent" if the ratio of geometric means of the pharmacokinetic (PK) responses, such as the area under the plasma concentration–time curve (AUC) and the maximal plasma concentration (Cmax), between the two formulations of the same drug is within 80–125%, with 90% confidence [66]. In practice, the SNEDDSs loaded with senicapoc and voxelotor must be compared with references in terms of oral bioavailability. Missing a reference on the market, senicapoc-loaded SNEDDSs can be compared to an equivalent dose of a free drug suspensions, tablets or capsules. For voxelotor-loaded SNEDDSs, the comparison should be done with Oxbryta®, the brand name of the drug. However, Oxbryta® contains 500 mg of voxelotor while our SNEDDSs only contain 50 mg. This can make it difficult to draw a conclusion.

IV. RECOMMANDATION ON SCD THERAPY

Although it seems likely that curative therapies such as gene editing and stem cell transplantation will gain traction in the years ahead, a range of issues, including safety, cost, and timing, mean that new disease-modifying drugs will be needed for the near future. Many emerging therapies for individuals with SCD will only be available in high-income settings and, thus, will only benefit a minority of the global SCD population. In countries with the highest number of people affected by SCD, the application of novel therapeutic agents and potential curative treatments will be limited by high costs and the need for advanced healthcare facilities. As new drugs and treatments are being developed, it will be essential to find ways to make them available to patients in low-income countries who stand to benefit most. Newly approved drugs, including L-Glutamine, voxelotor, and crizanlizumab are almost 20−50 times more expensive than hydroxyurea, which can be a hurdle in their extensive use in low-income regions [67]. Nevertheless, the arrival of these drugs on the market marks an exciting period of sickle cell pharmacotherapy.

Even though it has been decades since hydroxyurea was first licensed for treatment in SCD, its use in low- and middle-income countries remains limited. Hydroxyurea is now a widely available drug, but its application is still associated with obstacles that can be hard to overcome in settings like Africa and India. These include cost, blood counts monitoring and regular clinical evaluations. Despite hydroxyurea being relatively cheap, the drug continues to be unaffordable in many countries. This is particularly the case for pediatric formulations, an important problem to consider in settings where SCD is still very much a disease of childhood. We believe that local production of hydroxyurea, especially pediatric formulations could be an alternative to overcome this situation. Furthermore, evidence on efficacy and tolerance of hydroxyurea in low-income countries is still limited [68]. We recommand that clinical trials of hydroxyurea and other SCD drugs involve individuals from low-income countries, where the burden of disease is high.

Nerveless, my PhD thesis provides enough data to demonstrate the ability of SNEDDS to improve aqueous solubility and oral absorption of senicapoc and voxelotor. SNEDDS can be easily scaled-up, which is particularly advantageous for low-income countries where most of SCD patients are located. By increasing aqueous solubility and oral bioavailability of voxelotor, my PhD work will help solve problems associated with its clinical use.

REFERENCES

1. Rogers, K.; Balachandren, N.; Awogbade, M.; Johns, J. Sickle Cell Disease in Pregnancy. *Obstet. Gynaecol. Reprod. Med.* **2019**, *29*,61–69, https://doi.org/10.1016/j.ogrm.2019.01.006.
2. Kato, G. J.; Piel, F. B.; Reid, C. D.; Gaston, M. H.; Ohene-Frempong, K.; Krishnamurti, L.; Smith, W. R.; Panepinto, J. A.; Weatherall, D. J.; Costa, F. F.; Vichinsky, E. P. Sickle Cell Disease. *Nat. Rev. Dis. Prim.* **2018**, *4*, 1–22,https://doi.org/10.1038/nrdp.2018.10.
3. Palomo, M.; Diaz-Ricart, M.; Carreras, E. Is Sickle Cell Disease-Related Neurotoxicity a Systemic Endotheliopathy? *Hematol. Oncol. Stem Cell Ther.* **2020**, *13*, 111–115,https://doi.org/10.1016/j.hemonc.2019.12.005.
4. Piel, F. B.; Hay, S. I.; Gupta, S.; Weatherall, D. J.; Williams, T. N. Global Burden of Sickle Cell Anaemia in Children under Five, 2010-2050: Modelling Based on Demographics, Excess Mortality, and Interventions. *PLoS Med.* **2013**, *10*, https://doi.org/10.1371/journal.pmed.1001484.
5. Brandow, A. M.; Panepinto, J. A. Hydroxyurea Use in Sickle Cell Disease: The Battle with Low Prescription Rates, Poor Patient Compliance and Fears of Toxicities. *Expert Rev. Hematol.* **2010**, *3* , 255–260,https://doi.org/10.1586/ehm.10.22.
6. Niihara, Y.; Zerez, C. R.; Akiyama, D. S.; Tanaka, K. R. Oral L-Glutamine Therapy for Sickle Cell Anemia: I. Subjective Clinical Improvement and Favorable Change in Red Cell NAD Redox Potential. *Am. J. Hematol.* **1998**, *58*, 117–121,https://doi.org/10.1002/(SICI)1096-8652(199806)58:2<117::AID-AJH5>3.0.CO;2-V.
7. ASH Clinical News Home Page. Available online: https://www.ashclinicalnews.org/news/latest-and-greatest/fda-approves-crizanlizumab-tmca-sickle-cell-disease (accessed on 16 December 2020).
8. Marouf, R. Blood Transfusion in Sickle Cell Disease. *Hemoglobin* **2011**, *35*, 495–502, https://doi.org/10.3109/03630269.2011.596984.
9. Hutchaleelaha, A.; Patel, M.; Washington, C.; Siu, V.; Allen, E.; Oksenberg, D.; Gretler, D. D.; Mant, T.; Lehrer-Graiwer, J. Pharmacokinetics and Pharmacodynamics of Voxelotor (GBT440) in Healthy Adults and Patients with Sickle Cell Disease. *Br. J. Clin. Pharmacol.* **2019**, *85*, 1290–1302, https://doi.org/10.1111/bcp.13896.
10. US Food and Drug Administration Home Page. Available online: https://www.accessdata.fda.gov/drugsatfda_docs/label/2019/213137s000lbl.pdf (accessed on 10 December 2020).
11. McNaughton-Smith, G. A.; Burns, J. F.; Stocker, J. W.; Rigdon, G. C.; Creech, C.; Arlington, S.; Shelton, T.; De Franceschi, L. Novel Inhibitors of the Gardos Channel for the Treatment of Sickle Cell Disease. *J. Med. Chem.* **2008**, *51*, 976–982,https://doi.org/10.1021/jm070663s.
12. Rani, S.; Rana, R.; Saraogi, G. K.; Kumar, V.; Gupta, U. Self-Emulsifying Oral Lipid Drug Delivery Systems: Advances and Challenges. *AAPS PharmSciTech*. Springer New York LLC April 1, 2019. https://doi.org/10.1208/s12249-019-1335-x.
13. Pouton, C.W. Lipid Formulations for Oral Administration of Drugs: Non-Emulsifying, Self-Emulsifying and "Self-Microemulsifying" Drug Delivery Systems. *Eur. J. Pharm. Sci.* **2000**, *11*, 93–98, doi:10.1016/S0928-0987(00)00167-6.
14. Qian, J.; Meng, H.; Xin, L.; Xia, M.; Shen, H.; Li, G.; Xie, Y. Self-Nanoemulsifying Drug Delivery Systems of Myricetin: Formulation Development, Characterization, and in Vitro and in Vivo Evaluation. *Colloids Surfaces B Biointerfaces* **2017**, *160*, 101–109, doi:10.1016/j.colsurfb.2017.09.020.
15. Kollipara, S.; Gandhi, R.K. Pharmacokinetic Aspects and in Vitro–in Vivo Correlation Potential for Lipid-Based Formulations. *Acta Pharm. Sin. B* **2014**, *4*, 333–349, doi:10.1016/j.apsb.2014.09.001.
16. Mu, H.; Holm, R.; Mullertz, A. Lipid-Based Formulations for Oral Administration of Poorly Water-Soluble Drugs. *Int. J. Pharm.* **2013**, *453*, 215–224. https://doi.org/10.1016/j.ijpharm.2013.03.054.

17. Rajpoot, K.; Tekade, M.; Pandey, V.; Nagaraja, S.H.; Youngren-Ortiz, S.R.; Tekade, R.K. *Self-Microemulsifying Drug-Delivery System: Ongoing Challenges and Future Ahead*; Tekade, R.K., Ed.; Drug Delivery Systems: Academic Press, Cambridge, MA, USA, 2020; pp. 393–454, doi:10.1016/B978-0-12-814487-9.00009-0.
18. Li, L.; Zhou, C.H.; Xu, Z.P. Self-Nanoemulsifying Drug-Delivery System and Solidified Self-Nanoemulsifying Drug-Delivery System. In *Nanocarriers for Drug Delivery*; Elsevier: Amsterdam, The Netherlands, 2019; pp. 421–449, doi:10.1016/b978-0-12-814033-8.00014-x.
19. Yin, Y.M.; Cui, F.D.; Mu, C.F.; Choi, M.K.; Kim, J.S.; Chung, S.J.; Shim, C.K.; Kim, D.D. Docetaxel Microemulsion for Enhanced Oral Bioavailability: Preparation and in Vitro and in Vivo Evaluation. *J. Control. Release* **2009**, *140*, 86–94, doi:10.1016/j.jconrel.2009.08.015.
20. Mountfield, R.J.; Senepin, S.; Schleimer, M.; Walter, I.; Bittner, B. Potential Inhibitory Effects of Formulation Ingredients on Intestinal Cytochrome P450. *Int. J. Pharm.* **2000**, *211*, 89–92, doi:10.1016/S0378-5173(00)00586-X.
21. Rege, B.D.; Kao, J.P.Y.; Polli, J.E. Effects of Nonionic Surfactants on Membrane Transporters in Caco-2 Cell Monolayers. *Eur. J. Pharm. Sci.* **2002**, *16*, 237–246, doi:10.1016/S0928-0987(02)00055-6.
22. Čerpnjak, K.; Zvonar, A.; Gašperlin, M.; Vrečer, F. Lipid-Based Systems as a Promising Approach for Enhancing the Bioavailability of Poorly Water-Soluble Drugs. *Acta Pharm.* **2013**, *63*, 427–445, doi:10.2478/acph-2013-0040.
23. Zhang, L.; Zhang, L.; Zhang, M.; Pang, Y.; Li, Z.; Zhao, A.; Feng, J. Self-Emulsifying Drug Delivery System and the Applications in Herbal Drugs. *Drug Deliv.* **2015**, *22*, 475–486, doi:10.3109/10717544.2013.861659.
24. Zhu, J.X.; Tang, D.; Feng, L.; Zheng, Z.G.; Wang, R.S.; Wu, A.G.; Duan, T.T.; He, B.; Zhu, Q. Development of Self-Microemulsifying Drug Delivery System for Oral Bioavailability Enhancement of Berberine Hydrochloride. *Drug Dev. Ind. Pharm.* **2013**, *39*, 499–506, doi:10.3109/03639045.2012.683875.
25. Jain, S.; Jain, A. K.; Pohekar, M.; Thanki, K. Novel Self-Emulsifying Formulation of Quercetin for Improved in Vivo Antioxidant Potential: Implications for Drug-Induced Cardiotoxicity and Nephrotoxicity. *Free Radic. Biol. Med.* **2013**, *65*, 117–130, https://doi.org/10.1016/j.freeradbiomed.2013.05.041.
26. Li, F.; Song, S.; Guo, Y.; Zhao, Q.; Zhang, X.; Pan, W.; Yang, X. Preparation and Pharmacokinetics Evaluation of Oral Self-Emulsifying System for Poorly Water-Soluble Drug Lornoxicam. *Drug Deliv.* **2015**, *22*, 487–498, doi:10.3109/10717544.2014.885615.
27. Kovarik, J.M.; Mueller, E.A.; van Bree, J.B.; Tetzloff, W.; Kutz, K. Reduced Inter- and Intraindividual Variability in Cyclosporine Pharmacokinetics from a Microemulsion Formulation. *J. Pharm. Sci.* **1994**, *83*, 444–446, doi:10.1002/jps.2600830336.
28. Nielsen, F.S.; Petersen, K.B.; Müllertz, A. Bioavailability of Probucol from Lipid and Surfactant Based Formulations in Minipigs: Influence of Droplet Size and Dietary State. *Eur. J. Pharm. Biopharm.* **2008**, *69*, 553–562, doi:10.1016/j.ejpb.2007.12.020.
29. Feeney, O.M.; Crum, M.F.; McEvoy, C.L.; Trevaskis, N.L.; Williams, H.D.; Pouton, C.W.; Charman, W.N.; Bergström, C.A.S.; Porter, C.J.H. 50 Years of Oral Lipid-Based Formulations: Provenance, Progress and Future Perspectives. *Adv. Drug Deliv. Rev.* **2016**, *101*, 167–194, doi:10.1016/j.addr.2016.04.007.
30. Date, A.A.; Desai, N.; Dixit, R.; Nagarsenker, M. Self-Nanoemulsifying Drug Delivery Systems: Formulation Insights, Applications and Advances. *Nanomedicine* **2010**, 1595–1616, doi:10.2217/nnm.10.126.
31. Ataga, K. I.; Smith, W. R.; De Castro, L. M.; Swerdlow, P.; Saunthararajah, Y.; Castro, O.; Vichinsky, E.; Kutlar, A.; Orringer, E. P.; Rigdon, G. C.; Stacker, J. W. Efficacy and Safety of the Gardos Channel Blocker, Senicapoc (ICA-17043), in Patients with Sickle Cell Anemia. *Blood* **2008**, *111*, 3991–3997, https://doi.org/10.1182/blood-2007-08-110098.

32. Buya A.B; Beloqui A.; Memvanga P.B.; Préat V. Self-Nano-Emulsifying Drug-Delivery Systems: From the Development to the Current Applications and Challenges in Oral Drug Delivery. Pharmaceutics. **2020**; 12, 1194, https://doi.org/10.3390/pharmaceutics12121194.
33. Bahloul, B.; Lassoued, M. A.; Sfar, S. A Novel Approach for the Development and Optimization of Self Emulsifying Drug Delivery System Using HLB and Response Surface Methodology: Application to Fenofibrate Encapsulation. *Int. J. Pharm.* **2014**, *466*, 341–348, https://doi.org/10.1016/j.ijpharm.2014.03.040.
34. Tran, T.; Rades, T.; Müllertz, A. Formulation of Self-Nanoemulsifying Drug Delivery Systems Containing Monoacyl Phosphatidylcholine and Kolliphor® RH40 Using Experimental Design. *Asian J. Pharm. Sci.* **2018**, *13*, 536–545,https://doi.org/10.1016/j.ajps.2017.09.006.
35. Rantanen, J., & Khinast, J. (2015). The Future of Pharmaceutical Manufacturing Sciences. *Journal of Pharmaceutical Sciences*, *104*(11), 3612–3638. https://doi.org/https://doi.org/10.1002/jps.24594
36. Yi, T.; Wan, J.; Xu, H.; Yang, X. A New Solid Self-Microemulsifying Formulation Prepared by Spray-Drying to Improve the Oral Bioavailability of Poorly Water Soluble Drugs. *Eur. J. Pharm. Biopharm.* **2008**, *70*, 439–444, doi:10.1016/j.ejpb.2008.05.001.
37. Kamal, M.M.; Nazzal, S. Novel Sulforaphane-Enabled Self-Microemulsifying Delivery Systems (SFN-SMEDDS) of Taxanes: Formulation Development and in Vitro Cytotoxicity against Breast Cancer Cells. *Int. J. Pharm.* **2018**, *536*, 187–198, doi:10.1016/j.ijpharm.2017.11.063.
38. Buya, A.B.; Ucakar, B.; Beloqui, A.; Memvanga, P.B.; Préat, V. Design and Evaluation of Self-Nanoemulsifying Drug Delivery Systems (SNEDDSs) for Senicapoc. *Int. J. Pharm.* **2020**, *580*, 119180, doi:10.1016/j.ijpharm.2020.119180.
39. Zupančič, O.; Grießinger, J. A.; Rohrer, J.; Pereira de Sousa, I.; Danninger, L.; Partenhauser, A.; Sündermann, N. E.; Laffleur, F.; Bernkop-Schnürch, A. Development, in Vitro and in Vivo Evaluation of a Self-Emulsifying Drug Delivery System (SEDDS) for Oral Enoxaparin Administration. *Eur. J. Pharm. Biopharm.* **2016**, *109*, 113–121,https://doi.org/10.1016/j.ejpb.2016.09.013.
40. Yap, S.P.; Yuen, K.H. Influence of Lipolysis and Droplet Size on Tocotrienol Absorption from Self-Emulsifying Formulations. *Int. J. Pharm.* **2004**, *281*, 67–78, doi:10.1016/j.ijpharm.2004.05.015.
41. Kovarik, J.M.; Mueller, E.A.; van Bree, J.B.; Tetzloff, W.; Kutz, K. Reduced Inter- and Intraindividual Variability in Cyclosporine Pharmacokinetics from a Microemulsion Formulation. *J. Pharm. Sci.* **1994**, *83*, 444–446, doi:10.1002/jps.2600830336.
42. Xue, X.; Cao, M.; Ren, L.; Qian, Y.; Chen, G. Preparation and Optimization of Rivaroxaban by Self-Nanoemulsifying Drug Delivery System (SNEDDS) for Enhanced Oral Bioavailability and No Food Effect. *AAPS PharmSciTech* **2018**, *19*, 1847–1859,https://doi.org/10.1208/s12249-018-0991-6.
43. Cherniakov, I.; Domb, A.J.; Hoffman, A. Self-Nano-Emulsifying Drug Delivery Systems: An Update of the Biopharmaceutical Aspects. *Expert Opin. Drug Deliv.* **2015**, *12*, 1121–1133, doi:10.1517/17425247.2015.999038.
44. Wang, L.; Dong, J.; Chen, J.; Eastoe, J.; Li, X. Design and Optimization of a New Self-Nanoemulsifying Drug Delivery System. *J. Colloid Interface Sci.* **2009**, *330*, 443–448, doi:10.1016/j.jcis.2008.10.077.
45. Czajkowska-Kośnik, A.; Szekalska, M.; Amelian, A.; Szymańska, E.; Winnicka, K. Development and Evaluation of Liquid and Solid Self-Emulsifying Drug Delivery Systems for Atorvastatin. *Molecules* **2015**, *20*, 21010–21022, doi:10.3390/molecules201219745.
46. Parmar, N.; Singla, N.; Amin, S.; Kohli, K. Study of Cosurfactant Effect on Nanoemulsifying Area and Development of Lercanidipine Loaded (SNEDDS) Self Nanoemulsifying Drug Delivery System. *Colloids Surfaces B Biointerfaces* **2011**, *86*, 327–338, https://doi.org/10.1016/j.colsurfb.2011.04.016.
47. Qian, J.; Meng, H.; Xin, L.; Xia, M.; Shen, H.; Li, G.; Xie, Y. Self-Nanoemulsifying Drug Delivery Systems of Myricetin: Formulation Development, Characterization, and in Vitro and in Vivo Evaluation. *Colloids Surfaces B Biointerfaces* **2017**, *160*, 101–109, https://doi.org/10.1016/j.colsurfb.2017.09.020.

48. Mandal, S.; Mandal, S.S. Microemulsion Drug Delivery System: A Platform for Improving Dissolution Rate of Poorly Water Soluble Drug. *Int. J. Pharm. Sci. Nanotechnol.* **2011**, *3*, 1214–1219, doi:10.37285/ijpsn.2010.3.4.6.
49. Hedge, O. J.; Bergström, C. A. S. Suitability of Artificial Membranes in Lipolysis-Permeation Assays of Oral Lipid-Based Formulations. *Pharm. Res.* **2020**, *37*,9, https://doi.org/10.1007/s11095-020-02833-9.
50. Stillhart, C.; Kuentz, M. Comparison of High-Resolution Ultrasonic Resonator Technology and Raman Spectroscopy as Novel Process Analytical Tools for Drug Quantification in Self-Emulsifying Drug Delivery Systems. *J. Pharm. Biomed. Anal.* **2012**, *59*, 29–37, doi:10.1016/j.jpba.2011.10.018.
51. Thomas, N.; Holm, R.; Rades, T.; Müllertz, A. Characterising Lipid Lipolysis and Its Implication in Lipid-Based Formulation Development. *AAPS J.* **2012**, *14*, 860–871, doi:10.1208/s12248-012-9398-6.
52. Khan, J.; Hawley, A.; Rades, T.; Boyd, B. J. In Situ Lipolysis and Synchrotron Small-Angle X-Ray Scattering for the Direct Determination of the Precipitation and Solid-State Form of a Poorly Water-Soluble Drug During Digestion of a Lipid-Based Formulation. *J. Pharm. Sci.* **2016**, *105*, 2631–2639, https://doi.org/10.1002/jps.24634.
53. Bibi, H. A.; Holm, R.; Bauer-Brandl, A. Simultaneous Lipolysis/permeation in Vitro Model, for the Estimation of Bioavailability of Lipid Based Drug Delivery Systems. *Eur. J. Pharm. Biopharm.* **2017**, *117*, 300–307,https://doi.org/10.1016/j.ejpb.2017.05.001.
54. Tung, N. T.; Tran, C. S.; Pham, T. M. H.; Nguyen, H. A.; Nguyen, T. L.; Chi, S. C.; Nguyen, D. D.; Bui, T. B. H. Development of Solidified Self-Microemulsifying Drug Delivery Systems Containing L-Tetrahydropalmatine: Design of Experiment Approach and Bioavailability Comparison. *Int. J. Pharm.* **2018**, *537* (1-2), 9–21,https://doi.org/10.1016/j.ijpharm.2017.12.027.
55. Dantzig, A.H.; Bergin, L. Uptake of the Cephalosporin, Cephalexin, by a Dipeptide Transport Carrier in the Human Intestinal Cell Line, Caco-2. *BBA Biomembr.* **1990**, *1027*, 211–217, doi:10.1016/0005-2736(90)90309-C.
56. Yamashita, S.; Furubayashi, T.; Kataoka, M.; Sakane, T.; Sezaki, H.; Tokuda, H. Optimized Conditions for Prediction of Intestinal Drug Permeability Using Caco-2 Cells. *Eur. J. Pharm. Sci.* **2000**, *10*, 195–204, doi:10.1016/S0928-0987(00)00076-2.
57. Obringer, C.; Manwaring, J.; Goebel, C.; Hewitt, N.J.; Rothe, H. Suitability of the in Vitro Caco-2 Assay to Predict the Oral Absorption of Aromatic Amine Hair Dyes. *Toxicol. Vitr.* **2016**, *32*, 1–7, doi:10.1016/j.tiv.2015.11.007.
58. Mudie, D. M.; Amidon, G. L.; Amidon, G. E. Physiological Parameters for Oral Delivery and in Vitro Testing. *Mol. Pharm.* **2010**, *7* (5), 1388–1405. https://doi.org/10.1021/mp100149j.
59. Menzel, C.; Bernkop-Schnürch, A. Enzyme Decorated Drug Carriers: Targeted Swords to Cleave and Overcome the Mucus Barrier. *Adv. Drug Deliv. Rev.* **2018**, *124*, 164–174. https://doi.org/https://doi.org/10.1016/j.addr.2017.10.004.
60. Ataga, K. I., Reid, M., Ballas, S. K., Yasin, Z., Bigelow, C., James, L. S., … Stocker, J. W. (2011). Improvements in haemolysis and indicators of erythrocyte survival do not correlate with acute vaso-occlusive crises in patients with sickle cell disease: A phase III randomized, placebo-controlled, double-blind study of the gardos channel blocker senicapo. *British Journal of Haematology*, *153*(1), 92–104. https://doi.org/10.1111/j.1365-2141.2010.08520.x
61. Christophersen, P. C., Christiansen, M. L., Holm, R., Kristensen, J., Jacobsen, J., Abrahamsson, B., & Müllertz, A. (2014). Fed and fasted state gastro-intestinal in vitro lipolysis: In vitro in vivo relations of a conventional tablet, a SNEDDS and a solidified SNEDDS. *European Journal of Pharmaceutical Sciences*, *57*, 232–239. https://doi.org/https://doi.org/10.1016/j.ejps.2013.09.007
62. Telen, M. J., Malik, P., & Vercellotti, G. M. (2019). Therapeutic strategies for sickle cell disease: towards a multi-agent approach. *Nature Reviews Drug Discovery*, *18*(2), 139–158. https://doi.org/10.1038/s41573-018-0003-2

63. The Foundation for Sickle Cell Disease Research (FSCDR) Home Page. Available online: https://fscdr.org/wp-content/uploads/2019/08/01SEPT2016-SpecialJournal-Full.pdf (accessed on 9 May 2020).
64. Cui, W., Zhao, H., Wang, C., Chen, Y., Luo, C., Zhang, S., … He, Z. (2019). Co-encapsulation of docetaxel and cyclosporin A into SNEDDS to promote oral cancer chemotherapy. *Drug Delivery*, *26*(1), 542–550. https://doi.org/10.1080/10717544.2019.1616237
65. Vohra, A. M., Patel, C. V., Kumar, P., & Thakkar, H. P. (2017). Development of dual drug loaded solid self microemulsifying drug delivery system: Exploring interfacial interactions using QbD coupled risk based approach. *Journal of Molecular Liquids*, *242*, 1156–1168. https://doi.org/10.1016/j.molliq.2017.08.002
66. Crompton, D.; Vats, R.; Pradhan-Sundd, T.; Sundd, P.; Kameneva, M. V. Drag-Reducing Polymers Improve Hepatic Vaso-Occlusion in SCD Mice. *Blood Adv.* **2020**, *4* (18), 4333–4336. https://doi.org/https://doi.org/10.1182/bloodadvances.2020002779.
67. Chow, S.-C. Bioavailability and Bioequivalence in Drug Development. *Wiley Interdiscip. Rev. Comput. Stat.* **2014**, *6* (4), 304–312. https://doi.org/10.1002/wics.1310.
68. Ali, M. A., Ahmad, A., Chaudry, H., Aiman, W., Aamir, S., Anwar, M. Y., & Khan, A. (2020). Efficacy and safety of recently approved drugs for sickle cell disease: a review of clinical trials. *Experimental Hematology*, 1–9. https://doi.org/10.1016/j.exphem.2020.08.008
69. Power-Hays, A., & Ware, R. E. (2020). Effective use of hydroxyurea for sickle cell anemia in low resource countries. *Current Opinion in Hematology*, *27*(3), 172–180. https://doi.org/10.1097/MOH.0000000000000582.